INDIAN NATIONAL COMMITTEE ON SURFACE WATER (INCSW-CWC)

UID	**UK-2012-112**
Type (State whether final or draft report)	**Final Report**
Name of R&D Scheme	**HYDROLOGICAL RESPONSE OF A RIVER BASIN IN CHANGING CLIMATE**
Name of PI & Co-PI	**Dr. Ashish Pandey** **Associate Professor & PI** **Dept. of Water Resources Development and Management** **Indian Institute of Technology Roorkee** **Roorkee-247 667 (Uttarakhand)** **&** **Dr. S.K. Mishra** **Professor & Co-PI** **Dept. of Water Resources Development and Management** **Indian Institute of Technology Roorkee** **Roorkee-247 667 (Uttarakhand)** **&** **Dr.R.P. Pandey** **Scientist G & Co-PI** **NIH Roorkee-247667, Roorkee (Uttarakhand)**
Institute Address	**Indian Institute of Technology Roorkee** **Roorkee-247 667 (Uttarakhand)** **https://www.iitr.ac.in/**
Circulation (State whether Open for public or not)	**Open for Public**
Month & Year of Report Submission	**June 2019**

TEAM OF INVESTIGATORS

Principal Investigator

Dr. Ashish Pandey
Associate Professor
Department of Water Resources Development & Management
Indian Institute of Technology Roorkee
Roorkee-247 667, Uttarakhand

Co-Principal Investigators

1. **Dr. S.K. Mishra**
   Professor
   Department of Water Resources Development & Management
   Indian Institute of Technology Roorkee
   Roorkee-247 667, Uttarakhand

2. **Dr.R.P. Pandey**
   Scientist G
   National Institute of Hydrology, Roorkee
   Roorkee -247667, Uttarakhand

Supporting Research Staff

1. **Mr. Shakti Suryavanshi,** Junior Research Fellow, Dept. of WRD&M, IIT Roorkee
2. **Mr. Amarkant Gautam,** Senior Research Fellow, Dept. of WRD&M, IIT Roorkee
3. **Mr. Dheeraj Kumar,** Senior Research Fellow, Dept. of WRD&M, IIT Roorkee
4. **Mr. Deen Dayal,** Senior Research Fellow, Dept. of WRD&M, IIT Roorkee
5. **Mr. Harsh Vardhan Singh,** Junior Research Fellow, Dept. of WRD&M, IIT Roorkee
6. **Mr. Palmate Santosh Subhash,** Research Scholar**,** Dept. of WRD&M, IIT Roorkee

EXTENDED SUMMARY

The research project entitled "**Hydrological Response of a River Basin in Changing Climate**" was sanctioned to the Department of Water Resources Development and Management, Indian Institute of Technology (IIT) Roorkee by MoWR, PP Wing, R&D Division New Delhi vide letter no.23/72/2012-R&D/359-369; Dated March 6, 2012 under R&D programme of Ministry of Water Resources, RD&GR, New Delhi. The specific objectives of this research project are: (1) To study the long term changes in climatic variables in the Betwa basin; (2) To study the land use/land cover (LU/LC) changes in the Betwa basin using satellite data; (3) To study the spatial correlation of land use/land cover with climate parameter in the Betwa basin; (4) Application of the Soil & Water Assessment (SWAT) model for estimation of runoff and sediment yield under changing climate; and (5) Evaluation of optimal land use/land covers for the sustainable water resources development of the Betwa basin in changing climate.

The report is organized in eight chapters as follows:

Chapter 1: This chapter briefly describes the general subject background, land use/land cover & climatic changes, climate change impact assessment using models, importance of climate change study in Indian river basin and need of hydrological response study in Betwa Basin. It helps to motivate for the study and to achieve the specific research objectives.

Chapter 2: This chapter deals with the study area and data used in this study. It includes location of the Betwa basin, its climate, major crops grown, soils and water resources development and brief about Ken-Betwa Link Project. In this chapter, the data acquisition has also been discussed. It includes Digital Elevation Model, satellite data and Climate Data i.e. CMIP5 GCM data along with the discharge and sediment data, and soil data.

Chapter 3: This chapter deals with the long-term trend analysis of monthly climatic variables (rainfall, minimum, maximum and average temperature, diurnal temperature range, potential evapotranspiration and aridity index) has been carried out at station-wise, and basin scale. Seasonal and annual time-series data of climate was initially auto-correlated, and then trend analysis was carried out using modified Mann-Kendal (MK) test. The MK test statistics, Sen's slope, intercept, and percent change were estimated for each climate variable at each time-scale. In this study, the trend analysis was carried out at 1%, 5% and 10% significance level.

Chapter 4: This chapter deals with the Remote sensing and GIS techniques used to extract the spatial information of LU/LC using spatiotemporal satellite imagery data. Satellite imageries of the Landsat-1 Multispectral Scanner (MSS), Landsat-2 MSS, Landsat-5 Thematic Mapper (TM), Landsat-7 Enhanced Thematic Mapper Plus (ETM+), Landsat-8 Operational Land Imager (OLI), Indian Remote-sensing Satellite (IRS-P6) Linear Imaging and Self Scanning (LISS) III, and Resourcesat-2 LISS IV are analysed during this study. Maximum likelihood supervised image classification has been used to prepare land use maps for the years 1972, 1976, 1991, 2001, 2007, 2010, 2013 and 2015. Image pre-processing, classification of satellite data, and accuracy assessment of satellite-derived LU/LC maps are carried out using ERDAS Imagine 2014, and ArcGIS 10.2.2 version software packages. Furthermore, the vegetation area of LU/LC classification has been cross-verified using the vegetation maps generated by Normalized Difference Vegetation Index (NDVI) method.

Chapter 5: In this chapter the remotely sensed Moderate Resolution Imaging Spectroradiometer (MODIS) NDVI Terra (MOD13Q1), and MODIS Land Cover Type (MCD12Q1) time-series data products of collection 5 are used to assess relationship with numerous hydro-climatic variables, namely precipitation, Tmin, Tmax, Tdiff, R_H, PET, P/PET, discharge and sediment etc. All MODIS time-series datasets were initially re-projected to WGS 1984 UTM system. The MODIS NDVI data was further de-noised for smoothing using Savitzky-Golay filtering method in TIMESAT software. In this study, the correlation analyses is carried out at monthly, seasonal (pre-monsoon, monsoon, post-monsoon, winter), and annual time-scale. Multiple linear regression analysis is carried out to develop the empirical equations for land greening and degradation response of hydro-climatic variables. Furthermore, a conceptual model has been developed and used to furnish the relationships considering the dry years, wet years, and combined (dry + wet) year analyses results.

Chapter 6: In this chapter, a hydrological model, SWAT, is used to simulate the runoff and sediment considering the impacts of climatic change for the Betwa River basin. The downscaled and bias-corrected Global Climate Model (GCM) data of the Max-Planck-Institute-Earth System Model-Medium Resolution (MPI-ESM-MR) model is utilized to extract future climate change information, and to use as inputs in the calibrated and validated SWAT model for simulation of runoff and sediment. The GCM-derived climate variables are used for trend analysis and hydrological simulation over the periods of historical baseline 1986 (1986-2005) and the four future scenarios 2020 (2020-2039), 2040 (2040-2059), 2060 (2060-2079) and 2080 (2080-2099).

Chapter 7: In this chapter critical areas of the Betwa basin are identified and prioritized for the evaluation of structural and three non-structural Best Management Practices (BMPs) for sustainable management and development of the Betwa River Basin under changing climate. The calibrated and validated SWAT model is applied to simulate the BMP effectiveness on streamflow and sediment yield for future years. In this study, three overland BMPs (tillage management, contour farming, residue management etc.) as well as river channel BMPs (grassed waterways, streambank stabilization, grade stabilization structures etc.) are implemented and evaluated to recommend optimal solutions for sustainability of water resources in the Betwa river basin.

Chapter 8: This chapter provides the conclusions and recommendation of the study. Major conclusions, recommendations as well as limitations & future research scope of the study are briefly discussed.

CONTENTS

LIST OF TABLES

LIST OF FIGURES

ABBREVIATIONS

AI	:	Aridity Index
ASTER	:	Advanced Space-borne Thermal Emission and Reflection
BMP	:	Best Management Practice
BRB	:	Betwa River Basin
BSV	:	Barren or sparsely vegetated
CL	:	Croplands
CN	:	Curve Number
CSL	:	Closed Shrublands
CV	:	Coefficient of Variation
CWC	:	Central Water Commission
DBF	:	Deciduous Broadleaf Forest
DEM	:	Digital Elevation Model
DNF	:	Deciduous Needleleaf Forest
EBF	:	Evergreen Broadleaf Forest
ENF	:	Evergreen Needleleaf Forest
GCM	:	Global Circulation Model
GIS	:	Geographical Information System
GL	:	Grasslands
HRU	:	Hydrological Response Unit
IMD	:	India Meteorological Department
MCM	:	Million Cubic Meters
MK	:	Mann–Kendall
MLR	:	Multiple Linear Regression
MODIS	:	Moderate Resolution Imaging Spectro-radiometer
MP	:	Madhya Pradesh
MXF	:	Mixed Forest
NBSS&LUP	:	National Bureau of Soil Survey and Land Use Planning
NCCS	:	NASA Center for Climate Simulation
NCCS	:	NASA Center for Climate Simulation

NDVI	:	Normalized Difference Vegetation Index
NEX-GDDP	:	NASA Earth Exchange Global Daily Downscaled Projections
NRCS	:	National Resource Conservation Services
NRSC	:	National Remote Sensing Centre
NSE	:	Nash-Sutcliffe Efficiency
NV	:	Cropland/Natural Vegetation Mosaic
NWDA	:	National Water Development Agency
OSL	:	Open Shrublands
P	:	Precipitation
PBIAS	:	Percent Bias
PET	:	Potential Evapotranspiration
PWL	:	Permanent Wetlands
Q	:	Discharge
R^2	:	Coefficient of Determination
RH	:	Relative Humidity
RMSE	:	Root Mean Square Error
RSR	:	RMSE-Observations Standard Deviation Ratio
S&I	:	Snow and Ice
SCS	:	Soil Conservation Services
SI	:	Sensitivity Index
SRTM	:	Shuttle Radar Topography Mission
SV	:	Savannas
SW	:	South West
SWAT	:	Soil and Water Assessment Tool
Tdiff	:	Difference of Maximum and Minimum Temperature
Tmax	:	Maximum Temperature
Tmin	:	Minimum Temperature
U&B	:	Urban and builtup
UP	:	Uttar Pradesh
USDA	:	United States Department of Agriculture
USGS	:	United States Geological Survey

USLE	:	Universal Soil Loss Equation
WSV	:	Woody Savannas
WTR	:	Water
YBO	:	Yamuna Basin Organization

CHAPTER I

INTRODUCTION

1.1 GENERAL

From last few decades, climate change and climate variability has been studied throughout the world as they are expected to alter regional hydrologic conditions. Climate change impacts have been attributed to the associated long-term changes in the dominant meteorological variables such as precipitation and temperature (Chien et al., 2013). Climate change has many significant impacts on the hydrological processes such as frequency and distribution pattern of rainfall, evapo-transpiration, soil moisture, frequency and magnitude of runoff, and thus also impacts on hydrology and water resources system. Historical occurrence of extreme hydrological conditions has already exposed the vulnerability of human and natural systems to hydrological changes. Shifts in the availability of water resources are expected to be among the most significant consequences of projected climate changes (Kingston and Taylor, 2010). Consequently, the spatial and temporal availability of water resources can be significantly changes which in turn can affect agriculture, industry, and urban development (Frederick et al., 1997). These days the awareness of the effect of climate change due to human activities has been accelerating, and could be continued in the future also.

It is widely acknowledged that the climate has been changing is particularly vulnerable to changes in precipitation and temperature. The scientific community is beginning to realize that the hydrological response of catchment/watershed/river basin to the climate change is so far more complex than it was originally believed, especially, when the impacts of precipitation and temperature are considered. The hydrological response of a catchment depends on the sources of runoff, climatic conditions and physical characteristics of the catchment (Fontaine et al., 2001). The effect of temperature on the hydrological response of the basin has been studied independently, and also in combination with precipitation. The changes in temperature were applied as absolute amounts, whereas changes in precipitation were considered as percentage differences. In reality, changes in temperature and precipitation are likely to vary throughout the year, and such changes may also alter seasonal temperature patterns and consequently the distribution and frequency of precipitation events in the river basin area. These hydrological changes have pronounced the impact

on many sectors of the society. Therefore, estimation of the hydrological response of river basins under consideration of climate change is pre-requisite for appropriate planning and management in river basin.

1.2 LAND USE/LAND COVER & CLIMATIC CHANGES

Land use is characterized by conflict between conservation measures and subsistence farming. In some regions, the observed hydrological responses are affected by rapid land use change or other sources of hydrological alterations that may complicate the spatial generalization (Bari et al., 1996; Chiew et al., 2009; McIntyre and Marshall, 2010; Peel and Blöschl, 2011). It has also been suggested that empirical relationship between hydrological response and land use change, derived through spatial analysis, can be used to predict the temporal land use change impacts as an alternative or complement to the physical hydrological modeling (Wagener, 2007; Bulygina et al., 2012). This approach may be useful for sustainable land resource planning in regions having rapid changes.

Furthermore, climate change forms a complex and interactive system by linking a human action, viz. the land use change to environmental reactions, which in turn could have impact on hydrologic response analysis (Schulze, 2000). A major environment reaction to land use change occurs in hydrological responses such as changes in runoff components, erosion and groundwater recharge rates. With this response analysis being further complicated when accompanied by short or long term changes in climate.

Base on the literature studies, following issues or hypotheses are considered in the present study:

1. Indian hydrological regions are highly varying with time and space that climatic trends may be difficult to detect.
2. Fluctuations in the hydrological regions are amplified and exacerbated by climatic changes.
3. Hydrological response is highly sensitive to, and dependent upon the land use and climate change.
4. Abrupt changes in the land use at local scale is more significantly affects the hydrological cycle than the gradual land cover changes at regional to global scale.
5. Detailed spatial information is vital for assessing hydrological response in critical areas.

6. Major components of the hydrological system respond very differently between one region to the next when subjected to climate change.
7. Hydrological extremes are majorly concern in developing countries with the focus on inter-seasonal changes than the annual climatic change.
8. It is essential to identify hydrological sensitivity area in order to proactive in regard to the long term climatic changes.

1.3 CLIMATE CHANGE IMPACT ASSESSMENT USING MODELS

For evaluating climate change impacts on natural resources, normally a GIS based hydrologic model is being used to assess the effect of meteorological changes in drainage basin. Hydrological model provides a framework to conceptualize and investigate the relationships between climate, human activities and land resources (Jothityangkoon et al., 2001; Leavesley, 1994). They can be broadly classified into three categories: empirical or black-box, conceptual or grey-box, and physically based distributed or white-box models. Empirical models do not explicitly consider the governing physical laws of the process involved, but only relate input to output through some transform function. Conceptual models represent the effective response of an entire catchment, without attempting to characterize the spatial variability of the response explicitly. A critical shortcoming of lumped models is their inability to represent the spatial variability of hydrologic processes and catchment parameters (Moore et al., 1991; Refsgaard, 1987). The physically based distributed models are those which are able to explicitly represent the spatial variability of some of the important land surface characteristics such as topographic elevation, slope, aspect, vegetation, soil as well as climatic parameters including precipitation, temperature, and evapotranspiration. They relate model parameters directly to physical land surface characteristics. Nowadays, Soil and Water Assessment Tool (SWAT) is being widely used as physically-based semi-distributed model. Therefore, such spatially distributed hydrological models have important application for management purpose considering land use and climate change impacts.

1.4 IMPORTANCE OF CLIMATE CHANGE STUDY IN INDIAN RIVER BASIN

The vulnerability of climate change in Indian subcontinent is vital, because the major impact of climate change in this continent would be on the hydrology, land resources and agricultural economy. The major river systems of the Indian subcontinent, namely Ganga, Brahamaputra and

Indus which originate in the Himalayas, are expected to be more vulnerable to climate change because of the substantial flow contribution from snow and glaciers into these rivers. Possible impact of climatic changes on various aspects of the hydrological cycle has shown that little emphasis has been found on studying the hydrological processes in the Himalayan rivers.

Impact of climate change is going to be the most severe in the developing countries like India, because of their poor capacity to cope up with and adapt the climate change (Kulkarni et al. 2014). Divya and Mehrotra (1995) studied the climate change impact on hydrology of the India region. Precipitation changes show substantial spatial and temporal variability. The frequency of heavy precipitation events shows increasing trends over the central part of India (Goswami et al., 2006). Thus, it is necessary to assess the possible changes in the available water resources under the changing climatic conditions.

1.5 NEED OF HYDROLOGICAL RESPONSE STUDY IN BETWA BASIN

In present study, attempts have been made to investigate the effects of climatic change on hydrological response of a Betwa River basin which forms a part of the Yamuna River, tributary of Ganga river system. In central India, the Betwa River basin has dominant agriculture area which plays important role in rural economy. It falls under semi-arid to dry sub-humid climate region of the India. The air is being mostly dry in exception of south-west monsoon season. It has generally mild winter and hot summer climate. Betwa basin area varies from flat open wheat- growing areas to steep forest covered hilly areas, with change in the vegetation and topography in a fairly complex pattern. Forest is thick in hillier south-east; apart from the clay plains, some forest is also distributed over the basin and about one-fourth area of the basin contains vegetation which varies from scattered bush to thick forest. Betwa basin is dominated by black cotton soil. Most of the basin area is under cultivation of wheat and gram as the main crops in the post- monsoon or winter season and millet is also grow in the monsoon season. The increase of winter temperature may adversely affect the growth of Rabi crop (wheat and mustard) in the Betwa basin (Suryavanshi et al., 2014). Therefore, it is essential to study the hydrological response of Betwa basin under changing climate.

1.6 OBJECTIVES

The specific objectives of this study are as follows:

1. To study the long term (1901 – 2013) changes in climatic variables in the Betwa basin.

2. To study the land use/land cover changes in the Betwa basin using satellite data.
3. To study the spatial correlation of land use/land cover with climate parameter in the Betwa basin.
4. Application of the Soil & Water Assessment (SWAT) model for estimation of runoff and sediment yield under changing climate.
5. Evaluation of optimal land use/land covers for the sustainable water resources development of the Betwa basin in changing climate.

CHAPTER 2

STUDY AREA & DATA USED

2.1 STUDY AREA

2.1.1 Location of Betwa basin

Betwa River is a tributary of the Yamuna River, located in central part of the India. It is an interstate river between Madhya Pradesh and Uttar Pradesh. It originates from the Barkhera in Raisen district of Madhya Pradesh and then joins with the Yamuna River near Hamirpur in Uttar Pradesh. The total length of the river, from its origin to its confluence with the Yamuna River, is 590 km, out of which 232 km lies in Madhya Pradesh and the rest 358 km in Uttar Pradesh. During its course from the source up to the confluence with the Yamuna, the River is joined by a number of tributaries and sub-tributaries; some of the important rivers among them are Bina, Jamini, Dhasan, and Birma on the right bank and Kaliasote, Halali, Bah, Sagar, Narain, and Kaithan on the left Bank. The Betwa river basin is of saucer shape. It extends from 22°54′N to 26°05′N Latitude and 77°10′E to 80°20′E Longitude (Figure 2.1). Total area of the Betwa basin is about 43900 km^2 and its elevation ranges from 300 to 700 m above sea level (a.s.l.). It has undulating topography with the land slope varying from 0 to 67%. The catchment of the Betwa River is bounded by Southern Vindhyan plateau and northern alluvial plains. The study area is dominated by black cotton soil.

2.1.2 Climate of the Betwa Basin

The climate of the Betwa basin is moderate, mostly dry except during the southwest monsoons. The average annual rainfall varies from 700 to 1,200 mm with an average annual rainfall of 1,138 mm, the average annual evaporation losses are of the order of 1,830 mm, and the average annual runoff is about 13,430 million cubic meters (MCM), out of which nearly 80 % occurs in monsoon (Chaube 1988). The daily mean temperature ranges from a minimum of 8.1°C to a maximum of 42.3°C. The daily mean relative humidity varies from a minimum of 18 % (April and May) to a maximum of 90 % (August).

2.1.3 Major Crops Grown in Betwa Basin

The major crops grown in the Betwa basin are wheat, gram, paddy, oilseeds, pulses, sorghum, maize, vegetables and fodder. The agriculture informatics Division of National Informatics Centre,

Ministry of Communication & Information Technology, Government of India (http://dacnet.nic.in, presently http://www.nic.in/) has suggested wheat, paddy, maize and sorghum as the most suitable crop rotation in this region.

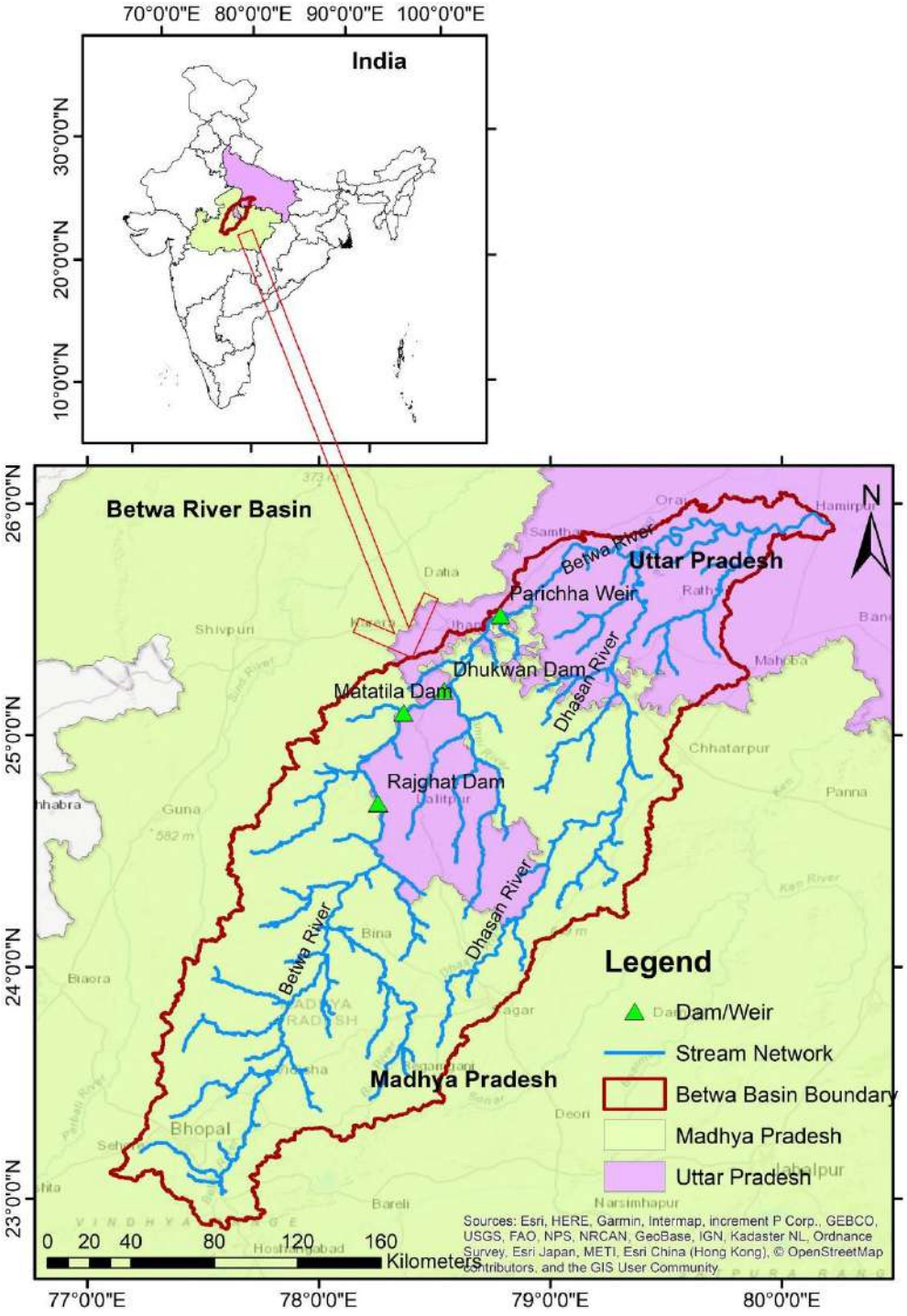

Figure 2.1: Location map of the Betwa river basin

2.1.4 Soils of the Betwa Basin

The Betwa basin falls under the Vindhyan sandstone, Deccan traps and Bundelkhand granite. Soils survey of the region has been carried out by the National Bureau of Soil Survey and Land Use Planning (NBSS&LUP), Nagpur. Based on the NBSS&LUP data, soils of the basin are classified as clay, silty clay, clay loam and sandy loam.

2.1.5 Water Resources Development in the Betwa Basin

(a) Rivers

The rivers in the Bundelkhand swell up with floods during rainy season, and dry up in the summers. Even in the Betwa River which is the mightiest river of the region, discharge remains only a few cusecs during the summer months. Therefore, if the water is not stored during the monsoon months, famine like conditions is created during the remaining part of the year. Even drinking water becomes scarce. Due to this, about 600 small tanks were constructed in this area during the time of Chandelas. Some of these tanks are still useful.

(b) Storage Reservoirs

Parichha dam was originally constructed in 1881 for 48.14 MCM and Betwa canal opened for irrigation in 1886. The storage fell short of the demand and, therefore, 6 ft high shutters were provided on the spillway weir in the year 1898 to increase its capacity to 68.64 MCM which was further increased. The supplies did not prove sufficient for the demand, and were augmented by another dam on Betwa River at Dhukwan in 1909. Originally the storage capacity of Dhukwan dam was 68.93 MCM after installation of 8 ft high shutters on the crest. The present storage capacities of these dams are 78.75 MCM and 64.67 MCM for Parichha and Dhukwan respectively. In order to supplement Dhukwan reservoir Matatila (a major project) was constructed in UP in 1958.

In the present condition the role of Parricha weir and Dhukwan dam is more or less limited to diversion only whereas Rajghat and Matatila dam in the basin acts as major storage reservoirs for irrigation, power production, municipal and industrial water supply and to feed water through water through Dhukwan and Parricha weir for irrigation releases.

2.1.6 Ken-Betwa Link Project

The Ken-Betwa link project is first Inter Basin Water Transfer project proposed under National Perspective Plan prepared by Ministry of Water Resources, Government of India. The schematic diagram of the proposed Ken-Betwa Link Project is presented in Figure 2.2.

This project envisages diversion of surplus waters of the Ken basin to water deficit Betwa basin. The water is proposed to be diverted from Ken basin, after considering in-basin demands and downstream commitments earmarked for providing irrigation in MP and UP. This link canal will provide irrigation to water short areas of Upper Betwa basin of MP by way of substitution. A dam is also proposed on River Ken at Daudhan 2.5 km upstream of existing Gangau weir. The 75% dependable yield of Ken up to Daudhan site has been assessed as 6188 Mm^3. The net water availability at dam site after accounting for all the upstream requirements including regeneration is 4364 Mm^3. The surplus water for diversion at Daudhan is 1074 MCM, out of which, 591 MCM is transferred to the Betwa river upstream of Parichha weir.

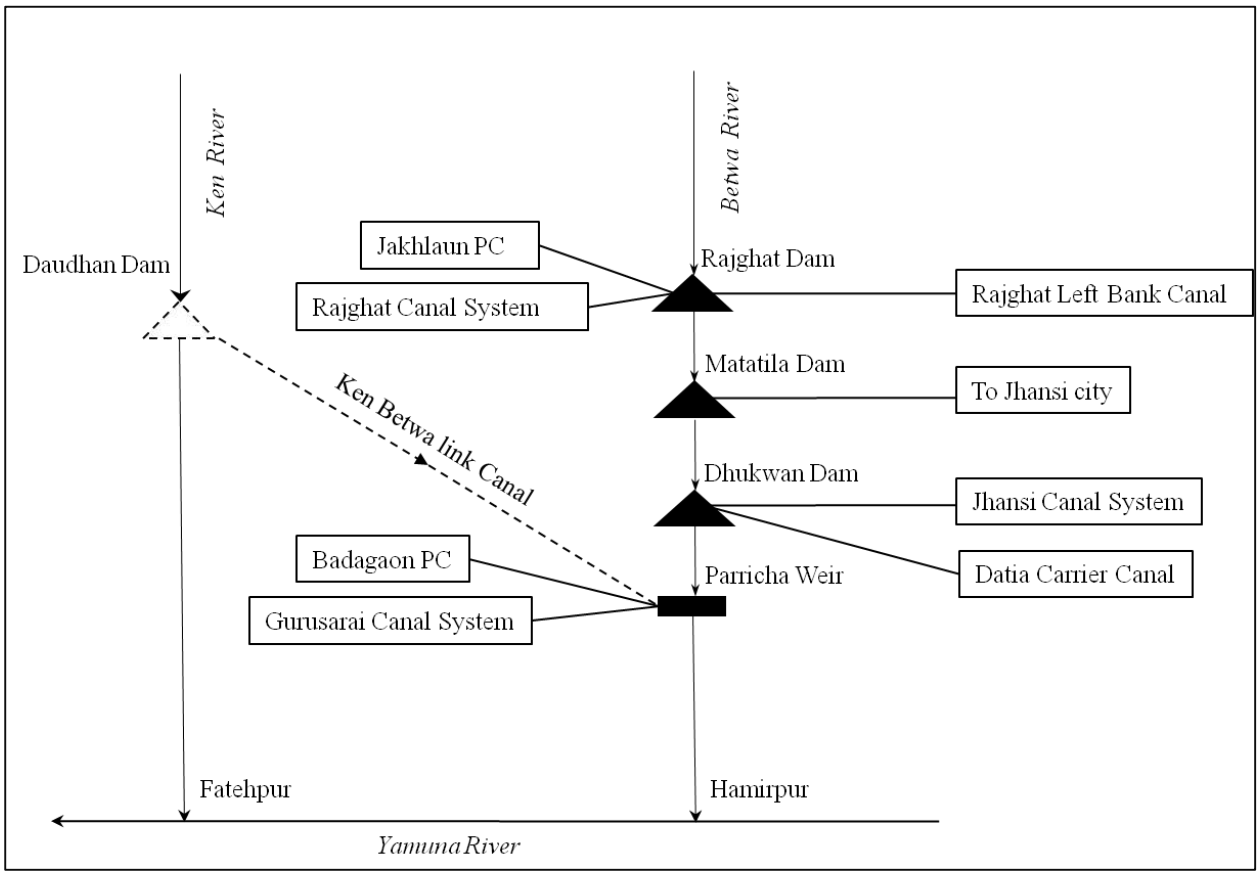

Figure 2.2: Schematic diagram of the proposed Ken Betwa Link Project

2.2 DATA ACQUISITION

2.2.1 Digital Elevation Model (DEM)

Freely available Advanced Space-borne Thermal Emission and Reflection (ASTER) Global Digital Elevation Model (GDEM) data of 30 m resolution (Figure 2.3) was obtained from the ASTER GDEM website (http://gdem.ersdac.jspacesystems.or.jp/index.jsp).

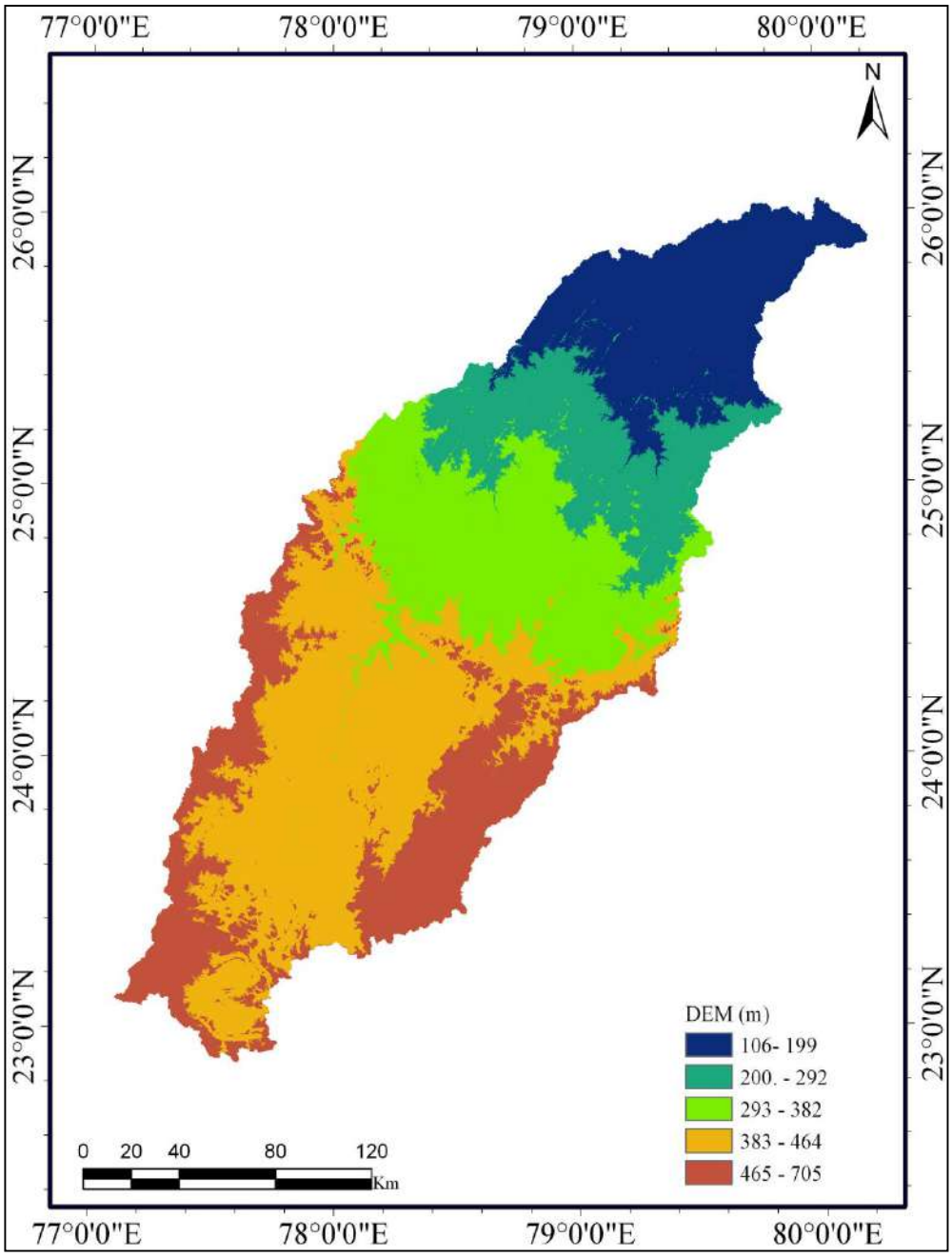

Figure 2.3: Digital Elevation Model (DEM) of Betwa basin

2.2.2 Satellite data

Satellite imageries of post-monsoon season were obtained to estimate spatio-temporal land use/land cover changes for the Betwa basin. Freely available Landsat satellite imagery data was downloaded from United States Geological Survey (USGS) Global Visualization Viewer (GloVis) website (http://glovis.usgs.gov/) for the years 1972 (Landsat-1 Multispectral Scanner (MSS)), 1976 (Landsat-2 MSS), 1991 (Landsat-5 Thematic Mapper (TM)), 2001 (Landsat-7 Enhanced Thematic Mapper Plus (ETM+)), 2010 (Landsat-5 Thematic Mapper), and 2013 (Landsat-8 Operational Land Imager (OLI)) as shown in Table 2.1.

Also, Indian Remote-sensing Satellite (IRS-P6) imagery of a Linear Imaging and Self Scanning (LISS-III) sensor was procured from National Remote Sensing Centre (NRSC) Hyderabad for the year 2007 and Resourcesat-2 LISS IV of the year 2015.

Table 2.1: Details of satellite data used for the study of Betwa basin

Year	Data type	Path - Row	Date of image	Spatial resolution (m)
1972	Landsat-1 MSS	155 - 42, 43, 44	30/Nov/1972	60
		156 - 42, 43, 44	1/Dec/1972	
1976	Landsat-2 MSS	155 - 42, 43, 44	13/Oct/1976	60
		156 - 42, 43, 44	1/Nov/1976	
1991	Landsat-5 TM	144 - 42, 43, 44	13/Dec/1991	30
		145 - 42	3/Feb/1991	
		145 - 43, 44	22/Feb/1991	
2001	Landsat-7 ETM+	144 - 42, 43, 44	27/Sep/2001	30
		144 - 44	11/Sep/2001	
		145 - 42, 43, 44	18/Sep/2001	
2007	IRS-P6 LISS III	97 - 54, 55, 56	27/Nov/2007	23.5
		98 - 53, 54, 55, 56	8/Nov/2007	
		99 - 53, 54, 55, 56	13/Nov/2007	
		100 - 53	18/Nov/2007	
2010	Landsat-5 TM	144 - 42, 43, 44	3/Feb/2011	30
		145 - 42, 43, 44	10/Feb/2011	
2013	Landsat-8 OLI	144 - 42, 43, 44	22/Oct/2013	30
		145 - 42, 43, 44	29/Oct/2013	
2015	Resourcesat-2 LISS IV	97-54_B, 97-54_D, 97-55_B, 97-56_B	04/Oct/2015	5.8
		97-55_D	21/Nov/2015	
		98-53_D, 98-54_B, 98-55_B, 98-54_D	09/Oct/2015	
		98-54_A, 98-54_C, 98-55_A, 98-55_C, 98-56_A	15/Sep/2015	
		98-55_D	26/Nov/2015	

		99-53_C, 99-54_A, 99-54_C, 99-55_A 99-55_C	25/Dec/2015	
		99-53_D	01/Dec/2015	
		99-54_B, 99-54_D	14/Oct/2015	

2.2.3 Climate data

Recent daily climate data of rainfall, temperature (maximum, minimum, dry bulb, wet bulb, dew point), evaporation, pressure (station level, mean sea level), wind (direction and speed), moisture (relative humidity, vapour pressure), sunshine (total hours of bright sunshine)) was procured from the India Meteorological Department (IMD) Pune for the years 2001-2013.

2.2.4 CMIP5 GCM data

Climate scenarios used were from the NASA Earth Exchange Global Daily Downscaled Projections (NEX-GDDP) dataset (Thrasher et al., 2012), prepared by the Climate Analytics Group and NASA Ames Research Center using the NASA Earth Exchange, and distributed by the NASA Center for Climate Simulation (NCCS). In this study, the Max-Planck-Institute-Earth System Model-Medium Resolution (MPI-ESM-MR) model has been used. From the recent literature, the MPI-ESM-MR model the best performing CMIP5 GCM data was selected for the present study based on the model performance and climate change impacts study over Indian regions (Sharmila et al., 2015; Guo et al., 2016; Roxy et la., 2016; Das et al., 2018). Therefore, we have selected the CMIP5 datasets of the MPI-ESM-MR model. Future daily precipitation, minimum temperature and maximum temperature data of the MPI-ESM-MR model was obtained from the Centre for Climate Change Research, Indian Institute of Tropical Meteorology, Pune (http://cccr.tropmet.res.in/).

The MPI-ESM-MR dataset at 0.25°×0.25° spatial resolution was used to prepare climate change data for the SWAT model simulation. In this study, RCP 8.5 scenario has been used because it is considered as the worst-case scenario and represents the most severe conditions, meaning that this scenario would be the upper limit for potential climate change impacts and responses. Firstly, future data was extracted for each station, and then bias-corrected by quantile mapping method (Thrasher et al., 2012). Based on empirical relationships between observed and simulated discharge and sediment datasets, the downscaled and bias-corrected MPI-ESM-MR dataset were further divided into five different scenarios. One historical scenario was used as baseline 1986 (1986-2005), and

four future scenarios i.e. scenario 2020 (2020-2039), scenario 2040 (2040-2059), scenario 2060 (2060-2079) and scenario 2080 (2080-2099) were used for future climate change impact studies.

2.2.5 Discharge & Sediment data

Daily discharge of Basoda, Garrauli, Mohana and Shahijina gauging stations (Figure 2.4) was procured from the Yamuna Basin Organization (YBO), Central Water Commission (CWC), New Delhi. Sediment data was available only for Garrauli and Shahijina stations only.

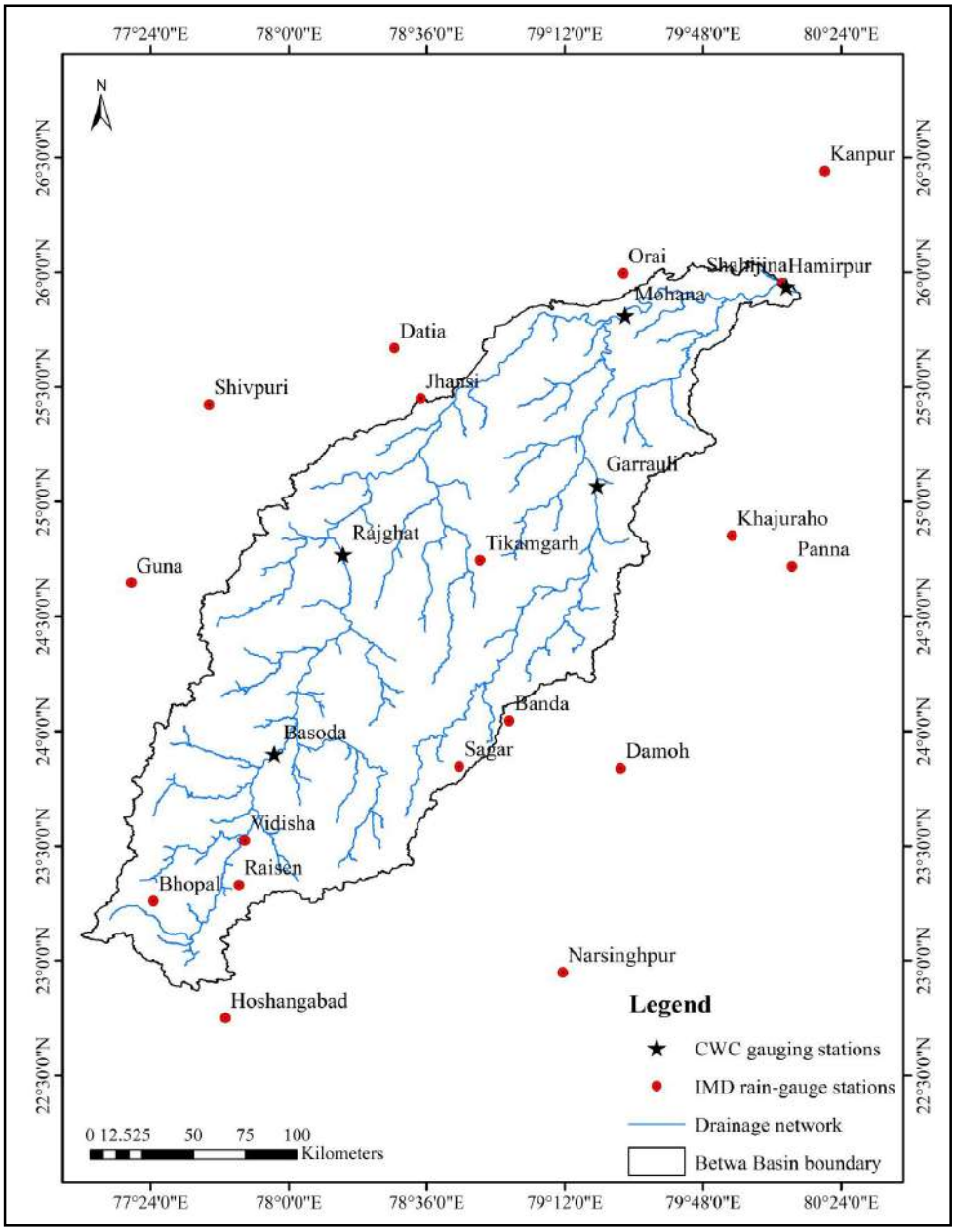

Figure 2.4: Gauging stations of IMD and CWC in the Betwa basin

2.2.6 Soil data

Soil data in the form of maps (Madhya Pradesh: 9 sheets and Uttar Pradesh: 6 sheets), soil series booklet and bulletin format were procured from the National Bureau of Soil Survey & Land Use Planning (NBSS & LUP) Nagpur. These soil maps were scanned first and then geometrically rectified to generate thematic layer for the Betwa basin (Figure 2.5). Based on the NBSS&LUP data, soils of the basin are classified as clay (40.89 %), Silty Clay (15.89 %), Clay Loam (16.25 %) and Sandy loam (26.97 %) with an area of 17782.8 km^2, 6912.15 km^2, 7068.75 km^2, 11727.6 km^2 respectively (Figure 3.2). The physical and chemical properties of the soils are taken from Soils of MP (NBSS, 1996) and are presented in Table 2.2.

Table 2.2: Physical and chemical properties of the soils in Betwa basin

Soil Properties	**Clay**				**Clay Loam**		**Sandy Loam**		**Silty Clay**					
	Layer 1	**Layer 2**	**Layer 3**	**Layer 4**	**Layer 1**	**Layer 2**	**Layer 1**	**Layer 2**	**Layer 1**	**Layer 2**	**Layer 3**	**Layer 4**	**Layer 5**	**Layer 6**
Depth (mm)	140	280	280	600	60	80	100	120	110	290	300	350	300	350
MBD (Mg/m^3)	1.32	1.43	1.48	1.53	1.47	1.71	1.70	1.70	1.35	1.43	1.53	1.57	1.58	1.58
OCC (%)	0.70	0.60	0.50	0.20	1.65	1.56	1.42	1.36	0.48	0.36	0.30	0.24	0.24	0.21
Clay (%)	52.10	55.30	64.20	65.10	34.20	37.1	14.20	35.70	46.40	48.60	49.80	48.30	43.1	38.50
Silt (%)	32.30	27.30	27.10	19.80	38.10	22.40	22.30	20.70	43.20	44.80	45.80	44.30	50.20	48.10
Sand (%)	15.60	17.00	8.70	15.10	22.70	40.50	63.50	43.60	10.40	6.66	4.20	7.40	6.70	13.40
SHC (mm/hr)	11.45	11.45	11.45	5.60	29.50	29.50	10.40	10.40	12.10	12.10	12.10	4.30	4.30	4.30
USLE K factor	0.20	0.17	0.12	0.12	0.28	0.26	0.55	0.30	0.25	0.24	0.23	0.24	0.29	0.34
MBD = Moist Bulk Density, OCC = Organic Carbon Content, SHC = Soil Hydraulic Conductivity														

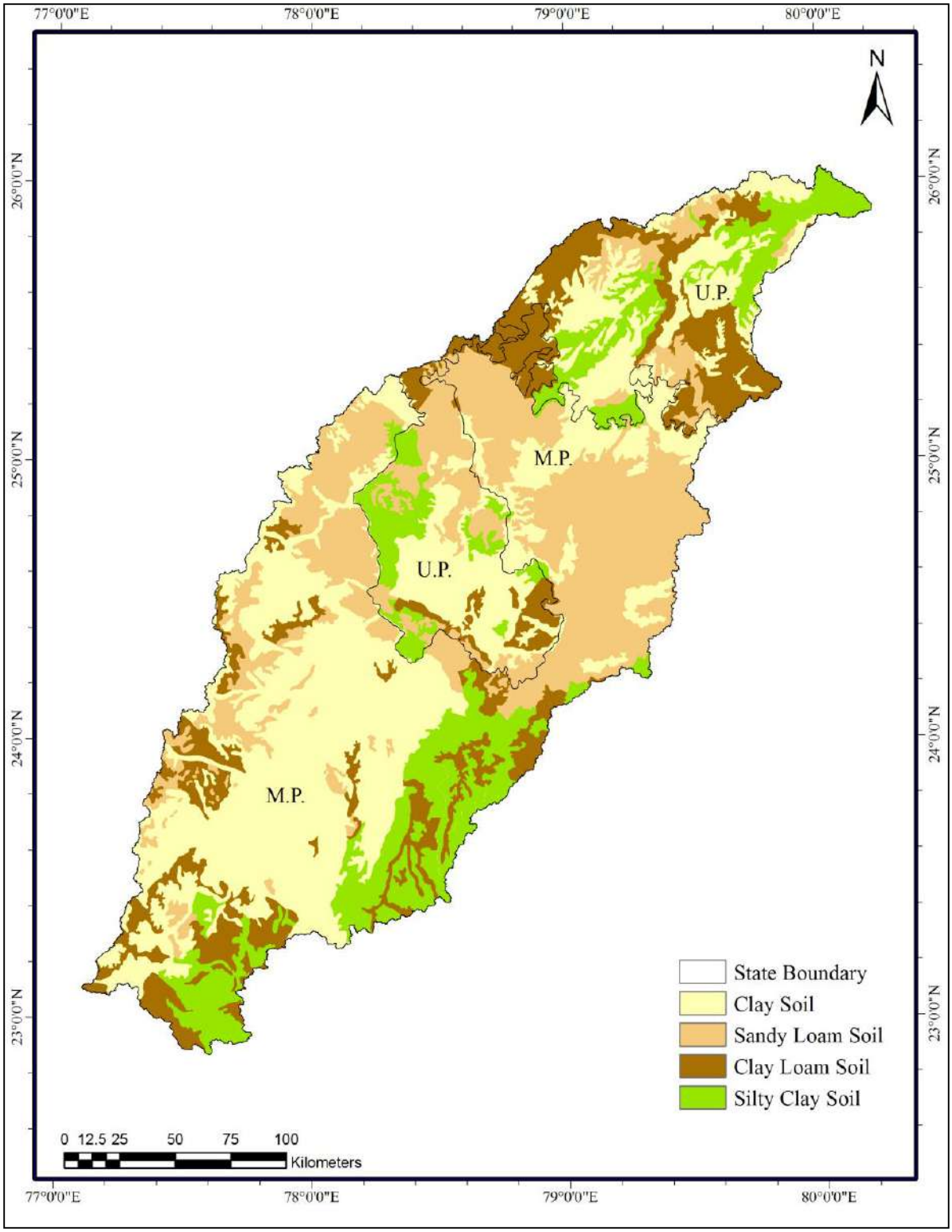

Figure 2.5: Soil map of the Betwa basin

CHAPTER 3

LONG TERM CHANGES IN CLIMATIC VARIABLES

3.1 BACKGROUND

Change and/or fluctuations in the hydrological cycle directly affect the availability and quantity of fresh water, which is a major environmental issue of the 21st century (Pal and Al-Tabbaa 2011). The rise in the mean annual temperature is mainly contributed by the rise of temperature during winter seasons (Kumar et al. 2011).

From the statistical point of view, variability of the climatic parameters can be identified by the presence of statistical evidence of persistence, cycles, trend and other non-random components. The spatial distribution and magnitude of rainfall, temperature, PET and aridity index trends would be highly relevant and useful from an agricultural and water management point of view (Subash et al. 2011).

Aridity index serve to identify, and locate regions that suffer from a deficit of available water. UNEP has proposed an index of aridity, defined as, AI = P/PET, where PET is the potential evapotranspiration and P is the precipitation (UNEP, 1992). Bannayan et al. (2010) employed Aridity index (UNEP, 1992) to quantify the drought occurrence as a numerical indicator of the degree of dryness of the climate at each study location. The trends in reference evapotranspiration and aridity index (AI) are of great significance for managing agricultural water resources (Huo at al., 2013).

Detection of trends in long-term series of climatic data is of paramount importance and is of practical significance. Studies on climate change are also important because of our need to understand the impact that man is having on the 'natural' world (WCDMP-45 2000). There are many approaches that can be used to detect trends and other forms of non-stationarity in climatic and hydrological data. In deciding which approach to take, it is necessary to be aware of which test procedures are valid (i.e. the data meets the required test assumptions) and which procedures are most useful.

A basin or its sub-basin is hydrologically a self-contained area and a natural unit for water resources planning (National Water Policy 2012). Basin level studies on climatic trends are limited (Rao

1993; Mirza et al. 1998; Ranade et al. 2008; Mishra et al. 2009), emphasizing urgent need to understand the climatic variations based on long-term historic data.

In this study, the variability of the climatic parameters of the Betwa basin is studied by employing the tests for trend. Betwa basin, though historically important, continues to be highly underdeveloped due to lack of irrigation facilities, the main stay of the people in the area, being agriculture. The area is prone to famines and droughts, particularly the upper and middle regions. There is a need to study the variability of the climatic parameters of the basin. Therefore, this study aims at analyzing trend of various climatic parameters such as rainfall, minimum, maximum and average temperature, potential evapotranspiration (PET) and aridity index (P/PET) of the Betwa basin. This study could serve as base line for preparation of a sustainable water resources development and management plan for the Betwa basin.

3.2 Methodology for Detection of Trend

There are two different approaches to analyze trend: (a) parametric method and (b) non-parametric method. Parametric testing procedures are widely used in classical statistics. In parametric testing, it is necessary to assume an underlying distribution for the data (often the normal distribution), and to make assumptions that data observations are independent of one another. For many climatic and hydrological series, these assumptions are not appropriate. Firstly, hydrological series rarely have a normal distribution. Secondly, there is often temporal dependence in hydrological series. If parametric techniques are to be used, it may be necessary to (a) transform data so that its distribution is nearly normal and (b) restrict analyses to annual series, for which independence assumptions are acceptable, rather than using the more detailed monthly, daily or hourly flow series. In non-parametric and distribution-free methods, fewer assumptions about the data need to be made. With such methods it is not necessary to assume a distribution. However, many of these methods still rely on assumptions of independence. The most popular non-parametric test for detecting trend in the time series is Mann–Kendall (MK) test (Mann 1945; Kendall 1975).

In this study, MK test was chosen over other trend detection tests due to the following advantage:

(1) The MK test is a rank based non-parametric test. When compared to parametric tests like Student t-test, the MK test has a higher power for non-normally distributed data which are frequently encountered in hydrological records (Onoz and Bayazit 2003; Yue and Pilon 2004).

(2) In comparison to other non-parametric tests, like Spearman's rho test, the capability of the MK test is similar to the point where both give indistinguishable results in practice (Yue et al. 2002).

(3) MK test does not require the assumption of normality or the assumption of homogeneity of variance.

(4) It compares medians rather than means and, as a result, if the data have one or two outliers, their influence is negated.

(5) In MK test, prior transformations are not required, even when approximate normality could be achieved.

(6) The greater power is achieved for the skewed distributions in the MK test

The MK test has been extensively used to determine trends in similar hydrologic studies previously (Hirsch et al. 1982; Hirsch and Slack 1984; Lettenmaier et al. 1994; Lins and Slack 1999; Douglas et al. 2000; Burn and Hag Elnur 2002; Burn et al. 2004; Zhang et al. 2005; Aziz and Burn 2006; Chen et al. 2007; Tabari et al. 2011; Tabari and Aghajanloo 2012).

However, the MK tests are based on the assumption that the time series is serially independent in nature, i.e. uncorrelated. In many cases, the observed climatic data are either serially correlated or auto-correlated. This autocorrelation leads to misinterpretation of the results. Therefore, in this study, modified MK test is used. MK test determines the change in the central value or median with time keeping the spreading of the distribution to be constant.

The variability of the climatic parameters can be identified by the presence of statistical evidence of persistence, cycles, trend and other non-random components. The spatial distribution and magnitude of rainfall and temperature trends would be highly relevant and useful from agriculture and water management point of view (Subash et al. 2011). The variability of the climatic parameters of the Betwa basin was investigated by employing the tests for trend.

In this study the following methodology has been adopted (Figure3.1):

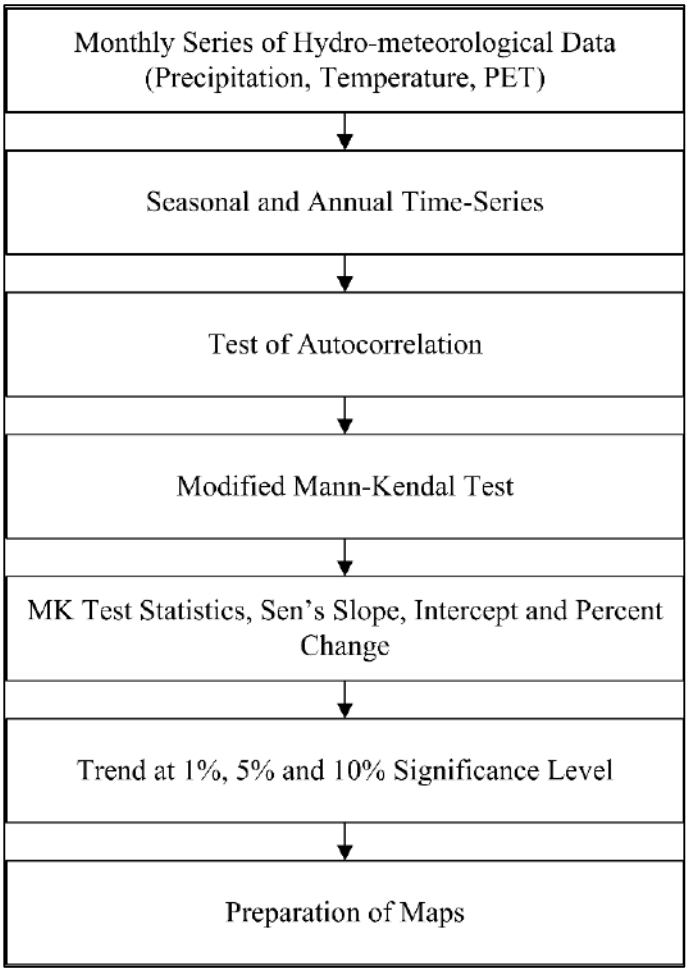

Figure 3.1: Flowchart of the methodology

3.2.1 Original MK test

The MK test, also called Kendall's tau test due to Mann (1945) and Kendall (1975), is the rank based non-parametric test for assessing the significance of a trend, and has been widely used in hydrological trend detection studies. It is based on the test statistic S as defined below:

$$S = \sum_{i=1}^{n-1} \sum_{j=i+1}^{n} \text{sign}(x_j - x_i) \quad \ldots(1)$$

where,

$$\text{sign}(x_j - x_i) = \begin{cases} 1 \ldots\ldots\ldots \text{if } (x_j - x_i) > 0 \\ 0 \ldots\ldots\ldots \text{if } (x_j - x_i) = 0 \\ -1 \ldots\ldots\ldots \text{if } (x_j - x_i) < 0 \end{cases} \quad \ldots(2)$$

$x_1, x_2, \ldots x_n$ represent n data points, where x_j represents the data point at time j.

A very high positive value of S is an indicator of an increasing trend, and a very low negative value indicates a decreasing trend.

It has been documented that when n ≥10, the statistic S is approximately normally distributed with the mean E (S) = 0, and its variance is

$$\mathrm{VAR(S)} = \frac{n(n-1)(2n+5)-\sum_{i=1}^{m} t_i(t_i-1)(2t_i+5)}{18} \quad \ldots(3)$$

Where n is the number of data points, m is the number of tied groups (a tied group is a set of sample data having the same value), and t_i is the number of data points in the i_{th} group.

The standardized test statistic Z is computed as follows:

$$Z = \begin{cases} \frac{S-1}{\sqrt{VAR(S)}} \text{ if } S > 0 \\ 0 \text{ if } S = 0 \\ \frac{S+1}{\sqrt{VAR\,(S)}} \text{ if } S < 0 \end{cases} \quad \ldots(4)$$

The null hypothesis, H_0, meaning that no significant trend is present, is accepted if the test statistic Z is not statistically significant, i.e., $-Z_{\alpha/2} < Z < Z_{\alpha/2}$, where $Z_{\alpha/2}$ is the standard normal deviate. In this study, three different significance levels, i.e., 1 %, 5 % and 10 % were considered.

3.2.2 Modified MK test

It is well known that the original Mann–Kendall test does not consider the autocorrelation factor that may be present in the time series being analyzed. The presence of an autocorrelation in a dataset may lead to inaccurate interpretations of the MK test. A time series exhibiting positive autocorrelation causes the effective sample size to be less than the actual sample size, thereby increasing the variance and the possibility of detecting significant trends when in fact, there are no trends (Hamed and Rao, 1998 and Ehsanzadeh et al., 2011).

Hirsch and Slack (1984) proposed a modified MK test that accounts for seasonality and serial dependence factors. This method separates observations into different seasons, which eliminates the dependence problem between seasons (Hirsch et al., 1982 and Hirsch and Slack, 1984). This method, however, is not as powerful when there is long-term persistence (with autoregressive parameter > 0.6) or when there are less than 5 years worth of monthly data (Hirsch and Slack, 1984).

Hamed and Rao (1998) proposed another modified version of the MK test in order to deal with the issue of autocorrelation structures for all lags in a dataset, because autocorrelations may still exist past the first lag. Since the presence of autocorrelation underestimates the variance if calculated using the MK formula for uncorrelated data, the method by Hamed and Rao (1998) modifies the calculation for the variance of the MK test statistics when the data are serially correlated by using an empirical formula. When applied to autocorrelated data with a large sample size, this test was found to be practically as powerful as when the original MK test is applied to independent data (Hamed and Rao, 1998).

Since using the original MK for autocorrelated data underestimates the variance of the data, the calculation of the variance of the test statistics S is altered and given by an empirical formula (equation 5) (Hamed and Rao, 1998):

$$V^*(S) = VAR(S) \cdot \frac{n}{n_s^*} = \frac{n\,(n-1)\,(2n+5) - \sum_{i=1}^{m} t_i(t_i-1)(2t_i+5)}{18} \cdot \frac{n}{n_s^*} \quad \ldots(5)$$

Where n/n_s^* represents a correction due to the autocorrelation in the data. The best approximation to the theoretical values was obtained by using n/n_s^* given by the empirical expression:

$$\frac{n}{n_s^*} = 1 + \frac{2}{n\,(n-1)(n-2)} \times \sum_{i=1}^{n-1}(n-i)(n-i-1)(n-i-2)\rho_s\,(i) \quad \ldots(6)$$

$$\rho_s(i) = \frac{\frac{1}{n-i}\sum_{t=i+1}^{n}(x_t-\bar{x})(x_{t-i}-\bar{x})}{\sqrt{\frac{1}{n}\sum_{t=1}^{n}(x_t-\bar{x})}\sqrt{\frac{1}{n}\sum_{t=i+1}^{n}(x_{t-i}-\bar{x})}} \quad \ldots(7)$$

Autocorrelation, which were significant in the time series at the 95% confidence level, was used for evaluating the modified variance of S using equations (5) and (6).

3.2.3 Slope and Intercept

Slope of the lines fit to the time series of climatic data provide a picture of changes that have occurred at any location over an extended period. The slope of the data set can be estimated using the Thiel–Sen Approach. This equation is used instead of a linear regression because it limits the influence that the outliers have on the slope (Hirsch et al., 1982).

$$\beta = Median\left[\frac{X_j - X_i}{j-i}\right] \;\; For\ all\ i < j \quad \ldots(8)$$

where, X_j and X_i are data values at times j and i (i > j), respectively.

$$Intercept = Median\,[X(i) - \beta \times i] \quad For\ i = 1\ to\ n \qquad \ldots(9)$$

3.2.4 Relative change (RC)

To compute the relative change of different climatic parameters, the following equation was used (Some'e et al. 2012)

$$RC = \frac{n*\beta}{|x|} * 100 \qquad \ldots(10)$$

where, n is the length of trend period (years), β is the magnitude of the trend slope of the time series which is determined by Sen's median estimator, and |x| is the absolute average value of the time series.

3.3 METEOROLOGICAL DATA

To study the temporal changes in climate of the Betwa basin trend analysis of the following climatic variables were carried out: (1) seasonal and annual rainfall, (2) seasonal and annual minimum, maximum and average temperature, (3) seasonal and annual (PET) and (4) seasonal and annual aridity index. Stations wise monthly data were obtained from the IMD and website of India Water Portal (www.indiawaterportal.org) for 113 years (1901–2013) except three stations (Sehore, Lalitpur and Mahoba) for which availability of data was only upto 2002. A list of stations is presented in Table 3.1. In this study, monthly data was used to compute annual and seasonal time series, and aridity index was computed using rainfall and PET data. To make the seasonal and annual time series, monthly temperature values in a season during a particular year were averaged whereas rainfall and PET values were added.

Table 3.1: List of stations and availability of the climatological data

Sl. No.	Station	Availability of data	Sl. No.	Station	Availability of data
1	Banda	1901-2013	12	Orai	1901-2013
2	Bhopal		13	Panna	
3	Damoh		14	Raisen	
4	Datia		15	Sagar	
5	Guna		16	Shivpuri	
6	Hamirpur		17	Tikamgarh	
7	Hoshangabad		18	Vidisha	
8	Jhansi		19	Lalitpur	1901-2002
9	Kanpur		20	Mahoba	
10	Khajuraho		21	Sehore	
11	Narsinghpur				

For seasonal analysis, the water year (i.e., 1 June to 31 May) was classified into four seasons which are pre-monsoon season (March to May), monsoon season (June to September), post-monsoon season (October and November) and winter season (December to February). In order to analyze the trend and statistical summary over the whole basin as an entity, Theissen polygon (Figure 3.2) method has been applied. The method used to convert point data at different stations into an average value over a catchment. This method is considered superior to the arithmetical averaging method since some weightage is assigned to each station.

3.4 RESULTS AND DISCUSSIONS

One of the most principal requirements of the studies about climatic and hydrological data is to analyze and discover historical changes in the climatic parameters (Some'e et al. 2012). Therefore, to study the temporal changes in climate of the Betwa basin, trend analysis of the climatic variables was carried out. In order to have a clearer idea about the magnitude to trend; the trend analysis was carried out at three different significance levels: 1 %, 5 % and 10 %. Only the significant results of slope, intercept and relative change are reported. First, station wise analysis was carried out for every parameter and spatial map of the trend were prepared. In Table 3.2, parameters depicting significant increasing or decreasing trend have been summarized. Further, average value of every parameter over the basin was estimated using Theissen polygon method and trend analysis was carried out on seasonal and annual basis. The Mann-Kendall Z value, slope, intercept and relative change for every parameter has been presented in Table 3.3. From the table it can be observed that maximum, minimum and average temperature depicted the most signification trend with high value of slope.

Table 3.2: Significant increasing or decreasing trend at various stations

Station	Parameters* depicting significant increasing or decreasing trend in different seasons at the station							
	Pre-monsoon		Monsoon		Post-monsoon	Winter	Annual	
	Increasing	Decreasing	Increasing	Decreasing	Increasing	Increasing	Increasing	Decreasing
Banda	P, MinT, MaxT, AvgT, AI			AI	MinT, MaxT, AvgT	MinT, MaxT, AvgT	MinT, MaxT, AvgT	P, AI
Bhopal	MinT, MaxT, AvgT				MinT, MaxT, AvgT	P, MinT, MaxT, AvgT, AI	MinT, MaxT, AvgT	
Damoh	MinT, MaxT, AvgT				MinT, MaxT, AvgT	MinT, MaxT, AvgT	MinT, MaxT, AvgT	
Datia	P, MinT, MaxT, AvgT, AI			MinT	MinT, MaxT, AvgT	MinT, MaxT, AvgT	MinT, MaxT, AvgT	
Guna	MinT, MaxT, AvgT				MinT, MaxT, AvgT	MinT, MaxT, AvgT	MinT, MaxT, AvgT, PET	
Hamirpur	P, MinT, MaxT, AvgT, AI				MinT, MaxT, AvgT	MinT, MaxT, AvgT	MinT, MaxT, AvgT	AI
Hoshangabad	MinT, MaxT, AvgT		MinT, MaxT, AvgT		MinT, MaxT, AvgT	MinT, MaxT, AvgT	MinT, MaxT, AvgT, PET	
Jhansi	P, MinT, MaxT, AvgT, AI				MinT, MaxT, AvgT	MinT, MaxT, AvgT	MinT, MaxT, AvgT	
Kanpur	P, MinT, AvgT, AI			MinT, MaxT, AvgT	MinT, MaxT, AvgT	MinT, MaxT, AvgT	MinT,	
Khajuraho	MinT, MaxT, AvgT, AI				MinT, MaxT, AvgT	MinT, MaxT, AvgT	MinT, MaxT, AvgT	
Lalitpur	MinT, MaxT, AvgT				MinT, MaxT, AvgT	MinT, MaxT, AvgT, PET	MinT, MaxT, AvgT	
Mahoba	P, MinT, MaxT, AvgT, AI			MaxT,	MinT, MaxT, AvgT	MinT, MaxT, AvgT, PET	MinT, MaxT, AvgT	
Narsinghpur	MinT, MaxT, AvgT		AvgT	AI	MinT, MaxT, AvgT	MinT, MaxT, AvgT	MinT, MaxT, AvgT	
Orai	P, MinT, MaxT, AvgT, AI			MinT, MaxT, AvgT	MinT, MaxT, AvgT	MinT, MaxT, AvgT	MinT, MaxT, AvgT	
Panna	MaxT, AvgT				MinT, MaxT, AvgT	MinT, MaxT, AvgT	MinT, MaxT, AvgT	
Raisen	MinT, MaxT, AvgT				MinT, MaxT, AvgT	MinT, MaxT, AvgT	MinT, MaxT, AvgT, PET	
Sagar	P, MinT, MaxT, AvgT, AI				MinT, MaxT, AvgT	MinT, MaxT, AvgT	MinT, MaxT, AvgT	
Sehore	MinT, MaxT, AvgT, PET				MinT, MaxT, AvgT	MinT, MaxT, AvgT, PET	MinT, MaxT, AvgT, PET	
Shivpuri	P, MinT, MaxT, AvgT, AI			MinT	MinT, MaxT, AvgT	MinT, MaxT, AvgT	MinT, MaxT, AvgT	
Tikamgarh	P, MinT, MaxT, AvgT, AI				MinT, MaxT, AvgT	MinT, MaxT, AvgT	MinT, MaxT, AvgT	
Vidisha	P, MinT, MaxT, AvgT, AI				MinT, MaxT, AvgT	MinT, MaxT, AvgT	MinT, MaxT, AvgT, PET	

*RF = Rainfall, MinT = Minimum Temperature, MaxT = Maximum Temperature, AvgT = Average Temperature, PET = Potential Evapotranspiration, AI = Aridity Index

Table 3.3: Mann-Kendall Z value, slope, relative change and intercept considering average value of parameter over the basin

Parameter	Pre-monsoon				Monsoon				Post-monsoon				Winter				Annual			
	ZMK	Slope	RC	Intercept	ZMK	Slope	RC	Intercept	ZMK	Slope	RC	Intercept	ZMK	Slope	RC	Intercept	ZMK	Slope	RC	Intercept
Rainfall	1.70	0.065	36.92	13.6	-0.73	-0.610	-7.18	1002.3	0.30	0.018	4.91	25.6	0.14	0.009	3.18	29.1	-0.59	-0.519	-5.57	1069.9
MinT	3.34	0.007	3.66	21.33	0.01	0.000	0.02	24.24	4.31	0.015	10.30	15.22	13.72	0.010	11.40	9.57	4.22	0.007	4.12	18.38
MaxT	4.07	0.008	2.49	37.28	0.60	0.001	0.42	33.04	4.33	0.015	5.41	29.88	5.47	0.008	3.45	25.27	4.46	0.007	2.43	31.69
AvgT	3.77	0.008	3.03	29.30	0.50	0.001	0.36	28.59	4.48	0.015	7.10	22.51	12.80	0.009	5.68	17.43	4.93	0.007	2.98	25.03
PET	0.59	0.013	0.20	750.6	-1.11	-0.030	-0.45	758.9	0.18	0.003	0.09	387.1	3.51	0.038	0.88	489.3	0.43	0.035	0.16	2385.4
AI	2.12	0.000	39.84	0.02	-1.28	-0.002	-15.81	1.37	0.36	0.000	5.36	0.07	0.34	0.000	8.54	0.06	-0.65	0	-6.56	0.45

3.4.1 Annual and seasonal rainfall

Autocorrelation and trend were analyzed for 21 rainfall stations. Monthly rainfall data was considered for this analysis. The Mann-Kendall Z value and significance level of the trend have been presented in Appendix B-1. The values of slope, intercept, and relative change of the stations having significant trend has been presented in Appendix B-2. From results it can be observed that, during pre-monsoon season, seven stations (Banda, Datia, Jhansi, Mahoba, Shivpuri, Tikamgarh and Vidisha) exhibited increasing trend at 90% confidence level, two stations (Hamirpur and Sagar) exhibited increasing trend at 95% confidence level and two stations (Kanpur and Orai) exhibited increasing trend at 99% confidence level with slope values ranging from 0.05 to 0.09. However, no significant trend has been observed during monsoon and post-monsoon season. Increasing trend at 90% confidence level has been observed during winter season in Bhopal station with slope value of 0.05. In case of yearly rainfall, only Banda station exhibited decreasing trend at 90% confidence level with slope of magnitude -1.25. Figure 3.2 shows the spatial distribution of the percent significant trend of seasonal and yearly rainfall within the Betwa basin.

In order to analyze the trend of rainfall over the basin, average value of rainfall was estimated from station data using Theissen Polygon method. The statistical summary of the average rainfall over the basin between the period of 1901 to 2013 is given in Table 3.4. Annual average rainfall over the basin varies from minimum 642 mm to maximum 1718 mm with an average value and standard deviation of 1053 mm and 217 mm respectively. More than 90% of rainfall over the basin occurs during the monsoon season.

Table 3.4: Statistical summary of average rainfall over the basin

Statistic	**Rainfall (mm) during various seasons between 1901-2013**				
	Pre-monsoon	**Monsoon**	**Post-Monsoon**	**Winter**	**Annual**
Max	85.2	1557.0	278.1	110.2	1718.2
Min	0.1	575.8	0.0	0.3	642.3
Avg	19.9	959.8	41.2	32.6	1053.6
SD	13.8	208.9	43.4	21.6	217.5
CV	0.7	0.2	1.1	0.7	0.2

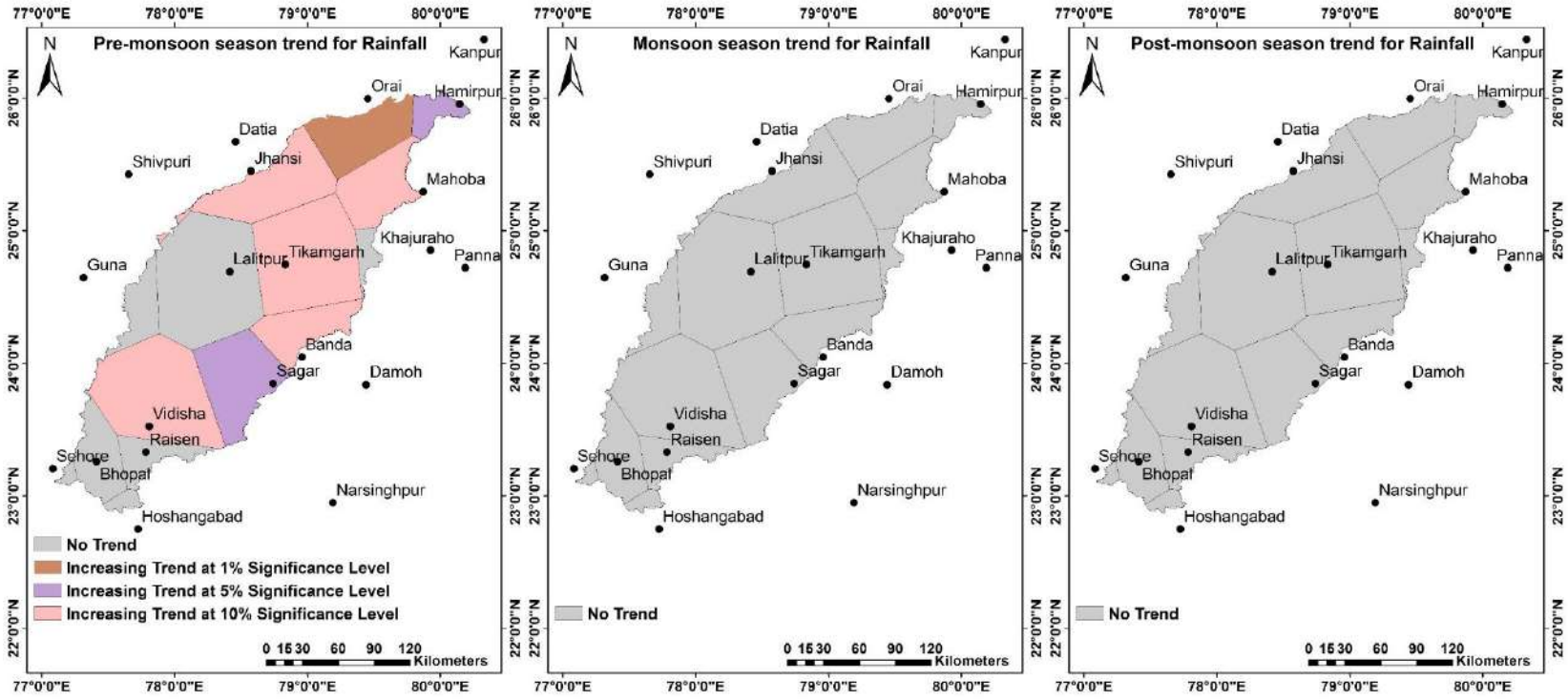

(a) (b) (c)

Figure 3.2 (a, b & c): Spatial distribution of the percentage significant trend of rainfall

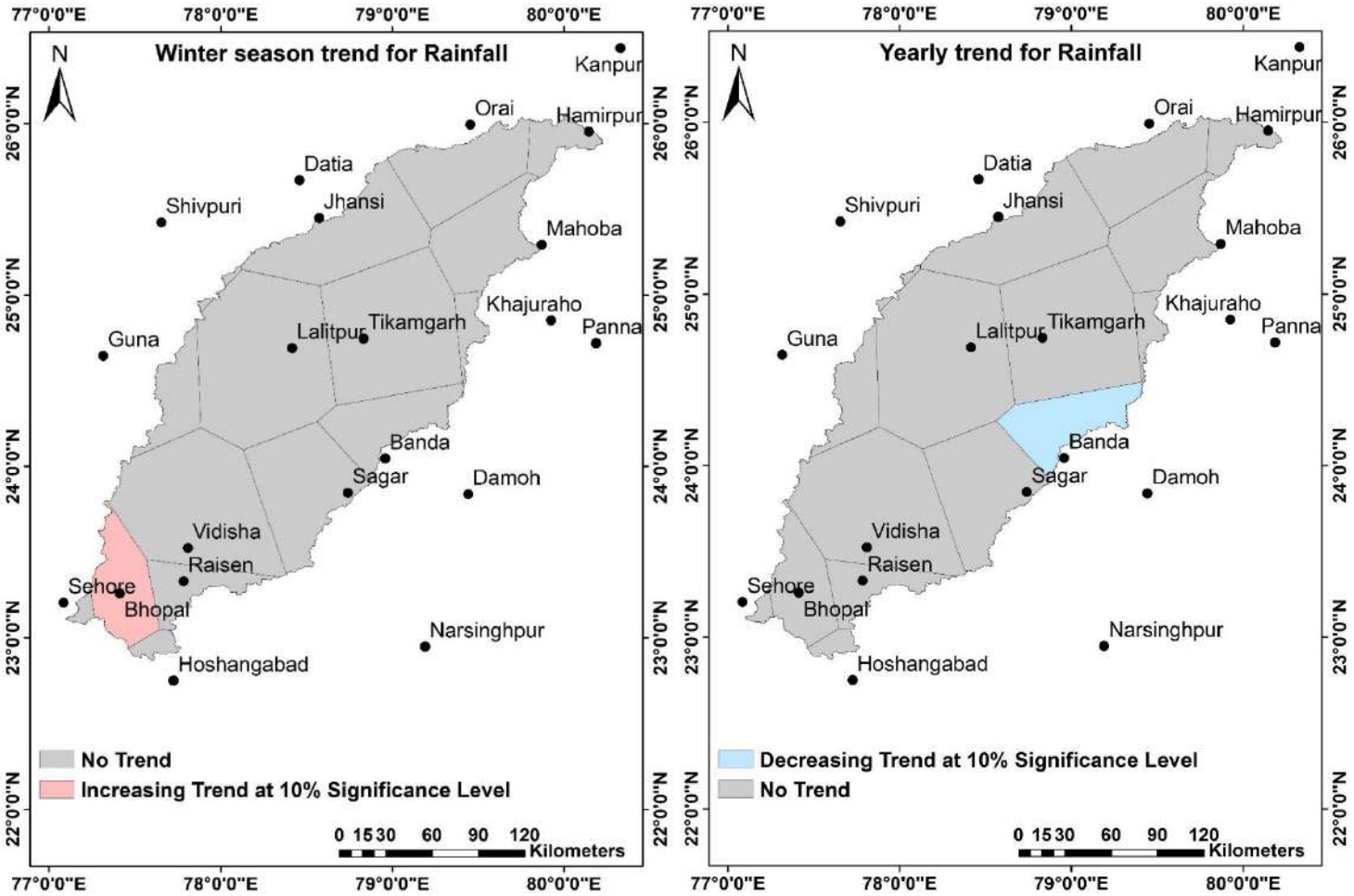

(d) (e)

Figure 3.2 (d & e): Spatial distribution of the percentage significant trend of rainfall

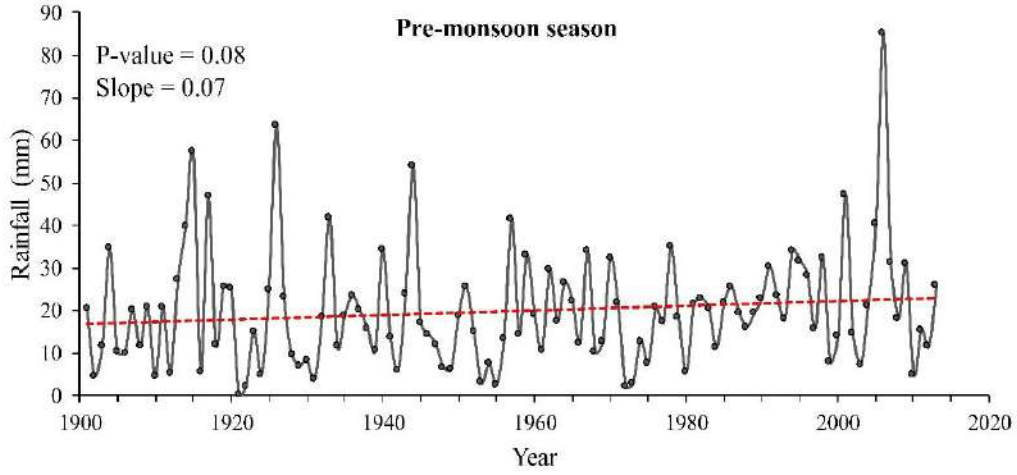

(a)

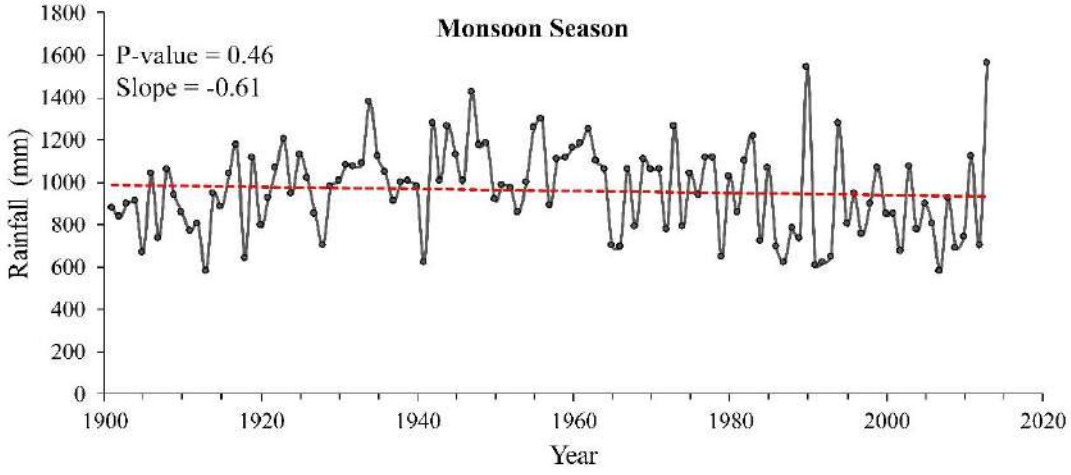

(b)

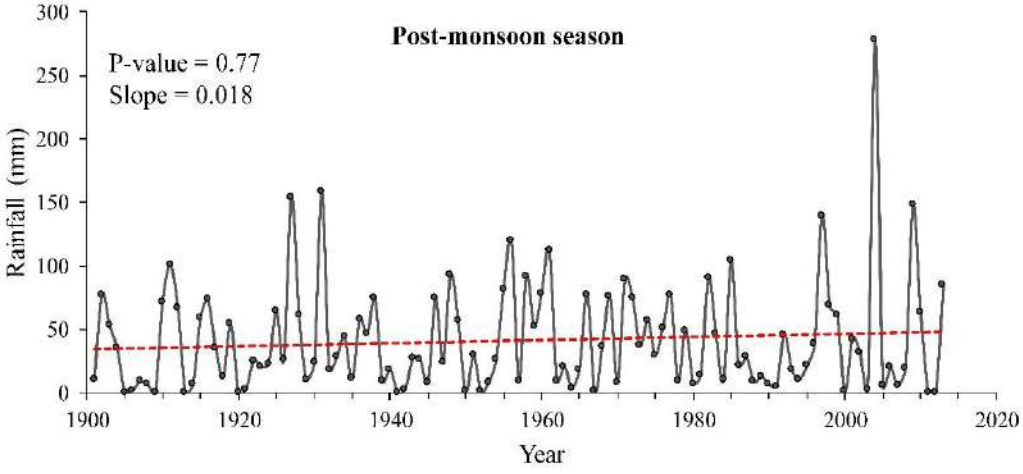

(c)

Figure 3.3 (a, b & c): Time series plot of average rainfall over Betwa basin during 1901-2013

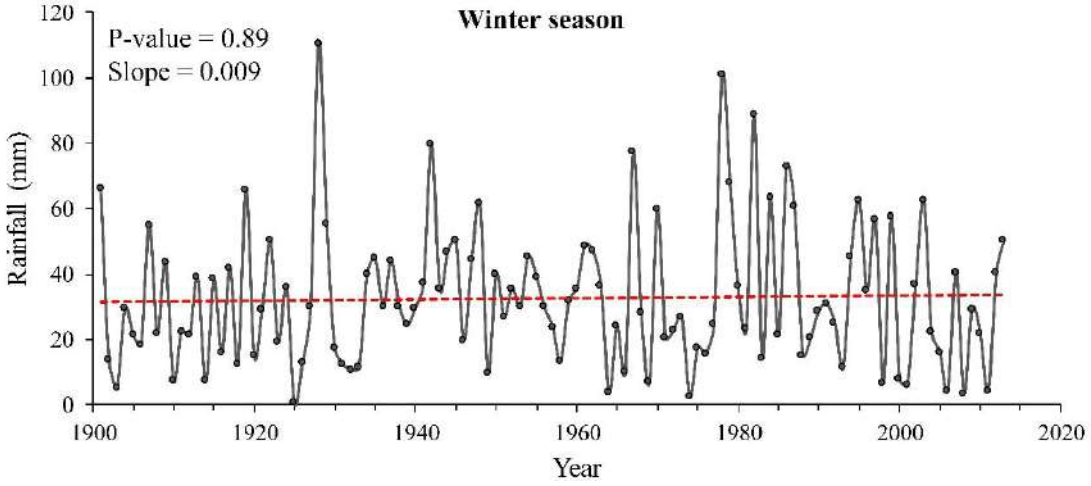

(d)

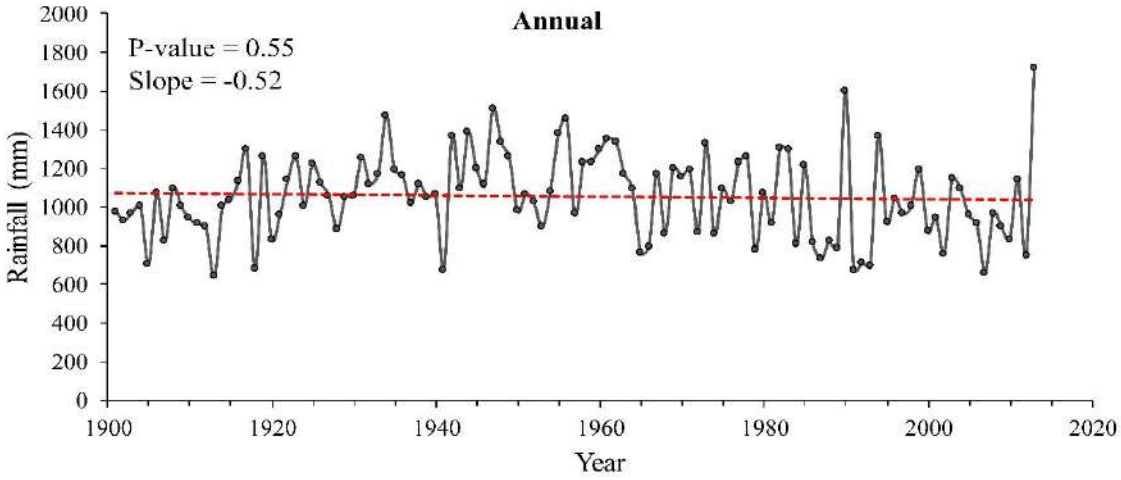

(e)

Figure 3.3 (d & e): Time series plot of average rainfall over Betwa basin during 1901-2013

From the time series plots (Figure 3.3) of rainfall, it can be observed that during Pre-monsoon season, there is a significant increasing trend with 90% confidence level, whereas slope value is very less. During monsoon season, the rainfall amount is declining specially after 1960 but the change is not significant. During post-monsoon season, winter season and total rainfall in a year over the basin depicted no significant trend.

3.4.2 Minimum temperature

Autocorrelation and trend were analyzed for 21 stations of seasonal and annual mean minimum temperature. Monthly mean minimum temperature data were considered for this analysis. The

Mann-Kendall Z values and significance level of the trend are presented in Appendix B-3. The values of slope, intercept, and relative change of the stations having significant trend are presented in Appendix B-4. Results shows that, during pre-monsoon season, five stations (Kanpur, Lalitpur, Mahoba, Raisen and Shivpuri) exhibited increasing trend at 90% confidence level, five stations (Damoh, Datia, Guna, Sehore and Tikamgarh) exhibited increasing trend at 95% confidence level and remaining stations except Panna exhibited increasing trend at 99% confidence level. During pre-monsoon season, slope of the increasing trend has been observed in range of 0.004 to 0.012. During monsoon season, four stations (Datia, Kanpur, Shivpuri and Orai) exhibited decreasing trend and only one station (Hoshangabad) exhibited increasing trend with slope ranging from 0.003 to 0.008. Strong increasing trend at 99% confidence level has been observed during post-monsoon in all the stations with slope value ranging from 0.009 to 0.019. However, increasing trend was observed at 95% confidence level at Damoh station and 99% confidence level in remaining stations during winter season with slope value ranging from 0.005 to 0.017. In case of yearly mean minimum temperature, five stations (Datia, Hamirpur, Jhansi, Panna and Shivpuri) exhibited increasing trend at 95% confidence level and remaining stations exhibited increasing trend at 99% confidence level with slope value ranging from 0.003 to 0.009. Figure 3.4 shows the spatial distribution of the percent significant trend of seasonal and yearly mean minimum temperature in the Betwa basin.

The statistical summary of mean minimum temperature over the basin between the period of 1901 to 2013 is given in Table 3.5. The mean minimum temperature during the year varies from minimum 17°C to maximum 20.2°C with an average value and standard deviation of 18.8°C and 0.5°C respectively. During the winter season, it varies from 8.3 to 12.1°C.

Table 3.5: Statistical summary of mean minimum temperature over the basin

Statistic	**Mean Minimum Temperature (°C) during various between during 1901-2013**				
	Pre-monsoon	**Monsoon**	**Post-Monsoon**	**Winter**	**Annual**
Max	24.0	25.8	18.8	12.1	20.2
Min	19.4	22.6	13.9	8.3	17.6
Avg	21.7	24.3	16.1	10.2	18.8
SD	0.9	0.6	1.0	0.7	0.5
CV	0.0	0.0	0.1	0.1	0.0

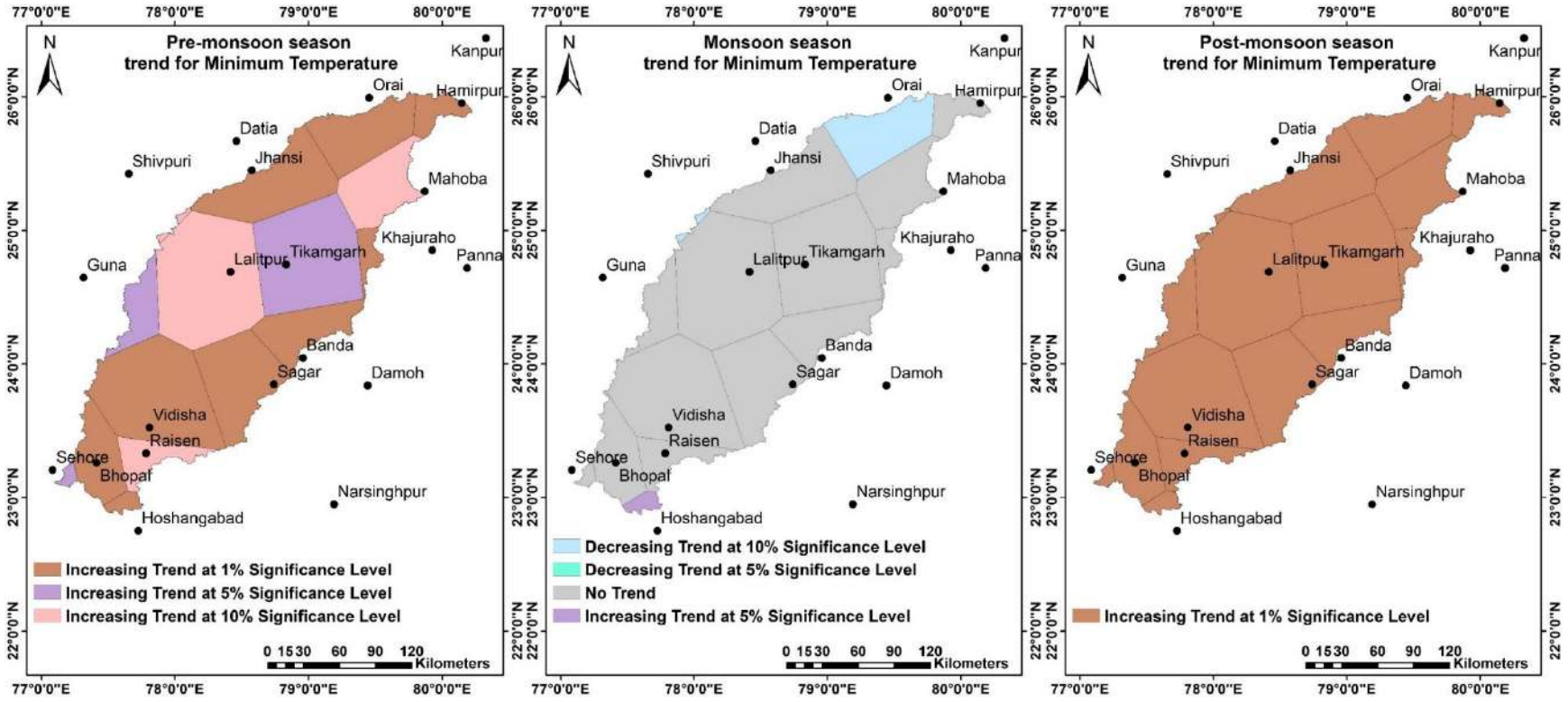

(a) (b) (c)

Figure 3.4 (a, b & c): Spatial distribution of the percentage significant trend of mean minimum temperature

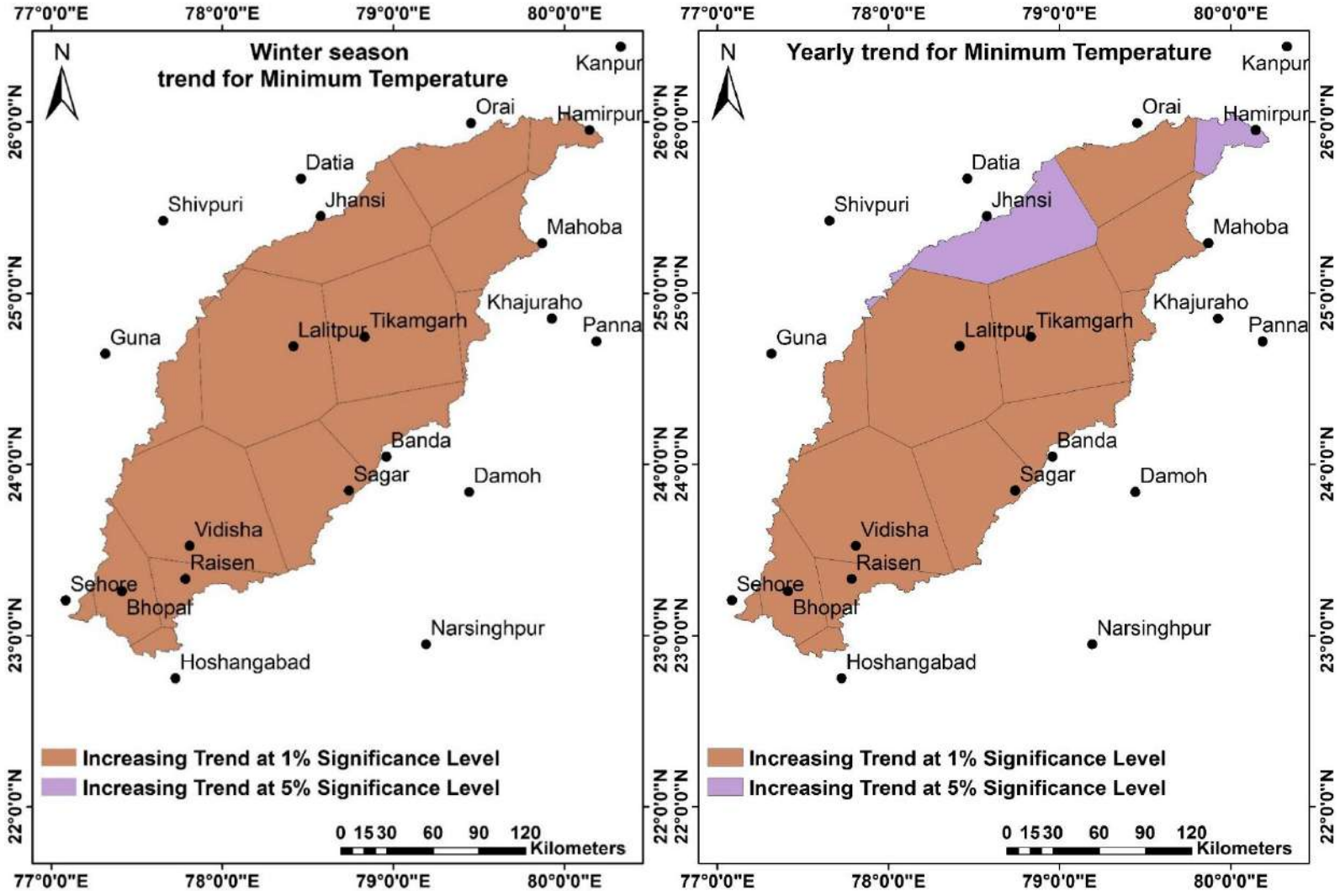

(d) (e)

Figure 3.4 (d & e): Spatial distribution of the percentage significant trend of mean minimum temperature

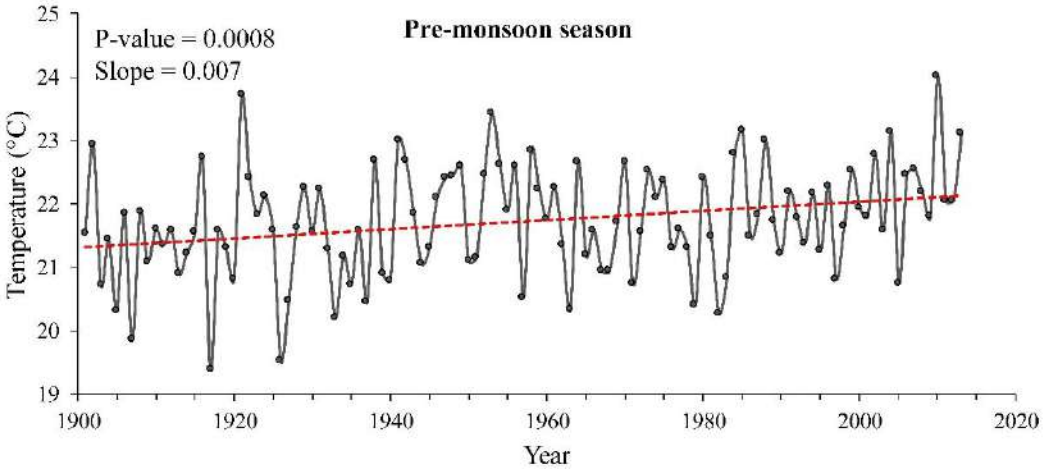

(a)

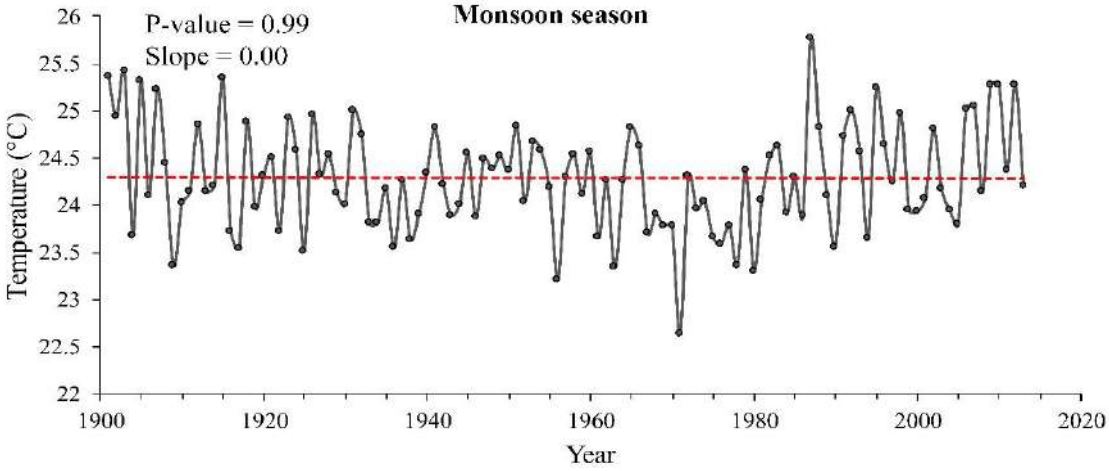

(b)

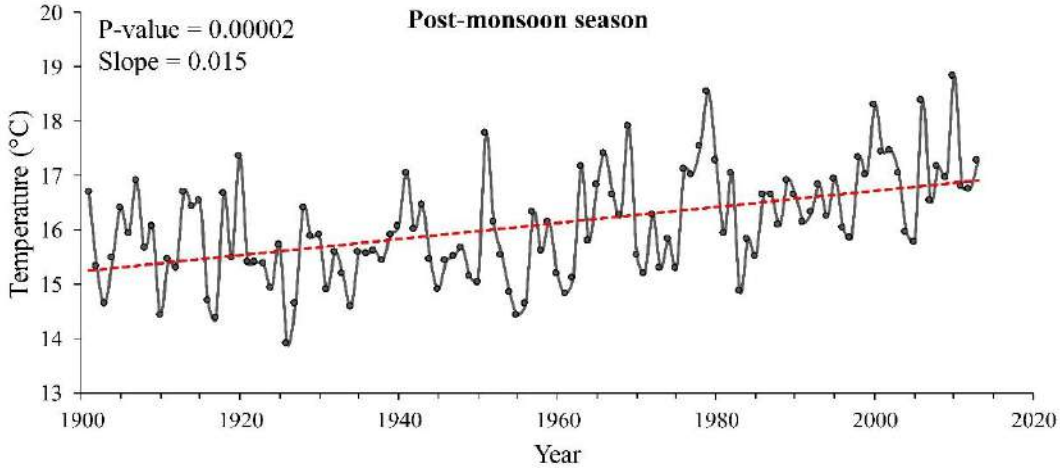

(c)

Figure 3.5 (a, b & c): Time series plot of mean minimum Temperature over Betwa basin

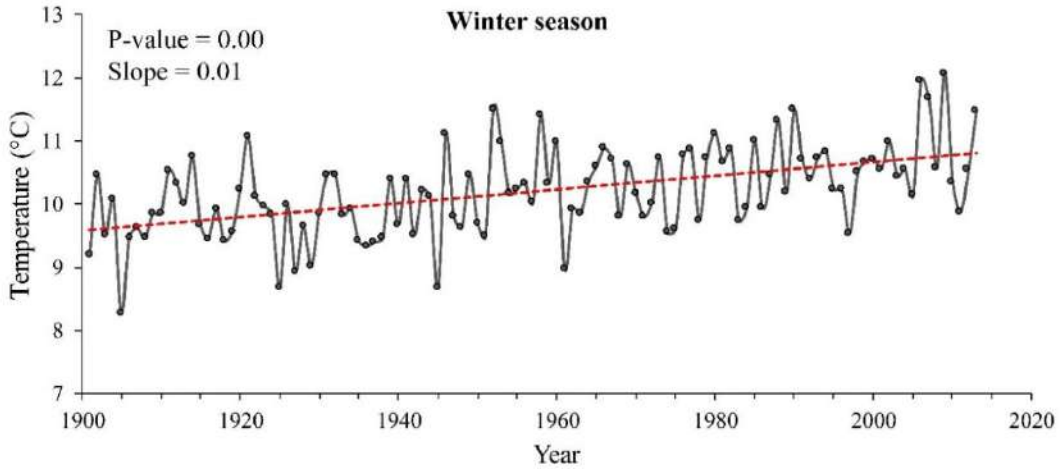

(d)

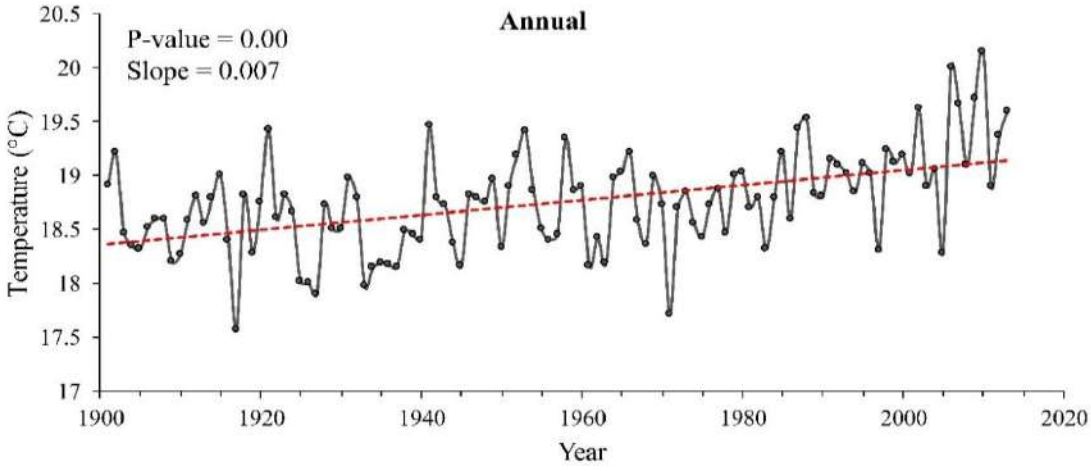

(e)

Figure 3.5 (d & e): Time series plot of mean minimum Temperature over Betwa basin

From the time series plots (Figure 3.5) of mean minimum temperature, it can be observed that during pre-monsoon, post-monsoon and winter season, there is a significant increasing trend with 99% confidence level. During the monsoon season, there is no significant trend. Highest rate of change (1.5°C/100 years) in the mean minimum temperature was observed during post monsoon season. While during the winter season rate of change is 1°C/100 years. The annual average minimum temperature is increasing with the rate of 0.7°C/100 years. This high rate of change may effect crops grown in the winter season.

3.4.3 Maximum temperature

Autocorrelation and trend were analyzed for 21 stations of seasonal and annual mean maximum temperature. Monthly mean maximum temperature data was considered for this analysis. The

Mann-Kendall Z value and significance level of the trend are presented in Appendix B-5. The values of slope, intercept, and relative change of the stations having significant trend are presented in Appendix B-6. From results it can be observed that, during pre-monsoon season, one station (Mahoba) exhibited increasing trend at 90% confidence level, four stations (Bhopal, Lalitpur, Raisen and Shivpuri) exhibited increasing trend at 95% confidence level and remaining stations except Kanpur exhibited increasing trend at 99% confidence level with slope value ranging from 0.004 to 0.012. During monsoon season, three stations (Kanpur, Mahoba and Orai) exhibited decreasing trend at 99%, 90% and 95% confidence level respectively and only one station (Hoshangabad) exhibited increasing trend at 95% confidence level. Increasing trend at 90% and 95% confidence level was observed in Kanpur and Shivpuri respectively during post-monsoon season. Further, remaining stations have shown increasing trend at 99% confidence level during post-monsoon season with slope value ranging from 0.006 to 0.019. Increasing trend was observed at 95% confidence level in two stations (Hamirpur and Kanpur) during winter season. Further, increasing trend at 99% confidence level was observed in remaining stations during winter season with the slope value ranging from 0.005 to 0.012. In case of yearly mean maximum temperature, two stations (Bhopal and Orai) exhibited increasing trend at 95% confidence level. However, remaining stations except Kanpur exhibited increasing trend at 99% confidence level with slope value ranging from 0.003 to 0.009. The spatial distribution of the percent significant trend of seasonal and yearly mean maximum temperature within the Betwa basin is presented in Figure 3.6.

The statistical summary of mean maximum temperature over the basin over the period of 1901 to 2013 is given in Table 3.6. The mean maximum temperature during the year varies from minimum 30.8°C to maximum 33.5°C with an average value and standard deviation of 32°C and 0.5°C respectively. During the pre-monsoon or summer season season, it varies from 35.4 to 40.7°C which is highest in all the seasons.

Table 3.6: Statistical summary of mean maximum temperature over the basin

Statistic	Mean Maximum Temperature (°C) during various seasons between 1901-2013				
	Pre-monsoon	Monsoon	Post-Monsoon	Winter	Annual
Max	40.7	35.0	32.9	28.7	33.5
Min	35.4	31.5	28.6	23.8	30.8
Avg	37.7	33.2	30.7	25.7	32.0
SD	0.9	0.7	1.0	0.7	0.5
CV	0.0	0.0	0.0	0.0	0.0

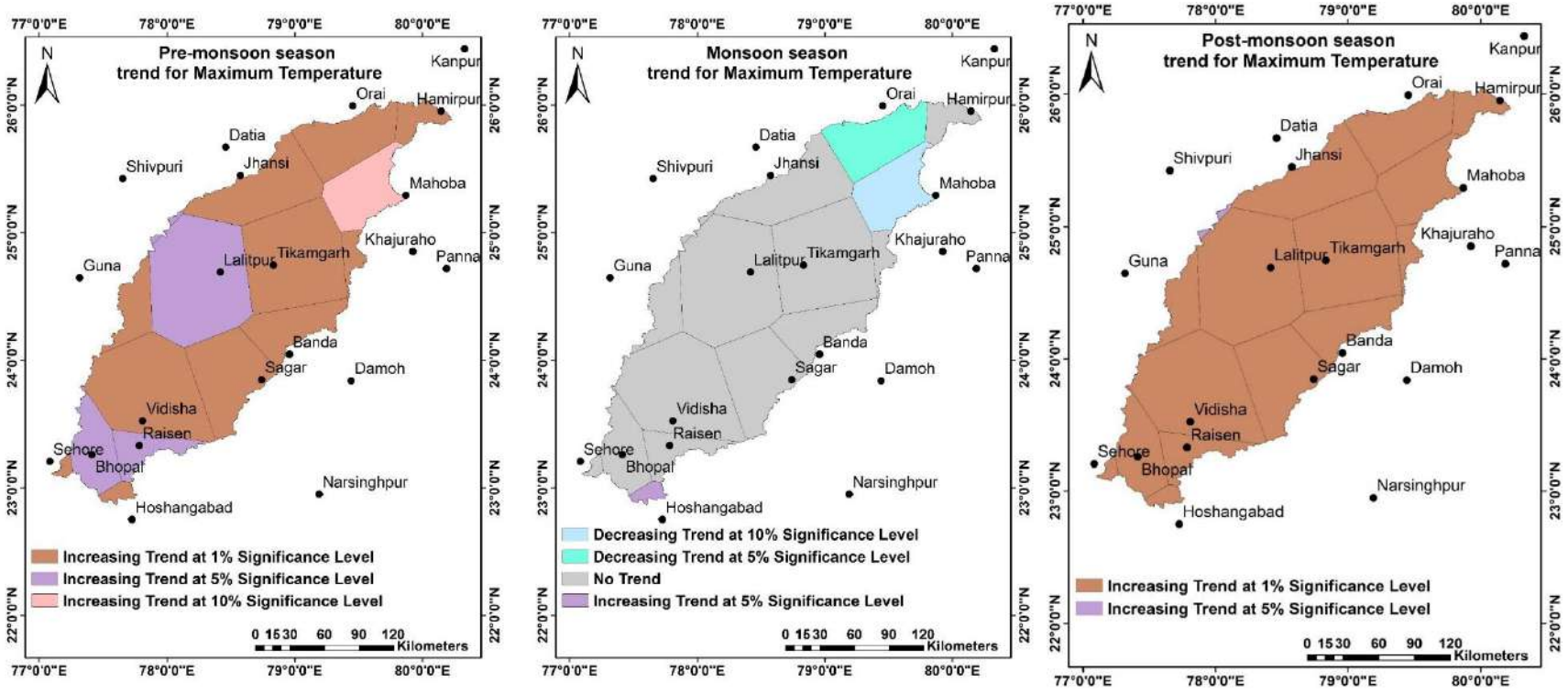

(a) (b) (c)

Figure 3.6 (a, b & c): Spatial distribution of the stations with percentage significant trend of mean maximum temperature

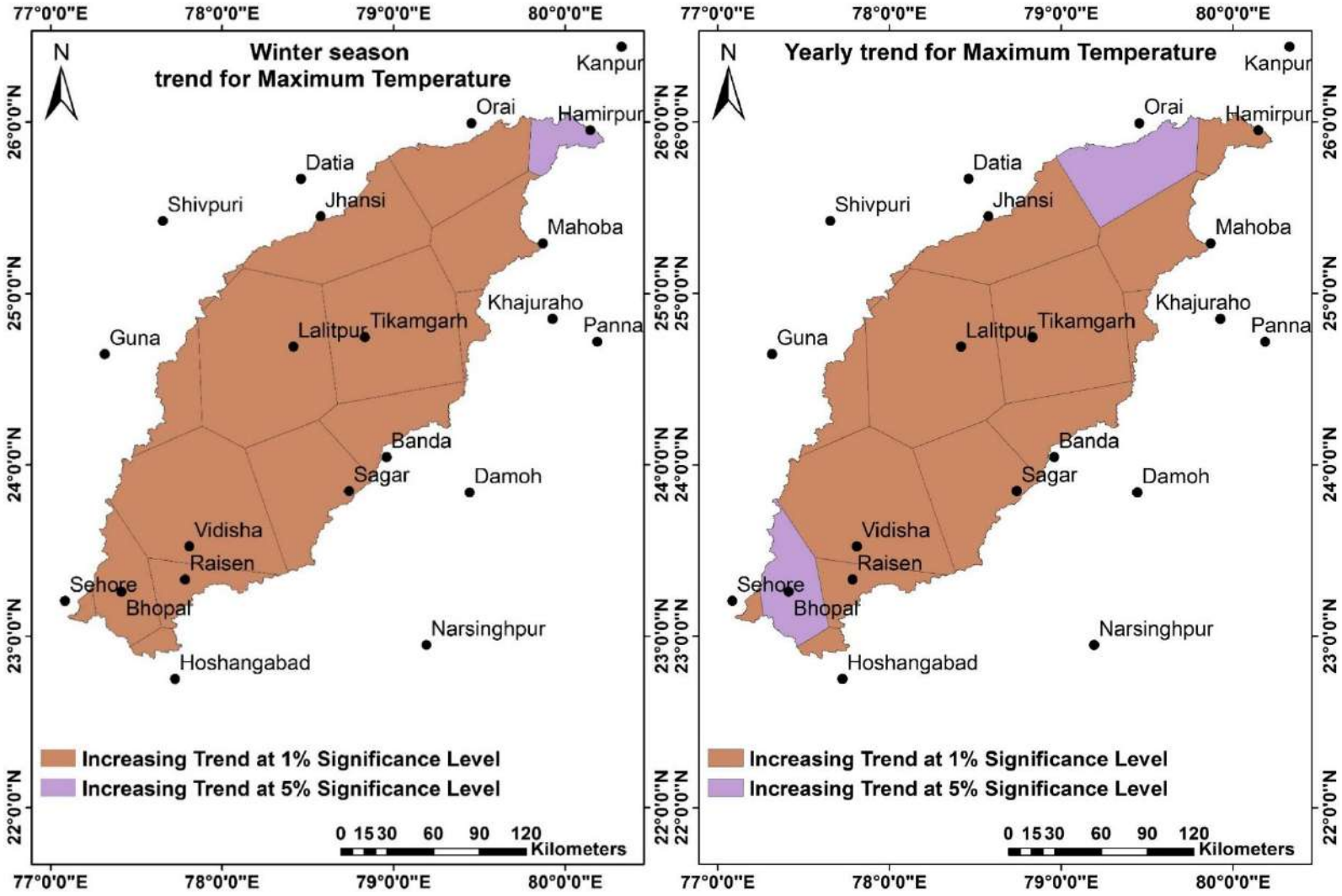

(d) (e)

Figure 3.6 (d & e): Spatial distribution of the stations with percentage significant trend of mean maximum temperature

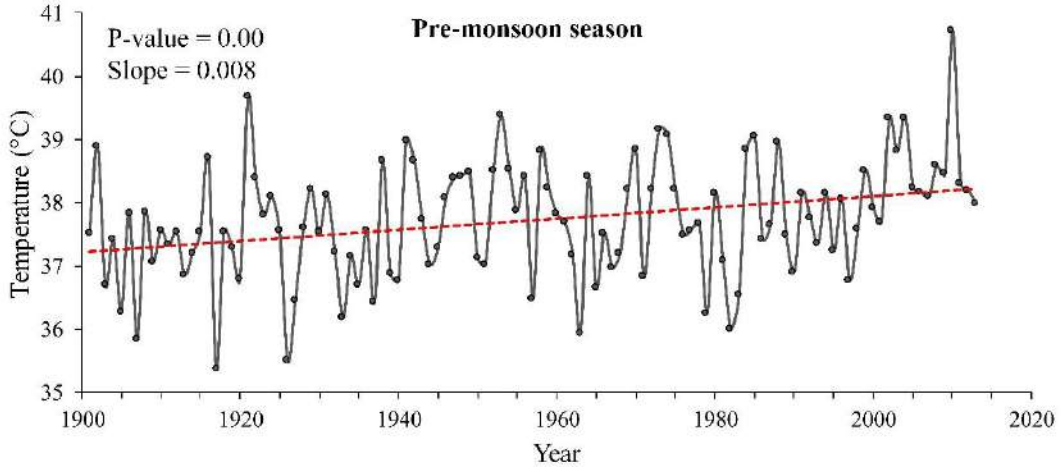

(a)

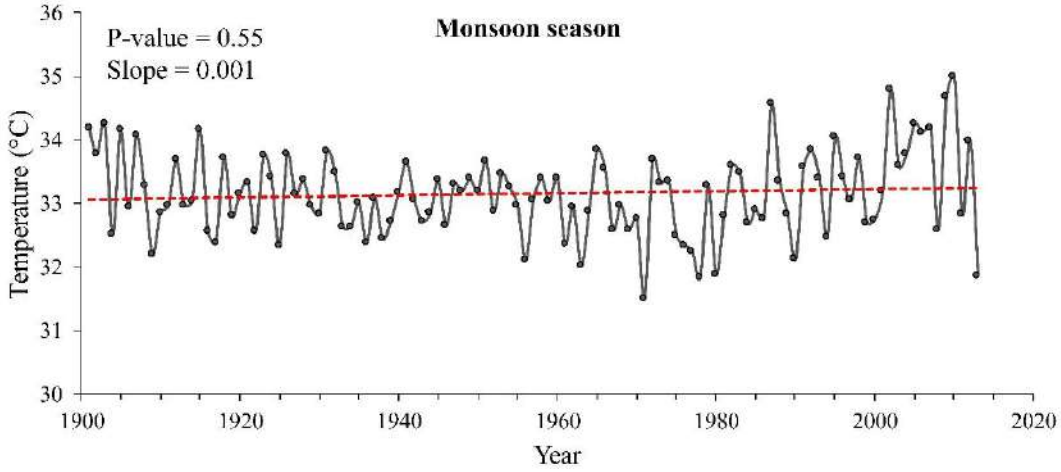

(b)

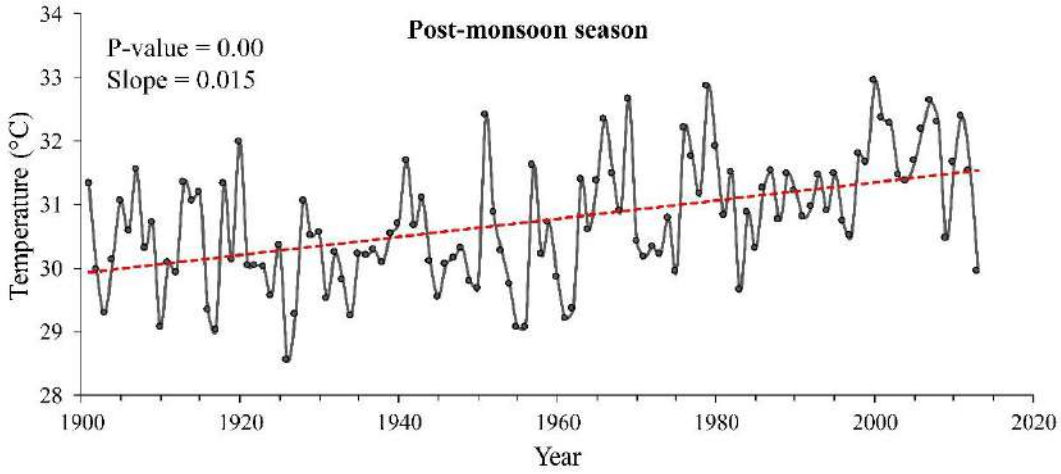

(c)

Figure 3.7 (a, b & c): Time series plots of mean maximum temperature over Betwa basin

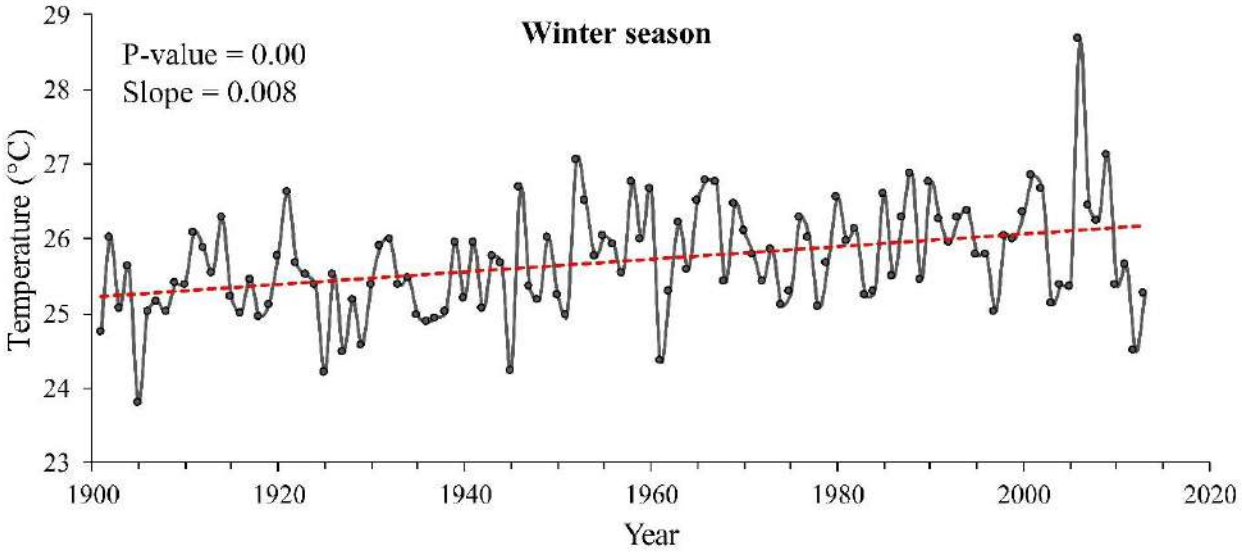

(d)

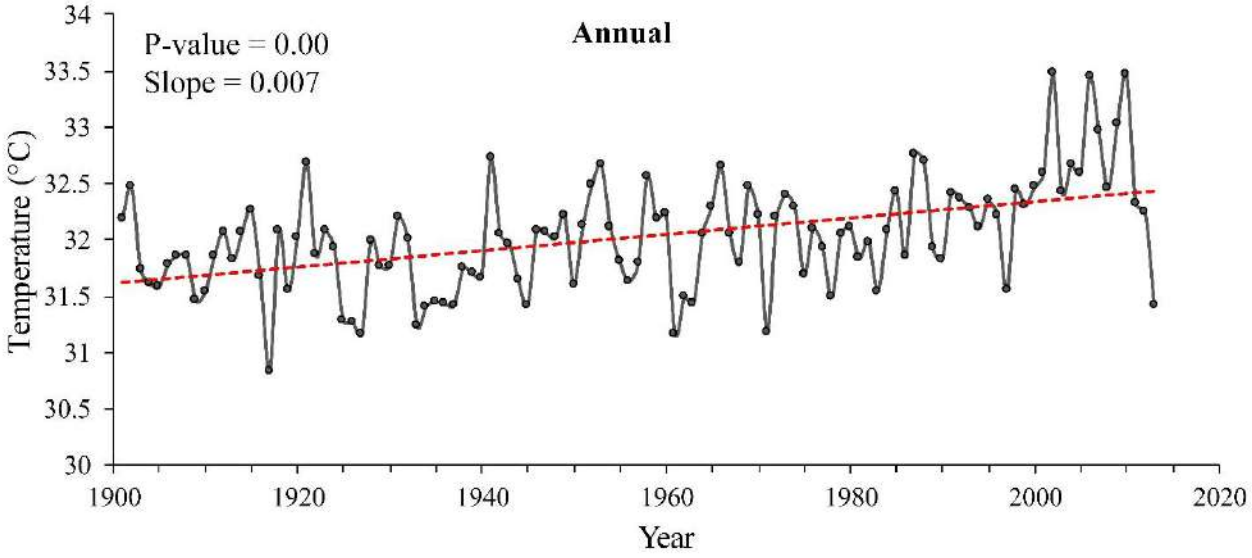

(e)

Figure 3.7 (d & e): Time series plots of mean maximum temperature over Betwa basin

From the time series plots (Figure 3.7) of mean maximum temperature, it can be observed that during pre-monsoon, post-monsoon and winter season, there is a significant increasing trend with 99% confidence level. Whereas, there is no significant trend during the monsoon season. Highest rate of change in the mean maximum temperature was observed during post monsoon season i.e. 1.5°C/100 years. While during the pre-monsoon season rate of change was observed as 0.8°C/100 years. The annual average maximum temperature is increasing with the rate of 0.7°C/100 years.

3.4.4 Average temperature

Autocorrelation and trend were analyzed for 21 stations of seasonal and annual average temperature. Monthly average temperature data were considered for this analysis. The Mann-Kendall Z value and significance level of the trend are presented in Appendix B-7. The values of slope, intercept, and relative change of the stations having significant trend are presented in Appendix B-8. During pre-monsoon season, three stations (Kanpur, Mahoba and Panna) exhibited increasing trend at 90% confidence level, three stations (Lalitpur, Raisen and Shivpuri) exhibited increasing trend at 95% confidence level and remaining stations exhibited increasing trend at 99% confidence level with slope value ranging from 0.004 to 0.012. During monsoon season, two stations namely Hoshangabad and Narsinghpur exhibited increasing trend and two stations (Kanpur and Orai) exhibited decreasing trend. Strong increasing trend at 99% confidence level has been observed during post-monsoon and winter season in all the stations with slope value ranging from 0.006 to 0.018. In case of yearly average temperature, all the stations except Kanpur (where there is no significant trend) exhibited increasing trend at 99% confidence level with slope value ranging from 0.005 to 0.009. Spatial distribution of the percent significant trend of seasonal and yearly average temperature within Betwa basin is presented in Figure 3.8.

The statistical summary of average temperature over the basin over the period of 1901 to 2013 is given in Table 3.7. The average temperature during the year varies from minimum 24.2°C to maximum 26.8°C with an average value and standard deviation of 25.4°C and 0.5°C respectively. During the pre-monsoon or summer season, it varies from 27.4 to 32.4°C with an average value of 29.7°C, which is highest in all the seasons.

Table 3.7: Statistical summary of average temperature over the basin

Statistic	Average Temperature (°C) during various seasons between 1901-2013				
	Pre-monsoon	Monsoon	Post-Monsoon	Winter	Annual
Max	32.4	30.2	25.7	20.3	26.8
Min	27.4	27.1	21.2	16.0	24.2
Avg	29.7	28.7	23.4	17.9	25.4
SD	0.9	0.6	1.0	0.7	0.5
CV	0.0	0.0	0.0	0.0	0.0

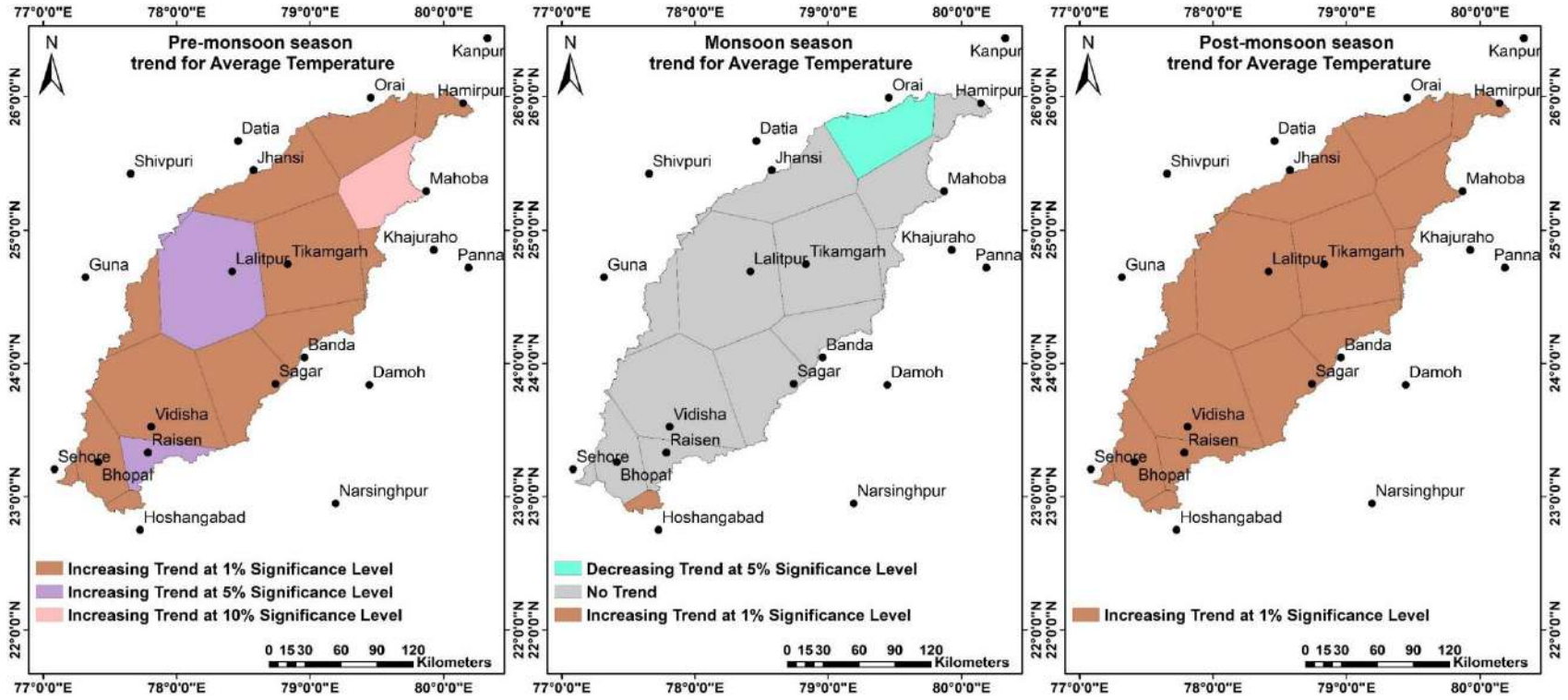

(a) (b) (c)

Figure 3.8 (a, b &c): Spatial distribution of the stations with percentage significant trend of maximum temperature

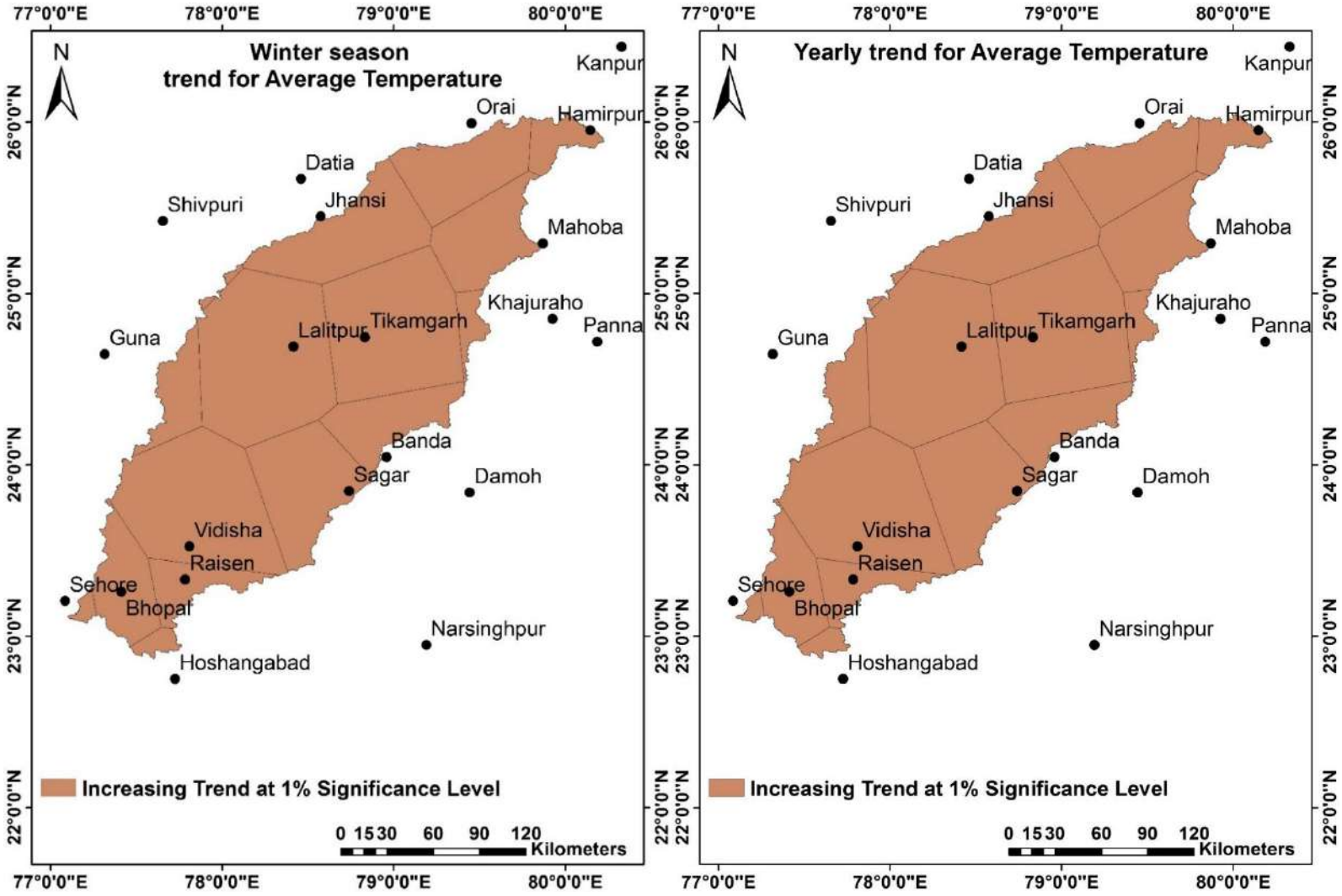

(d) (e)

Figure 3.8 (d & e): Spatial distribution of the stations with percentage significant trend of maximum temperature

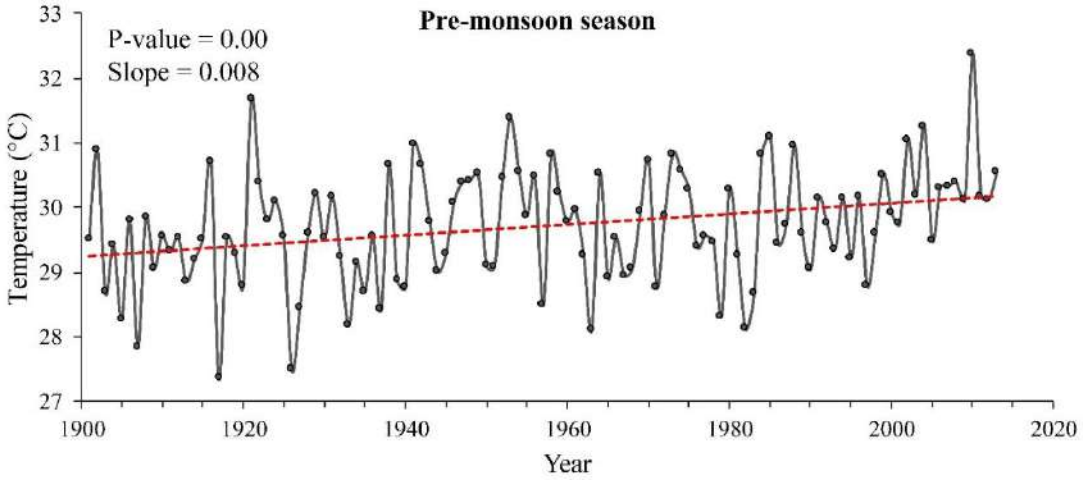

(a)

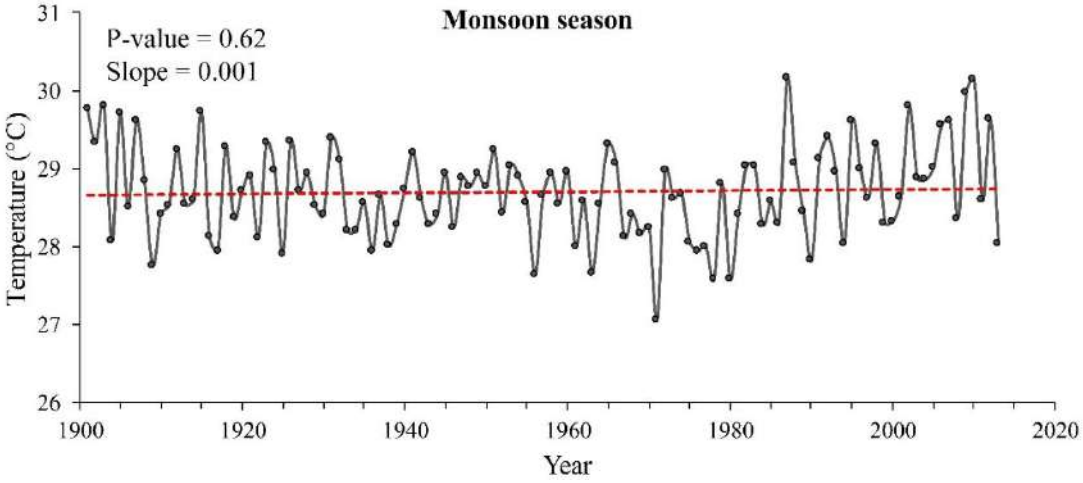

(b)

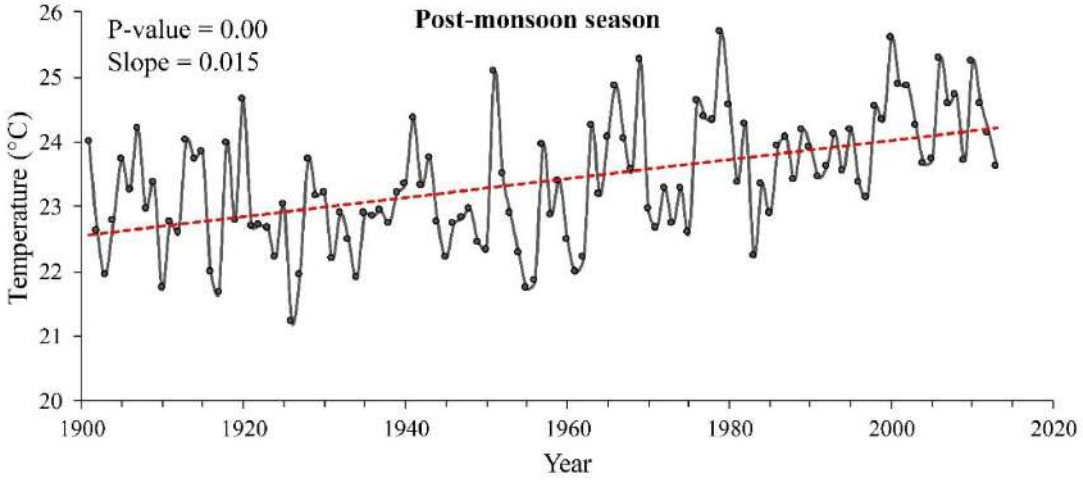

(c)

Figure 3.9 (a, b & c): Time series plot of average temperature over Betwa basin

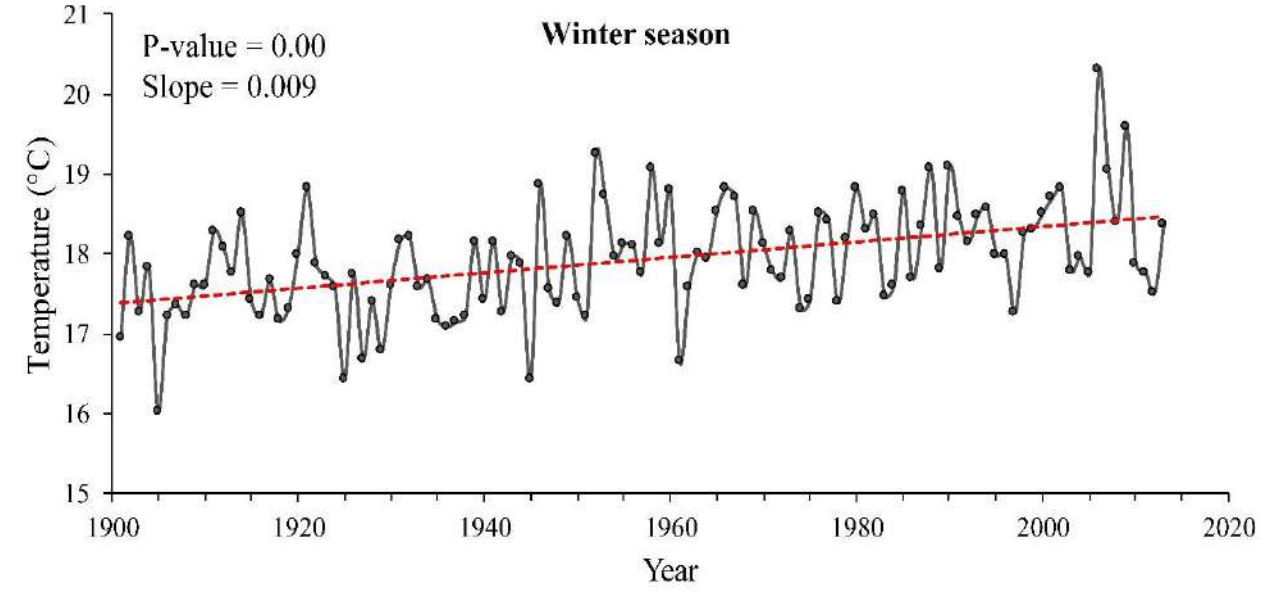

(d)

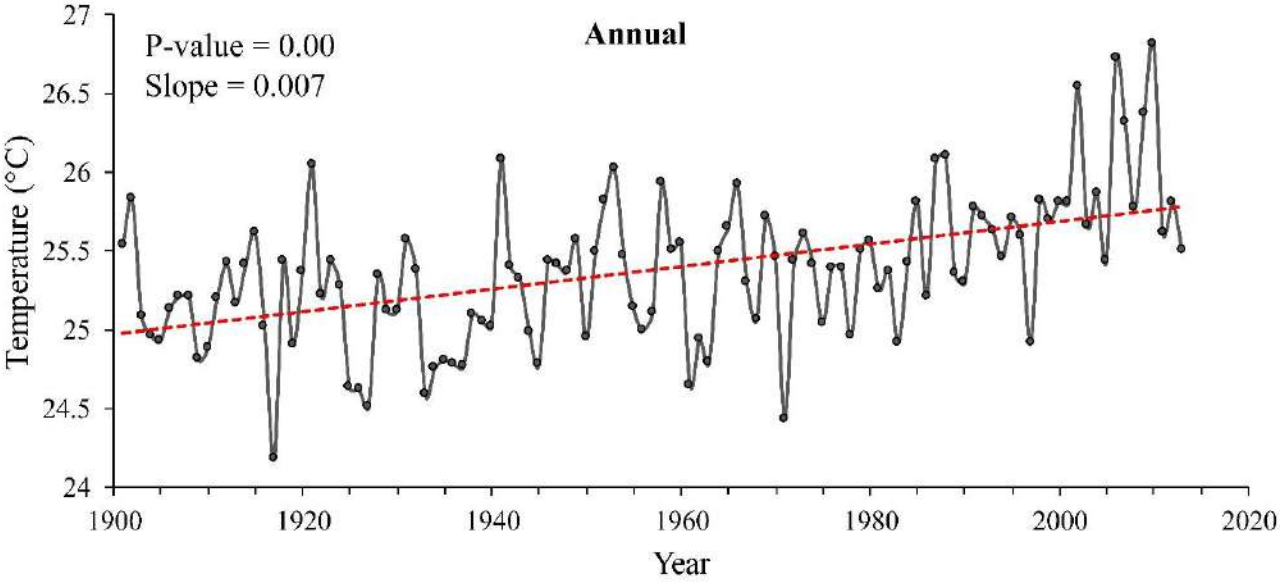

(e)

Figure 3.9 (d & e): Time series plot of average temperature over Betwa basin

From the time series plots (Figure 3.9) of average temperature, it can be observed that during pre-monsoon, post-monsoon and winter season, there is a significant increasing trend with 99% confidence level. Whereas, there is no significant trend observed during the monsoon season. Highest rate of change in the average temperature was observed during post monsoon season i.e. 1.5°C/100 years. While during the winter season rate of change was observed as 0.9°C/100 years. The annual average temperature is increasing with the rate of 0.7°C/100 years.

3.4.5 Potential Evapotranspiration (PET)

Autocorrelation and trend were analyzed for 21 stations for seasonal and annual PET. Monthly PET data were considered for this analysis. The Mann-Kendall Z value and significance level of the trend are presented in Appendix B-9. The values of slope, intercept, and relative change of the stations having significant trend are presented in Appendix B-10. During pre-monsoon season, only one station (Sehore) exhibited increasing trend at 90% confidence level with slope value of 0.04. However, no significant trend was observed during monsoon and post-monsoon season. Increasing trend at 99% confidence level in three stations (Lalitpur, Mahoba and Sehore) were observed during winter season with slope value ranging from 0.046 to 0.062. In case of yearly PET, only one station (Sehore) exhibited increasing trend at 90% confidence level and four stations (Guna, Hoshangabad, Raisen and Vidisha) exhibited increasing trend at 95% confidence level with slope value ranging from 0.105 to 0.223. The spatial distribution of the percent significant trend of seasonal and yearly PET within Betwa basin is presented in Figure 3.10.

The statistical summary of the average PET over the basin during the period of 1901 to 2013 is given in Table 3.8. Annual average PET over the basin varies from minimum 2328 mm to maximum 2446 mm with an average value and standard deviation of 2388 mm and 19 mm respectively. The maximum amount of PET can be observed during the monsoon season i.e. 757 mm.

Table 3.8: Statistical summary of Potential Evapotranspiration (PET) over the basin

Statistic	PET (mm) during various seasons between 1901-2013				
	Pre-monsoon	Monsoon	Post-Monsoon	Winter	Annual
Max	780.9	793.5	403.5	512.6	2446.4
Min	734.9	726.8	369.0	474.2	2328.0
Avg	752.3	757.3	387.4	491.6	2388.5
SD	8.2	10.5	5.6	7.1	19.0
CV	0.0	0.0	0.0	0.0	0.0

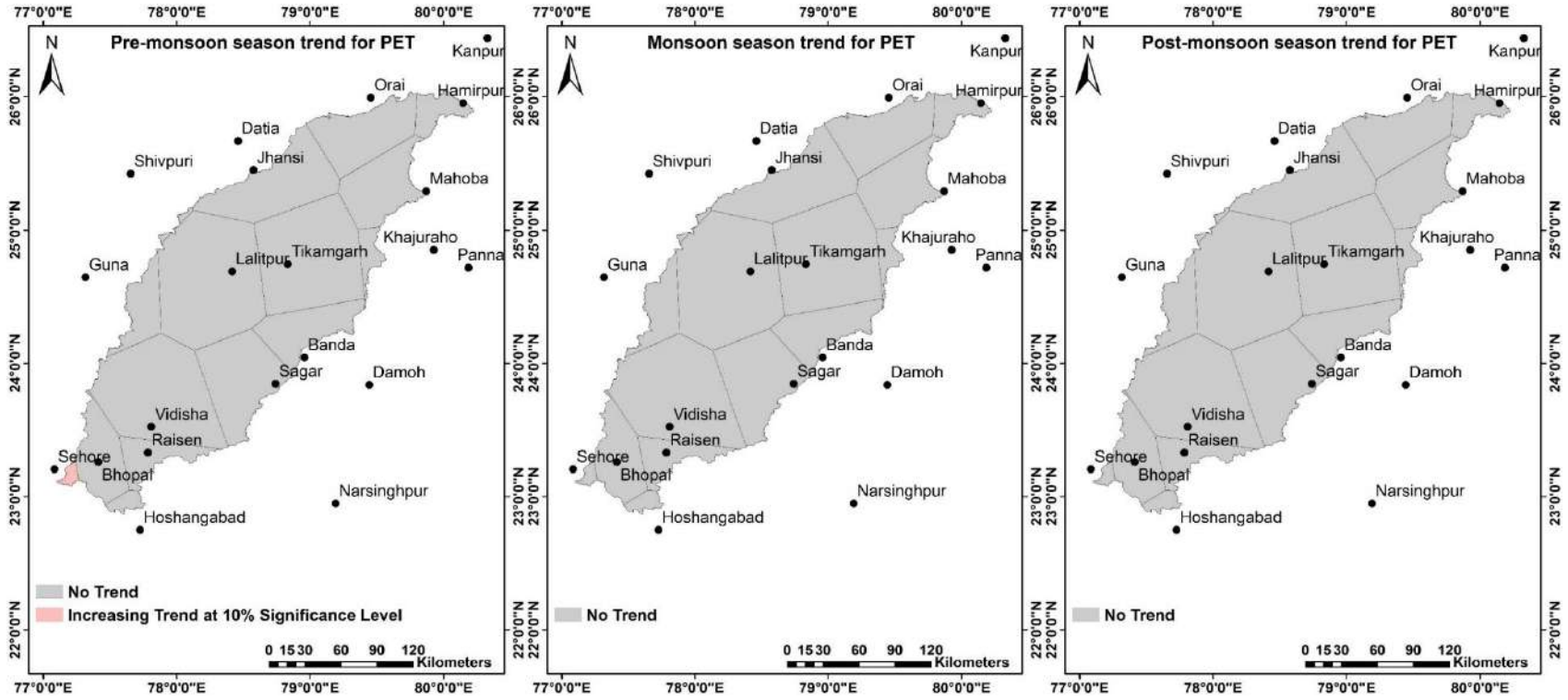

(a) (b) (c)

Figure 3.10 (a, b & c): Spatial distribution of the stations with percentage significant trend of PET

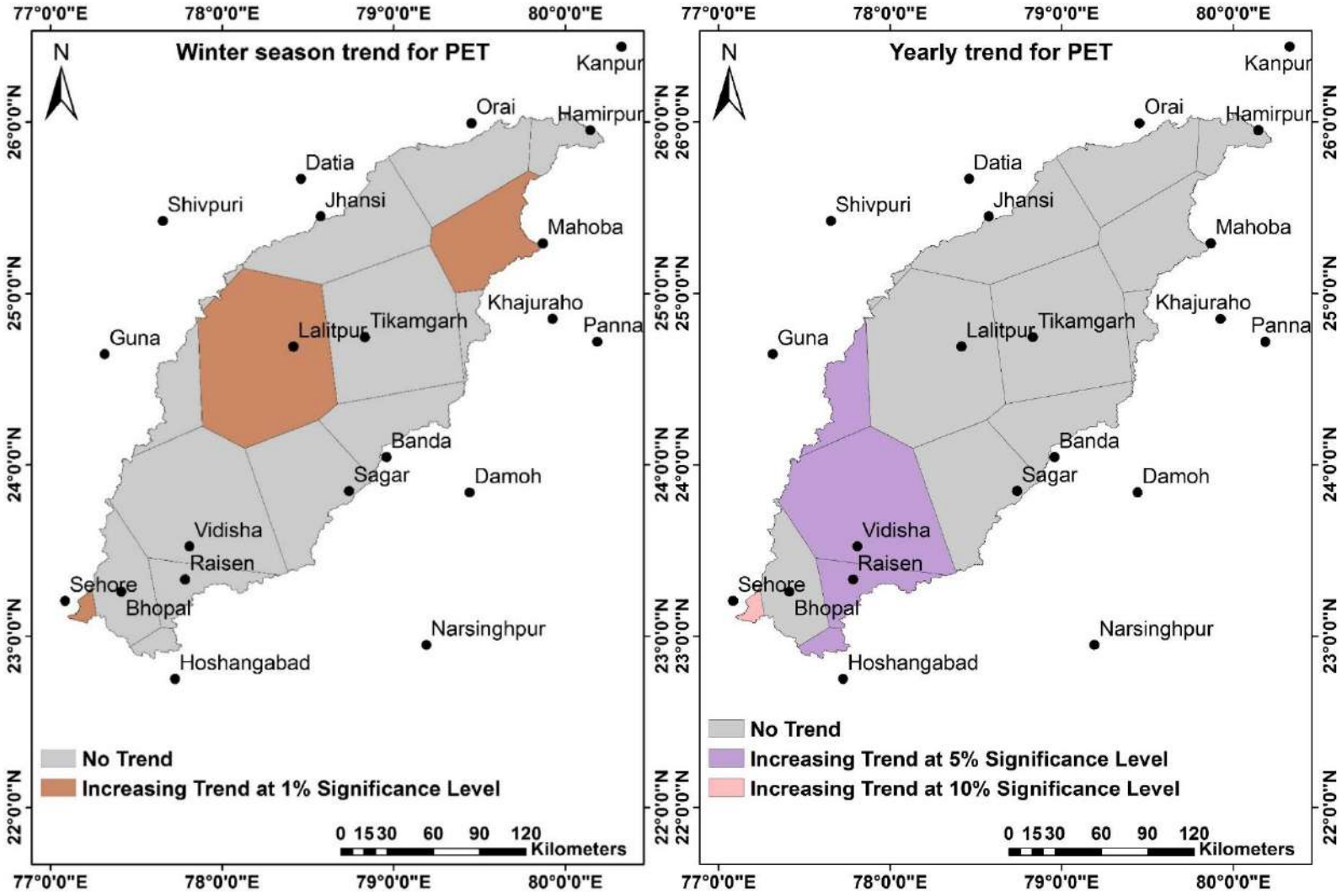

(d) (e)

Figure 3.10 (d & e): Spatial distribution of the stations with percentage significant trend of PET

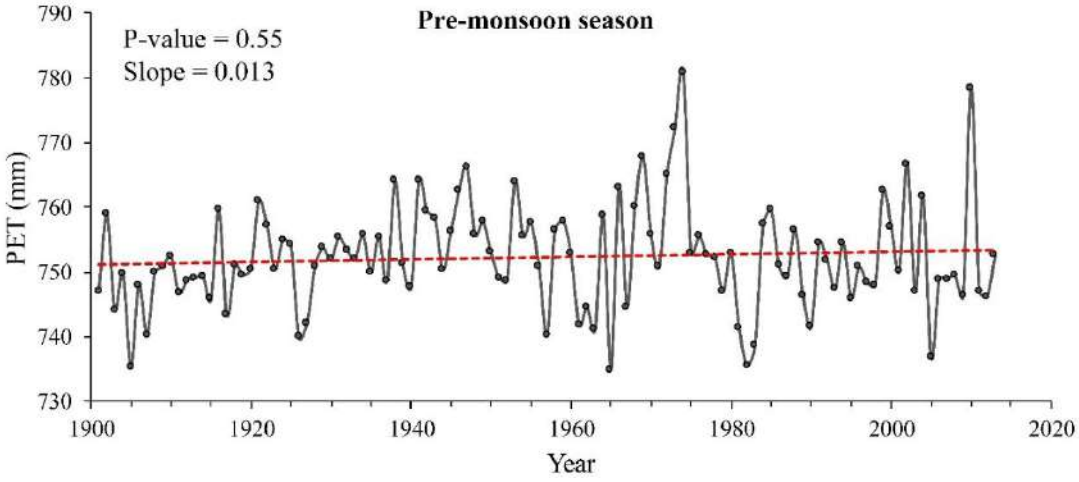

(a)

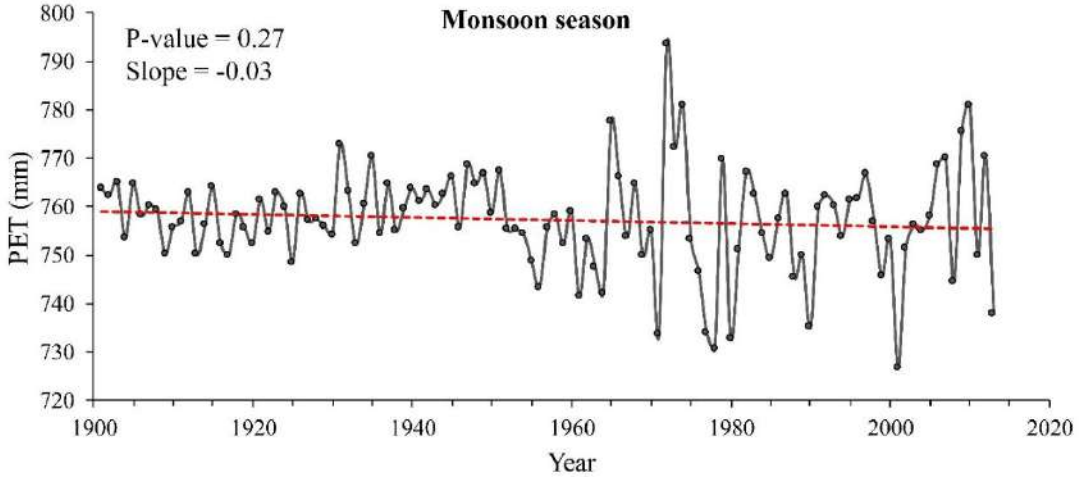

(b)

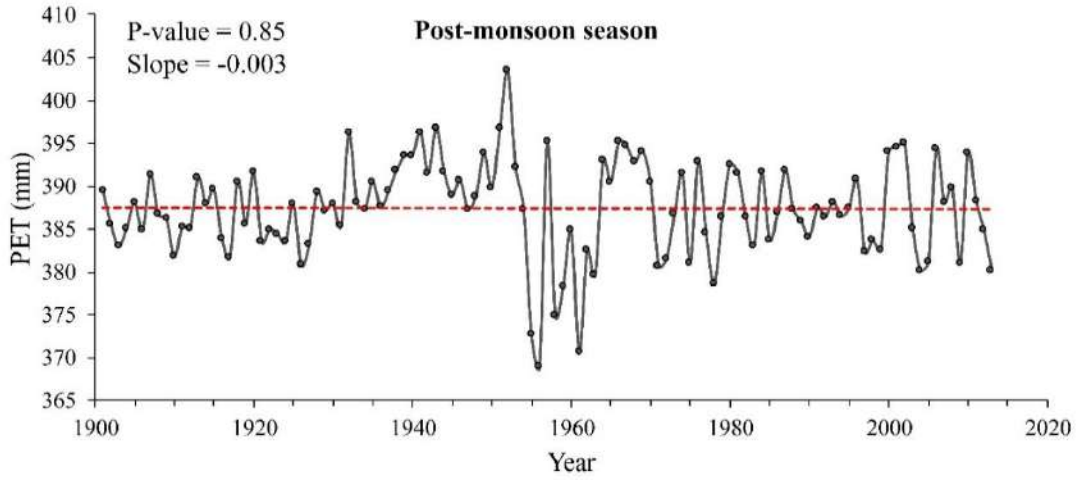

(c)

Figure 3.11 (a, b & c): Time series plot of PET over Betwa basin during 1901-2013

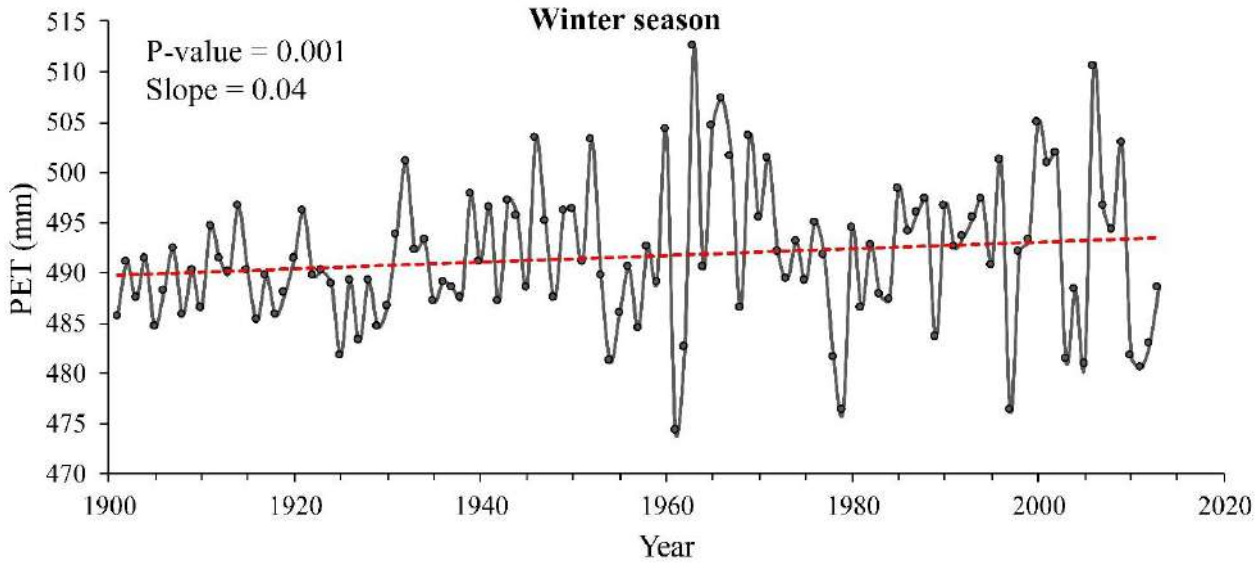

(d)

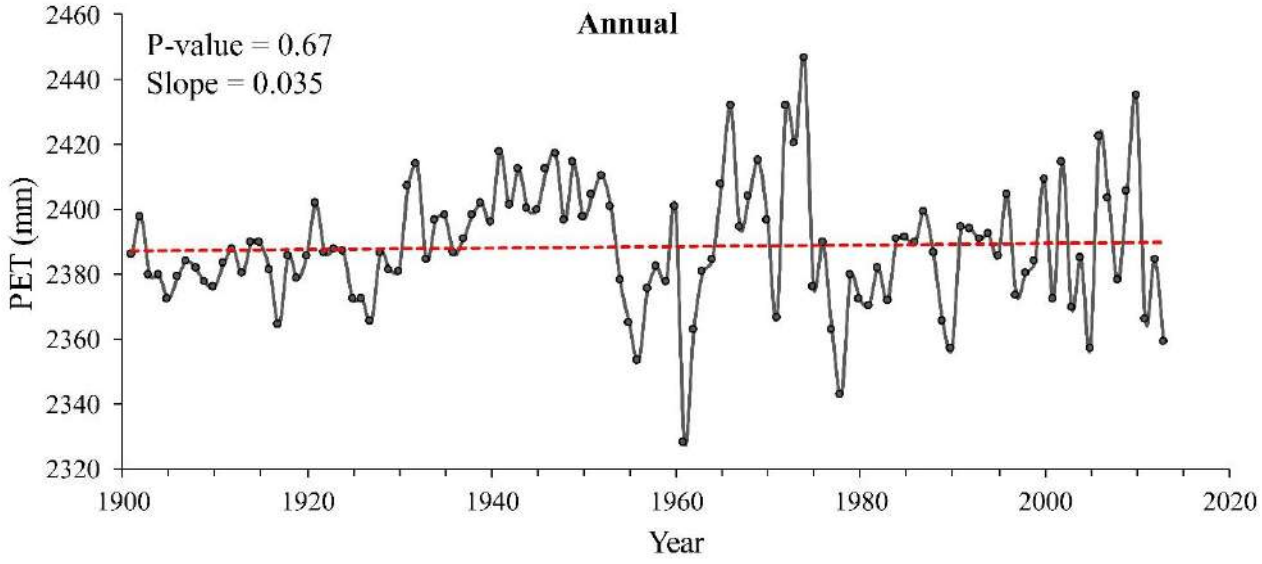

(e)

Figure 3.11 (d & e): Time series plot of PET over Betwa basin during 1901-2013

From the time series plots (Figure 3.11) of PET, it can be observed that during pre-monsoon, post-monsoon and winter season, there is no significant trend was observed. Whereas, during winter season there is a significant positive trend observed with 99% confidence level. This change is due to high rate of change in the minimum and maximum temperature during the winter season. The annual PET does not show any significant trend over the basin.

3.4.6 Aridity Index

Autocorrelation and trend were analyzed for 21 stations for seasonal and annual aridity index. Monthly rainfall and PET data (both are in same unit) were considered for the calculation of the AI by UNEP method. The Mann-Kendall Z value and significance level of the trend are presented in Appendix B-11. The values of slope, intercept, and relative change of the stations having significant trend are presented in Appendix B-12. During pre-monsoon season, four stations (Khajuraho, Mahoba, Shivpuri and Tikamgarh) exhibited increasing trend at 90% confidence level, six stations (Banda, Datia, Hamirpur, Jhansi, Sagar and Vidisha) exhibited increasing trend at 95% confidence level and two stations (Kanpur and Orai) exhibited increasing trend at 99% confidence level. During monsoon season, two stations (Banda and Narsinghpur) exhibited decreasing trend at 90% confidence level. However, no significant trend was observed during post-monsoon season. Increasing trend at 95% confidence level has been observed during winter season in only one station (Bhopal). In case of yearly aridity index, two stations (Banda and Hamirpur) exhibited decreasing trend at 90% confidence level. The spatial distribution of the percent significant trend of seasonal and yearly aridity index within the Betwa basin is presented in Figure 3.12.

The statistical summary of the aridity index over the basin between the period of 1901 to 2013 is given in Table 3.9. Annual average aridity index over the basin varies from minimum 0.27 to maximum 0.72 with an average value and standard deviation of 0.44 and 0.09 respectively. The highest value of aridity index was observed during monsoon season i.e. 1.24 whereas lowest value was observed during pre-monsoon season.

Table 3.9: Statistical summary of Aridity Index (AI) over the basin

Statistic	Aridity Index during various seasons between 1901-2013				
	Pre-monsoon	Monsoon	Post-Monsoon	Winter	Annual
Max	0.12	2.09	0.79	0.23	0.72
Min	0.00	0.62	0.00	0.00	0.27
Avg	0.03	1.24	0.11	0.07	0.44
SD	0.02	0.29	0.12	0.04	0.09
CV	0.71	0.23	1.08	0.66	0.21

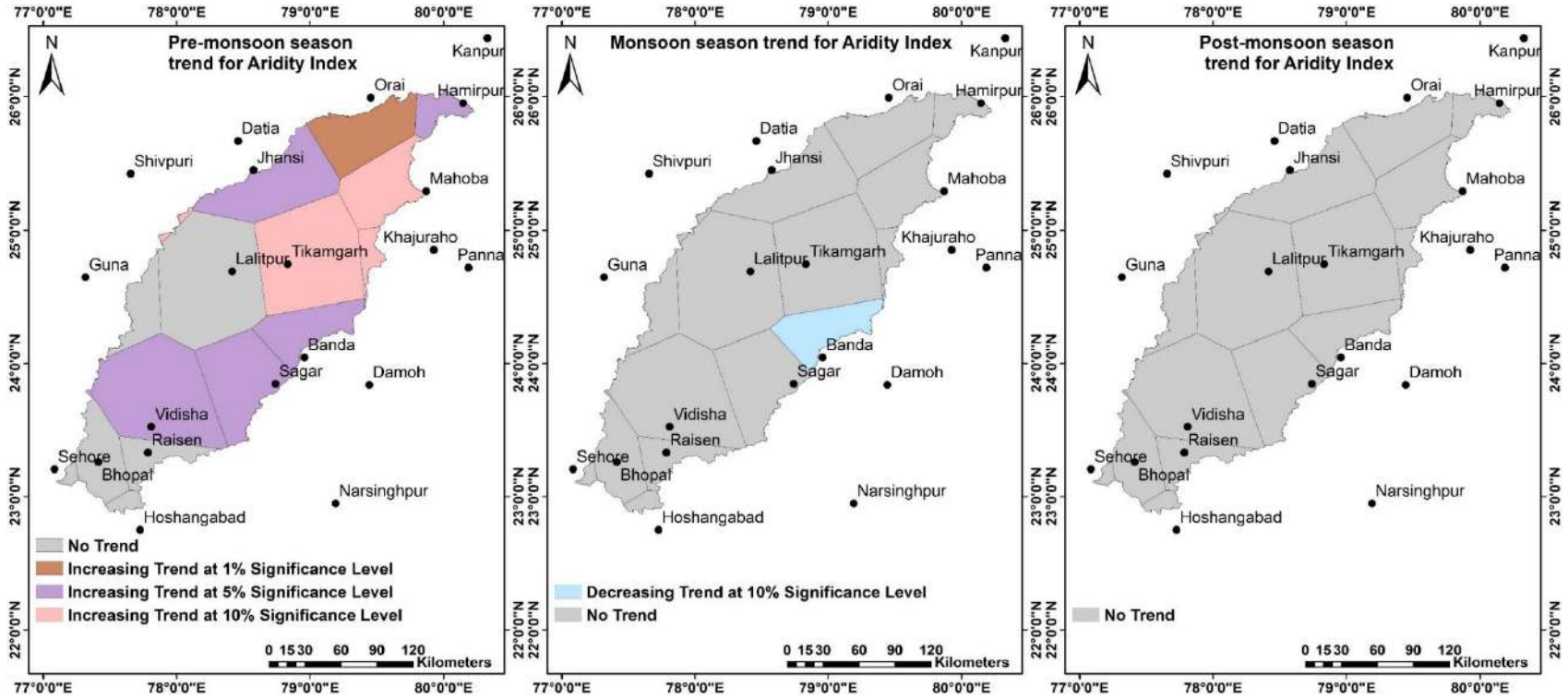

(a) (b) (c)

Figure 3.12 (a, b & c): Spatial distribution of the stations with percentage significant trend of aridity index

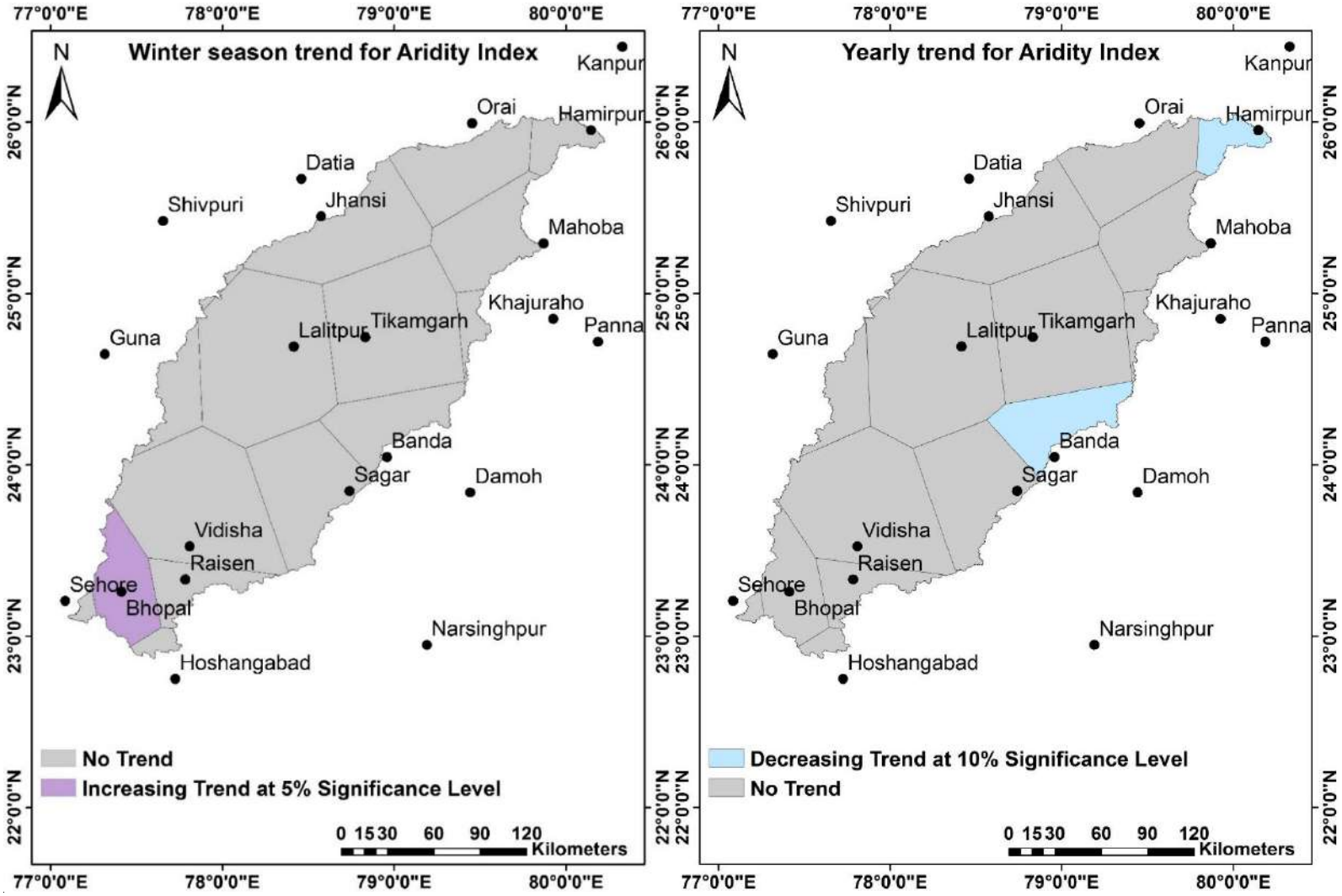

(d) (e)

Figure 3.12 (d & e): Spatial distribution of the stations with percentage significant trend of aridity index

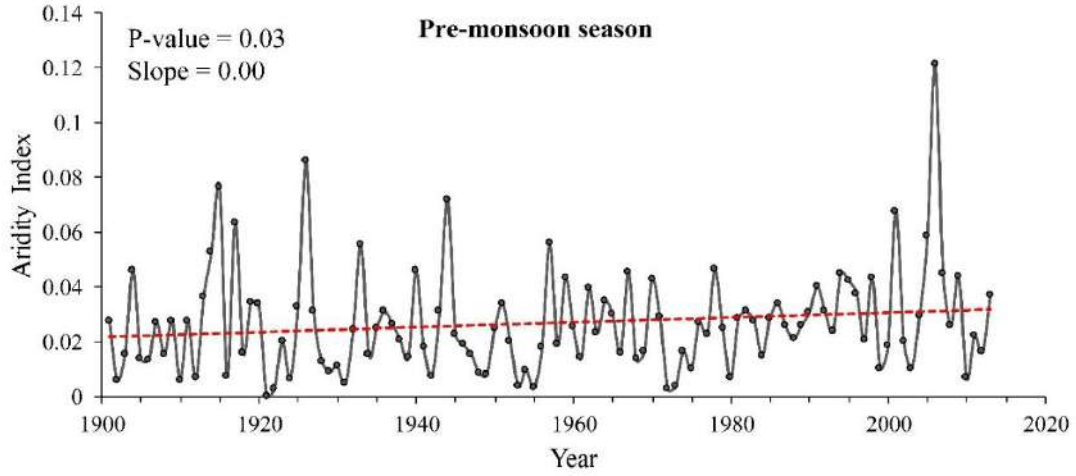

(a)

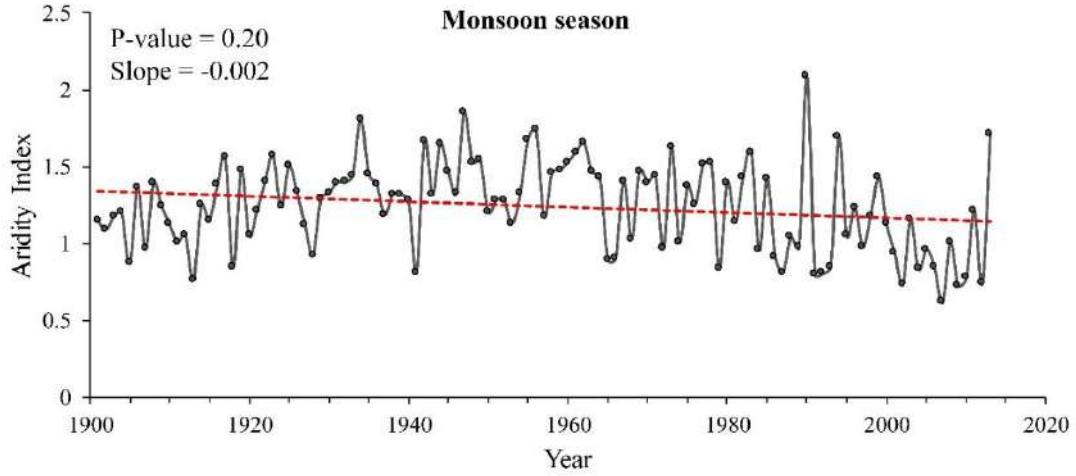

(b)

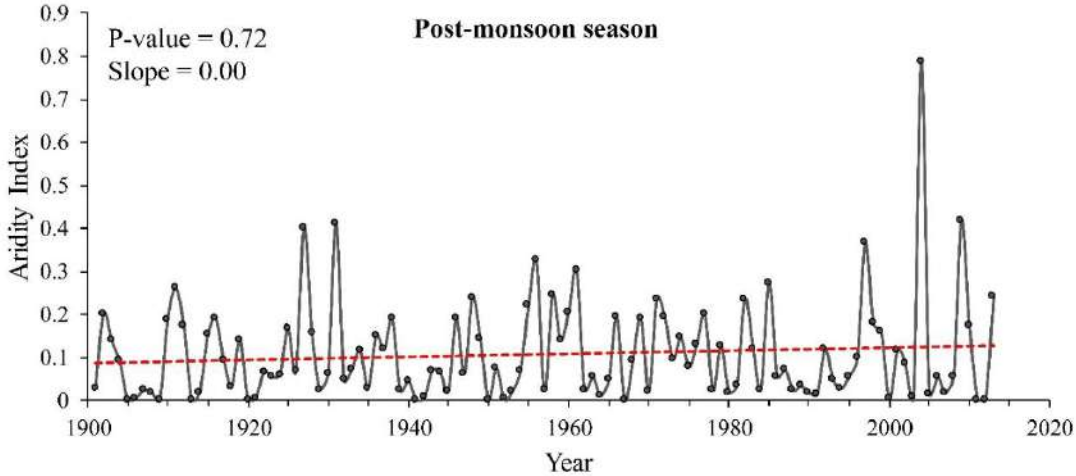

(c)

Figure 3.13 (a, b & c): Time series plot of Aridity Index over Betwa basin during 1901-2013

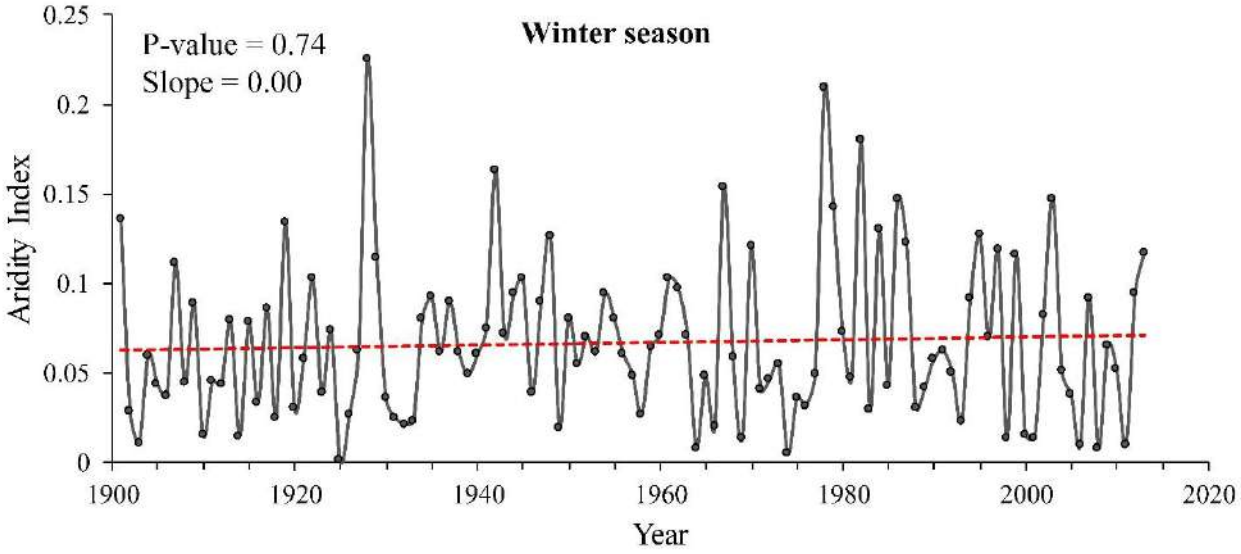

(d)

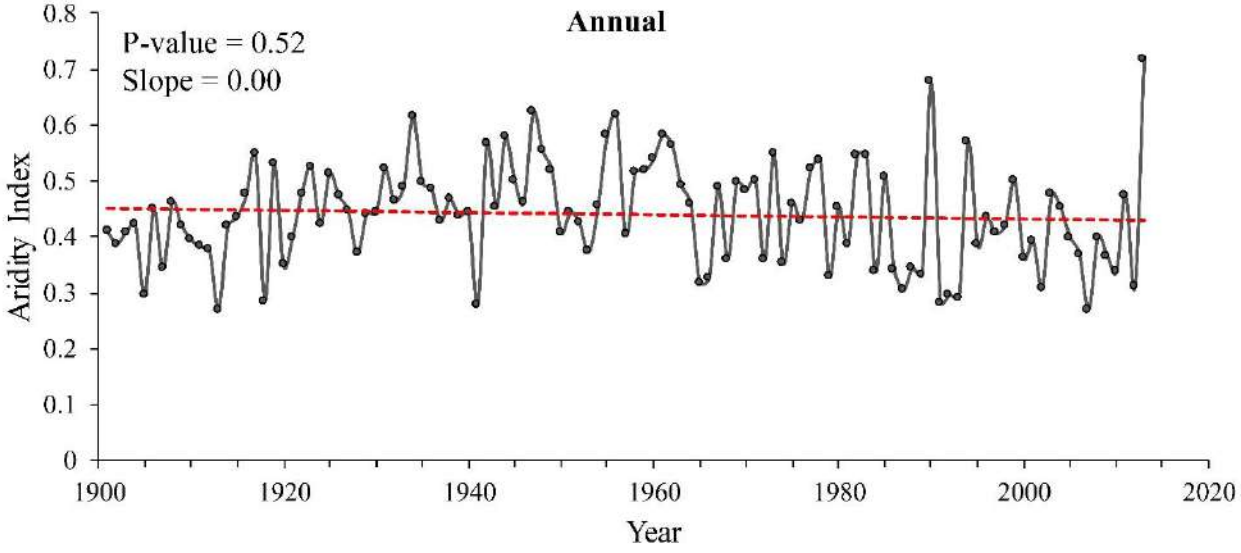

(e)

Figure 3.13 (d & e): Time series plot of Aridity Index over Betwa basin during 1901-2013

From the time series plots (Figure 3.13) of AI, it can be observed that during pre-monsoon, there is a significant increasing trend with 95% confidence level. Whereas, no significant trend was observed during other seasons. From Figure 3.15b, a very less decreasing trend can be observed that but the change is not statistically significant. Increasing trend in the pre-monsoon rainfall is the main cause for increase in AI during the pre-monsoon season.

3.5 SUMMARY

In this study, trend analysis of different climatic variables was carried out on station basin and basin as a whole. From the results, it was found that, except for pre-monsoon season rainfall, no significant trend was observed in the seasonal rainfall. In case of pre-monsoon rainfall, an increasing trend was observed at twelve stations. However, in case of yearly rainfall one station exhibited decreasing trend. Decrease of rainfall may lead to low crop productivity in the Betwa river basin. Minimum, maximum and average temperature is found to be increased for all the stations in all seasons except monsoon season. The increase of air temperature in the study area will increase dry conditions in the region by increasing potential evapotranspiration and consequently places it in serious risk of desertification. This temperature increase may lead to a significant change in the growth stages and water use of winter wheat. PET doesn't show any trend in pre-monsoon and monsoon season except at one station (which is showing increasing trend during pre-monsoon), however, during winter season it shows increasing trend at three stations. In case of yearly PET five stations shows increasing trend. Climate Change could potentially affect PET due to changes in air temperature, humidity, wind speed, and effects on cloudiness and atmospheric turbidity which affect net radiation. AI shows increasing trend at twelve stations during pre-monsoon season. This trend may be due to increasing trend in pre-monsoon rainfall. However, during monsoon season AI decreased at two stations which shows the change in the dryness during monsoon season. During post-monsoon and winter season there is not much trend in the AI. In case of yearly aridity index, two stations shows decreasing trend. Study of long-term changes in climatic variables and spatio-temporal distribution plays very important role in water resources development and management.

On the basis of average value of parameters over the basin, it was found that the minimum, maximum and average temperature were depicting the significant increasing trend. Whereas trend in the other parameters were not significant. The rate of change of minimum temperature during the winter and post monsoon season was higher than the maximum temperature whereas it was opposite during the pre-monsoon season.

CHAPTER 4

STUDY ON LAND USE/ LAND COVER CHANGE

4.1 INTRODUCTION

Land use/land cover (LU/LC) is two separate terminologies which are often used interchangeably (Dimyati et al., 1996). Land cover refers to the physical characteristics of earth's surface, captured in the distribution of vegetation, water, soil and other physical features of the land, including those created solely by human activities e.g., settlements. While land use refers to the way in which land has been used by humans and their habitat, usually with accent on the functional role of land for economic activities. The LU/LC pattern of a region is an outcome of natural and socio-economic factors and their utilization by man in time and space. Information on LU/LC and possibilities for their optimal use is essential for the selection, planning and implementation of land use schemes to meet the increasing demands for basic human needs and welfare. This information also assists in monitoring the dynamics of land use resulting out of demands of increasing population.

Changes in land cover by land use do not necessarily imply degradation of the land. However, many shifting land use patterns driven by a variety of social causes, result in land cover changes that affects biodiversity, water and radiation budgets, trace gas emissions and other processes that come together to affect climate and biosphere (Riebsame et al., 1994). Thus, the LU/LC change detection is essential for better understanding of landscape dynamic during a known period of time having sustainable management. Changes in LU/LC is a widespread and accelerating process, mainly driven by natural phenomena and anthropogenic activities, which in turn drive changes that would impact natural ecosystem (Turner and Ruscher, 2004). Understanding landscape patterns, changes and interactions between human activities and natural phenomenon are essential for proper land management and decision improvement. Today, earth resource satellites data are very applicable and useful for land use/cover change detection studies. In this study, an attempt has been made to map out the status of LU/LC in the Betwa River Basin to detect the changes that has taken place during the last five decades using geospatial techniques.

4.2 LAND USE/LAND COVER (LU/LC) CLASSIFICATION

In this study, remote sensing and GIS techniques were used to extract spatial information of the Betwa basin using satellite data of different spatial and temporal resolution. Image classification is carried out to identify the features occurring in an image which are actually present on the ground. Image processing satellite data and analysis of interpreted maps were carried out using ERDAS Imagine 2014 and ArcGIS 10.2.2 version software packages. Detailed methodology flowchart is shown in Figure 4.1.

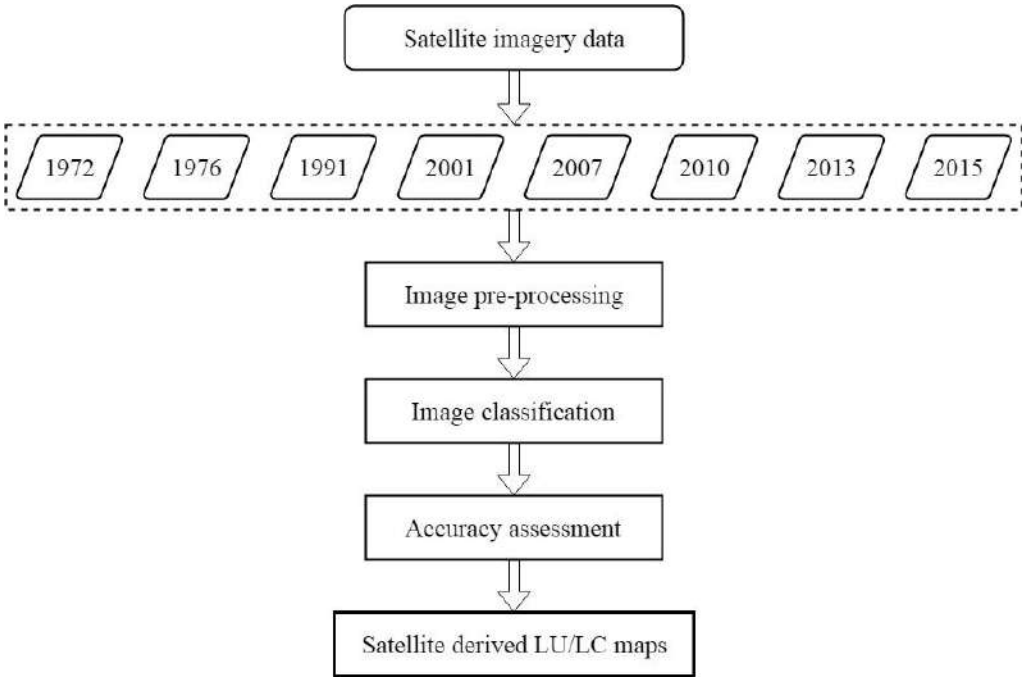

Figure 4.1: Methodology flowchart of historical LU/LC analysis

4.2.1 Image pre-processing

Satellite data was available in different layers of Geo TIFF format, and the study area falls under more than one satellite imagery. Therefore, these layers were stacked and then mosaicing of the stacked imagery were carried out using ERDAS Imagine 2014 software. Further, image enhancement, contrast stretching and false colour composites was carried out to make easy visual interpretation and understanding of the satellite imagery. Satellite imagery data follows some processes which includes radiometric and geometric corrections, image segmentation, image enhancement and classification using spectral and spatial information. Geometric and radiometric

corrections of satellite imagery were also carried out to improve image accuracy for further analysis.

4.2.2 Image classification

There are two types of classification methods i.e. supervised and unsupervised classification. In this study, supervised classification method was used to prepare LU/LC map for the Betwa basin. Supervised classification is based on the idea that a user can select sample pixels in an image that are representative of specific classes and then direct the image processing software to use these training sites as references for the classification of all other pixels in the image. Training sites are selected based on the knowledge of the user. This method uses the spectral signatures file which can be obtained from training samples of an image. In signature analysis, simple or complex distinctive reflectances on band were analyzed. Then, digital image has been classified by determining the reflectance for each pixel. In this study, an image classification categorizes six LU/LC classes namely dense forest, degraded forest, agriculture area, barren land, waterbody and settlement etc.

4.2.3 Accuracy assessment

Accuracy assessment is essential to understand accurate and valid results of the classified imagery, without which the LU/LC map is a simply an untested hypothesis. Accuracy assessment of LU/LC map is required to evaluate its utility suitable for the application.

In this method, certain pixels in the classified subset were compared to the reference pixels for which the correct class is known (known pixels may come from ground truth data or previously tested maps, photos or other data). In this study, five hundred stratified random accuracy assessment points were generated across the LU/LC map. It is calculated in terms of overall classification accuracy (%) and Kappa coefficient using ERDAS Imagine 2014 software. Also, ground truth verification of the LU/LC map was carried out using GPS for the assessment of classification accuracy as shown in Figure 4.2. Ground Truth locations reported during field visits August-2013, May-2014, November-2014 and November-2016 are presented in Figure 4.2.

Based on inter-transitions calculated by confusion matrix between reference data and classified imagery data, several statistical measures namely user's accuracy, producers accuracy, overall accuracy and Kappa coefficient were estimated for all satellite-derived LU/LC maps. Higher percentage of user's accuracy/producers accuracy/overall accuracy indicates more precise

classification of satellite imagery. Kappa coefficient value ranges from 0 to 1. High value of Kappa coefficient indicates more accuracy in the LU/LC map, and low value indicates less accuracy. In this study, these statistical terms have been used as accuracy assessment measures.

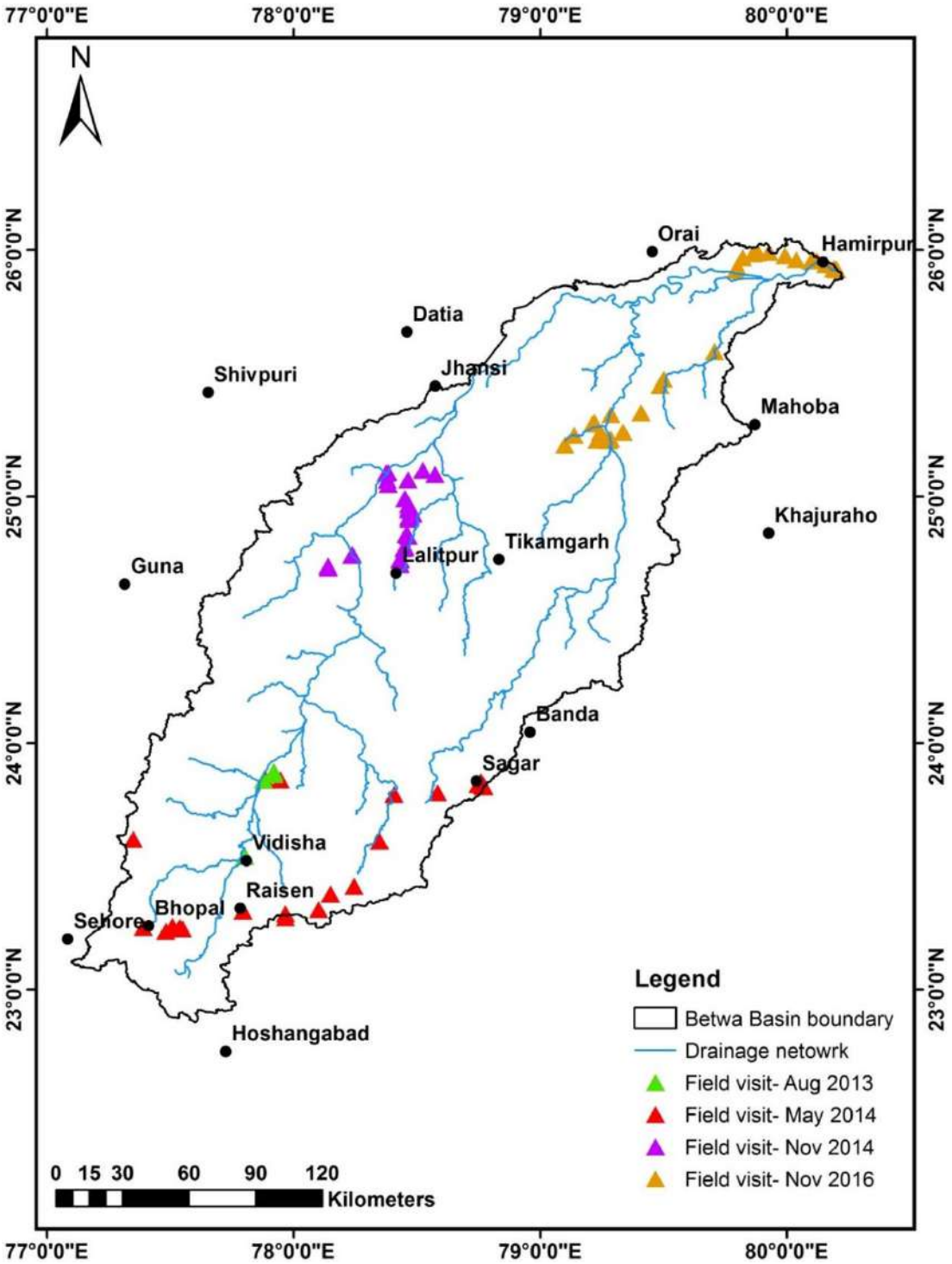

Figure 4.2: GPS locations during ground truth verification

4.3 NORMALIZED DIFFERENCE VEGETATION INDEX (NDVI)

Different vegetation indices have been used for the vegetation monitoring. NDVI has been used to prepare spectral vegetation indices which separate green vegetation using Landsat data. It depends on the different interactions between electromagnetic spectrum of near infrared and red wavelengths and vegetation. Red wavelength (about 0.6 - 0.7μ) shows low reflectance because chlorophyll of leaf pigment absorbs more red wavelengths and infrared wavelength (about 0.8 - 0.9 μ) is of high reflectance because cell structure of the leaves scatters more infrared wavelength.

NDVI can be easily determined with the comparison of infrared wavelength band to that of red wavelength band. NDVI is the ratio of difference between the near infrared (NIR) and red (RED) wavelength bands and sum of those two bands. It is expressed using the following Equation 4.1.

$$NDVI = (NIR - RED)/(NIR + RED) \quad \ldots(4.1)$$

This is the most commonly used vegetation index. It has the value in the range of -1 to 1, and 0 value of NDVI shows no vegetation. Positive value of NDVI shows vegetation surface while negative values of NDVI shows non-vegetation surfaces.

4.4 HISTORICAL LAND USE/LAND COVER CHANGE (LU/LC) ANALYSIS

In the present study, LC/LC analysis was carried out using remote sensing data of post-monsoon season. The classified LU/LC classes are dense forest, degraded forest, agriculture area, barren land, waterbody and settlement. Tables 4.1 and 4.2 show LU/LC areas (in terms of km^2 and % respectively) in the Betwa basin for the years 1972, 1976, 1991, 2001, 2007, 2010, 2013 and 2015.

Area statistics of different LU/LC classes for the years 1972, 1976, 1991, 2001, 2007, 2010, 2013 and 2015 are presented in Tables 4.1 and 4.2. In the study area, dense forest area has declined from 10285.98 km^2 (23.39%) to 5141.64 km^2 (11.70%) during the years 1972 to 2015 respectively, and resulted 5144.34 km^2 (11.69%) decrease in the last four decades. During the years 1972 to 2015, the area under degraded forest has increased from 8.54% to 11.87%, agriculture area has increased from 63.75% to 72.30%, barren land has decreased from 2.98% to 1.42%, waterbody surface area has increased from 1.22% to 2.11% and settlement area has increased from 0.12% to 0.59%. In the Betwa basin, waterbody area depends mainly upon monsoon season rainfall. Present analysis shows that, increase in agriculture area by 3735.13 km^2 (8.55%) during the years 1972 to 2015 is due to 0.89% increase in waterbody area. However, decrease in dense forest area (11.69%) cease to

increase in degraded forest area by 3.33%. Analysis reveals that 11.69% reductions in the forest area is due to increased anthropogenic activity in the Betwa basin.

Table 4.1: Area (sq km) under land use/land cover classification of the Betwa River Basin

LULC Class Name	Area under land use/land cover classification (km^2)							
	1972 Post	1976 Post	1991 Post	2001 Post	2007 Post	2010 Post	2013 Post	2015 Post
Dense forest	10285.98	9304.48	7918.29	6519.50	5259.82	5673.80	6286.53	5141.64
Degraded/Open forest	3756.39	4254.87	4019.72	5558.82	6353.25	6109.88	5874.10	5216.89
Agriculture area	28032.76	28678.13	30430.88	30403.44	29071.87	29581.24	29835.85	31767.89
Barren land	1311.09	1064.53	1118.50	577.74	2619.18	1955.31	559.89	624.14
Waterbody	535.45	616.89	367.82	780.11	515.83	485.75	1246.08	926.88
Settlement	52.56	55.35	81.37	96.98	124.21	130.61	134.15	259.38
Total area (km^2) =	**43974.23**	**43974.23**	**43936.59**	**43936.59**	**43944.17**	**43936.59**	**43936.59**	**43936.63**

Table 4.2: Area (%) under land use/land cover classification

LULC Class Name	Area under land use/land cover classification (%)							
	1972 Post	1976 Post	1991 Post	2001 Post	2007 Post	2010 Post	2013 Post	2015 Post
Dense forest	23.39	21.16	18.02	14.84	11.97	12.91	14.31	11.70
Degraded/Open forest	8.54	9.68	9.15	12.65	14.46	13.91	13.37	11.87
Agriculture area	63.75	65.22	69.26	69.20	66.16	67.33	67.91	72.30
Barren land	2.98	2.42	2.55	1.31	5.96	4.45	1.27	1.42
Waterbody	1.22	1.40	0.84	1.78	1.17	1.11	2.84	2.11
Settlement	0.12	0.13	0.19	0.22	0.28	0.30	0.31	0.59
Total area (%) =	**100.00**	**100.00**	**100.00**	**100.00**	**100.00**	**100.00**	**100.00**	**100.00**

Table 4.3 shows that overall classification accuracy and Kappa coefficient were calculated for LU/LC map of the years 1972, 1976, 1991, 2001, 2007, 2010, 2013 and 2015. Overall classification accuracy was found to be 86%, 84%, 77%, 78%, 82%, 87%, 82% and 80%, and kappa coefficient was found to be 0.824, 0.797, 0.709, 0.722, 0.775, 0.836, 0.775 and 0.746 for the year 1972, 1976, 1991, 2001, 2007, 2010, 2013 and 2015 respectively. Figure 4.3 shows the LU/LC maps obtained in the present study.

In this study, dense forest, degraded forest and agriculture area are taken into consideration for vegetation class category. Overall, the study area is dominated by agricultural and forest area, whereas settlement area only accounts for about 0.3%, even though Bhopal city, which is located in the upstream basin, has been rapidly growing due to industrialization and urbanization (around 1798218 inhabitants; Chandramouli and Sinha, 2014). Hence, rapid changes in urbanization and increase in population may have pronounced impact on LU/LC of the Betwa basin.

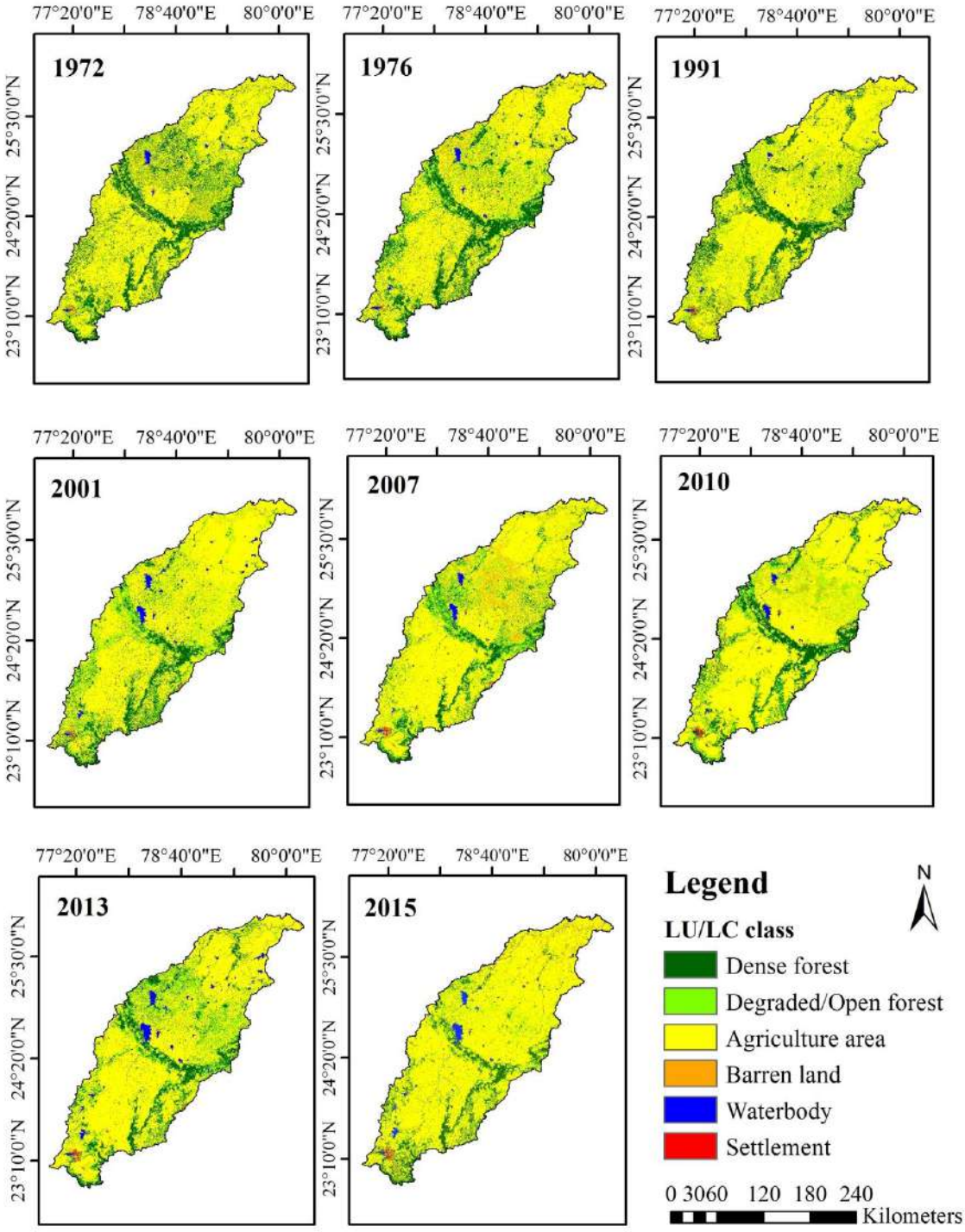

Figure 4.3: Historical LU/LC maps of the Betwa basin

Table 4.3: Accuracy assessment results of land use/land cover classification

LULC Class Name	Accuracy (%)	Classification Accuracy Assessment							
		1972 Post	1976 Post	1991 Post	2001 Post	2007 Post	2010 Post	2013 Post	2015 Post
Dense forest	Producers Accuracy	94.44	88.24	92.31	93.33	93.33	100.00	93.75	93.85
	Users Accuracy	85.00	75.00	60.00	70.00	70.00	90.00	75.00	71.00
Degraded/Open forest	Producers Accuracy	73.91	88.89	71.43	83.33	83.33	77.27	77.27	84.54
	Users Accuracy	85.00	80.00	75.00	75.00	75.00	85.00	85.00	77.00
Agriculture area	Producers Accuracy	78.79	71.79	68.42	65.79	79.41	81.82	80.65	67.79
	Users Accuracy	86.67	93.33	86.67	83.33	90.00	90.00	83.33	84.33
Barren land	Producers Accuracy	100.00	88.89	63.64	66.67	53.85	77.78	58.33	67.67
	Users Accuracy	80.00	80.00	70.00	80.00	70.00	70.00	70.00	81.00
Waterbody	Producers Accuracy	100.00	100.00	100.00	100.00	100.00	100.00	100.00	100.00
	Users Accuracy	100.00	100.00	90.00	90.00	100.00	100.00	90.00	90.00
Settlement	Producers Accuracy	100.00	100.00	100.00	90.00	90.00	100.00	100.00	90.00
	Users Accuracy	80.00	70.00	80.00	70.00	90.00	80.00	90.00	75.00
Overall Classification Accuracy (%)		**86.00**	**84.00**	**77.00**	**78.00**	**82.00**	**87.00**	**82.00**	**80.00**
Kappa coefficient		**0.824**	**0.797**	**0.709**	**0.722**	**0.775**	**0.836**	**0.775**	**0.746**

4.5 ESTIMATION OF VEGETATION AREA USING NDVI METHOD

The popular NDVI method was used for monitoring temporal changes in vegetation area of the Betwa basin. NDVI were generated using ERDAS Imagine 2014 version software package. Figure 4.4 shows the NDVI maps obtained in the present analysis.

The NDVI maps were used to estimate the total vegetation area of Betwa basin, and then compared with the total vegetation area calculated by LU/LC classification. Main purpose of this analysis is to validate the dominant vegetation area of Betwa basin employing NDVI method.

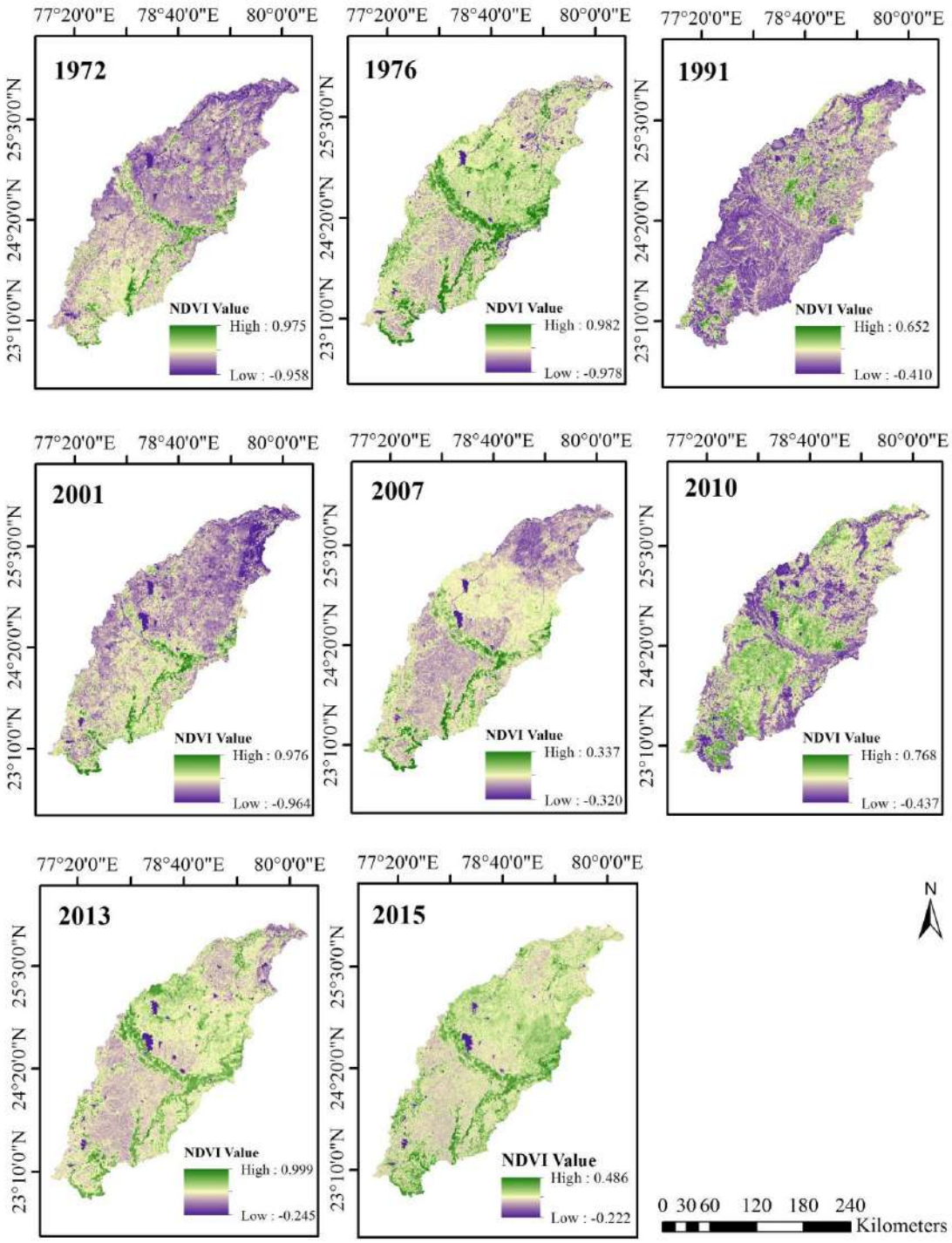

Figure 4.4: NDVI maps for the Betwa basin

4.6 CROSS VERIFICATION OF VEGETATION AREA

Vegetation area obtained from LU/LC analysis and NDVI method were verified using the simple linear regression method. Regression analysis method is used to describe the relationship between

the percentage of vegetation area estimated from LU/LC analysis and NDVI. In this method, regression coefficient value exhibit correlation between these two variables. Table 4.4 shows the percentage of vegetation area obtained from LU/LC and NDVI analysis.

The coefficient of determination value of $R^2 = 0.846$ shows a good agreement between vegetation area obtained from the LU/LC and NDVI analyses. This result implies that vegetation area is correctly accounted in the present study.

Table 4.4: Vegetation area under land use/land cover and NDVI

Year	LU/LC results (%)	NDVI area (%)
1972	95.66	95.62
1976	96.03	96.60
1991	96.41	96.49
2001	96.67	96.22
2007	92.55	94.31
2010	94.11	94.70
2013	95.55	95.37
2015	95.88	96.5

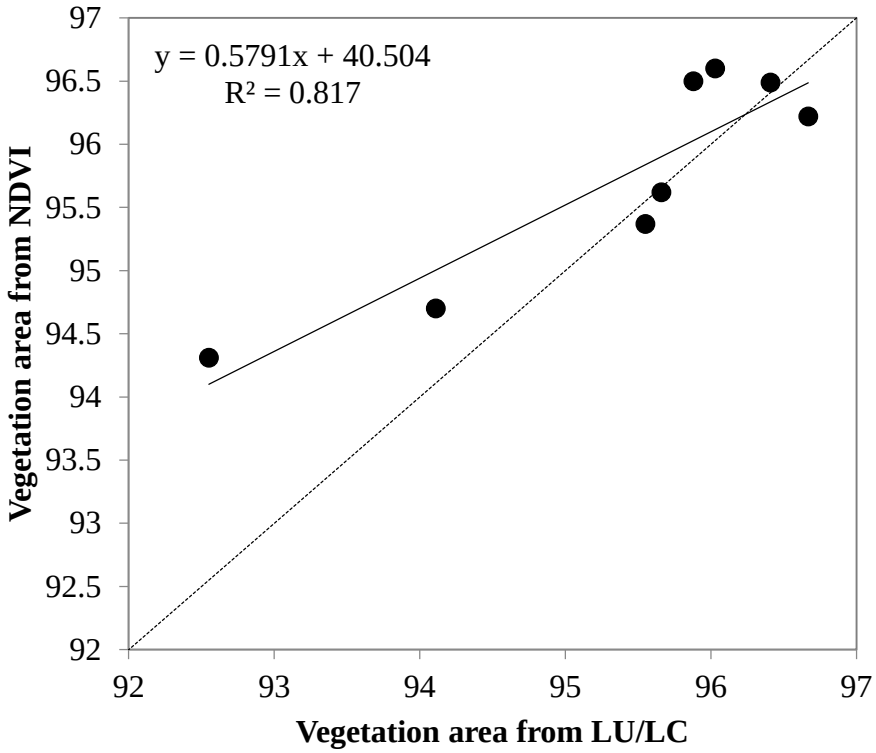

Figure 4.5: Correlation between vegetation areas obtained from LU/LC analysis and NDVI

4.7 WATER AVAILABILITY AND LU/LC CHANGES IN BETWA BASIN

Water availability in the Betwa basin shows significant effect on changes in the LU/LC area. The initial years (1972 and 1976) of analysis shows less agriculture area due to the drought effect (Pandey et al., 2008). However, water availability from reservoir, lake and pond is mainly responsible for positive changes in the agriculture area. After the year 2007, accrued in agriculture area (1.75%) is due to increase in water availability from Rajghat reservoir, having a large water storage capacity. It is newly accomplished reservoir in the middle part of the Betwa basin, and was put in operation from 2006. Therefore, Rajghat reservoir serves great significance to water storage for irrigation releases in the Betwa basin area. Thus, the results demonstrated that river basin sustainability can be further continued with joint inter-state planning, management and development of water resources at middle and lower part of the BRB.

4.8 SUMMARY

In this study, historical LU/LC analysis of the Betwa basin has been carried out using satellite data of the years 1972, 1976, 1991, 2001, 2007, 2010, 2013 and 2015. Following conclusions are drawn from the present study:

1. The historical spatiotemporal LU/LC change analysis shows accrued in agriculture area by 8.55% due to increase in waterbody area (0.89%) and reduced dense forest area (11.69%) cease to increase in degraded forest area by 3.33% in the Betwa basin.
2. After 2007, about 6.14% increase in agriculture area shows dependency to more water availability (0.94%) from Rajghat reservoir.
3. The overall classification accuracy varies from 77% to 87%, and Kc value varies from 0.709 to 0.836 shows satisfactory classification of the satellite-derived LU/LC maps.
4. Cross verification of vegetation area showed significant regression value (R^2 = 0.817) for LU/LC and NDVI results.

CHAPTER 5

CORRELATION ANALYSIS OF HYDRO-CLIMATIC PARAMETERS WITH NDVI AND LAND COVER

5.1 INTRODUCTION

The interaction between land surface and climate plays an important role in the hydrology (Poveda and Mesa, 1997) and vegetative land cover (Zhou et al., 2001). It has been recognized that, climate determine the Earth's surface characteristics, such as land use/land cover and energy balances (Small and Kurc, 2003; Weiss et al., 2004). Land surface reflects to the climate through changes in evapotranspiration, soil moisture (Zribi et al., 2010), albedo etc. Therefore, recent research work has been mainly focused on the response between land cover i.e. vegetation, and climate parameters.

Vegetation plays an important role, and proven to be a crucial component of ecosystem (Sun et al., 1998) responsive to climate. It helps to reduce greenhouse gases, regulate carbon balance and maintain climate suitability at spatial and temporal scales (Barichivich et al., 2013; Dubovyk et al., 2015). Nowadays, vegetation changes can be quantified using available satellite observations of global time series datasets (Lanorte et al., 2014; Du et al., 2015; Dubovyk et al., 2015). Globally, vegetation monitoring were carried out for drought assessment (Gu et al., 2008), net primary productivity (Running, 1990), crop yield forecasting (Rasmussen, 1997), crop classification (Wardlow and Egbert, 2008), long-term vegetation changes (Panday and Ghimire, 2012), and assessment of growing period.

From last few decades, responses of climate were studied using statistical correlation analysis between land characteristics and climate variables (Weiss et al., 2004). The correlation method was employed to establish relationship between climate variables and NDVI for mapping climatic variations (Tucker and Nicholson, 1999). The correlation analyses of first to higher order have been successfully used in hydrology and water resources to understand response analysis (Burn, 2008). In this study, pre-monsoon (March to May), South West (SW)-monsoon (June to September) post-monsoon (October and November) and winter (December to February), seasons (Kumar and Hingane, 1988) were considered to categorize hydro-climatic variables and MODIS time-series dataset values for relationship analysis. In addition to this, monthly and annual analyses were also carried out for the BRB area.

5.2 DATA USED

5.2.1 Hydro-climatic data

Daily observed surface climate data of precipitation (P), minimum and maximum temperature (Tmin and Tmax) and relative humidity (RH) were obtained from India Meteorological Department, Pune for January-2001 to December-2013. Prior to analysis, data was checked, and missing data were filled with average sampling method using neighboring station values. Further, discharge (Q) and sediment data were obtained from the Yamuna Basin Organization (YBO), Central Water Commission (CWC), New Delhi. In this study, discharge and sediment data of Betwa basin outlet i.e. Shahijina gauging station has been utilized for the correlation analysis.

5.2.2 MODIS NDVI & Land Cover data products

In this study, remotely sensed time-series datasets of MODIS NDVI (collection 5) Terra (MOD13Q1) and MODIS Land Cover Type (MCD12Q1) products have been used to assess relationship with hydro-climatic variables. These datasets were retrieved from the online Reverb tool (http://reverb.echo.nasa.gov/reverb/). The Betwa basin area is covered within one MODIS tile (h25v06). Details of MODIS data products are given in Table 5.1.

Table 5.1: Details of MODIS data products

MODIS data type	Spatial resolution	Temporal resolution	Data availability
MODIS NDVI	250 m	16 days	January-2001 to December-2013
MODIS Land Cover	500 m	1 year	2001 to present

For NDVI data, the scale factor 0.0001 was multiplied to obtain NDVI values (https://lpdaac.usgs.gov/dataset_discovery/modis/modis_products_table/mod13q1_v006). Then, average NDVI values were calculated from an attributes of each MODIS imagery tile. From MODIS land cover data, histogram values were obtained from their attributes, and used to calculate the area wise distribution of all present land cover classes.

The NDVI data quality was also assessed using corresponding quality assessment (QA) information that describes the utility of NDVI values. Invalid data were eliminated and interpolated linearly. The Savitzky-Golay filtering method was employed to de-noise and to smooth the NDVI time-series data as shown in Figure 5.1. This method uses local polynomial regression to determine the

smoothed data values at each data point. Therefore, it performed best to de-noise the temporal NDVI data (Geng et al., 2014). The reliability band of MOD13Q1 data composite has been used to weight each data point in the NDVI time-series. For this, good data (value 0) had full weight (1), marginal data (values 1-2) had half weight (0.5), and cloudy data (value 3) had minimum weight (0.1). The function-fitting was carried out using TIMESAT software (Jönsson & Eklundh, 2004).

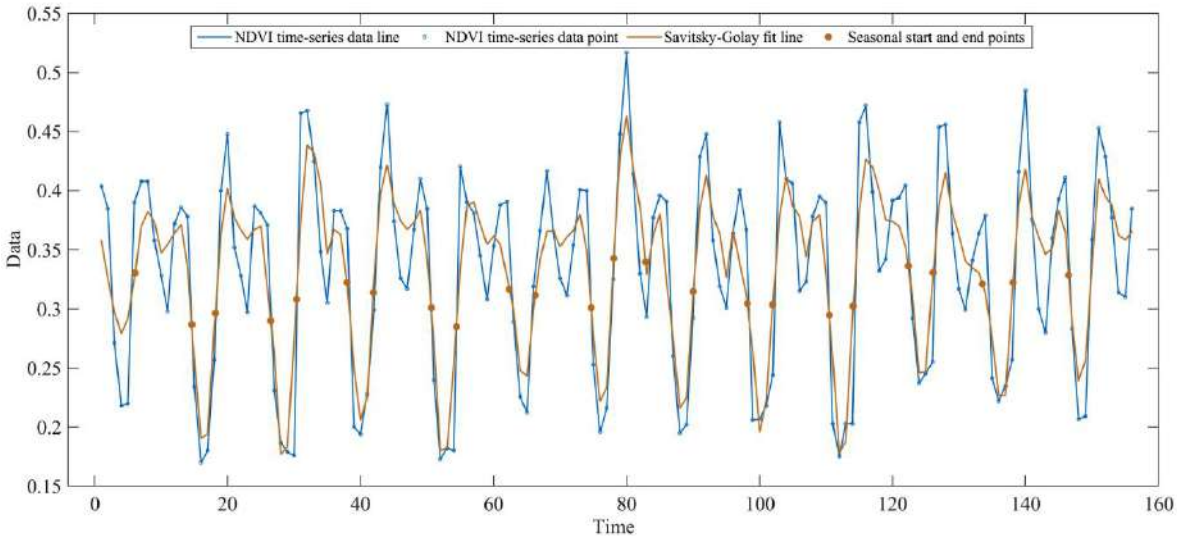

Figure 5.1: Smoothed NDVI time-series illustrating original MODIS NDVI values (blue line) and de-noised temporally interpolated NDVI values (brown line)

5.3 METHODOLOGY

Detailed methodology flowchart is given in Figure 5.2.

5.3.1 Blaney-Criddle method

In this study, the temperature based Blaney-Criddle method (Blaney and Criddle, 1962) has been used for estimation of potential evapotranspiration (PET) using the Equation 5.1.

$$PET = K \times p \times (0.46 \times T_{mean} + 8.13) \quad \text{...(5.1)}$$

where, PET is the daily potential evapotranspiration (mm/day); K is the monthly consumptive use coefficient depending upon the vegetation type, location and season (Vangelis et al., 2013); p is the mean daily percentage of maximum possible annual day light hours; and T_a is the mean temperature (°C).

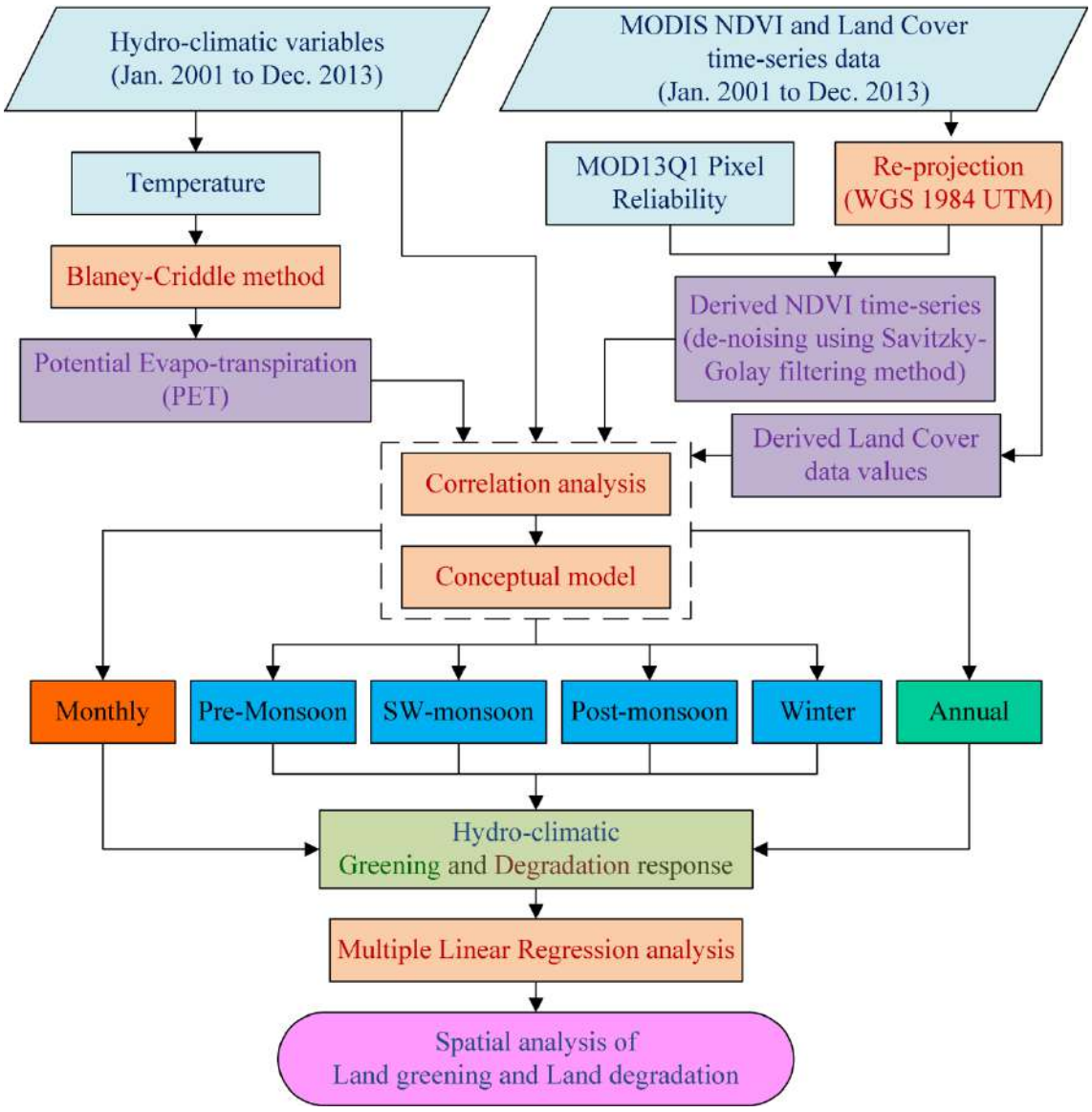

Figure 5.2: Methodology flowchart used in this study

5.3.2 Dry and Wet spells

In this study, dry and wet spell effects are mainly focused on land greening and degradation response analysis. The 13 years of time-series data were categorized into dry and wet years employing standardized anomalies of the annual rainfall time-series (Figure 5.3). Negative and positive anomaly values were categorized as dry and wet years respectively. Thus, the total analysis period was categorized into nine dry years (2001, 2002, 2005, 2006, 2007, 2008, 2009, 2010 and 2012) and four wet years (2003, 2004, 2011 and 2013). It is inferred that annual rainfall is skewed

towards dry years. However, based on standard deviations the 2007 and 2013 were found to be an extreme dry and wet years respectively.

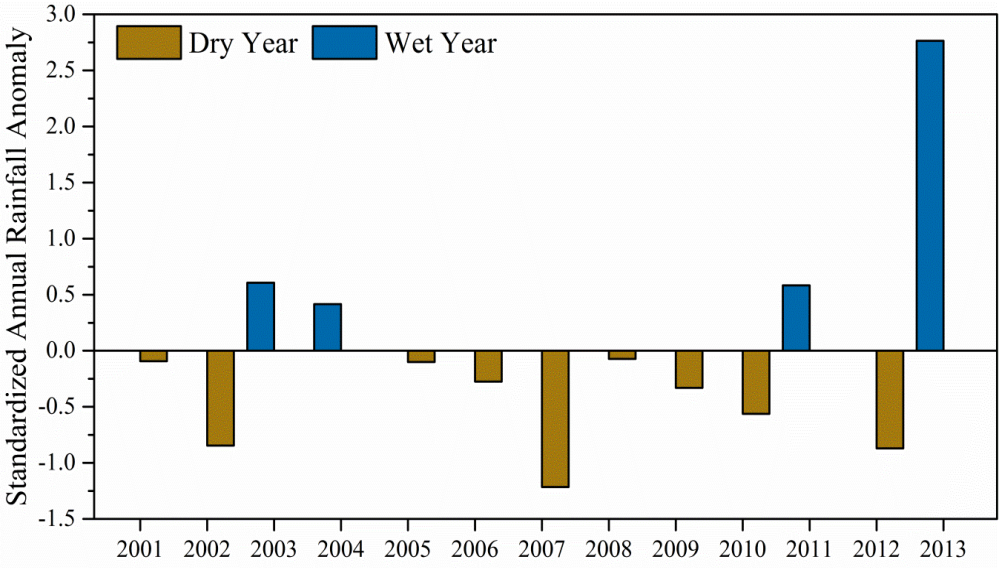

Figure 5.3: Standardized annual rainfall anomalies over the years 2001 to 2013

From the hydro-climatic variables, few variables were selected for the relationship analysis i.e. aridity index (P/PET) and temperature difference (Tmax-Tmin). Depending on the temporal scale of satellite data, these variables were calculated on monthly, seasonal and annual basis to measure dry and wet spell effects over the BRB. These data sets were further used for relationship analysis using correlation and multiple linear regression methods.

5.3.3 Correlation method

There are two types of correlation i.e. positive correlation and negative correlation.

(a) Positive Correlation

The correlation is said to be positive correlation if, the values of two variables *x* and *y* changing with same direction and indicated by '+' sign.

- As *x* is increasing, *y* is increasing
- As *x* is decreasing, *y* is decreasing

(b) Negative Correlation

The correlation is said to be negative when the values of variables *x* and *y* change with opposite direction, and indicated by '-' sign.

- As *x* is increasing, *y* is decreasing
- As *x* is decreasing, *y* is increasing

Relationship between two variables is expressed in the terms of correlation coefficient (r). The value of r varies from -1 to +1, where -1 shows perfect negative relation and +1 indicate perfect positive relation. However, zero value shows that there exist no relationship. It is expressed as shown in Equation 5.2.

$$r = cor(x, y) = \frac{\sum_{i=1}^{n}(x_i - \bar{x})(y_i - \bar{y})}{\sqrt{\left[\sum_{i=1}^{n}(x_i - \bar{x})^2\right]\left[\sum_{i=1}^{n}(y_i - \bar{y})^2\right]}} \quad ...(5.2)$$

where, x_i be the independent variable and y_i be the dependent variable, and $\bar{x}$ and $\bar{y}$ are the mean values of x_i and y_i variables respectively.

5.3.4 Regression method

There are two types of regression methods:

(a) Simple Regression method

Regression analysis is one of the statistical tools that can be used for the investigation of relationship between two variables. Relationship between two variables associated with their changes, analyzed graphically in direct or indirect category. Direct relationship between two variables means a positive relationship in which they increase or decrease in conjunction. While, indirect relationship between two variables means negative relationship in which one decreases when the other increases and vice-versa.

The relationship between two variables plotted on co-ordinate system is linear by drawn straight line through all the data points. To examine the graphs and the data points, straight line is drawn to get the Equation 5.3:

$$y = c \times x + b \quad \ldots(5.3)$$

where, *y* is the dependent variable, *c* is the slope, *x* is the independent variable and *b* is the intercept (the point where the line crosses the y-axis).

Analysis between dependent variables (NDVI and land cover) and independent variables (hydro-climatic variables) has been carried out employing correlation analysis and plotting their pair of data values in the graph. In this study, analysis was performed using MS-Excel. Regression analysis has been also used in combination with the statistical techniques to determine the data validity points within a data set. The regression value is termed as R^2 on the graph which shows goodness-of-fit of the line through given points. It means, $R^2 = 1$ indicates that all points lies exactly on the same line.

(b) Multiple Linear Regression method

In the present study, the MLR method was employed to establish the relationship of MODIS NDVI and land cover data to hydro-climatic variables. The MLR equation is expressed as:

$$y = c + (m_1 \times x_1) + (m_2 \times x_2) + ... + (m_n \times x_n)$$

where, y is the NDVI or land cover class; c is the intercept; and m_1, m_2 ..... m_n are the coefficients of the variables x_1, x_2 ..... x_n.

To compare the relative importance of each variable, the standardized coefficient (β, beta coefficient) has been estimated to measure how many standard deviations of a dependent variable changes per standard deviation increase in the predictor variable. This coefficient standardizes all variables to have a variance equal to 1. It is very helpful to know the effect of independent variables on the dependent variables in a MLR analysis.

5.3.5 Conceptual model for relationship analysis

Four conceptual models namely climatic greening, climatic degradation, non-climatic degradation and non-climatic greening have been developed and utilized for spatiotemporal relationship analysis between hydro-climatic variables and MODIS (NDVI and land cover) datasets.

5.4 RESULTS AND DISCUSSIONS

5.4.1 Pattern analysis

Initially, the time-series pattern of hydro-climatic parameters and MODIS NDVI has been analyzed on monthly, seasonal (winter, pre-monsoon, SW-monsoon and post-monsoon) and annual basis to

understand their trend over the BRB (Figures 5.4a to 5.4d). For MODIS land cover data, only annual analysis has been carried out as this dataset is available on annual time-scale only.

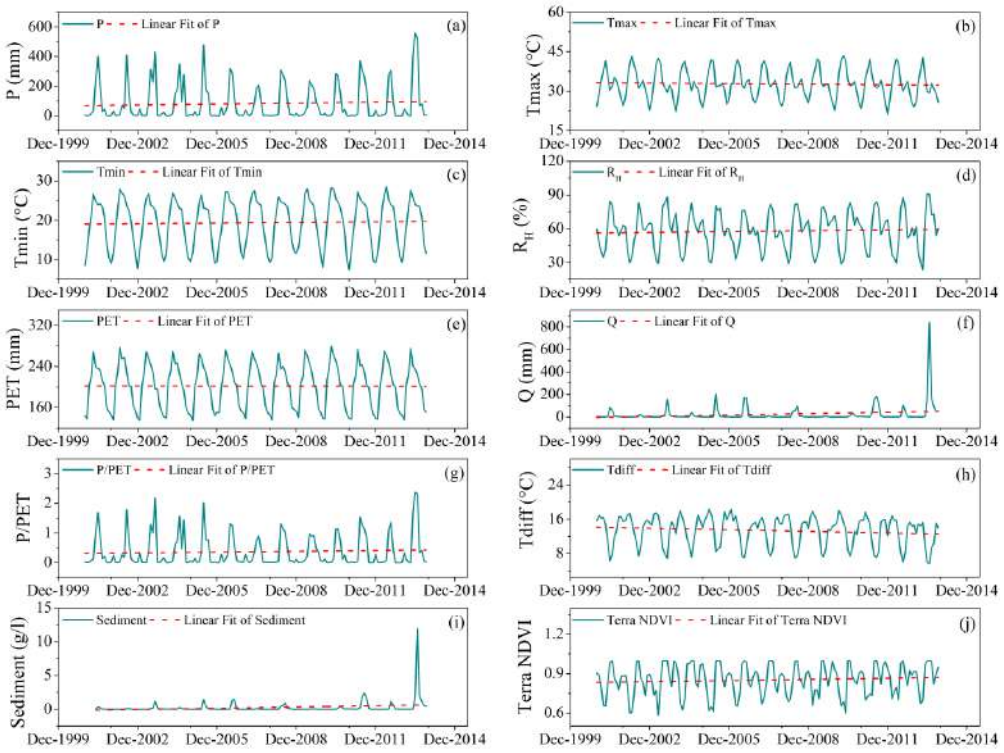

Figure 5.4a: Monthly time series graph of hydro-climatic variables and MODIS NDVI values

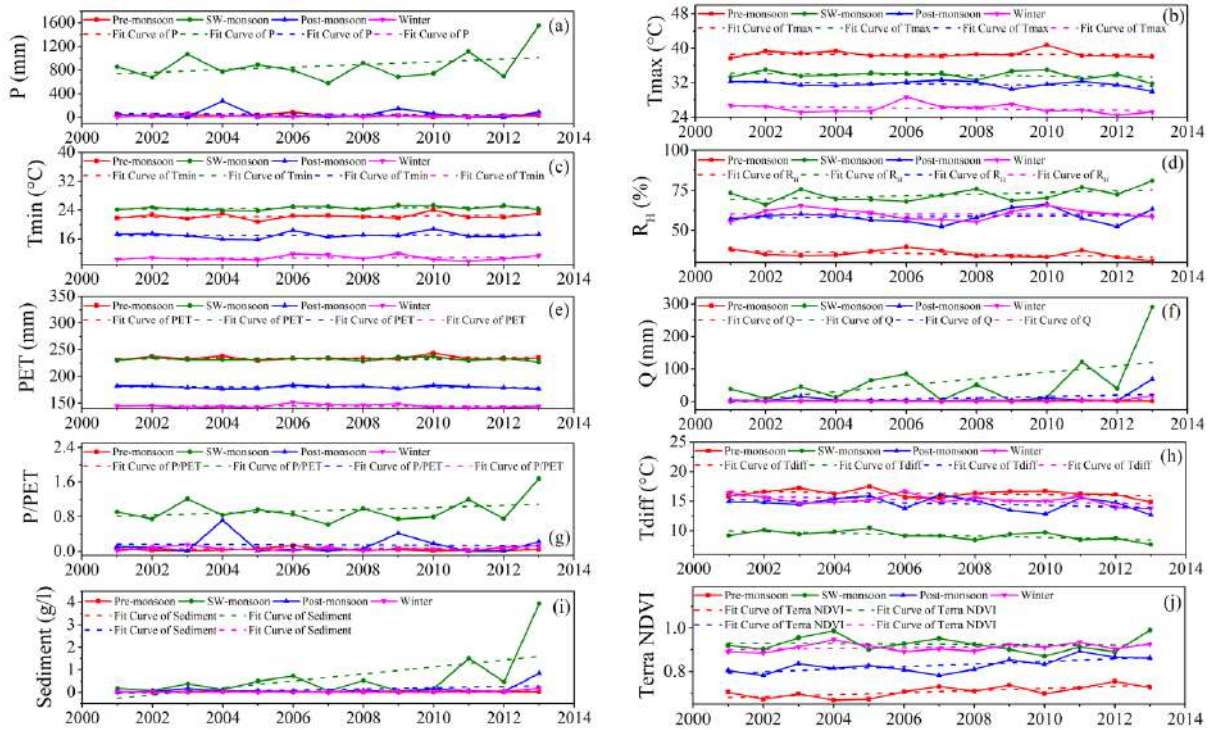

Figure 5.4b: Seasonal time series graph of hydro-climatic variables and MODIS NDVI values

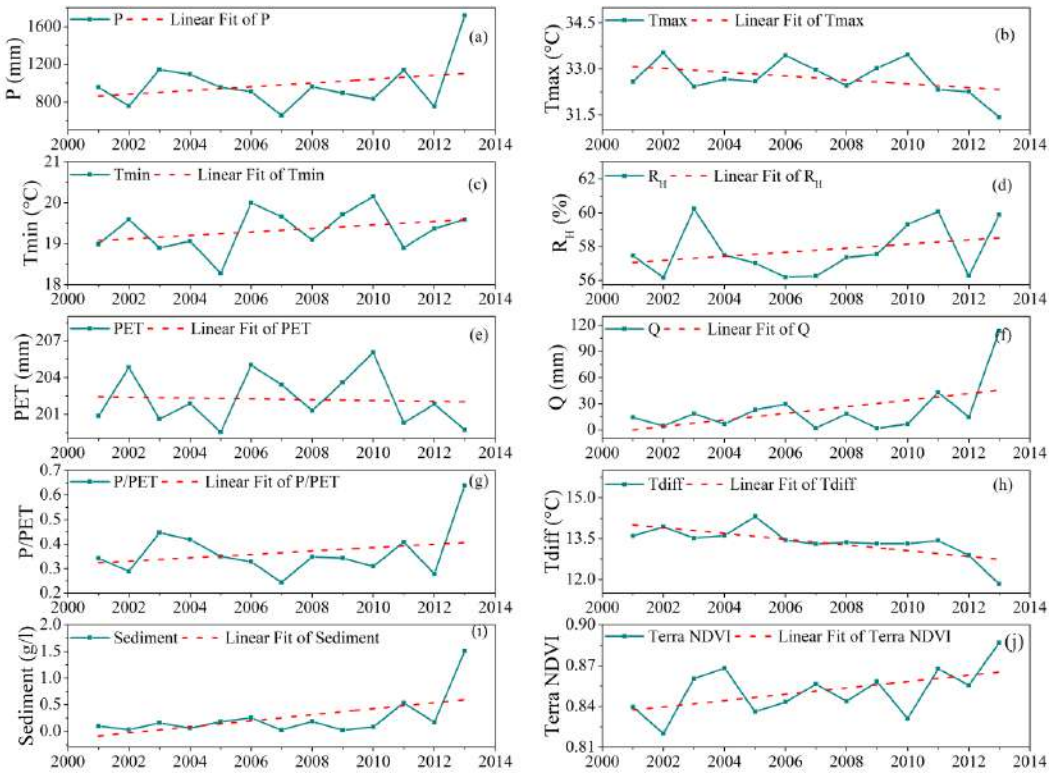

Figure 5.4c: Annual time series graph of hydro-climatic variables and MODIS NDVI values

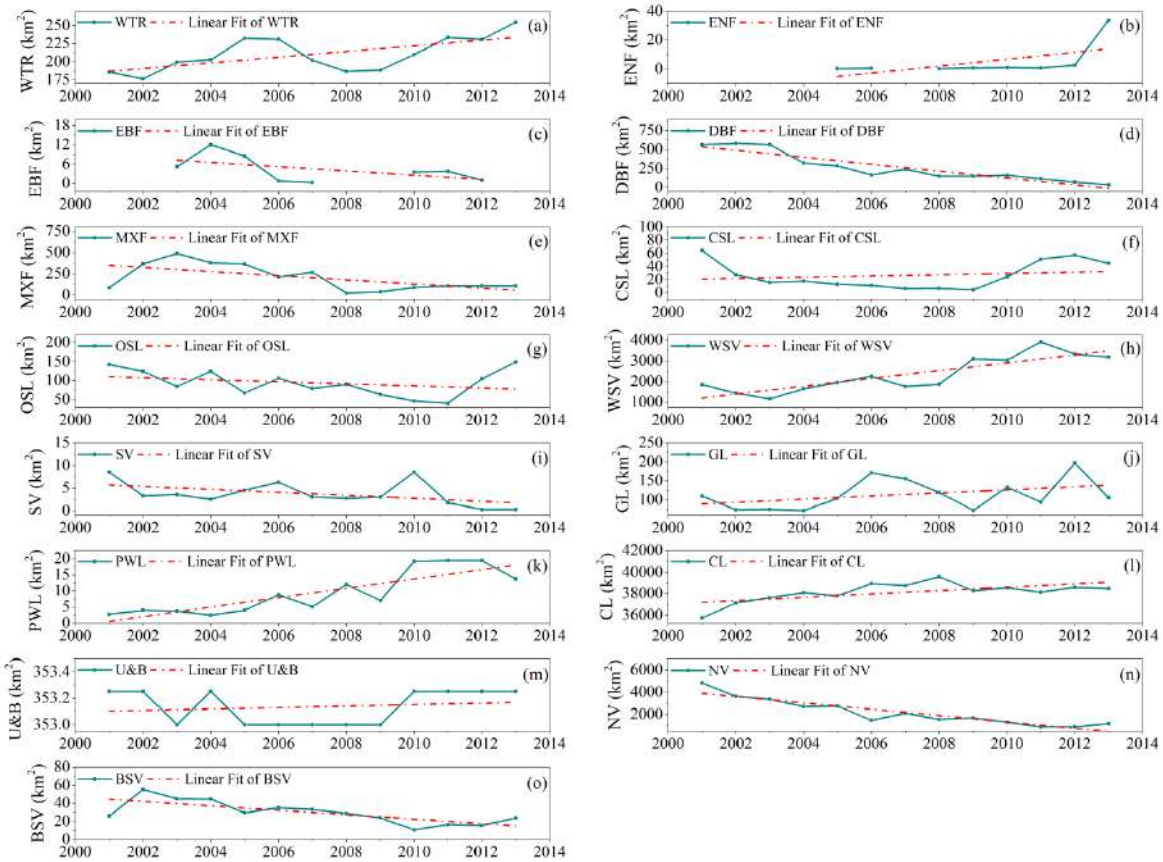

Figure 5.4d: Annual time series graph of MODIS Land Cover classes

a) Pattern of Hydro-climatic variables

The highest annual rainfall of 1718.19 mm was recorded for the year 2013 (Figure 5.4c). Precipitation was increased for SW-monsoon, post-monsoon, winter seasons, and on annual basis by 699.09 mm, 41.65 mm, 45.21 mm and 761.66 mm respectively over the years 2001-2013. Due to precipitation increase, discharge increases by 252.23 mm, 64.49 mm, 16.79 mm and 98.98 mm for SW-monsoon, post monsoon, winter and annual basis respectively (Figures 5.4b and 5.4c). Similarly, sediment yield was also increased by 3.79 g/l, 0.83 g/l, 0.17 g/l and 1.41 g/l (Figure 5.4b). In SW-monsoon season, changes in precipitation brought a significant rise in R_H and P/PET by 7.64% and 0.77 respectively (Figure 5.4b). These variations in the hydro-climatic variable can have strong association with changes in the vegetation and the land cover of the BRB area.

In this study, three temperature parameters, i.e. Tmax, Tmin and Tdiff, were used to understand their response with NDVI and land cover. Among these, Tmax and Tmin showed decreasing (1.16°C) and increasing (0.61°C) annual trends respectively (Figures 5.4b and 5.4c). This opposite pattern has manifested to decrease the trend of temperature difference (Tdiff) over the BRB (Figure 5.4b). This may turn out to be an inadequate seasonal temperature condition for proper plant growth.

Further, the R_H parameter has significant increase in the SW-monsoon season (by 7.64%) and the value of R_H was decreased significantly in the pre-monsoon season (by 7.64%) during the years 2001-2013. The result shows that R_H has a complete reverse pattern for pre-monsoon (decreased by -7.64%) and SW-monsoon season (increased by +7.64%) as shown in Figure 5.4b. This R_H pattern may be induced due to opposite rainfall and temperature pattern in both seasons. Furthermore, more PET losses were also found in pre-monsoon and SW-monsoon seasons as shown in Figure 5.4b. The slight increasing trend of PET (4.01 mm) has been observed in the pre-monsoon season due to increase in Tmin (1.30°C). However, due to varying vegetation pattern and temperature condition, the PET losses were decreased by 5.38 mm and 6.78 mm in post-monsoon (Figure 5.4b) and monthly scale respectively (Figures 5.4a & 5.4b). Further, the aridity index pattern showed slight decrease (0.03) in pre-monsoon season and increase (0.77) in SW-monsoon season. Overall, the annual aridity index pattern was found to be increased by 0.30 (Figure 5.4c). As per the aridity index classification given by Kukal and Irmak (2016), the present analysis reveals that the BRB

area had experienced semi-arid to dry-sub humid climatic condition over the recent years 2001-2013.

b) Pattern of MODIS NDVI and land cover

The significant positive trend of NDVI time-series were observed for pre-monsoon and winter seasons (Figure 5.4b). The BRB area has many small to large capacity water storage structures like tributaries, lake and reservoirs. This might be the reason to show the non-climatic or hydrologic greening response during non-monsoon season. During SW-monsoon season, NDVI has slightly decreasing trend under the increase in SW-monsoon rainfall as shown in Figure 5.4b. This climatic degradation response might be due to wetland condition or flooding condition in the study area.

Further, different MODIS land cover (MCD12Q1) classes showed a significant trend during the years 2001 to 2013 (Figure 5.4d). Among them, significant increase in the area of WSV (1342.50 km^2) and CL (2731.75 km^2) areas were observed. However, a large amount of land degradation about 3652.25 km^2 was obtained for NV. Also, slight decrease in OSL (6.25 km^2) and slight increase in CSL (19.50 km^2) pattern has been also detected in the present study. These changes in shrub land were took place due to the varying hydro-climatic response in the sub-tropical region. The area under ENF and EBF were changed during 2001 to 2013 (Figure 5.4d). These classes have limited data points, therefore not considered in the present study. Further, the result shows that the increase in WTR area from 0.42% to 0.58% indicates increase in surface water availability in the BRB. From last decade, a newly constructed interstate project Rajghat reservoir also gives a major contribution to increase WTR area and to provide water for irrigation, drinking and rehabilitation purpose. Figure 5.4d also shows a greening response to CSL, WSV, GL, PWL and CL areas and degradation response for DBF, OSL, SV, NV and BSV areas of the BRB.

5.4.2 Relationship analysis

The present study also reveals that the more significant correlations was obtained in the wet year analysis as compared to dry year analysis. The WTR class was the most sensitive MODIS land cover area with hydro-climatic variables in dry, wet and all year analysis.

a) Relationship with MODIS NDVI

From hydro-climatic variables, monthly rainfall exhibited a moderate positive correlation with NDVI i.e. a climatic greening response for vegetation in dry, wet and all year analysis (Table 5.2).

Moreover, annual rainfall has good correlation with the NDVI in wet year as compare to dry year. Among temperature parameters, monthly Tmax exhibited a moderate negative correlations with NDVI i.e. a climatic degradation response in dry (r = -0.676), wet (r = -0.649) and all year (r = -0.669) analysis (Table 5.2). Similarly, the difference between maximum and minimum temperature (Tdiff) has moderate negative correlations to the monthly NDVI in dry (r = -0.653), wet (r = -0.642) and all year (r = -0.651) analysis (Table 5.2). This analysis also shows a climatic degradation response to the monthly NDVI. The result shows that, inadequate Tmax and Tdiff may be caused to have a climatic degradation response for monthly vegetative growth in the BRB. From Table 5.2, the Tmax parameter also exhibited significant negative correlation with dry year NDVI in post-monsoon season (r = -0.838) and on annual basis (r = -0.732), and with wet year NDVI in pre-monsoon season (r = -0.983). In wet year, Tmin also exhibited a significant negative correlation (r = -0.776) with NDVI in SW-monsoon season. These results show that increase in Tmax and Tmin could degrade the wet year vegetation cover. The present analysis demonstrated the effect of dry and wet spells to have climatic greening response due to rainfall and a climatic degradation response due to temperature in the BRB.

In addition to this, monthly R_H has a significant positive correlation to the NDVI in dry (r = 0.864), wet (r = 0.854) and all year (r = 0.861) analysis (Table 5.2). Result depict that, effect of dry and wet spells had not altered the positive response between R_H and vegetation cover. The PET parameter has few moderate negative correlations to the NDVI. Annual NDVI (r = -0.668) in dry year analysis, pre-monsoon NDVI (r = -0.704) in wet year analysis and SW-monsoon NDVI (-0.621) in all year analysis showed degradation response to the vegetation cover. During wet years, a positive moderate response (r = 0.653) also exhibited during post-monsoon seasone. Thus, PET parameter has been undergone different response to the vegetation under dry and wet spells effect.

According to the rainfall pattern analysis, the runoff (Q) and the sediment parameters also showed similar response in the wet years (Table 5.2). On monthly basis, the vegetation cover showed a moderate positive response to both Q and sediment in dry, wet and all year analyses. However, a small negative correlation in pre-monsoon season had not changed under dry and wet spells. The result reveals that, small increase in the vegetation cover could decreases runoff and sediment losses, i.e. a negative response. It is also observed that, both Q and sediment have similar response to the vegetation under dry and wet spells (Table 5.2).

During wet years, the aridity index, i.e. P/PET, parameter has significant correlation to the NDVI in post-monsoon (r = -0.712) and winter seasons (r = -0.806) as shown in Table 5.3. It means, the vegetation greening may be responded to deflect the aridity due to wet spell effect. The combined dry and wet spells showed none significant relationship between aridity index and vegetation cover of the BRB (Table 5.2).

In the present study, the most satisfactory correlation results have been observed on the monthly basis. This study demonstrated that NDVI has a more significant relationship in wet years as compared to dry year analysis (Table 5.2). However, the combined dry and wet spells effect showed a moderate response between hydro-climatic variables and vegetation (Table 5.2). But, the R_H parameter is an exceptional parameter possesses significant positive correlations to the monthly NDVI in all year analysis. Under dry spell effect, three temperature parameters were negatively correlated to the NDVI, and hence strongly affected the vegetation cover. However, due to wet spell, the effect of temperature on vegetation cover was resulted moderate positive response in the BRB.

Table 5.2: Correlation between hydro-climatic parameters and MODIS NDVI for dry, wet and all (dry+wet) years

Spells	Analysis	P	Tmax	Tmin	RH	PET	Q	P/PET	Tdiff	Sediment
Dry	Monthly	0.544	-0.676	-0.232	**0.864**	-0.316	0.388	0.561	-0.653	0.382
	Pre-monsoon	-0.090	-0.330	0.023	-0.256	-0.167	-0.120	-0.120	-0.529	-0.192
	SW-monsoon	-0.063	-0.493	-0.237	0.282	-0.441	0.158	-0.087	-0.387	0.077
	Post-monsoon	0.368	-0.838	-0.096	0.244	-0.529	0.173	0.383	-0.424	0.252
	Winter	0.263	-0.333	0.081	0.507	-0.245	-0.123	0.225	-0.547	0.434
	Annual	0.259	-0.732	-0.633	0.332	-0.668	0.228	0.221	0.033	0.288
Wet	Monthly	0.459	-0.649	-0.208	**0.854**	-0.317	0.304	0.464	-0.642	0.277
	Pre-monsoon	0.130	-0.983	-0.188	-0.118	-0.704	-0.285	0.283	-0.454	-0.078
	SW-monsoon	0.115	-0.082	-0.776	-0.134	-0.285	0.186	0.117	0.066	0.214
	Post-monsoon	-0.712	0.262	0.557	-0.220	**0.653**	0.161	-0.712	-0.044	0.180
	Winter	-0.802	**0.651**	-0.173	-0.278	0.443	-0.112	-0.806	0.316	-0.079
	Annual	0.411	-0.264	**0.658**	-0.720	0.281	0.300	0.407	-0.424	0.336
Combined Dry+Wet	Monthly	0.510	-0.669	-0.226	**0.861**	-0.317	0.294	0.520	-0.651	0.243
	Pre-monsoon	-0.024	-0.446	-0.041	-0.173	-0.259	-0.206	-0.034	-0.464	-0.177
	SW-monsoon	0.490	-0.585	-0.511	0.447	-0.621	0.450	0.498	-0.350	0.459
	Post-monsoon	-0.023	-0.494	-0.096	0.240	-0.388	0.334	-0.012	-0.278	0.344
	Winter	0.125	-0.458	-0.165	0.469	-0.383	0.371	0.116	-0.448	0.455
	Annual	-0.054	-0.203	-0.144	-0.332	-0.150	0.017	-0.082	-0.078	0.028

b) Relationship with MODIS Land Cover

In this study, annual MODIS land cover (MCD12Q1) time-series data set has been also well correlated with hydro-climatic variables as shown in Table 5.3. The low annual rainfall in dry years showed none significant response to the vegetation. But in wet years, more annual rainfall showed many significant correlations with all MODIS land cover classes. Due to wet spell, the rainfall was responded to increase surface water availability, i.e. WTR area (r = 0.823). Thus, it induces a climatic greening response to OSL, GL and CL with correlation value r = 0.648, 0.812 and 0.730, respectively (Table 5.3). Further, the climatic degradation response was observed for the DBF, MXF and SV with correlation value r = -0.623, -0.569 and -0.842 respectively. The combined effect of dry and wet spells resulted a moderate rainfall response only with WTR (0.525) area as shown in Table 5.3. The result demonstrated that, the prolonged dry spell might suppress the effect of wet year rainfall on the land cover area.

In dry year analysis, the Tmax and Tmin parameters have none significant effect on land cover area (Table 5.3). Nevertheless, the difference between maximum and minimum temperature (Tdiff) showed several moderate relationships with DBF (0.602), MXF (0.704), WSV (-0.634), GL (-0.602), PWL (-0.677) and NV (0.606). But, in wet years, the Tmax was significantly affected on WTR and GL area with correlation values of r = -0.885 and -0.894, respectively. However, the SV area (r = 0.849) was responded positively by the Tmax parameter as shown in Table 5.3. The Tmin parameter also showed few significant correlations with OSL, SV and CL under correlation value of r = 0.815, -0.838 and 0.801 respectively. The result shows that, crop growth is very sensitive to the changes in the Tmin under the wet spell effect. Moreover, the developed temperature parameter Tdiff showed a significant positive correlation with SV (r = 0.870), i.e. climatic greening response. The Tdiff parameter also showed climatic degradation response to WTR, GL and CL under correlation value of r = -0.852, -0.837 and -0.762, respectively. The result shows that the rise in temperature difference may induce climatic degradation response to the crop land. Hence, it could affect agriculture production in the BRB. From Table 5.3, the combined effect of dry and wet spells shows only moderate responses in the present study.

Among other hydro-climatic parameters, R_H has a moderate response to MODIS land cover in dry and wet year analysis (Table 5.3). However, in all year analysis, R_H has none good response to land cover. During a wet spell, the PET parameter exhibited significant negative response with WTR (r =

-0.790) and GL area (r = -0.867). From Table 5.3, the PET and the aridity index have some moderate correlations with the land cover in wet year analysis.

Moreover, two hydrologic parameters, Q and sediment, exhibited a moderate positive correlation to the WTR area in dry years as shown in Table 5.3. With respect to the rainfall, more Q and sediment losses were produced under the wet spell. In the present study, the Q parameter shows the significant positive response with WTR, GL and CL with a correlation value of r = 0.939, 0.940 and 0.776, respectively. It means, these land cover classes helps to induce more runoff during wet years. Also, the Q parameter shows the negative response with DBF, MXF and SV areas with correlation values of r = -0.753, -0.748 and -0.907 (Table 5.3). The result reveals that the DBF, MXF and SV area have significant impact on minimizing surface runoff. Furthermore, the sediment parameter has a positive correlation to the increased area of WTR, GL and CL with correlation values of r = 0.945, 0.940 and 0.801 respectively (Table 5.3). Also, sediment was negatively correlated to decrease in the area of DBF, MXF and SV with correlation values of r = -0.774, -0.761 and -0.922 respectively. This shows that both Q and sediment parameters were similarly responded to all land cover classes. Among them, the DBF, MXF and SV classes helps to reduce Q and sediment losses during wet years. On an annual basis, the combined dry and wet spell effect shows only moderate positive response of Q and sediment parameters to WTR area with correlation values of r = 0.728 and 0.707 respectively (Table 5.3).

This study also reveals more significant correlations in the wet year analysis as compare to the dry year analysis. It is observed that, the WTR class was the most sensitive land cover class to the hydro-climatic variables in dry, wet and all year analysis. In wet years, other land cover classes were also well responded to the hydro-climatic variables due to the effect of wet spells.

Development of MLR models for land greening and degradation

In this study, MLR models were developed between hydro-climatic variables and MODIS (NDVI and land cover) datasets (2001-2008), and then validated for the years 2009 to 2013. Each MLR model was evaluated using coefficient of correlation (r) value and enables to be utilized for better prediction. Multiple Linear Regression (MLR) models were developed for the relationship between hydro-climatic variables and MODIS NDVI and land cover for the years 2001-2008.

Table 5.3: Correlation between hydro-climatic parameters and MODIS land cover for dry, wet and all (dry+wet) years

Spells	LC class	P	Tmax	Tmin	RH	PET	Q	P/PET	Tdiff	Sediment
Dry	WTR	0.008	-0.163	-0.096	-0.144	-0.126	**0.609**	-0.046	-0.055	**0.656**
	DBF	0.040	0.201	-0.264	-0.148	-0.097	-0.172	0.027	**0.602**	-0.373
	MXF	-0.316	0.315	-0.242	-0.518	-0.005	0.085	-0.317	**0.704**	-0.056
	CSL	-0.037	-0.365	-0.168	-0.002	-0.241	0.038	-0.096	-0.190	0.030
	OSL	0.046	-0.159	-0.181	-0.538	-0.207	0.220	-0.031	0.068	0.124
	WSV	-0.054	-0.111	0.362	0.391	0.210	-0.109	0.013	-0.634	0.056
	SV	0.420	0.416	0.155	0.595	0.230	0.167	0.362	0.267	0.043
	GL	-0.340	-0.243	0.229	-0.262	0.053	0.379	-0.455	-0.602	0.515
	PWL	-0.171	-0.106	0.397	0.382	0.285	0.033	-0.171	-0.677	0.268
	CL	-0.156	0.007	0.330	-0.025	0.240	0.148	-0.153	-0.454	0.339
	U&B	-0.249	0.065	0.160	0.225	0.198	-0.267	-0.252	-0.147	-0.241
	NV	0.208	0.009	-0.426	-0.086	-0.307	-0.088	0.179	**0.606**	-0.306
	BSV	-0.157	0.384	-0.067	-0.635	0.113	-0.024	-0.140	0.539	-0.161
Wet	WTR	**0.823**	-0.885	**0.733**	0.406	-0.790	**0.939**	**0.736**	-0.852	**0.945**
	DBF	-0.623	**0.659**	-0.624	-0.076	0.496	-0.753	-0.514	**0.665**	-0.774
	MXF	-0.569	**0.652**	-0.501	-0.286	**0.627**	-0.748	-0.447	**0.612**	-0.761
	CSL	0.480	-0.602	0.352	0.464	-0.711	**0.696**	0.354	-0.523	**0.701**
	OSL	**0.648**	-0.484	**0.815**	-0.416	0.054	0.432	**0.715**	-0.627	0.446
	WSV	0.386	-0.503	0.285	0.359	-0.604	**0.610**	0.253	-0.433	**0.620**
	SV	-0.842	**0.849**	-0.838	-0.135	**0.600**	-0.907	-0.765	**0.870**	-0.922
	GL	**0.812**	-0.894	**0.682**	0.532	-0.867	**0.940**	**0.726**	-0.837	**0.940**
	PWL	0.349	-0.498	0.187	0.549	-0.709	0.591	0.220	-0.392	0.592
	CL	**0.730**	-0.704	**0.801**	-0.118	-0.374	**0.776**	**0.654**	-0.762	**0.801**
	U&B	0.290	-0.262	0.430	-0.418	0.017	0.374	0.193	-0.335	0.410
	NV	-0.490	0.585	-0.415	-0.297	**0.605**	-0.688	-0.363	0.536	-0.701
	BSV	-0.431	0.564	-0.290	-0.495	**0.711**	-0.658	-0.303	0.474	-0.662
Dry+Wet	WTR	0.525	-0.516	-0.042	0.295	-0.357	**0.728**	0.488	-0.489	**0.707**
	DBF	-0.211	0.300	-0.307	-0.089	0.007	-0.416	-0.173	0.584	-0.450
	MXF	-0.046	0.163	-0.344	-0.053	-0.075	-0.203	0.016	0.478	-0.240
	CSL	0.254	-0.449	-0.141	0.226	-0.343	0.357	0.211	-0.332	0.362
	OSL	0.341	-0.294	0.025	-0.247	-0.173	0.338	0.344	-0.323	0.326
	WSV	0.230	-0.285	0.251	0.327	-0.037	0.405	0.188	-0.518	0.446
	SV	-0.336	0.598	0.181	-0.063	0.426	-0.384	-0.36	0.448	-0.428
	GL	-0.363	0.052	0.358	-0.421	0.244	-0.008	-0.408	-0.271	-0.02
	PWL	0.114	-0.228	0.304	0.341	0.066	0.326	0.073	-0.507	0.363
	CL	-0.004	-0.035	0.352	-0.050	0.200	0.136	-0.009	-0.354	0.161
	U&B	0.223	-0.188	0.103	0.224	-0.009	0.235	0.209	-0.285	0.280
	NV	-0.140	0.190	-0.373	-0.164	-0.111	-0.340	-0.118	0.531	-0.378
	BSV	-0.072	0.273	-0.142	-0.292	0.089	-0.231	-0.017	0.408	-0.256

(a) MLR models for NDVI

$$NDVI_{monthly} = 1.287 + (0.632\times10^{-3}\times V1) + (0.101\times10^{-3}\times V2) + (-0.879\times10^{-2}\times V3) + (0.246\times10^{-2}\times V4) + (-0.223\times10^{-3}\times V5) + (-0.239\times10^{-3}\times V6) + (-0.171\times V7) + (-0.026\times V8) + (0.043\times V9)$$

$$NDVI_{winter} = 0.315 + (-0.868\times10^{-3}\times V1) + (0.055\times V2) + (0.037\times V3) + (0.212\times10^{-3}\times V4) + (-0.826\times10^{-2}\times V5) + (0.968\times10^{-2}\times V6) + (-0.015\times V7) + (-0.013\times V8) + (0.465\times V9)$$

$$NDVI_{pre-monsoon} = -14.953 + (-0.019\times V1) + (-1.375\times V2) + (-0.832\times10^{-2}\times V3) + (-0.041\times V4) + (0.260\times V5) + (0.044\times V6) + (12.686\times V7) + (0.543\times V8) + (-1.053\times V9)$$

$$NDVI_{SW-monsoon} = 110.990 + (0.199\times10^{-2}\times V1) + (7.527\times V2) + (-0.011\times V3) + (-0.743\times10^{-2}\times V4) + (-1.425\times V5) + (-0.022\times V6) + (-0.663\times V7) + (-3.687\times V8) + (1.765\times V9)$$

$$NDVI_{post-monsoon} = -6.935 + (2.026\times10^{-5}\times V1) + (-0.644\times V2) + (-0.086\times V3) + (-0.816\times10^{-2}\times V4) + (0.141\times V5) + (0.302\times10^{-2}\times V6) + (0.062\times V7) + (0.304\times V8) + (0.074\times V9)$$

$$NDVI_{annual} = 8.474 + (-0.763\times10^{-3}\times V1) + (0.163\times V2) + (0.261\times10^{-4}\times V3) + (-0.025\times V4) + (-0.048\times V5) + (2.005\times10^{-4}\times V6) + (2.244\times V7) + (-0.141\times V8) + (-0.312\times10^{-3}\times V9)$$

where**,** $V1$=P, $V2$=Tmax, $V3$=Tmin, $V4$=RH, $V5$=PET, $V6$=Q, $V7$=P/PET, $V8$= Tdiff, and $V9$=sediment

(b) MLR models for land cover

$$WTR = 11507.874 + (-1.259\times V1) + (276\times V2) + (13.392\times V3) + (-41.492\times V4) + (-77.306\times V5) + (2.376\times V6) + (3476.170\times V7) + (-178.685\times V8) + (185.612\times V9)$$

$$DBF = -35761.686 + (7.636\times V1) + (845\times V2) + (16.547\times V3) + (317.650\times V4) + (-50.582\times V5) + (-24.771\times V6) + (-19627.450\times V7) + (246.937\times V8) + (-460.871\times V9)$$

$$MXF = 36847.059 + (-7.811\times V1) + (1310\times V2) + (50.715\times V3) + (-102.597\times V4) + (-325.337\times V5) + (3.418\times V6) + (21140.321\times V7) + (-588.630\times V8) + (-594.803\times V9)$$

$$CSL = -1605.085 + (1.270\times V1) + (180\times V2) + (16.051\times V3) + (24.966\times V4) + (-26.550\times V5) + (-3.441\times V6) + (-3065.313\times V7) + (-29.525\times V8) + (14.595\times V9)$$

$$OSL = -4760.006 + (1.676\times V1) + (113\times V2) + (13.017\times V3) + (22.545\times V4) + (-1.977\times V5) + (-4.559\times V6) + (-3788.459\times V7) + (5.052\times V8) + (10.991\times V9)$$

$$WSV = 8.081 + (-1.404\times V1) + (1633\times V2) + (-373.379\times V3) + (-398.541\times V4) + (-4.645\times V5) + (15.579\times V6) + (6159.441\times V7) + (-1246.464\times V8) + (-1218.800\times V9)$$

$$SV = 345.139 + (0.087 \times V1) + (32 \times V2) + (-1.763 \times V3) + (1.183 \times V4) + (-6.171 \times V5) + (-0.185 \times V6) + (-201.841 \times V7) + (-12.029 \times V8) + (2.479 \times V9)$$

$$GL = 11650.714 + (-0.894 \times V1) + (275 \times V2) + (13.38831 \times V3) + (-34.822 \times V4) + (-75.166 \times V5) + (2.842 \times V6) + (1213.185 \times V7) + (-233.603 \times V8) + (-128.883 \times V9)$$

$$PWL = -1025.608 + (0.032 \times V1) + (-62 \times V2) + (-8.810 \times V3) + (1.350 \times V4) + (14.053 \times V5) + (0.425 \times V6) + (-142.190 \times V7) + (25.919 \times V8) + (-13.021 \times V9)$$

$$CL = -58951.618 + (-54.844 \times V1) + (-14400 \times V2) + (4875.467 \times V3) + (-1366.348 \times V4) + (2522.247 \times V5) + (197.662 \times V6) + (130038.607 \times V7) + (2875.467 \times V8) + (-7532.667 \times V9)$$

$$U\ \&\ B = 333.014 + (0.661 \times 10^{-2} \times V1) + (0.180 \times V2) + (-0.136 \times V3) + (0.078 \times V4) + (-0.317 \times 10^{-2} \times V5) + (-0.023 \times V6) + (-84.572 \times V7) + (0.149 \times V8) + (18.980 \times V9)$$

$$NV = -11332460 + (55.742 \times V1) + (0.850 \times V2) + (612885 \times V3) + (1578.825 \times V4) + (-1515.232 \times V5) + (-189.166 \times V6) + (-136849.016 \times V7) + (-885.452 \times V8) + (-6.240 \times V9)$$

$$BSV = -2480 + (-0.028 \times V1) + (-51 \times V2) + (-5.2466 \times V3) + (5.483 \times V4) + (16.927 \times V5) + (-0.240 \times V6) + (92.424 \times V7) + (42.280 \times V8) + (1.881 \times V9)$$

These models were validated for the years 2009-2013 using coefficient of correlation (r) values (Tables 5.4 & 5.5) that enables to be utilized for better prediction.

Table 5.4. Validation of MLR model for MODIS NDVI

NDVI analysis	**Correlation coefficient (r)**
Monthly	0.832
Winter	0.550
Pre-monsoon	0.508
SW-monsoon	0.728
Post-monsoon	0.375
Annual	0.828

Table 5.5. Validation of MLR model for MODIS land cover

Land cover class	Correlation coefficient (r)
WTR	0.752
DBF	0.958
MXF	0.807
CSL	0.517
OSL	0.939
WSV	0.857
SV	0.608
GL	0.645
PWL	0.642
CL	0.705
U&B	0.833
NV	0.656
BSV	0.651

5.4.3 Effects of Dry, Wet and all year analysis

The result shows the significant effect of dry and wet spells on relationship analysis between hydro-climatic variables and MODIS NDVI, and land cover data sets.

(a) Dry spell effects

In dry year analysis, vegetation has similar responses (i.e. positive or negative) on monthly basis (Table 5.2). However, seasonal and annual analysis results varied under dry spell effects over the BRB area. In this study, Tmax and Tdiff showed climatic degradation responses to monthly and seasonal NDVI that declined the vegetation pattern under prolonged dry spell effect. On annual basis, Tmax and Tmin were significantly degraded vegetation area. Deficient and uneven rainfall distribution (Duhan & Pandey, 2013) adversely affected the crop development and growth in the Madhya Pradesh (Lal et al., 1999). The aridity index resulted moderate correlation value of r = 0.50, for NDVI, which shows the inadequate soil moisture condition. In BRB, forest growth was limited by low SW-monsoon rainfall (Shah et al., 2007) and less moist climate condition (Chauhan & Quamar, 2010). The study depicted that the Tdiff is the most affecting climate variable during dry spells which showed more responses to the land cover area.

(b) Wet spell effects

For wet years, monthly correlation analysis between NDVI and some hydro-climatic variables (Tmax, R_H and Tdiff) showed the same response (positive or negative) with vegetation cover (Table 5.2). The increase in the rainfall amount resulted significant climatic degradation response to vegetation cover during post-monsoon and winter seasons. This may be due to saturated cereal-based agriculture area (Chauhan & Quamar, 2012; Quamar & Chauhan, 2014). Previously, similar responses were observed by Chauhan & Quamar (2012) for the South-West forest area of Madhya Pradesh with respect to increased rainfall. The vegetative land shows significant climatic greening response to monthly R_H, however climatic degradation response to annual R_H. The study also depicted that the land degradation response of Tmax in the pre-monsoon season was decreased from SW-monsoon to winter season and upraised climatic-greening response to vegetation.

In wet year analysis, nearly all land cover classes showed good correlations with hydro-climatic variables (Table 5.3). Here, the DBF and MXF showed similar positive response for Tmax, PET and Tdiff parameters; however, negative response to P, Q and sediment (Table 5.3). The prominent CL area exhibited a significant negative correlation with Tmax and Tdiff; as well as positive correlation with P, Tmin, Q, P/PET and sediment in wet year analysis (Table 5.3). The result shows that WTR, DBF, MXF, SV, GL and CL were the most influenced land cover classes due to wet spell effect over the BRB.

(c) Combined Dry & Wet spell effects

The correlation analysis for the full time period, i.e. dry plus wet years, were carried out to investigate combined dry and wet spell effects over the BRB. Very few good correlations were observed between hydro-climatic variables and vegetation as shown in Table 5.2. It is clearly emphasized that vegetation was well responded to hydro-climatic variables in monthly and SW-monsoon season analysis. On a monthly basis, certain parameters (Tmax, R_H and Tdiff) showed the similar response to vegetation cover. The moderate response of monthly rainfall showed somewhat climatic greening response. It is observed that, more good correlation results were obtained in the monthly and SW-monsoon season analysis; however, other seasonal and annual analysis showed very less response. This analysis demonstrated that the combined effects of dry and wet spells induced variations in the vegetation response over the BRB area.

In all year analysis, MODIS land cover classes have moderate correlations with hydro-climatic variables as shown in Table 5.3. The WTR class shows more and better response with hydro-climatic variables. These classes were changed under the positive response of P and PET variables. The significant decrease in the annual Tmax shows significant negative response to the increased WTR area.

5.5 SUMMARY

In the present study, a relationship between hydro-climatic variables and MODIS time-series data sets for the years 2001 to 2013 have been developed. MODIS NDVI and land cover data sets were correlated on monthly, seasonal (pre-monsoon, SW-monsoon, post-monsoon and winter,) and annual basis.

Following conclusions are drawn from the analysis:

1. Monthly rainfall exhibited a climatic greening response to vegetation cover in dry, wet and all year analyses. However, Tmax and Tdiff exhibited a climatic degradation response to NDVI. The positive response between monthly R_H and vegetation were not altered under dry and wet spells.
2. In pre-monsoon season, the vegetation cover was positively increased under non-climatic or hydrologic greening response due to available surface water resources. However, insufficient temperature condition in SW-monsoon season caused the climatic degradation response to vegetation growth.
3. On annual basis, MODIS land cover experienced climatic greening response for ENF, CSL, WSV, GL, PWL and CL area due to increased annual rainfall (761.66 mm) and WTR area of the BRB. However, the non-climatic degradation response for DBF, CSL, SV, GL, NV and BSV area were mainly caused owing to increased anthropogenic activities within the study area.
4. In dry years, Tdiff parameter is the most sensitive parameter that affected the WSV, GL, PWL and CL areas under climatic degradation response. The prolonged dry spell effects were significantly induced climatic degradation of land due to changes in temperature on monthly, seasonal and annual basis. Moreover, the aridity index shows inadequate moisture condition for vegetation growth under the dry spells.
5. In wet years, more rainfall affects the vegetation growth in post-monsoon and winter season. The R_H shows climatic greening response with monthly NDVI, however climatic degradation

response to annual NDVI. Under wet spells, rainfall responded to increase surface WTR area (r = 0.823), and tends to cause a climatic greening response to OSL, GL and CL. Among temperature parameters, Tdiff shows the significant climatic greening response to SV (0.870), and significant climatic degradation response to WTR (-0.852), GL (-0.837) and CL area (-0.762) of the BRB. Further, both Q and sediment parameters showed similar positive and negative responses to the land cover areas.

6. The combined effects of dry and wet spells show the moderate responses to vegetation in monthly and SW-monsoon season analysis only. Moreover, the hydro-climatic variables were also well responded to WTR area of the BRB.
7. The dominant CL area showed significantly positive response with P, Tmin, Q, aridity index and sediment with values of r = 0.730, 0.801, 0.776, 0.654 and 0.801 respectively. It was affected by the Tmax (-0.704) and Tdiff (-0.762) in the wet year analysis. However, in dry and all year analysis, none good correlation has been observed for CL area during the years 2001-2013.
8. Present analysis revealed that MODIS time-series data set has more significant relationships in wet years as compared to dry year analysis. However, combined dry and wet spell effects in all year analysis reduced their responses, and shows moderate correlations with hydro-climatic variability.

CHAPTER 6

APPLICATION OF SWAT MODEL FOR ESTIMATION OF RUNOFF AND SEDIMENT YIELD UNDER CHANGING CLIMATE

In this chapter, the Soil and Water Assessment Tool (SWAT) model has been used to estimate the runoff and sediment yield considering climatic changes in the Betwa River basin. This chapter includes description of the SWAT model, basin attributes, model setup, sensitivity analysis, calibration, validation and the model performance evaluation. Moreover, the bias-corrected and downscaled GCM data has been utilized to simulate the future runoff and the sediment yield for four scenarios 2020 (2020-2039), 2040 (2040-2059), 2060 (2060-2079) and 2080 (2080-2099).

6.1 DESCRIPTION OF THE SWAT MODEL

The SWAT model is a continuous time-scale model that operates on a daily/sub-daily time step. It is a physically based model, and can operate on large basins for long period of time (Arnold et al., 1998). It was developed to predict the impact of land management practices on water, sediment and agricultural chemical yields in large watersheds with varying spatial and temporal conditions (Neitsch et al., 2005). The SWAT model underlies the ArcSWAT interface where ArcGIS is used to provide geographic analyses, which feed into the SWAT model and provide hydrological outputs. The SWAT as described by Bian et al. (1996) is a semi-empirical and semi-physically based model. It adopts existing mathematical equations approximating the physical behavior of the hydrologic system. It is also an advanced lumped or semi-distributed model dividing the catchment into discrete area units for analysis which makes it suitable for integration with a GIS.

The basic model inputs are climatic parameters (rainfall, maximum and minimum temperature, radiation, wind speed, relative humidity), land use/land cover (LU/LC) map, soil map and elevation data (DEM). The study basin is subdivided into sub-basins that are spatially related to one another. This configuration preserves the natural channels and flow paths of the basin. Further, the sub-basins are divided into Hydrological Response Units (HRU's). These HRUs are discrete areas of similar slope, soil and LU/LC through which water is expected to flow in a more or less homogenous fashion. It lumps the results at the outflow of each unique area. Final results are then summarized for the whole basin at the final outlet. Each of these is analyzed separately to improve the accuracy of the model, but results are lumped per sub-basin and averaged for the entire catchment in the present report.

No matter what physical problem is studied using SWAT, water balance is the driving force behind everything that happens in the watershed (Neitsch et al., 2005). Water Balancing simply means; finding out how much water comes into the system and then finding out where that water goes. In terms of water balance storages for each HRU in the watershed, four layered storage possibilities exist. Snow is the first, then a soil profile of up to 2 meters, followed by a shallow aquifer underneath it comprising the next 18 meters up to 20 meters, and a deep aquifer sitting below 20 meters underground is the final storage space from which water is ultimately completely lost to the SWAT system. Water balance equation used by the SWAT model is given below:

$$SW_t = SW + \sum_{t-1}^{t} (R - Q - ET - P - QR) \quad \ldots (6.1)$$

where, SW_t is the final soil water content (mm), SW is the initial soil water content (mm), t is the time (days), R is the amount of precipitation (mm), Q is the amount of surface runoff (mm), ET is the amount of evapotranspiration (mm), P is percolation (mm) and QR is the amount of return flow (mm).

6.1.1 Surface runoff

In SWAT, surface runoff amounts can be estimated either by using the SCS curve number or the Green & Ampt infiltration method. In the present study, the SCS curve number method has been used for estimation of runoff. It is an empirical model that estimates the amounts of runoff under varying land use and soil types. The SCS curve number equation used in the model is as follows (USDA, 1972):

$$Q = \frac{(R - 0.2s)^2}{(R + 0.8s)} \qquad R \geq 0.2s \quad \ldots (6.2)$$

$$Q = 0.0, \qquad R \leq 0.2s \quad \ldots (6.3)$$

where, Q is the daily runoff, R is the daily rainfall, and s is a retention parameter. The retention parameter, s, varies (a) among sub-basins because of the variation in soils, land use, management, and slope (b) with time because of changes in soil water content. The parameter s is related to curve number (CN) by the SCS equation (USDA, 1972):

$$s = 254\left(\frac{100}{CN} - 1\right) \quad \ldots (6.4)$$

The constant, 254, in the above equation gives *s* in mm. Thus, *R* and *Q* are also expressed in mm. *CN* is the curve number for antecedent moisture condition (AMC) II. The values of curve number for different land use conditions and hydrologic soil groups are applied to AMC II only, i.e. for average condition. The equation gives the value (Q) in terms of runoff depth. In this study, runoff curve numbers (AMC-II) values for the Indian conditions were adopted from Narayana (1993).

6.1.2 Percolation

The percolation component of the SWAT uses a storage routing technique combined with a crack-flow model to predict flow through each soil layer. Once water percolates below the root zone, it is lost from the watershed (becomes groundwater or appears as return flow in downstream basins). The storage routing technique is based on the following equation:

$$SW_i = SW_{oi} \exp\left(\frac{-\Delta t}{TT_i}\right) \quad \ldots (6.5)$$

where, SW_i and SW_{oi} are the soil water contents at the beginning and end of the day in mm, Δt is the time interval (24 h), and TT_i is the travel time through layer *i*. Thus, subtracting SW_{oi} from SW_i can compute the percolation:

$$O_i = SW_{oi}\left[1 - \exp\left(\frac{-\Delta t}{TT_i}\right)\right] \quad \ldots (6.6)$$

where, O_i is the percolation rate in mmd^{-1}.

The travel time, TT_i, is computed for each soil layer with the linear storage equation:

$$TT_i = \frac{(SW_i - FC_i)}{H_i} \quad \ldots (6.7)$$

where, H_i is the hydraulic conductivity in mmh^{-1} and *FC* is the field capacity minus wilting point water content for layer *i* in mm. The hydraulic conductivity varies from the saturated conductivity value at saturation to near zero at field capacity.

$$H_i = SC_i\left(\frac{SW_i}{UL_i}\right)^{\beta_i} \quad \ldots (6.8)$$

where, SC_i is the saturated conductivity for layer *i* in mmh^{-1}, UL_i is soil water content at saturation in mm mm^{-1}. β_i is a parameter that causes H_i to approach zero as SW_i approaches FC_i. The equation for estimating β is

$$\beta_i = \frac{-2.655}{\log_{10}\left(\frac{FC_i}{UL_i}\right)} \quad \ldots (6.9)$$

The constant (-2.655) in equation (4.9) was set to assure H_i = 0.002SC_i at field capacity. Upward flow may occur when a lower layer exceeds field capacity. The soil water to field capacity ratios of the two layers regulates movement from a lower layer to an adjoining upper layer. Percolation is also affected by the soil temperature. If the temperature in a particular layer is at 0°C or below, no percolation is allowed from that layer.

6.1.3 Lateral subsurface flow

Lateral subsurface flow in the soil profile (0-2 m) is calculated simultaneously with percolation. A kinematic storage model (Sloan et al., 1983) is used to predict lateral flow in each soil layer.

$$q_{lat} = 0.024\frac{(2S\ SC\sin(\alpha))}{\theta_d \times L} \quad \ldots (6.10)$$

where, q_{lat} is lateral flow (mm d^{-1}), S is drainable volume of soil water (mh^{-1}), α is slope (m/m), θ_d is drainable porosity (mm^{-1}), and L is flow length (m). If the saturated zone rises above the soil layer, water is allowed to flow to the layer above (back to the surface for the upper soil layer), to account for multiple layers, the model is applied to each soil layer independently, starting at the upper layer.

6.1.4 Ground water flow

Ground water flow contribution to total stream flow is simulated by creating shallow aquifer storage. The water balance for the shallow aquifer is

$$Vsa_i = Vsa_{i-1} + Rc - revap - rf - perc_{gw} - WU_{SA} \quad \ldots (6.11)$$

where, *Vsa* is the shallow aquifer storage (mm), *Rc* is recharge (percolate from the bottom of the soil profile) (mm), *revap* is root uptake from the shallow aquifer (mm), *rf* is the return flow (mm), $perc_{gw}$ is the percolation to the deep aquifer (mm), WU_{SA} is the water use (withdrawal) from the shallow aquifer (mm), and *i* is the day.

Return flow from the shallow aquifer to the stream is estimated with the equation (Arnold et al., 1993):

$$rf_i = rf_{i-1}e^{-\alpha\Delta t} + Rc(1.0 - e^{-\alpha\Delta t}) \quad \ldots (6.12)$$

where, α is the constant of proportionality or the reaction factor.

The relationship for water table height is (Arnold et al., 1993):

$$h_i = h_{i-1} e^{-\alpha \Delta t} + \frac{Rc}{0.8 \mu \alpha} (10 - e^{-\alpha \Delta t}) \quad \text{... (6.13)}$$

where, h is the water table height, (m above stream bottom), and μ is the specific yield.

6.1.5 Evapotranspiration

Evapotranspiration (*ET*) is one of the most basic components of the hydrologic cycle. It affects the water balance from the time of precipitation until the residual reaches the ocean. There are three methods for estimating PET in the SWAT model: (1) Penman-Monteith (Monteith, 1965). (2) Hargreaves (Hargreaves and Samani, 1985) and (3) Priestley-Taylor (Priestley and Taylor, 1972). The Priestley-Taylor method requires solar radiation and air temperature as input, while the Hargreaves method requires air temperature only. If wind speed, relative humidity, and solar radiation data are not available, the Hargreaves methods provide options that give realistic results in most cases (Arnold et al., 1998 and Williams et al., 2008). In the present study, Hargreaves method was used for estimating the evapotranspiration.

$$\lambda E_O = 0.0023 H_O (T_{mx} - T_{mn})^{0.5} (T_{av} + 17.8) \quad \text{… (6.14)}$$

where, λ is the latent heat of vaporization (MJ/kg), E_o is the potential evapotranspiration (mm/d), H_0 is the extraterrestrial radiation (MJ/m^2/d), T_{mx} is the maximum air temperature for a given day (°C), T_{mn} is the minimum air temperature for a given day (°C), and T_{av} is the mean air temperature for a given day (°C).

6.2 BASIN ATTRIBUTES

The attributes of sub-watersheds, tributary channels and main channels are determined in the ArcSWAT interface as follows (Neitsch et al., 2004):

6.2.1 Subbasin

The first level of subdivision is the subbasin or sub-watershed. Subbasins possess a geographic position in the watershed, and are spatially related to one another. The subbasin delineation may be obtained from subwatershed boundaries that are defined by surface topography so that the entire area within a subbasin flows to the subbasin outlet.

6.2.2 Hydrologic Response Units (HRU)

The land area in a subbasin may be divided into hydrologic response units (HRUs). Hydrologic response units are portions of a subbasin that possess unique landuse/management/soil attributes.

6.2.3 Reach/Main channels

Reach or Main channel is associated with each subbasin in a watershed. Loadings from the subbasin enter the channel network of the watershed in the associated reach segment. Outflow from the upstream reach segment(s) will also enter the reach segment.

6.2.4 Tributary channels

The term tributary channel is used to differentiate inputs for channelized flow of surface runoff generated in a subbasin. Tributary channel inputs are used to calculate the time of concentration for channelized flow of runoff generated within the subbasin and transmission losses from runoff as it flows to the main channel.

6.2.5 Ponds/Wetlands/Reservoirs

Water bodies within a watershed were modelled as ponds, wetlands or reservoirs.

6.3 SWAT MODEL SETUP

The SWAT model setup was carried out with ArcGIS interface. The interface helped to create the stream network, delineate the catchment boundary from the SRTM DEM and further subdivide the catchment into subbasins. The land cover, soil layers and DEM were used to generate HRUs. The climatic data was integrated spatially to assign these data as the main drivers of the model to the different subbasins. The workflow diagram for the model setup was adopted from Lewarne (2009) and further modified as shown in Figure 6.1.

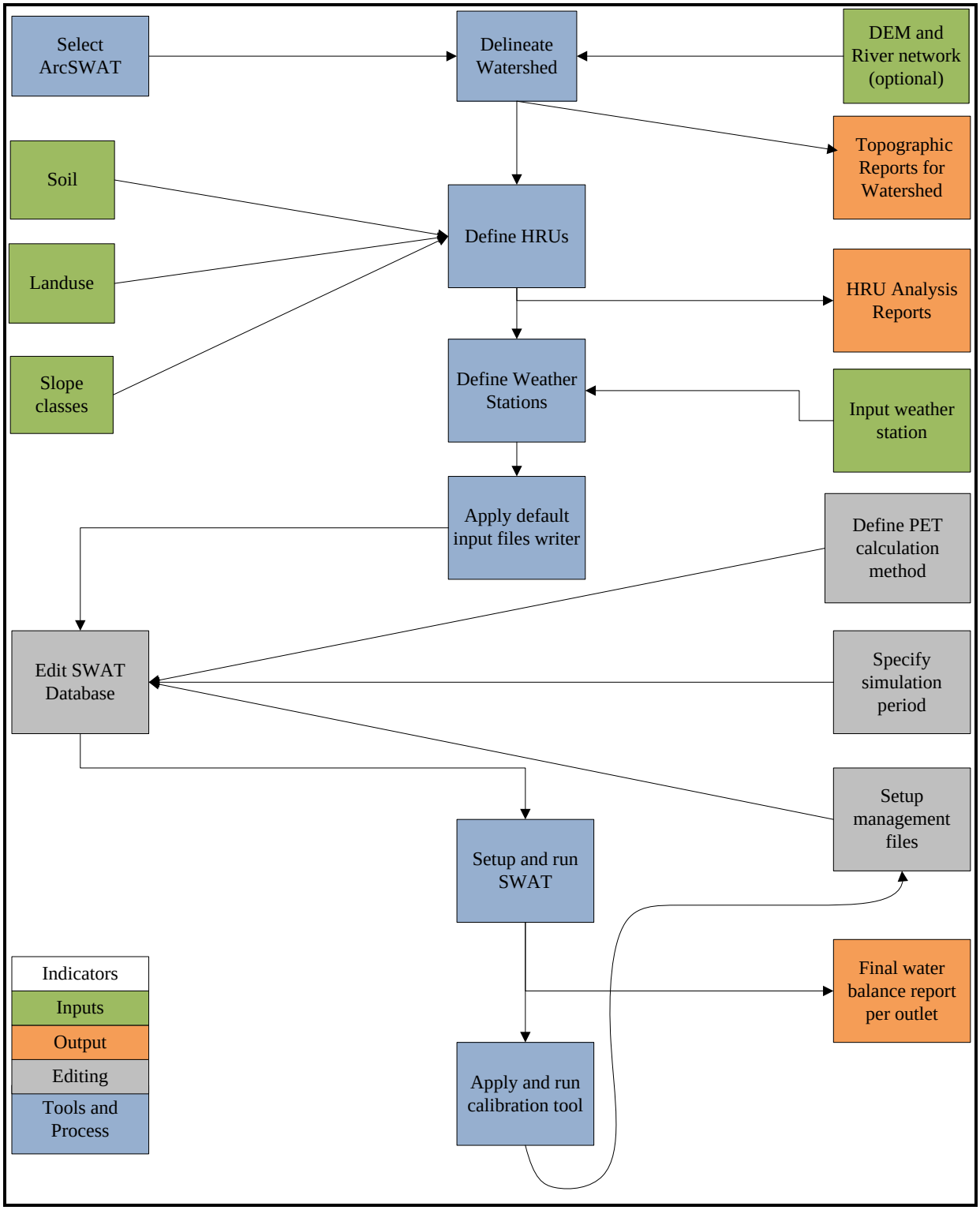

Figure 6.1: Workflow diagram for the SWAT model setup and run

6.3.1 Watershed Delineation

The study area comprises the entire Betwa river which is a tributary of river Yamuna River. The delineation of the study area was done from the DEM of ASTER data sets. The area of the basin (Betwa basin) up to confluence of the Betwa river with the Yamuna (near

Hamirpur) is found to be 43936.59 km^2 from the DEM based delineation. This area fairly matches with the area of the Betwa basin reported in technical report of the Betwa basin (43895 km^2) carried out by (National Water Development Agency) NWDA in 1993 year. The percentage deviation between the reported value and DEM based value used in this study is found to be 0.91. The variation in the drainage area of the Betwa river used in the present study and that reported by NWDA may be due to fixing of the outlet point at the confluence of the Betwa with the Yamuna River in watershed delineation. However, the variation (< 1%) is very small and is considered to be negligible.

6.3.2 Sub basin and HRU definition

The minimum and maximum elevations for the Betwa basin were found to be 61 meters and 715 meters respectively. The study area was divided into 57 sub-basins (Figure 6.2) by strategically selecting outlet points which include the four hydrologic data sites (Basoda, Garrauli, Mohana and Shahijina) and nine reservoirs to facilitate the calibration and validation of the model. Each subbasin boundary marks the end of a reach, the end point of which is the accumulation point for all flow data from upstream which is then fed into the downstream sub basin and reach. Once flow lines are established, the model uses other physical layers to determine HRUs. These unique hydrological response units were defined in the model. The initial run of the model produced 3874 HRUs.

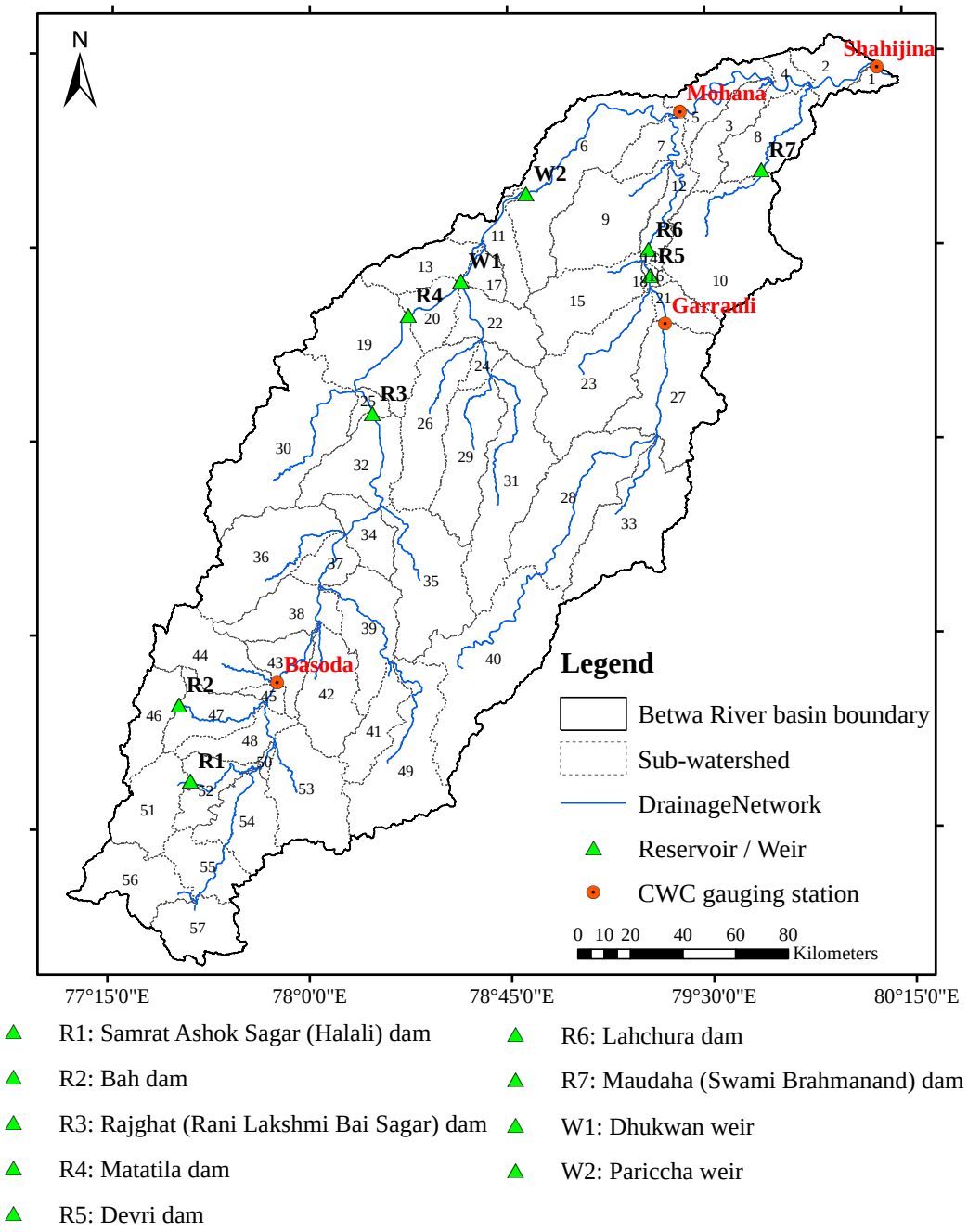

Figure 6.2: Study area (Betwa River basin) details used in SWAT model

6.4 MODEL EVALUATION CRITERIA

Evaluation always involved a comparison of the model outputs to some corresponding measured variable. When presenting model results, the model developers typically do not provide consistent or standard statistical evaluation criteria to assist the readers or users in determining how well their model reproduces the measured data and how well their model compares to other models (ASCE Task Committee 1993). Haan et al. (1982) suggested that the graphical representation of the results could easily be interpreted if the calibration is done

for only one watershed at one stream gauge location. Continuous time series of the recorded and simulated data were used in the present study.

6.4.1 The coefficient of determination (R^2)

It describes the proportion of the total variance in the observed data that can be explained by the model. It is given by:

$$R^2 = \left[\frac{\sum_{i=1}^{n}(x_i - \bar{x})(y_i - \bar{y})}{\sqrt{\sum_{i=1}^{n}(x_i - \bar{x})^2 \sqrt{\sum_{i=1}^{n}(y_i - \bar{y})^2}} \right]^2 \quad \ldots(6.15)$$

where, X_i is the i^{th} observed data, $\bar{x}$ is mean of observed data, Y_i^{sim} is the i^{th} simulated value, $\bar{y}$ is the mean of model simulated value, and n is the total number of events.

The correlation or correlation based measurements (R^2) have been widely used to evaluate the goodness of fit of hydrologic models. It ranges from 0.0 to 1.0, with higher values indicating better agreement. These measures are over sensitive to extreme values and are insensitive to additive and proportional difference between the model simulations and observations (Willmott, 1981, and Leagates and McCabe, 1999).

6.4.2 Nash-Sutcliffe Efficiency (NSE)

The Nash-Sutcliffe efficiency (NSE) is a normalized statistic that determines the relative magnitude of the residual variance ("noise") compared to the measured data variance ("information") (Nash and Sutcliffe, 1970). NSE indicates how well the plot of observed versus simulated data fits the 1:1 line. NSE is computed using the following equation:

$$NSE = 1 - \frac{\sum_{i=1}^{n}(x_i - y_i)^2}{\sum_{i=1}^{n}(x_i - \bar{x})^2} \quad \ldots (6.16)$$

where, X_i is the i^{th} observation for the constituent being evaluated, Y_i is the i^{th} simulated value for the constituent being evaluated, $\bar{x}$ is the mean of observed data for the constituent being evaluated, and n is the total number of observations.

The NSE values can vary from 0 to 1, where 1 indicating a perfect fit. If the daily measured flows approach the average value, the denominator of the Equation 6.16 goes to zero and

NSE approach minus infinity with only minor model miss predictions. This statistics works best when the coefficient of variation for the observed data set is large. The NSE represents an improvement over R^2 for model evaluation as it is sensitive to the differences in the observed and model simulated means and variances. The NSE has been widely used to evaluate the performance of hydrologic models (Wilcox et al., 1990).

6.4.3 Percent bias (PBIAS)

Percent bias (PBIAS) measures the average tendency of the simulated data to be larger or smaller than their observed counterparts (Gupta et al., 1999). The optimal value of PBIAS is 0.0, with low-magnitude value indicating accurate model simulation. Positive values indicate model underestimation bias, and negative value indicates model overestimation bias (Gupta et al., 1999). PBIAS is calculated by using following equation:

$$PBIAS = \left[\frac{\sum_{i=1}^{n} (x_i - y_i) \times 100}{\sum_{i=1}^{n} (x_i)} \right] \quad \ldots (6.17)$$

where, PBIAS is the deviation of data being evaluated, expressed as a percentage.

6.4.4 RMSE-Observations Standard Deviation Ratio (RSR)

RMSE is one of the commonly used error index statistics (Chu and Shirmohammadi, 2004; Singh et al., 2004; Vasquez-Amábile and Engel, 2005). It is commonly accepted that lower the RMSE the better the model performance. Singh et al. (2004) suggested a model evaluation statistic, named the RMSE-observations standard deviation ratio (RSR). The RSR standardizes RMSE using the observations standard deviation, and it combines both an error index, and the additional information recommended by Legates and McCabe (1999). RSR is calculated as the ratio of the RMSE and standard deviation of measured data, as shown in the following equation:

$$RSR = \frac{RMSE}{STDEV} = \frac{\sqrt{\sum_{i=1}^{n} (x_i - y_i)^2}}{\sqrt{\sum_{i=1}^{n} (x_i - \bar{x})^2}} \quad \ldots (6.18)$$

where, *Xmean* is the mean of observed data for the constituent being evaluated, and *n* is the total number of observations. RSR varies from the optimal value of 0, which indicates zero

RMSE or residual variation and therefore perfect model simulation, to a large positive value. The lower is the RSR, the lower the RMSE, and better is the model simulation performance (Moriasi et al., 2007). In this study, criterion suggested by Moriasi et al. (2007) has been adopted to corroborate the monthly performance of the SWAT model (Table 6.1).

Table 6.1: General performance ratings for recommended statistics for a monthly time-step

Performance rating	RSR	NSE	Pbias (%)
Very good	0.00 < RSR < 0.50	0.75 < NSE < 1.00	Pbias < ± 10
Good	0.50 < RSR < 0.60	0.65 < NSE < 0.75	± 10 < Pbias < ± 15
Satisfactory	0.60 < RSR < 0.70	0.50 < NSE < 0.65	± 15 < Pbias < ± 25
Unsatisfactory	RSR > 0.70	NSE < 0.50	Pbias > ± 25

6.5 SWAT MODEL CALIBRATION & VALIDATION

The successful application of a hydrologic model depends on how well the model is calibrated. In this study, manual calibration of the SWAT model has been carried out on monthly basis. After each parameter adjustment and simulation run, the simulated and observed hydrographs were visually compared to examine the improvement in the results. Before starting the calibration, few important observations of the model developer and users of the model were studied; this helped in deciding the parameters to be adjusted. The parameters such as plant uptake compensation factor, soil evaporation compensation factor, groundwater delay, effective hydraulic conductivity in main channel alluvium were taken into consideration for calibration of the model. Different values between the lower limits and upper limits were chosen and the model was run to simulate runoff and sediment. Since many of the input parameters were available for the basin, they were not to be calibrated. The calibration were carried out carried out for Basoda, Garrauli, Mohana and Shahijina gauging stations for the years 2001-2013. The first two years (2001-2002) of the modeling period were reserved for “model warm-up” in order to realistically set-up the states of its internal hydrological components, e.g. groundwater store, soil moisture content etc. Changes in the parameter affecting hydrology were done in a distributed way for selected reach. Parameters were modified by replacement and by multiplication of a relative change depending on nature of the parameter. However, a parameter has never been allowed to go beyond the predefined absolute parameter ranges during the calibration. Thus, the model can be applied for further analysis.

Further, the model outputs have been used for calibration and validation by employing SUFI-2 (Sequential Uncertainty Fitting version 2) algorithm of the SWAT-CUP (SWAT Calibration and Uncertainty Programs). The SUFI-2 algorithm is used to calibration, validation, sensitivity and uncertainty analysis (Abbaspour, 2007; Abbaspour et al, 2007). Monthly observed discharge data of seven years (2003-2009) and four years (2010-2013) were used for calibration and validation, respectively.

6.5.1 Sensitivity analysis

i. One-at-a-time (OAT) sensitivity analysis

In this method, the sensitivity of a variable to the changes in a parameter is analyzed while keeping other parameters constant at some value. The parameter sensitivity has been assessed firstly for runoff, and then for sediment.

ii. Global sensitivity analysis

After selection of sensitive parameters, a global sensitivity analysis was performed to estimate changes in the objective function resulting from changes in each parameter while all other parameters are changing. This gives relative sensitivity based on linear approximations, and provides partial information about sensitivity of the objective function to the model parameters.

The SWAT model calibration parameters and their fitted values are presented in Table 6.2.

Table 6.2: Calibrated parameters and their fitted values for runoff and sediment

Variable	Calibration parameter	Details	Fitted value	Method of variation
Runoff	CN2.mgt	SCS runoff curve number	-0.17	Relative
	ALPHA_BF.gw	Baseflow alpha factor (days)	0.41	Absolute
	GW_DELAY.gw	Groundwater delay (days)	31.70	Absolute
	GWQMN.gw	Treshold depth of water in the shallow aquifer required for return flow to occur (mm)	0.07	Absolute
	SURLAG.bsn	Surface runoff lag time	1.64	Absolute
	GDRAIN.mgt	Drain tile lag time	0.63	Absolute
	SOL_AWC().sol	Available water capacity of the soil layer	0.08	Relative
	ESCO.hru	Soil evaporation compensation factor	0.58	Relative
	RCHRG_DP.gw	Deep aquifer percolation fraction	0.36	Replace
Sediment	PRF.bsn	Peak rate adjustment factor for sediment routing in the main channel.	1.90	Absolute
	SPEXP.bsn	Exponent parameter for calculating sediment reentrained in channel sediment routing.	0.76	Absolute
	ADJ_PKR.bsn	Peak rate adjustment factor for sediment routing in the subbasin (tributary channels)	0.85	Absolute
	LAT_SED.hru	Sediment concentration in lateral flow and groundwater flow.	7.54	Absolute

CH_ERODMO().rte	Jan. channel erodability factor	0.03	Absolute
CH_COV1.rte	Channel erodibility factor	0.08	Absolute
CH_COV2.rte	Channel cover factor.	0.50	Absolute
USLE_P.mgt	USLE equation support practice factor	0.65	Relative
USLE_K().sol	USLE equation soil erodibility (K) factor.	0.13	Relative
USLE_C{1}.plant.dat_____ _AGRL	Min value of USLE C factor applicable to the land cover/plant.	0.15	Replace
USLE_C{7,8}.plant.dat____ __FRSD,FRSE		0.23	Replace
RES_STLR_CO.bsn	Reservoir sediment settling coefficient	0.76	Replace
RES_SED.res	Initial sediment concentration in the reservoir.	1133.79	Absolute
RES_NSED.res	Normal sediment concentration in the reservoir.	19.48	Absolute

6.5.2 Calibration, validation and the SWAT model performance

The SWAT model calibration and validation have been carried out using the SUFI-2 algorithm of the SWAT-CUP. The model performance was assessed at four gauging stations, namely Basoda, Garrauli, Mohana and Shahijina. Different graphs were compared for observed monthly runoff data to the runoff simulated by the SWAT model at the gauging stations (Figure 6.6), which was built into the model as subbasin outlets (outlet no. 2, 6, 27 and 45).

In order to utilize the calibrated model for estimating the effect of different scenarios on water balancing of the Betwa basin, the model was tested against an independent set of measured data. The model was validated with observed data at four gauging sites for independent validation period (2010-2013). Ideally, for large river basins the validation process has to be multisite and based on sensitivity analyses performed in advance. This is especially important when the model has to be further applied at the regional scale and/or for climate variability.

a) Runoff

Firstly, the model was calibrated and validated for runoff. The model showed satisfactory to good performance in calibration and validation on the monthly time scale (Table 6.3). Also, the model results were visualized to check the simulation accuracy (Figure 6.3). In calibration, high values of the R^2 (0.90, 0.94, 0.91 and 0.92), NSE (0.88, 0.91, 0.91 and 0.92), low values of PBIAS (-14.20, -11.10, -7.70 and -16.30) and RSR (0.34, 0.30, 0.31 and 0.29) indicates satisfactory calibration and accurate simulation of runoff at the Basoda, Garrauli, Mohana and Shahijina sites, respectively. For validation, the model performance results R^2 (0.90, 0.92, 0.90 and 0.88), NSE (0.84, 0.91, 0.89 and 0.86), low values of PBIAS (-13.60, -

16.50, -3.90 and -7.50) and RSR (0.41, 0.30, 0.33 and 0.38) indicates satisfactory validation and accurate simulation of runoff at the Basoda, Garrauli, Mohana and Shahijina sites, respectively. Results show that the model performs satisfactory to very good during calibration and validation of runoff.

Table 6.3: SWAT model performance during calibration and validation for runoff

Gauging station	Calibration				Validation			
	R^2	NSE	PBIAS	RSR	R^2	NSE	PBIAS	RSR
Basoda	0.90	0.88	-14.20	0.34	0.90	0.84	-13.60	0.41
Garrauli	0.94	0.91	-11.10	0.30	0.92	0.91	-16.50	0.30
Mohana	0.91	0.91	-7.70	0.31	0.90	0.89	-3.90	0.33
Shahijina	0.92	0.92	-16.30	0.29	0.88	0.86	-7.50	0.38

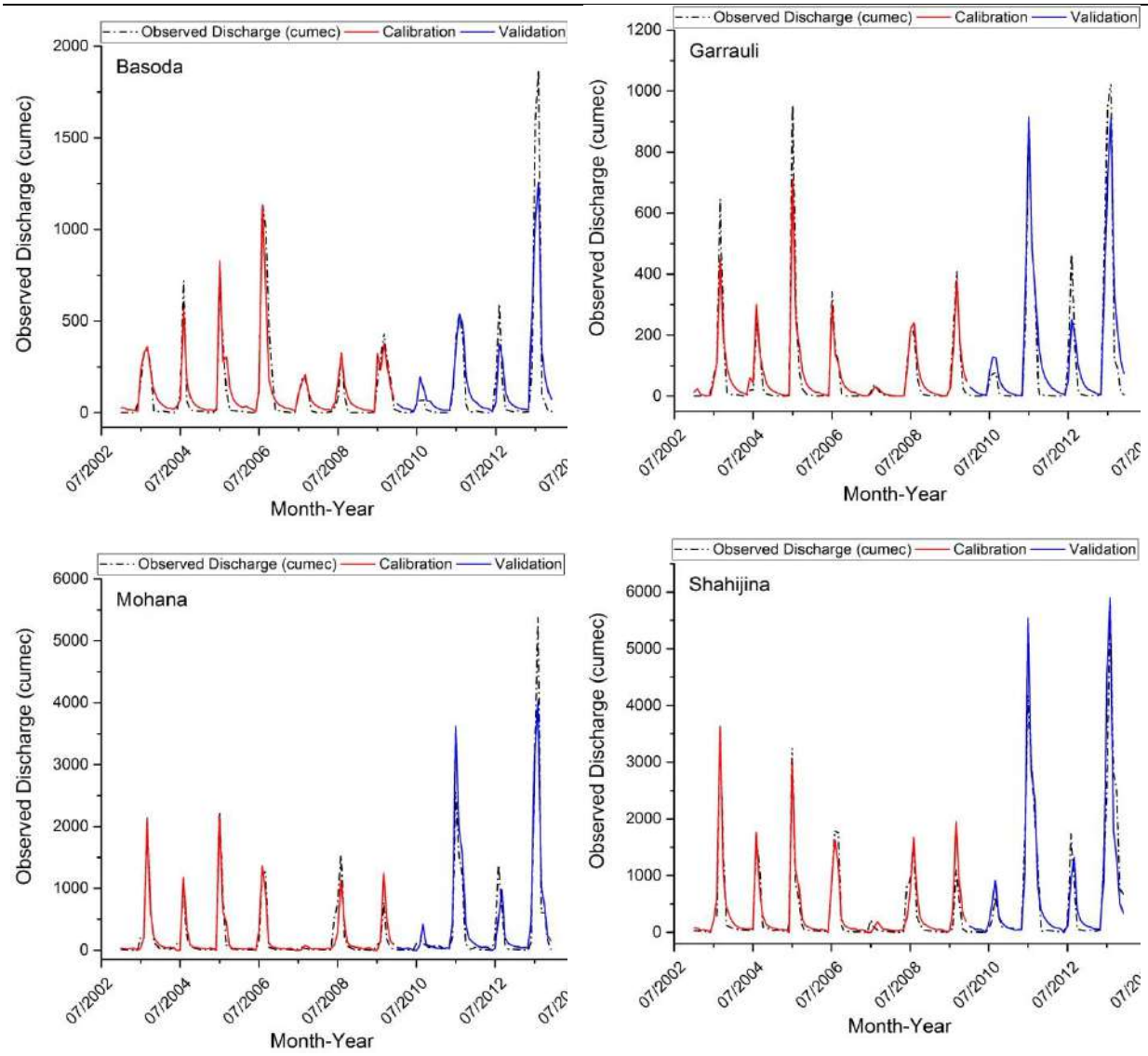

Figure 6.3: Calibration and Validation plots for runoff

b) Sediment

Similarly, the SWAT model was calibrated and validated for the sediment yield. During calibration of sediment, high values of the R^2 (0.89 and 0.78), NSE (0.89 and 0.77), low values of PBIAS (-9.30 and -4.10) and RSR (0.33 and 0.48) indicates satisfactory calibration and accurate simulation of sediment at Garrauli and Shahijina sites, respectively. During validation, the SWAT model performance shows R^2 (0.90 and 0.81), NSE (0.90 and 0.81), low values of PBIAS (0.70 and 1.60) and RSR (0.32 and 0.44) indicates satisfactory to good validation and accurate simulation of sediment at Garrauli and Shahijina sites, respectively (Table 6.4 and Figure 6.4). Thus analysis showed overall good model performance at Garrauli and Shahijina stations.

Table 6.4: SWAT model performance during calibration and validation for sediment

Gauging station	Calibration				Validation			
	R^2	NSE	PBIAS	RSR	R^2	NSE	PBIAS	RSR
Garrauli	0.89	0.89	-9.30	0.33	0.90	0.90	0.70	0.32
Shahijina	0.78	0.77	-4.10	0.48	0.81	0.81	1.60	0.44

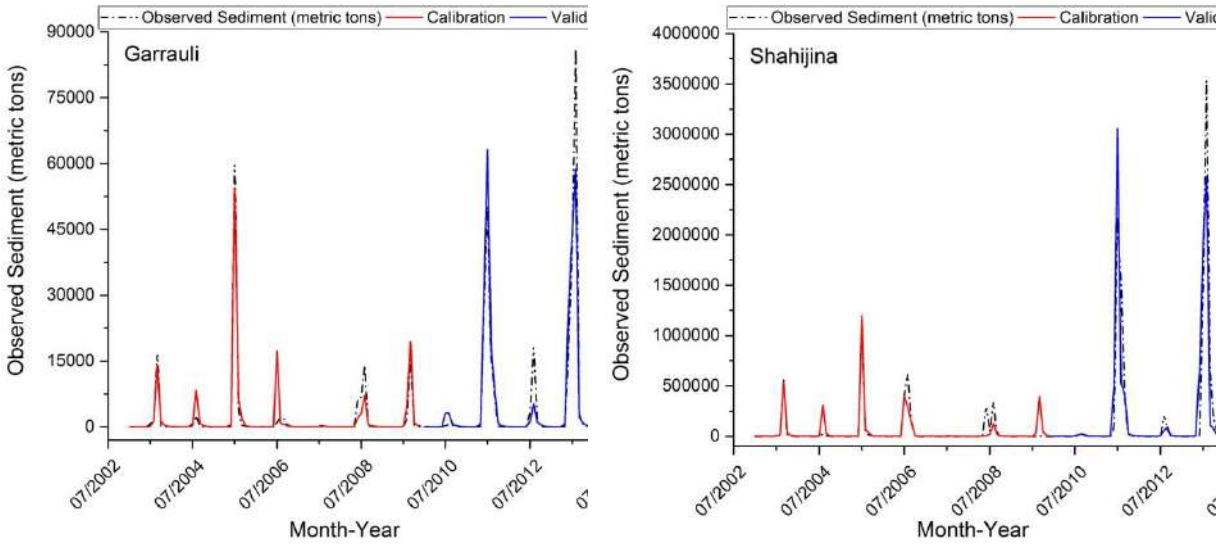

Figure 6.4: Calibration and Validation plots for sediment

A high R^2 value 0.94 for runoff at Garrauli site indicates that there is a very good agreement between the observed and simulated discharge during the calibration period. Other gauging site has lower values which might be due to dam management effect on the SWAT simulation. In case of sediment also, the Garrauli site showed high R^2 value 0.89 compare to Shahijina (R^2 = 0.78). Similar model performance has been also observed during validation

(Tables 6.3 and 6.4). Thus, the results indicate that the overall prediction of monthly discharge by the SWAT model during the calibration and validation period was satisfactory and therefore, accepted for further analysis.

6.6 FUTURE SWAT SIMULATION USING GCM DATA

In the present study, the downscaled and bias-corrected CMIP5 MPI-ESM-MR model datasets (discussed in Chapter-2) were used to prepare the future climate change data for the simulation of runoff and sediment employing SWAT model. Following scenarios were considered and used for the climate change impact study on SWAT simulations:

- Baseline 1986: Historical time-period 1986-2005
- Scenario 2020: Future time-period 2020-2039
- Scenario 2040: Future time-period 2040-2059
- Scenario 2060: Future time-period 2060-2079
- Scenario 2080: Future time-period 2080-2099

Before future simulation using the SWAT model, monthly variation of climate parameters were studied for each future scenario compare to baseline scenario.

6.6.1 Monthly climatic changes

(a) Rainfall

Figure 6.5 shows the rainfall variations in four future scenarios (i.e. scenarios 2020, 2040, 2060 and 2080) with respect to the baseline scenario (1986-2005). Very slight changes are visible in rainfall during the non-monsoon period; however, the monsoon variations are gradual to a very high level in the future scenarios.

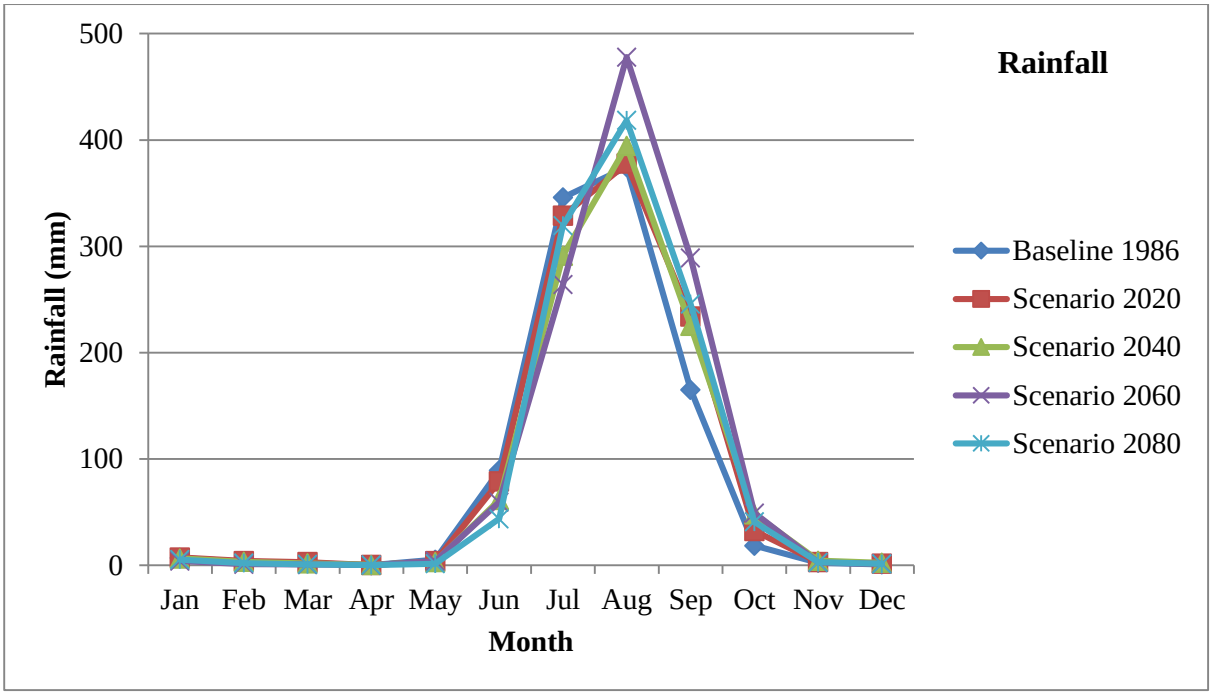

Figure 6.5: Monthly variation of rainfall during climate scenarios

In scenario 2020, maximum decrease of rainfall about 17.18 mm is observed in the month of July, and maximum increase in rainfall of about 68.93 mm is observed for September. During scenario 2040, maximum reduction of monthly rainfall about 54.61 mm is observed in July, and maximum increase of monthly rainfall of about 60.07 mm observed for September. In future scenario 2060, highest decrease of rainfall about 81.94 mm is observed in July, and maximum increase in the monthly rainfall about 123.99 mm observed in September. Subsequently in scenario 2080, maximum reduction of rainfall is observed in June of about 45.35 mm, and maximum rainfall increase of about 80.52 mm is observed in September month.

Overall, the scenario 2060 has a great monsoon rainfall changes than other future scenario changes. There is great reduction in rainfall for June and July; however in August to September, rainfall increases significantly.

(b) Maximum temperature

Figure 6.6 represents the variation of maximum temperature during four future scenarios (i.e. scenarios 2020, 2040, 2060 and 2080) with respect to the baseline scenario (1986). The scenarios of maximum temperature, from baseline 1986 to future scenario 2080, show a clear distinct variation with respect to following scenario.

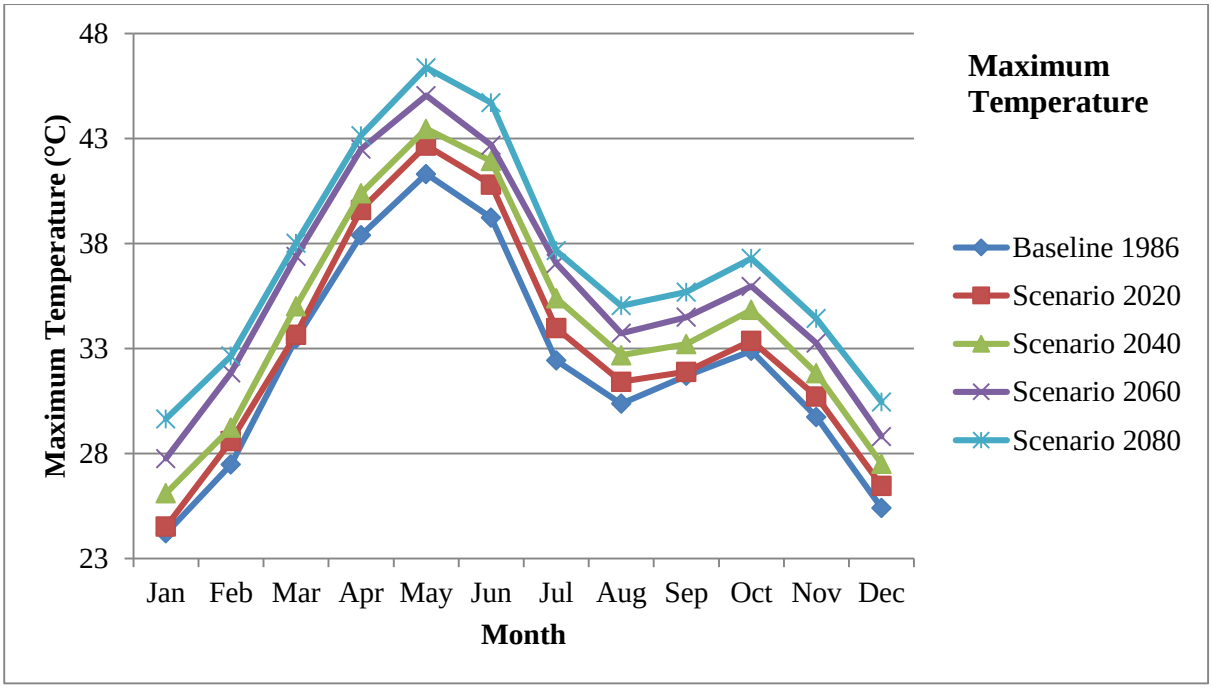

Figure 6.6: Monthly variation of maximum temperature during climate scenarios

In this study, scenario 2020 shows significant rise in maximum temperature from 0.19 °C (March and September) to 1.57 °C (June). From the scenario 2040, the more increase in maximum temperature about 2.97 °C and less increase in maximum temperature about 1.51°C has been observed in July and September, respectively. Succeeding scenario 2060 showed more increase of maximum temperature (about 4.63 °C) in July, and low rise in maximum temperature about 2.79 °C in September is observed. Also, the future scenario 2080 has increase in maximum temperature from 3.99 °C (September) to 5.47 °C (June).

In this study, it is clearly observed that there is gradual rise in maximum temperature in every scenario with respect to the baseline scenario and to every preceding scenario. More changes in maximum temperature (3.99 °C to 5.47 °C) are observed in the last future scenario 2080. The maximum temperature showed less variation at its peaks time during the summer. However, in monsoon the more abrupt changes in maximum temperature have been observed for all the scenarios.

(c) Minimum temperature

Changes in minimum temperature during all the future scenarios with respect to baseline are illustrated in Figure 6.7. The behavior of minimum temperature is nearly similar to the changes in the maximum temperature.

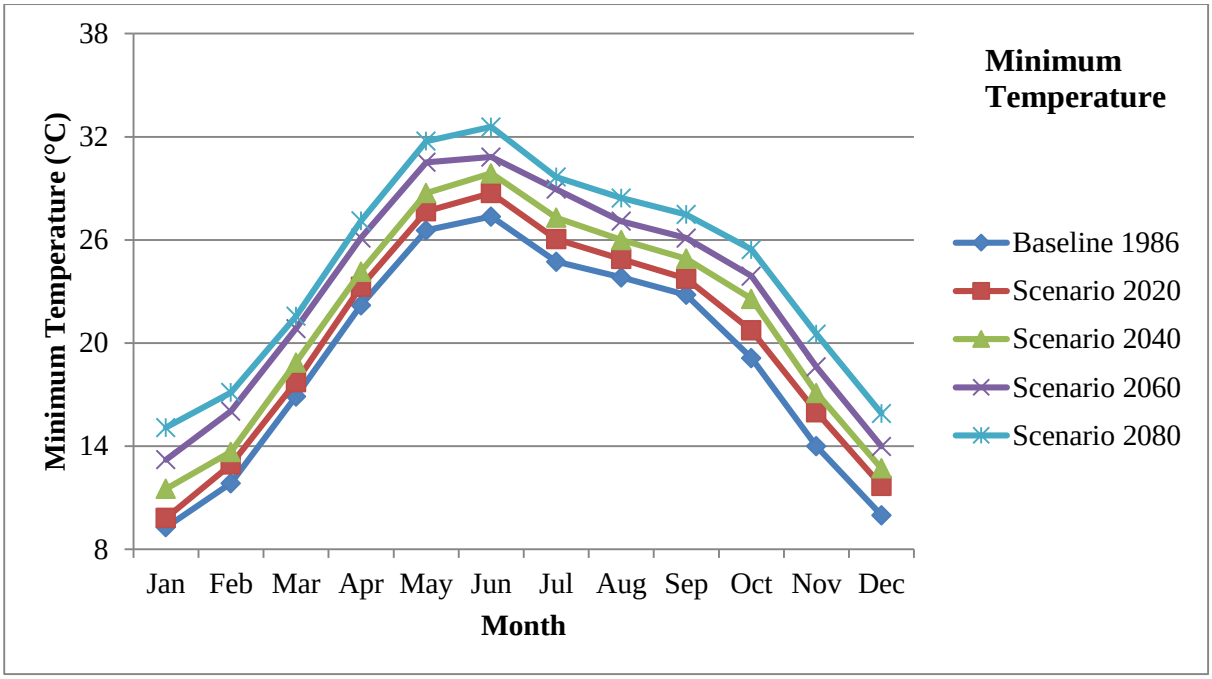

Figure 6.7: Monthly variation of minimum temperature during climate scenarios

In scenario 2020, changes in minimum temperature are observed from 0.54 °C (January) to 1.99 °C (November) with respect to the baseline scenario. During scenario 2040, minimum temperature rise from about 1.82°C observed for February to about 3.44°C observed in October month. In Scenario 2060, August month having low rise in minimum temperature of about 3.27°C and high rise of minimum temperature of about 4.77°C in October has been observed. For scenario 2080, minimum temperature increases less about 4.62°C in the month of August, and increases more about 6.53°C in November month.

Concluding from the results, the minimum temperature increases rapidly in each future scenario. In this study, more increase in minimum temperature (from 4.62°C to 6.53°C) has been observed for the scenario 2080 with respect to the baseline scenario 1986. In future, initial two scenarios 2020 and 2040 shows more changes in post-monsoon and winter. Later, more changes in minimum temperature observed for the scenarios 2060 and 2080 will occur in monsoon and post-monsoon season. Hence, in future the pattern of rise in minimum temperature could be shifted for the present study area.

6.6.2 Climate change impact on monthly SWAT simulation

In this study, monthly model simulation has been used to assess the climate change impact on runoff, sediment yield, ET and water yield in the Betwa basin.

(a) Runoff

Based on the model simulation, monthly runoff during baseline 1986 maximize about 1409.39 cumec in August (monsoon season), and minimumize about 15.78 cumec in June month (Figure 6.8). In future, the peak runoff about 1303.69 cumec in scenario 2020, 1367.34 cumec in scenario 2040, 2017.44 cumec in scenario 2060, and 1640.40 cumec in scenario 2080 has been observed for August month (Figure 6.8). However, the decrease in runoff about 14.79 cumec in scenario 2020, 17.05 cumec in scenario 2040, 4.07 cumec in scenario 2060 and 6.56 cumec in scenario 2080 has been observed for June month. Results show that, scenario 2060 has more changes in low and high runoff, due to changes in future precipitation. These results revealed that increase in runoff is mainly observed in August, and decrease in runoff is observed in June month. Thus, monsoon changes may affect future runoff as compare to historical flows, especially due to precipitation decrease in June and increase in August. Monthly runoff changes for one baseline scenario and four future climate scenarios are illustrated in Figure 6.8.

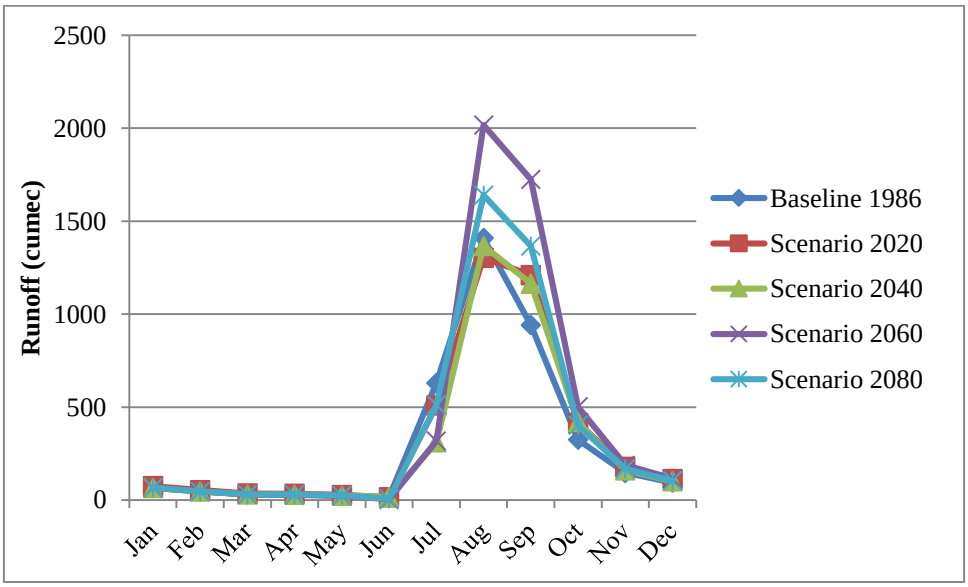

Figure 6.8: Monthly variations in simulated runoff

(a) Sediment yield

Figure 6.9 represents monthly sediment yield in baseline 1986 and four future climatic scenarios. Monthly high sediment yield during baseline 1986 is observed to be 80.65 t/ha in August. In future, sediment yield has been estimated about 70.05 t/ha in scenario 2020, 78.82 t/ha in scenario 2040, 119.92 t/ha in scenario 2060, and 96.28 t/ha in scenario 2080 for August month. In this analysis also, sediment yield is higher in monsoon months during scenario 2060. The pattern of change in sediment yield is very similar to the runoff pattern, hence both runoff and sediment yield should exhibited a significant relationship under

climatic changes. Thus, change in monsoon flow may have high impact on changes in sediment yield of the Betwa basin.

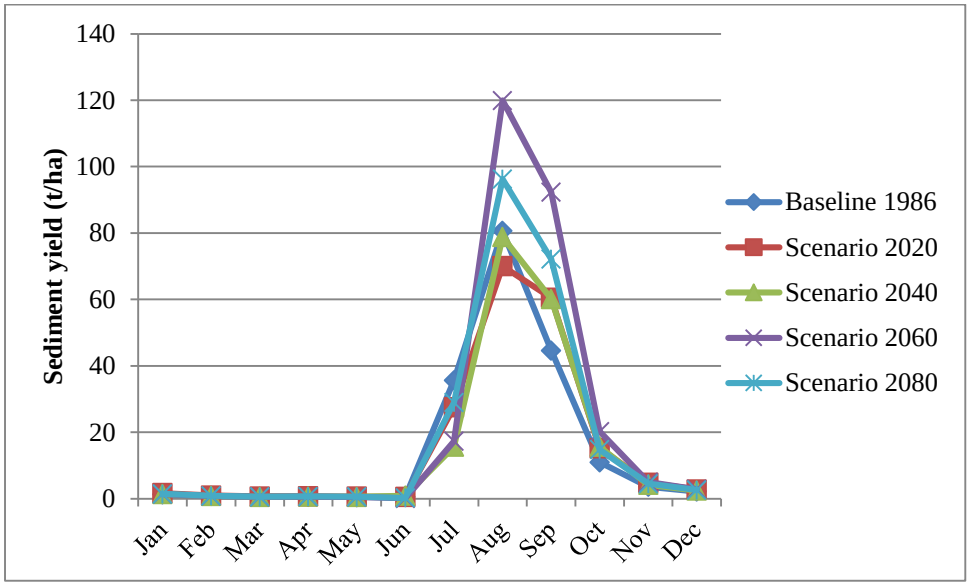

Figure 6.9: Monthly variations in simulated runoff

6.7 Annual changes in GCM-derived climate variables and SWAT simulations

6.7.1 GCM-derived climate variables

(a) Trend analysis

Results show that precipitation has increasing trend during baseline 1986 period (1986-2005). The trend of precipitation change later decreases in the future scenarios 2020, 2040 and 2080 as shown in Figure 6.10. Only the scenario 2060 has significant increasing trend in future which shows more number of high precipitation events.

The trend of temperature parameters shows significant change in trend of all future scenarios as compare to the baseline trend of maximum temperature, minimum temperature, mean temperature and temperature difference (Figure 6.10). In this study, the mean and difference of temperature were estimated based on the original maximum and minimum temperature data. Trend analysis result shows that the increase in trend of future temperature variables increases in each climate scenario from scenario 2020 to scenario 2080. Only the trend of temperature difference has been decreasing from baseline to future climate scenarios.

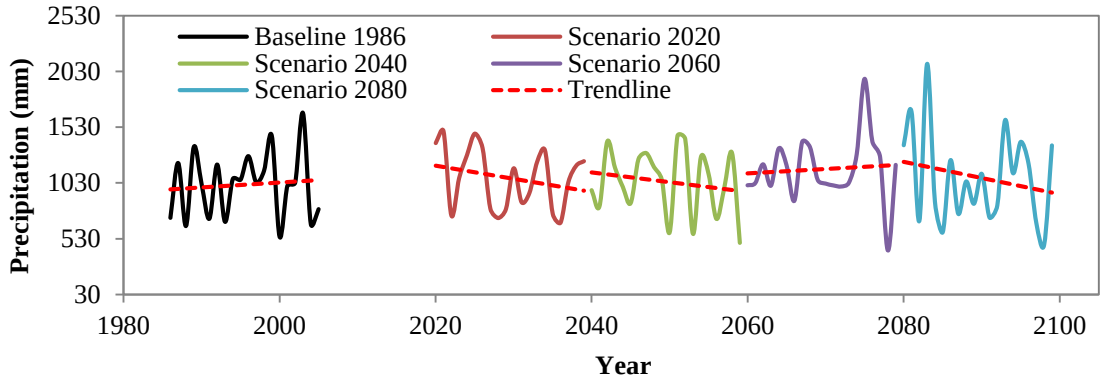
Precipitation (mm)
2530
2030
1530
1030
530
30
Baseline 1986
Scenario 2020
Scenario 2040
Scenario 2060
Scenario 2080
Trendline
1980
2000
2020
2040
2060
2080
2100
Year

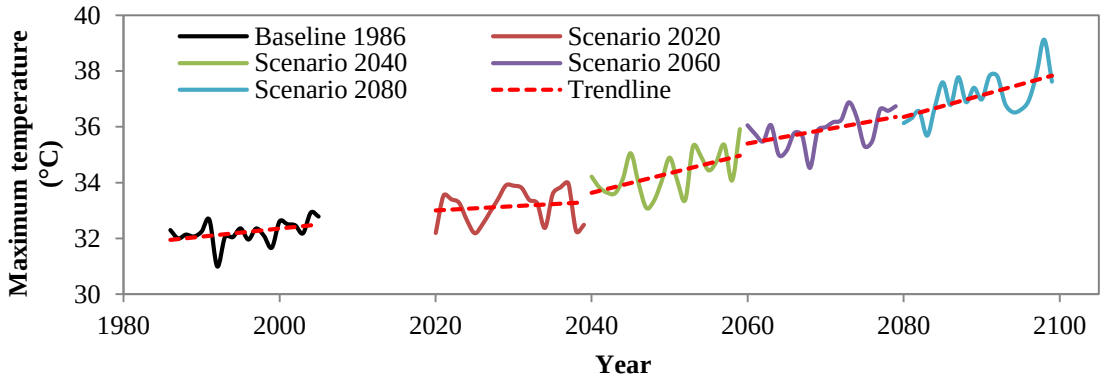
Maximum temperature (°C)
40
38
36
34
32
30
Baseline 1986
Scenario 2020
Scenario 2040
Scenario 2060
Scenario 2080
Trendline
1980
2000
2020
2040
2060
2080
2100
Year

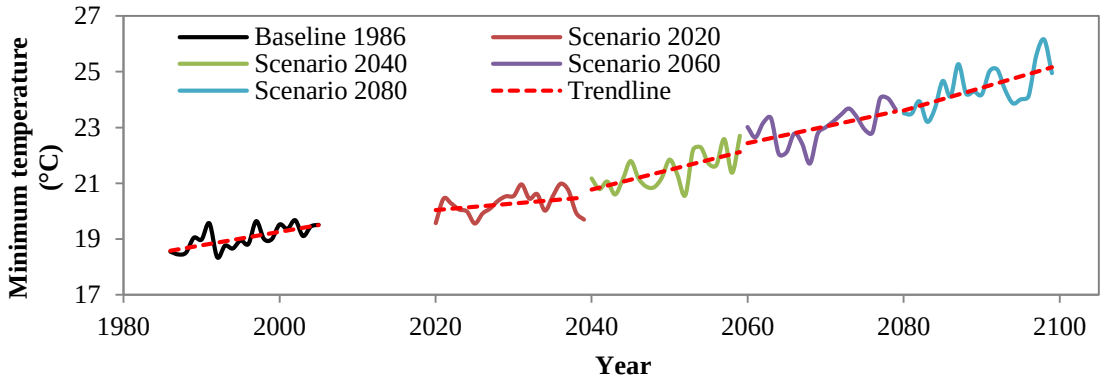
Minimum temperature (°C)
27
25
23
21
19
17
Baseline 1986
Scenario 2020
Scenario 2040
Scenario 2060
Scenario 2080
Trendline
1980
2000
2020
2040
2060
2080
2100
Year

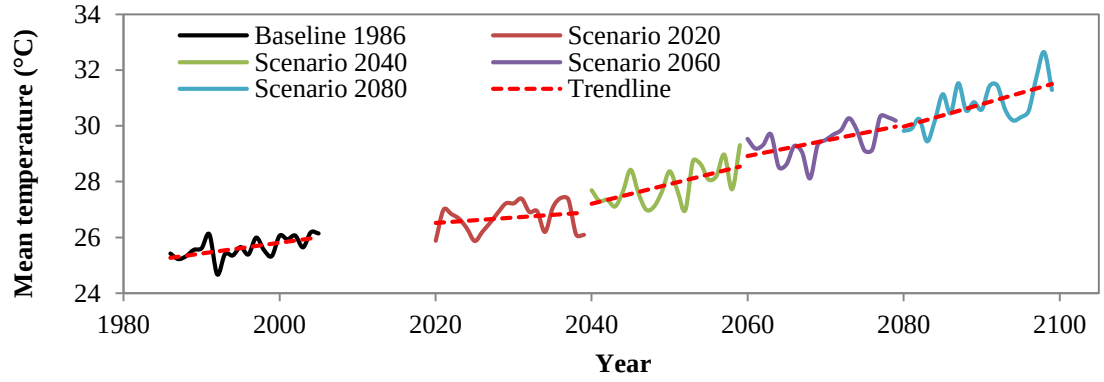
Mean temperature (°C)
34
32
30
28
26
24
Baseline 1986
Scenario 2020
Scenario 2040
Scenario 2060
Scenario 2080
Trendline
1980
2000
2020
2040
2060
2080
2100
Year

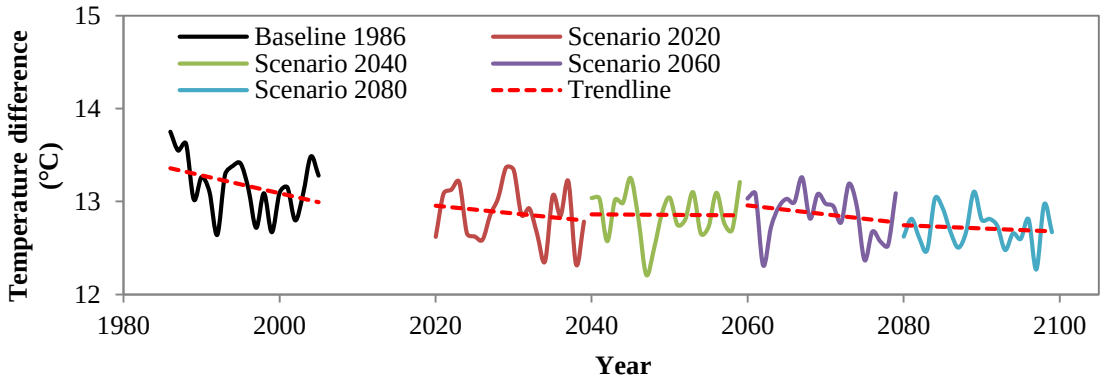

Figure 6.10: Trend analysis of GCM-derived climate variables for baseline and future climate scenarios

(b) Statistical summary

In addition, the statistical summary of GCM-derived annual climate variables has been calculated to understand the changes in maximum, minimum, average values, standard deviation and coefficient of variation from baseline to future scenarios (Table 6.7). Results shows the decrease in coefficient of variation in scenario 2020 (CV = 0.25), 2040 (CV = 0.28), and 2060 (CV = 0.26) as compare to the baseline CV = 0.30. Only the scenario 2080 has significantly increased coefficient of variation (CV = 0.38) due to high standard deviation in precipitation.

Furthermore, the study of coefficient of variation has been carried out for the original temperature variables i.e. maximum and minimum temperature. The analysis results show the increase in coefficient of variation of maximum temperature in future scenarios (CV = 0.02) as compared to the baseline CV = 0.01. Result also shows an increase in coefficient of variation of minimum temperature from baseline to future climate scenarios with increasing standard deviations (Table 6.7).

Table 6.7: Statistical summary of GCM-derived annual climate variables

Statistic	GCM-derived annual climate variables				
	Baseline 1986	Scenario 2020	Scenario 2040	Scenario 2060	Scenario 2080
	Precipitation (mm)				
Max	1657.31	1493.86	1449.19	1964.16	2096.98
Min	547.97	672.93	492.11	424.51	475.98
Avg	1012.88	1073.52	1041.14	1152.55	1081.66
SD	298.85	271.40	293.32	294.05	415.66
CV	0.30	0.25	0.28	0.26	0.38
	Maximum temperature (°C)				
Max	32.93	33.97	35.92	36.87	39.12

Min	30.99	32.19	33.10	34.52	35.68
Avg	32.22	33.14	34.30	35.88	37.10
SD	0.42	0.63	0.76	0.61	0.78
CV	0.01	0.02	0.02	0.02	0.02
Minimum temperature (°C)					
Max	19.67	20.98	22.71	24.05	26.16
Min	18.35	19.56	20.57	21.70	23.20
Avg	19.04	20.27	21.45	23.01	24.38
SD	0.42	0.42	0.63	0.63	0.76
CV	0.02	0.02	0.03	0.03	0.03

Note: Max = maximum value; Min = minimum value; Avg = average value; SD = standard deviation, and CV = coefficient of variation

6.7.2 SWAT simulations

(a) Trend analysis of SWAT simulations

In this study, the SWAT model outputs have been used for trend analysis of the runoff, sediment yield, evapotranspiration and water yield (Figure 6.11). Results shows that both runoff and sediment yield have similar trends in baseline and future climate scenarios. Historical baseline period has increasing trend, while only future scenario 2060 has increase in trends for runoff and sediment yield simulations. In future, other three scenarios 2020, 2040 and 2080 have decreasing trends.

Two water balance components, ET and water yield, shows varying trends under changing climate. During baseline period (1986-2005), the ET has insignificant decreasing trend while the water yield has increasing trend. Similarly, the ET and water yield components have opposite trends, except for the scenario 2040 where a less precipitation may induce an insignificant change in future period (2040-2059).

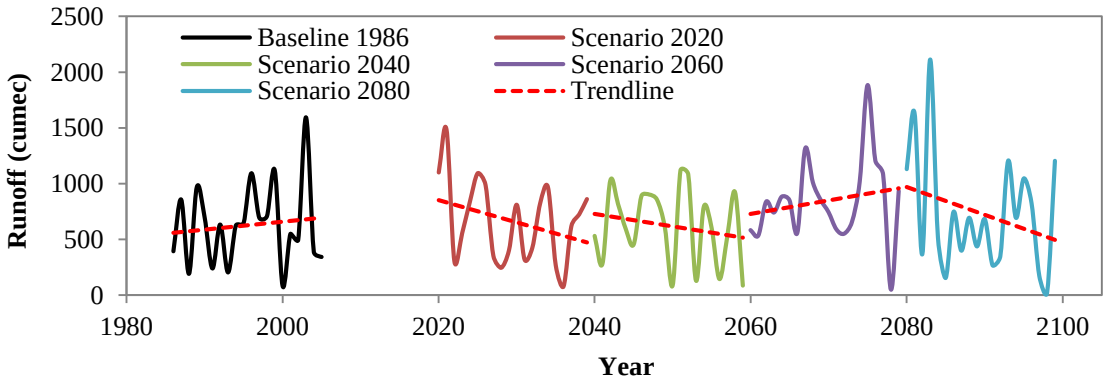

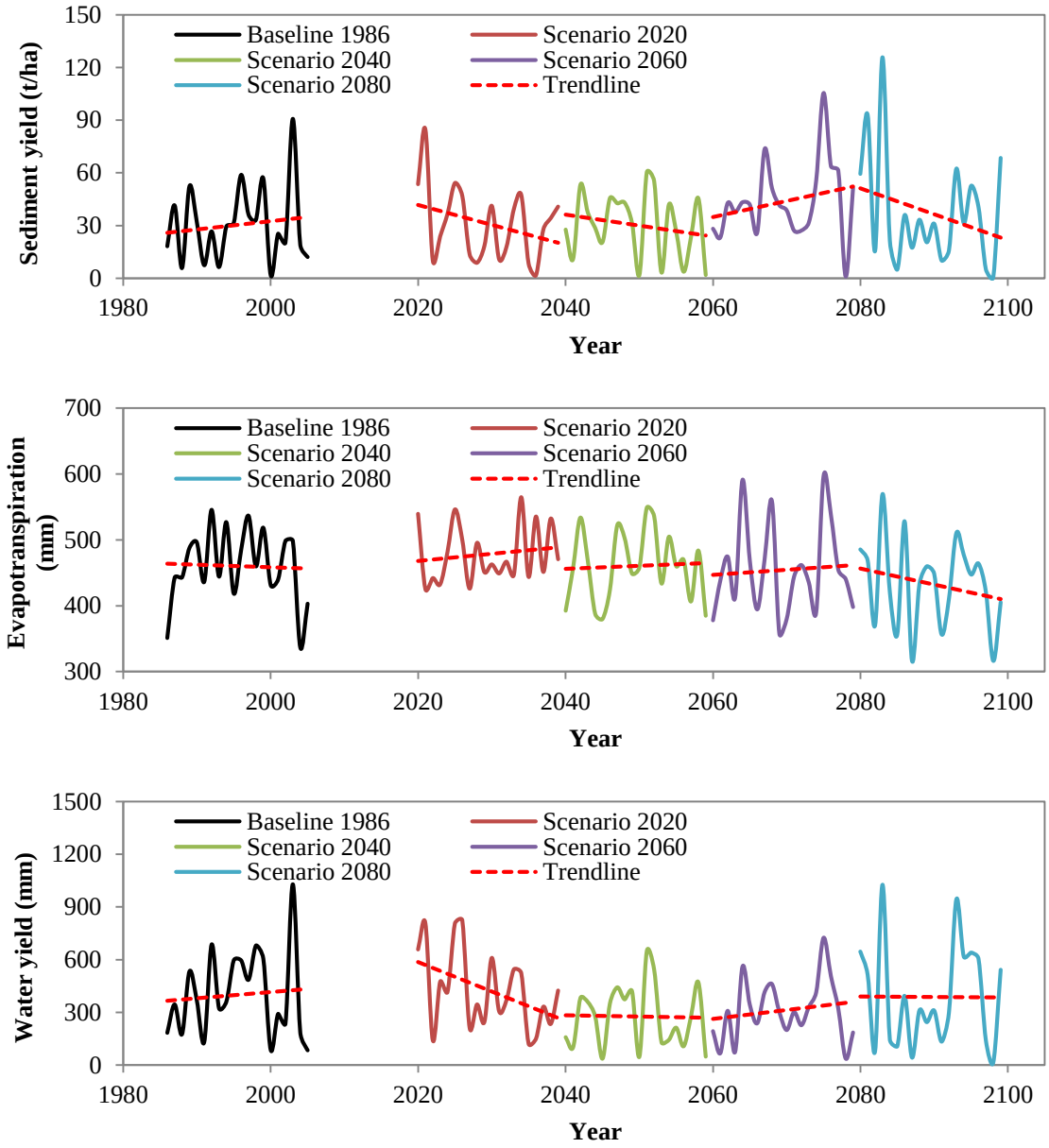

Figure 6.11: Trend analysis of SWAT simulations for baseline and future climate scenarios

(b) Statistical summary

The statistical summary result for runoff shows that coefficient of variation decreases from baseline 1986 (CV = 0.59) to scenario 2060 (CV = 0.44), and then suddenly increases in scenario 2080 (CV = 0.72) due to increased standard deviation (Table 6.8). Similarly, the sediment yield has decreased coefficient of variation (from CV = 0.72 to CV = 0.51) from baseline 1986 to scenario 2060, and then rise in CV = 0.86 during scenario 2080.

The ET parameter has the lowest values of coefficient of variation which represents low ET variation under climatic changes. Result shows the increase in ET coefficient of variation due to increase in temperature parameters which induces more water vaporization in future years.

The result for water yield shows more values of coefficient of variation under changing climate. Highest CV = 0.76 is observed for scenario 2080 where a large standard deviation (SD = 294.16 mm) produces more variations in water yield (Table 6.8). In contrary, the low coefficient of variation for scenario 2020 has been observed due to high average value (427.13 mm) of water yield.

Table 6.9: Statistical summary of SWAT simulation on annual time-scale

Statistic	SWAT simulation annual summary				
	Baseline 1986	Scenario 2020	Scenario 2040	Scenario 2060	Scenario 2080
			Runoff (cumec)		
Max	1593.67	1481.72	1117.82	1882.35	2111.39
Min	83.05	78.07	86.47	50.10	25.92
Avg	625.98	662.05	622.74	844.32	733.35
SD	370.49	364.09	339.56	372.42	528.72
CV	0.59	0.55	0.55	0.44	0.72
			Sediment yield (t/ha)		
Max	90.78	84.62	60.30	105.44	125.88
Min	1.72	1.66	1.84	0.98	0.49
Avg	30.31	30.99	30.29	43.60	37.25
SD	21.87	20.74	18.67	22.04	31.98
CV	0.72	0.67	0.62	0.51	0.86
			Evapo-transpiration (mm)		
Max	545.80	564.80	548.90	596.92	569.39
Min	337.19	425.22	380.01	357.86	316.42
Avg	460.20	478.28	460.34	454.27	433.34
SD	56.81	43.92	53.49	69.62	67.34
CV	0.12	0.09	0.12	0.15	0.16
			Water yield (mm)		
Max	1029.96	824.28	647.66	724.96	1025.85
Min	84.57	120.73	36.90	36.79	14.19
Avg	399.69	427.13	276.80	310.38	387.09
SD	247.50	225.14	178.76	172.10	294.16
CV	0.62	0.53	0.65	0.55	0.76

Note: Max = maximum value; Min = minimum value; Avg = average value; SD = standard deviation, and CV = coefficient of variation

6.7.3 Change in dependable flows

The change in river flows in future has been studied by plotting the flow duration curves for baseline and future scenarios (Figure 6.12). It is observed that scenario 2060 has the highest

changes in dependable flow for first 20% probability as compare to the dependable flows in other climate scenarios.

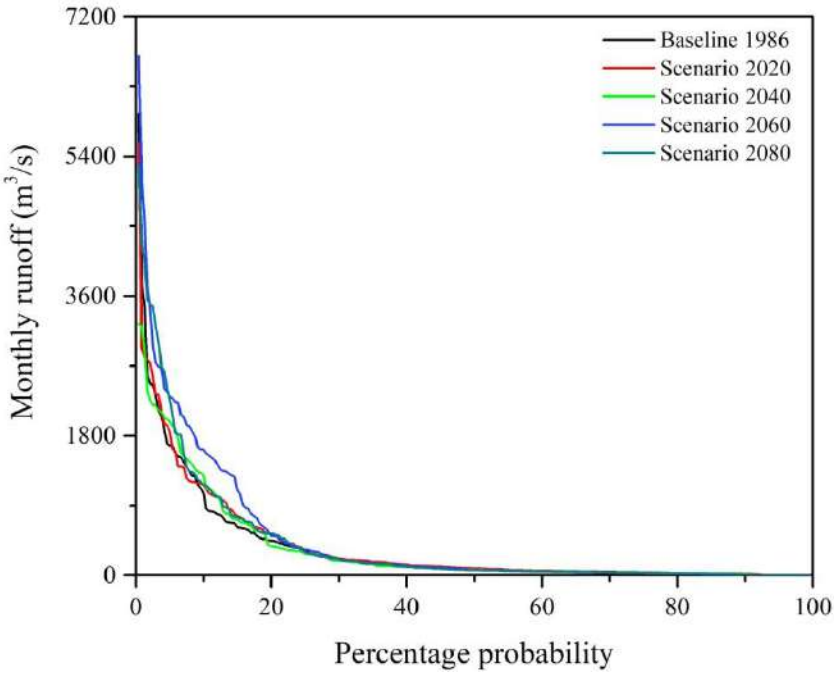

Figure 6.12: Changes in flow duration curve under changing climate scenarios

Based on the previous results, the future flow has great variation in future years with the changes in future climatic variables. Thus, the dependability of river flows has been also assessed at the 50%, 75%, 90% and 99% probability (Table 6.9). Results show that dependable flow decreases in future years at all percentage probabilities. Thus, the future climate change induces a negative impact on the dependable flow in future years.

Table 6.9: Dependable flows at 50, 75, 90 and 99 percentage probability

Percentage probability	Annual dependable flows (cumec)				
	Baseline 1986	Scenario 2020	Scenario 2040	Scenario 2060	Scenario 2080
50	71.40	90.20	71.10	68.85	63.60
75	31.88	33.70	30.64	28.50	27.24
90	6.06	18.79	14.40	0.00	6.30
99	0.00	0.00	0.00	0.00	0.00

6.8 Summary

Following conclusions are drawn from the SWAT model simulation study under changing climate:

1. In this study, future climate analysis shows that rainfall could change significantly in monsoon season compared to non-monsoon season of the Betwa basin. The maximum

and minimum temperature increases gradually in all climate scenarios, hence change in temperature could have more impact in the future.

2. Change analysis shows that rainfall decreases in June and July months, however in August and September rainfall could increase in the future. Due to high amount rainfall in the scenario 2060, maximum runoff could produce flooding in the future.
3. Based on runoff and sediment simulations, the critical sub-watersheds can identify and prioritize to implement proper conservation and management practices for sustaining basin productivity.
4. Trend analysis shows increasing trends for temperature parameters, while the decreasing trend in precipitation pattern in future except the scenario 2060 where increasing trend observed due to more wet years during 2060-2079. As a result, the coefficient of variation for minimum and maximum temperature increases from baseline to future scenarios. While, the precipitation has high coefficient of variation during scenario 2080.
5. The trend analysis of SWAT simulation shows a very similar response for both runoff and sediment yield, i.e. increase in baseline and scenario 2060, however the decrease in scenario 2020, 2040 and 2080.
6. The study also shows that future climate change impact induces negative impact on dependable flow in future years at 50%, 75%, 90% and 99% probabilities. Thus, in future sustainable management is required to combat the climate change impact.

CHAPTER 7

EVALUATION OF BEST MANAGEMENT PRACTICES (BMPs) FOR SUSTAINABLE WATER RESOURCES DEVELOPMENT UNDER CHANGING CLIMATE

This chapter deals with the evaluation of Best Management Practice (BMPs) for sustainable development of the Betwa River Basin under changing climate. The SWAT model has been applied to simulate the effect of BMPs on streamflow and sediment yield for future scenarios. In this study, six sets of BMPs including overland as well as river channel treatments, namely tillage management, contour farming, residue management, grassed waterways, streambank stabilization and grade stabilization structures has been employed to provide solution for sustainability of water resources in the Betwa river basin.

7.1 INTRODUCTION

Increasing rate of watershed development and utilization for various purposes has focused attention on the application of physically based hydrological models to deal with constantly changing environment. Many watershed management programs (Sharda et al., 2012) have suggested modelling strategies for development and implementation of sustainable watershed plans. In the absence of a standard procedure for representing conservation practices with watershed models, Best management practices (BMPs) are generally accepted as an effective measure to control watershed losses in terms of streamflow and sediment.

Soil erosion is a major concern for environment and natural resources leading to reduction in the field productivity and soil quality resulting to land degradation. The process of soil erosion includes removal of soil material from one location via natural erosive agents such as water. Thus, erosive agents influence the process of detachment, transportation, and deposition of soil materials (Foster and Meyer, 1972). Soil erosion is mainly affected by natural factors, such as climate, soil, topography, vegetation and anthropogenic activities, such as soil conservation measures and tillage systems (Kuznetsov et al., 1998). Crucial information about erosion patterns and trends can be obtained by modelling of the water-induced soil erosion which allows scenario analysis in relation to current or potential land uses (Millington, 1986).

Many watershed management programs suggested modelling strategies to investigate effects of management practices at the watershed level (Pandey et al., 2005, 2009d; Lam et al., 2011; Jang et al., 2017). Best management practices (BMPs) are generally accepted as effective

control measures for agricultural non-point sources of streamflow and sediment. Effective control of soil erosion and nutrient losses require proper implementation of BMPs in critical erosion prone areas of the watershed (Tripathi et al., 2005). The SWAT model which has been widely used in Indian sub-continent, is a tool that predicts the impact of BMPs on streamflow and sediment yields in complex watersheds (Ullrich and Volk, 2009; Arnold and Fohrer, 2005, Murty et al., 2014).

After calibration and validation of the SWAT model for streamflow and sediment simulation over the Betwa river basin, it is crucial to evaluate optimal BMPs for sustainability of the Betwa river basin area employing the SWAT model. Soil erosion status in the Betwa basin was accomplished to provide the priority of sub-watersheds for soil conservation measures. In this study, the SWAT model was employed for evaluating the effectiveness of different management strategies in reducing sediment yield considering different BMPs i.e. tillage management, contour farming, residue management, grassed waterways, streambank stabilization and grade stabilization structures. The primarily evaluation of the SWAT model was carried out in Chapter-6. In this chapter, identification of critical soil erosion prone areas and evaluation of best management practices has been carried out for recommendation of suitable soil conservation measures using the SWAT model.

7.2 DATA ACQUISITION

The details of data pertaining to metrological, hydrological and satellite data are briefly discussed in Chapter-2. Methodology flowchart used in this study is provided in Figure 7.1.

7.3 BASELINE SIMULATION

The baseline values for the input parameters were selected by model calibration, suggested values from the literature, and prior experience of the analyst. Specific management operations used for the baseline simulation include conventional tillage practice (using mould board plough), ploughing, sowing, fertilization, pesticide application, irrigation, inter-culture operations and harvesting. The baseline simulation was carried out for the historical time period 1986-2005 (baseline scenario 1986) and it was compared with the future climate scenarios 2020, 2040, 2060 and 2080.

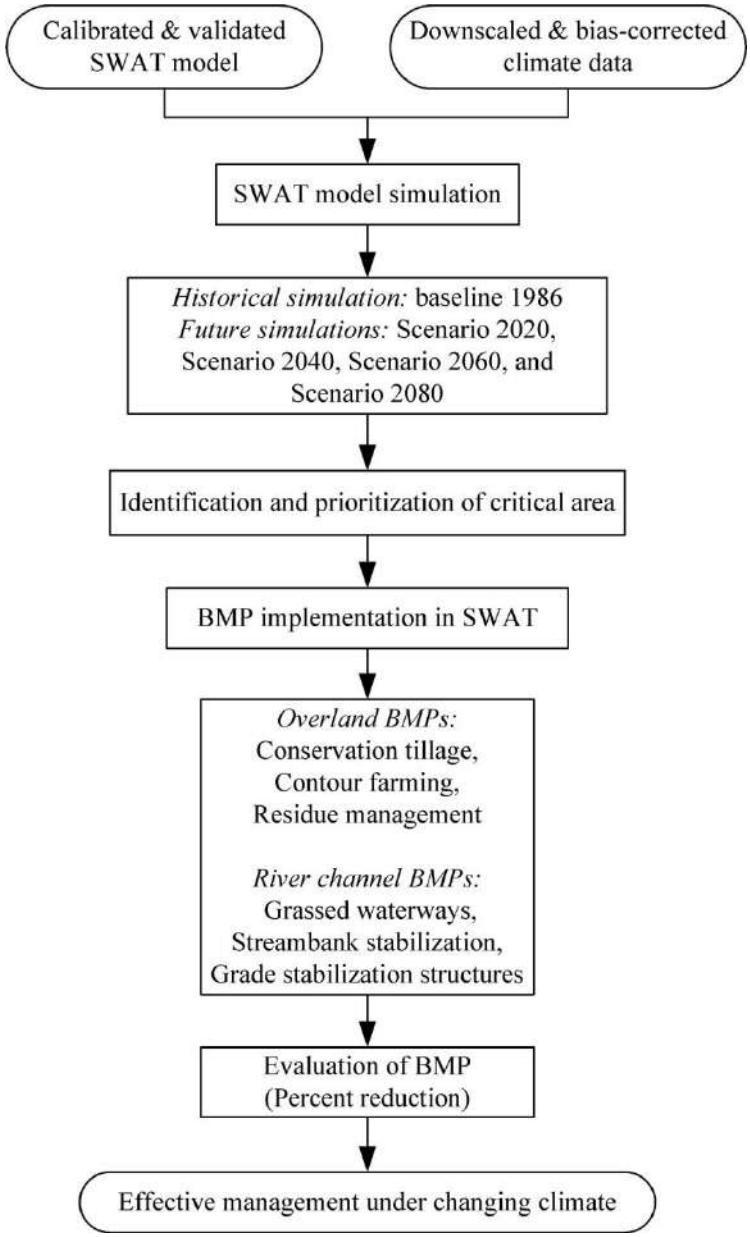

Figure 7.1: Methodology flowchart for BMP evaluation under changing climate

7.4 IDENTIFICATION AND PRIORITIZLATION OF CRITICAL SUB-WATERSHEDS

A particular sub-watershed may get top priority due to various reasons but often the intensity of land degradation/sediment/nutrient losses is taken as the basis (Niraula et al., 2013). This approach of prioritizing watersheds based on actual measurement of sediment yield rates may be possible only when the number of sub-watersheds to be prioritized are less and necessary sediment data can be collected easily. In this study, the critical sub-watersheds were identified on the basis of the SWAT simulated average annual sediment yields. Priorities were fixed on the basis of ranks assigned to each critical sub-watersheds based on the susceptibility to erosion (Singh et al., 1992; Dabral and Pandey, 2007; Pandey et al., 2009c,

2009d). The sub-watersheds were arranged in descending order of sediment yield and then priorities were fixed for the treatment, and soil and water conservation measures.

In this study, average annual sediment yield from the sub-watersheds not only provides the basis for identification and prioritization of critical sub-watersheds but also helps for planning of agricultural and structural management of the watershed. Since, the simulated sediment yield of the Betwa basin for all the scenarios are in close agreement with the measured values, it may be quite appropriate to use the average of model outputs (sediment yield) of different sub-watersheds for identification and prioritization of critical sub-watersheds. With this in view, the simulated sediment yields for all fifty-seven sub-watersheds of the Betwa river basin for climate scenarios and the average value for each sub-watershed were determined and presented in Table 7.1.

Table 7.1: Sub-watershed wise identification and prioritization of critical sub-watersheds

Sub-watershed	Area (ha)	Sediment yield (tons/ha)					Average Sediment yield (tons/ha)	Priority Rank	Average Slope
		Baseline 1986	Scenario 2020	Scenario 2040	Scenario 2060	Scenario 2080			
SW-1	11253.78	196.29	202.60	196.65	280.00	240.08	223.13	1	3.08
SW-2	43520.13	54.79	52.06	50.56	71.95	61.71	58.21	6	3.91
SW-3	52576.11	0.00	0.00	0.00	0.00	0.00	0.00	56	3.89
SW-4	19452.24	122.34	123.20	121.14	175.16	147.91	137.95	4	4.52
SW-5	55177.92	47.06	43.30	42.59	61.59	52.00	49.31	7	4.62
SW-6	176287.41	15.10	11.08	11.30	15.79	13.09	13.27	13	6.04
SW-7	40620.06	21.32	20.47	18.44	25.91	23.16	21.86	12	5.05
SW-8	76524.30	0.14	0.26	0.20	0.26	0.26	0.22	29	5.17
SW-9	119800.98	0.00	0.00	0.00	0.00	0.00	0.00	54	5.38
SW-10	179577.09	0.01	0.00	0.00	0.00	0.00	0.00	45	5.40
SW-11	48750.66	39.24	37.88	39.24	54.74	45.13	43.25	9	5.89
SW-12	33527.34	25.24	24.72	22.29	31.31	27.98	26.31	11	5.07
SW-13	55269.09	0.00	0.00	0.00	0.00	0.00	0.00	57	4.89
SW-14	4012.83	163.60	174.47	159.13	226.77	200.62	184.92	2	6.12
SW-15	94267.53	0.00	0.00	0.00	0.00	0.00	0.00	47	5.53
SW-16	4704.93	138.14	146.92	134.07	191.48	169.27	155.98	3	5.58
SW-17	21368.52	87.35	91.76	94.19	129.13	106.74	101.83	5	5.37
SW-18	2070.63	40.23	43.74	40.30	55.94	49.43	45.93	8	4.54
SW-19	141855.21	1.39	1.14	1.23	1.48	0.97	1.24	24	4.96
SW-20	43248.69	33.22	34.22	37.05	50.65	40.89	39.21	10	4.96
SW-21	30941.64	1.91	1.91	1.78	2.48	2.18	2.05	22	5.99
SW-22	64202.58	0.47	0.41	0.35	0.50	0.46	0.44	26	4.56
SW-23	153413.46	0.01	0.00	0.00	0.00	0.00	0.00	43	5.93
SW-24	16729.02	0.61	0.60	0.52	0.73	0.67	0.63	25	5.56
SW-25	14033.16	6.61	7.40	7.95	8.69	4.72	7.07	16	5.56

SW-26	109016.91	0.00	0.00	0.00	0.00	0.00	0.00	52	4.41
SW-27	136146.33	0.38	0.29	0.28	0.38	0.33	0.33	28	5.94
SW-28	159767.28	0.13	0.09	0.09	0.12	0.10	0.11	34	5.24
SW-29	98769.60	0.00	0.00	0.00	0.00	0.00	0.00	51	4.01
SW-30	197607.15	0.00	0.00	0.00	0.00	0.00	0.00	53	5.07
SW-31	161891.37	0.00	0.00	0.00	0.00	0.00	0.00	49	4.05
SW-32	90014.94	3.73	3.42	3.83	4.72	3.86	3.91	19	4.73
SW-33	134213.76	0.01	0.00	0.00	0.00	0.00	0.01	38	6.69
SW-34	47748.51	5.04	5.21	5.87	7.19	5.85	5.83	18	3.99
SW-35	135564.39	0.01	0.00	0.00	0.00	0.00	0.00	46	4.14
SW-36	135404.55	0.00	0.00	0.00	0.00	0.00	0.00	55	4.35
SW-37	32159.52	5.68	6.20	7.01	8.52	6.93	6.87	17	3.46
SW-38	68338.44	2.20	2.21	2.52	3.01	2.44	2.48	21	3.52
SW-39	86532.03	0.15	0.14	0.14	0.19	0.16	0.16	32	3.36
SW-40	196250.58	0.01	0.00	0.00	0.00	0.00	0.00	42	5.47
SW-41	52138.35	0.00	0.00	0.00	0.00	0.00	0.00	48	5.65
SW-42	84435.48	0.01	0.00	0.00	0.00	0.00	0.00	41	4.23
SW-43	43345.89	2.50	2.72	3.09	3.66	2.97	2.99	20	3.86
SW-44	85231.17	0.01	0.01	0.01	0.01	0.00	0.01	35	4.45
SW-45	10735.56	7.81	9.43	10.65	12.55	10.18	10.12	14	3.63
SW-46	56537.46	0.01	0.01	0.01	0.01	0.00	0.01	37	4.07
SW-47	59029.74	0.28	0.38	0.38	0.44	0.35	0.37	27	3.43
SW-48	44285.76	1.19	1.24	1.45	1.70	1.38	1.39	23	3.36
SW-49	143310.15	0.00	0.00	0.00	0.00	0.00	0.00	50	4.98
SW-50	4810.50	6.28	7.36	8.64	10.05	8.16	8.10	15	3.15
SW-51	73755.72	0.00	0.00	0.00	0.00	0.00	0.00	44	3.51
SW-52	45707.85	0.18	0.19	0.21	0.24	0.20	0.20	31	5.34
SW-53	110209.14	0.01	0.00	0.00	0.00	0.00	0.00	39	4.39
SW-54	74063.25	0.20	0.19	0.23	0.26	0.21	0.22	30	6.30
SW-55	54460.62	0.13	0.13	0.15	0.17	0.14	0.14	33	4.97
SW-56	78435.63	0.00	0.00	0.00	0.00	0.00	0.00	40	4.74
SW-57	63491.31	0.01	0.01	0.01	0.01	0.00	0.01	36	5.91

Table 7.2 shows the area under six soil erosion classes in the critical sub-watersheds of the Betwa river basin. The whole watershed was classified in 57 sub-watersheds, which were further classified in six erosion severity classes according to the sediment yield (t $ha^{-1}year^{-1}$) in ascending order. Most of the sub-watersheds are (about 80.63% of the Betwa basin area) falling under the slight erosion class (0-5 t $ha^{-1}year^{-1}$). About 8.60% of the area of the watershed comes under the moderate soil erosion class with soil loss of about 5-10 t $ha^{-1}year^{-1}$. Two sub-watersheds (i.e. 6 and 45) are falling under high soil erosion class (10-20 t $ha^{-1}year^{-1}$) covers around 3.15% of the total basin area. The sub-watersheds with very high soil erosion class with the soil loss of 20-40 t $ha^{-1}year^{-1}$ covers around 3.18% of the total basin area. The sub-watersheds with severe soil erosion class covers area of 2.44% with soil loss

rate of 40-80 t $ha^{-1}year^{-1}$. About 2% area of the whole watershed comes under very severe zone of soil erosion class, from where the sediment yield is about greater than 80 t $ha^{-1}year^{-1}$ are identified as critical sub-watersheds which needs more attention to apply Best Management Practices (BMPs) and to reduce the soil erosion in the future scenarios.

As per the guidelines suggested by Singh (1995) for Indian conditions, the average annual sediment yield was regrouped into six soil erosion classes as shown in Table 7.2.

Table 7.2: Area under different soil erosion classes in critical sub-watersheds of Betwa basin

Sediment yield (t ha−1 year−1)	**Sub-watershed**	**Area (%)**	**Soil erosion class**
0–5	3,8,9,10,13,15,19,21,22,23,24,26,27,28,29,30,31,32, 33,35,36,38,39,40,42,42,43,44,46,47,48,49,51,52,53, 54,55,56,57	80.63	Slight
5–10	25, 34, 37, 50	8.60	Moderate
10–20	6, 45	3.15	High
20–40	7, 12, 20	3.18	Very high
40–80	2, 5, 11, 18	2.44	Severe
>80	1, 4, 14, 16, 17	2.00	Very severe

At sub-watershed level, the highest soil loss is about 223.13 t $ha^{-1}year^{-1}$ (from SW-1). The soil loss rates are higher in the areas which are under agricultural land use. The areas with higher soil loss rate are those areas which experiences the maximum streamflow generation in the watershed. These areas are covered by forest land having least rate of soil loss apart from of the slope gradient. These results provide the priority of sub-watersheds for soil conservation measures. It can be used to provide a framework to develop soil and water conservation programs to control further reduction in the soil erosion and to avoid the land degradation.

Based on the annual sediment yield estimation, all sub-watersheds are divided into four priority categories for conservation intervention. Five sub-watersheds were assigned as the first priority (very severe soil erosion class), four sub-watersheds fall under the second priority (severe erosion class), three sub-watersheds under third priority (very high erosion class), two sub-watersheds under the forth priority (high erosion class), and three sub-watersheds under fifth priority (moderate erosion class). These results were further used for application of BMPs in the critical sub-watersheds.

The sub-watershed wise annual average sediment yield map is presented in Figure 7.2. The higher rate of erosion may be attributed to the fact that the particular sub-watershed may have

undergone streambank erosion. Further, faulty method of cultivation practices is prevalent in agricultural land contributing more sediment yield.

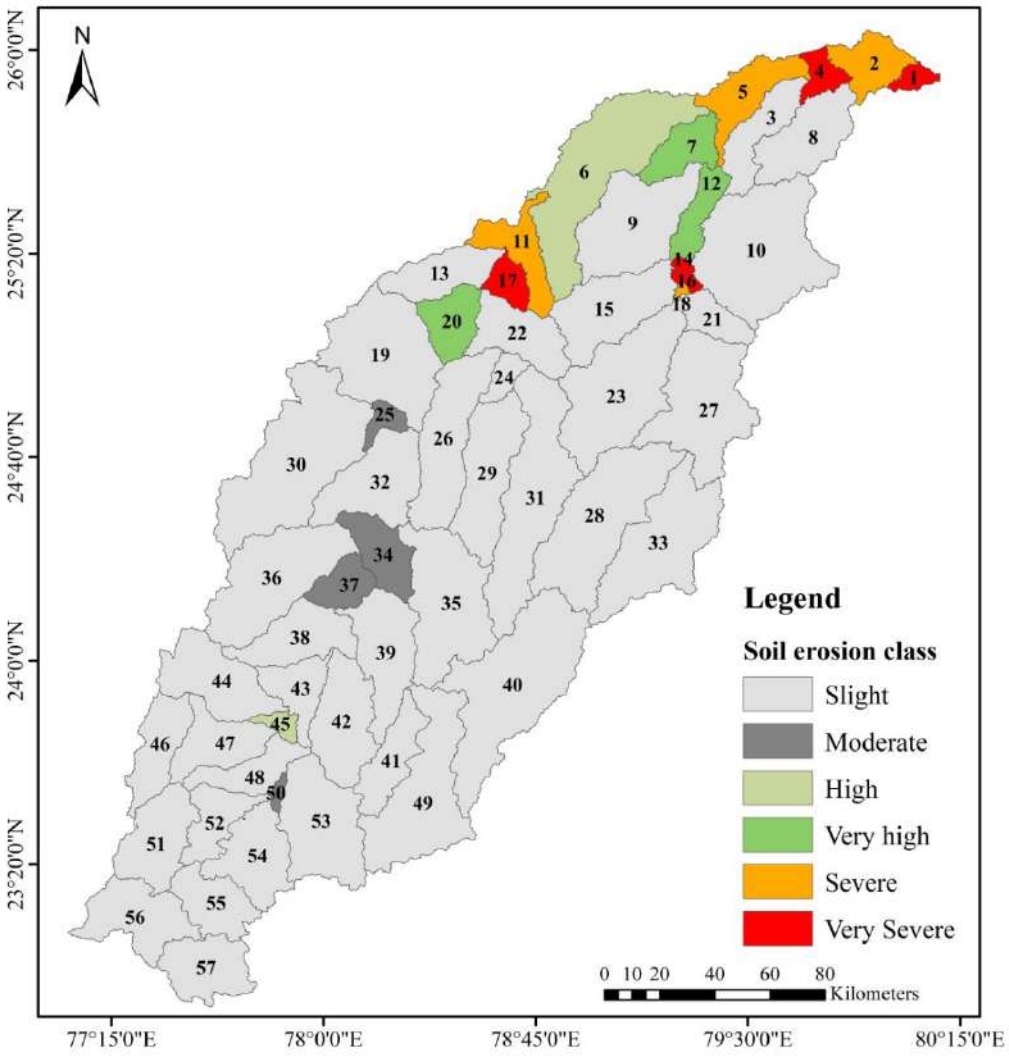

Figure 7.2: Critical sub-watersheds under different soil erosion classes in Betwa basin

7.5 APPLICATION OF BEST MANAGEMENT PRACTICES

The assessment of BMP impacts using a watershed model is helpful in establishing a watershed conservation and protection plan. In this study, the SWAT model was used to analyze future scenarios of the management practices for the critical sub-watersheds. Treatments were considered based on the information available in the literature and collected by the personal communication with the farmers, scientists and agricultural development officers. Based on the available field data and existing practices of cultivation, the treatments of the watershed were decided for evaluating the BMPs.

In order to evolve an appropriate management strategy suited to the farmers as river development organization of the Betwa River basin, following overland as well as river channel BMPs were applied and evaluated in the present study:

1. Conservation tillage (*overland BMP*)
2. Contour farming (*overland BMP*)
3. Residue management (*overland BMP*)
4. Grassed waterways (*river channel BMP*)
5. Streambank stabilization (*river channel BMP*)
6. Grade stabilization structures (*river channel BMP*)

Definition and purpose of BMPs were obtained from national conservation practice standards—NHPS (USDA-NRCS, 2005). Based on the function of a conservation practice, a method was suggested for representing the practice in SWAT.

7.5.1 Conservation tillage (NRCS practice code-328)

Conservation tillage includes various practices that cause less soil disturbance than the conventional tillage. In the SWAT model, tillage practices are differing in terms of mixing efficiency and tillage depth. Mixing efficiency represents the fraction of materials (residue, nutrient and pesticides) on the soil surface that are mixed uniformly throughout the soil depth. The tillage depth represents the depth of mixing caused by tillage operation.

Table 7.3: Tillage treatments considered for effective management in the Betwa basin

Tillage treatments	Tillage code	Tillage depth	Mixing efficiency
Mould board plough	MLDBOARD	150	0.95
Conservation tillage	CONSTILL	100	0.25

In the study area, mould board plough is used for conventional tillage practice by farmers. All farmers do not use advanced tillage implements due to financial constraints, and poor knowledge towards improved agricultural implements. In the present study tillage treatments were selected on the basis of previous studies (Triphati et al., 2005; Behera and Panda, 2006; Pandey et al., 2009c, 2009d) undertaken in the different Indian watersheds for evaluation of the BMPs. Tillage treatments and their respective mixing efficiencies as suggested by Neitsch et al. (2011) are given in Table 7.3.

7.5.2 Contour farming (NRCS practice code-330)

Contour farming consists of performing field operations including plowing, planting, cultivating and harvesting along the contour of the field. This practice is specially implement to reduce surface runoff by impounding water in small depressions, to reduce sheet and rill erosion by reducing erosive power of surface streamflow, and preventing or minimizing development of rills. Curve number (CN) and USLE support practice factor (USLE_P) were used to represent the contour farming practice in the SWAT model.

7.5.3 Residue management (NRCS practice code-345)

Implementation of residue management practice helps to lower the surface runoff and peak flow, to increase infiltration and to reduce sheet and rill erosion by reducing surface flow volume, overland flow rate, raindrop impact, providing more surface cover and preventing development of rills. In this study, curve number (CN), Manning's roughness coefficient for overland flow (OV_N) and USLE cover factor (USLE_C) were utilized for representation of residue management practice using SWAT model.

7.5.4 Grassed waterways (NRCS practice code-412)

Grassed waterways helps to increase sediment trapping in the channel by reducing flow velocity. Also, increase in flow roughness can reduce peak flow rate/flow velocity in the channel segment. Moreover, gully erosion in the channel segment will be reduced by establishing channel cover. In this study, Manning's roughness coefficient (CH_N2) and channel cover factor (CH_COV) were used for installation of grassed waterways in the channel segments.

7.5.5 Streambank stabilization (NRCS practice code-580)

The main purpose of streambank stabilization is to prevent bank erosion. This practice uses vegetation or structural techniques to stabilize and protect the banks of river or constructed channels, and the shorelines of lakes and reservoirs against scour and erosion. Hence, it refers to the lined waterways with erosion resistant material in the channel segment. In SWAT model, streambank stabilization can influence channel erodibility (CH_EROD) and channel roughness (CH_N2).

7.5.6 Grade stabilization structures (NRCS practice code-410)

Grade stabilization structures are used to control the grade and head cutting in natural or artificial channels in the river basin area. This practice will increase sediment trapping,

decrease peak flow rate/flow velocity, and reduces gully erosion in the channel segment. In this case, slope of the channel segment (CH_S2) and channel erodibility factor (CH_EROD) represents the grade stabilization structures in the SWAT model.

7.6 EVALUATION OF BEST MANAGEMENT PRACTICES

7.6.1 Percent reduction

Effects of BMP implementation is evaluated as percent reduction in an average annual surface streamflow and sediment yield. The sub-watershed level evaluation represents erosion load reductions for overland as well as in-stream/channel network. Watershed level reduction comprises cumulative load reductions in pre-BMP and post-BMP conditions. All the proposed BMPs were simulated individually, where pre-BMP condition represents baseline simulation, and during post-BMP condition all input parameters except parameters representing a BMP were held constant in SWAT model.

Percent reduction can be calculated as:

$$reduction(\%) = \frac{100 \times (BMPpre - BMPpost)}{BMPpre} \quad \ldots (7.1)$$

Also, change in percent reduction of streamflow and sediment yield was calculated for future climate scenarios. At post-BMP condition, difference between baseline simulation and climate scenario simulation was estimated to understand the effect of BMP implementation from historical baseline to future climate scenarios.

7.6.2 Sensitivity index (SI)

Based on the SWAT simulation at watershed outlet, the sensitivity analysis of BMP representative parameters has been carried out to understand the influence of change in BMP parameter values.

$$SI = \frac{(X_2 - X_1)}{X_{preBMP}} \quad \ldots (7.2)$$

where, X_2 and X_1 are the model output values corresponding to minimum and maximum values of a BMP parameter, and X_{preBMP} is the pre-BMP model output at nominal or baseline value.

Figure 7.3 shows the SI values for streamflow and sediment in critical sub-watersheds of the Betwa basin.

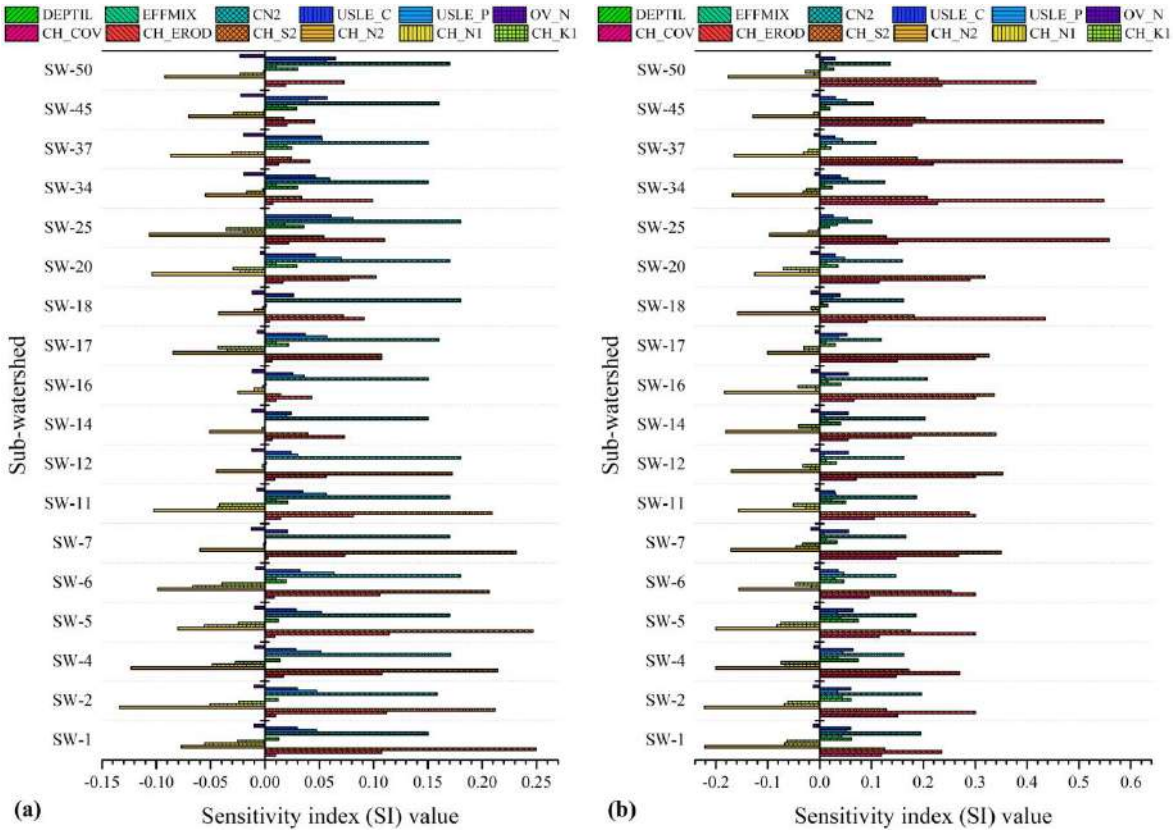

Figure 7.3: Sensitivity index values of BMP parameters for (a) streamflow and (b) sediment

In this analysis, a positive *SI* value represents direct response of change in BMP parameter value to the model output, i.e. increase in parameter value increases the model outputs, and vice versa. However, a negative *SI* value indicates indirect response between change in parameter value and model outputs, i.e. increase in parameter value decreases the model outputs, and vice versa. Hence, a negative value of SI represents that the BMP parameter and the model outputs (here streamflow and/or sediment yield) are inversely related to each other.

7.7 RESULTS & DISCUSSION

The results of overland as well as within channel BMP implementation in critical sub-watershed, and their effect on streamflow and sediment yield reduction are evaluated and discussed for sustainable development of the Betwa river basin.

7.7.1 Effective management of Conservation tillage practice

In the present analysis, the effect of conservation tillage in agriculture land has been evaluated for critical sub-watersheds of the Betwa river basin. This practice reduces the depth (DEPTIL) and mixing efficiency (EFFMIX) of tillage operation as well as decrease in the curve number (CN2) to lower the surface flow and soil erosion, and for sediment settling. Results show that reduction in sediment yield (6.84% to 24.27%) is higher than the reduction

in streamflow (5.38% to 9.53%) for baseline as well as future horizons (Table 7.4). Although the streamflow reduction in critical sub-watersheds (SW-25, SW-34, SW-37, SW-45 and SW-50) located at upper basin part is high, the conservation tillage practice can effectively reduce the soil erosion by decreasing depth and mixing efficiency of tillage operation. Sensitivity of conservation tillage parameters, i.e. DEPTIL, EFFMIX and CN2, is low for streamflow and high for sediment yield (Figure 7.3). The sub-watersheds located in lower basin part have high sensitivity of DEPTIL, EFFMIX and CN2 resulting high (more than 20%) sediment yield reduction (Figure 7.3 & Table 7.4). These BMP parameters also reduces the flow but in lower extent (about 6%). Thus, the conservation tillage is an effective management practice for streamflow and sediment yield reduction in the Betwa basin.

Table 7.4: (%) reduction in post-BMP simulation after implementation of conservation tillage

Sub-watershed	Streamflow (% reduction)					Sediment yield(% reduction)				
	Baseline 1986	Horizon 2020	Horizon 2040	Horizon 2060	Horizon 2080	Baseline 1986	Horizon 2020	Horizon 2040	Horizon 2060	Horizon 2080
SW-1	6.07	5.38	6.07	5.91	6.59	13.33	23.69	22.88	21.52	24.27
SW-2	6.77	6.03	5.38	5.91	5.98	13.32	23.74	22.92	22.32	23.44
SW-4	5.38	6.08	6.11	5.94	6.67	23.58	22.29	21.41	21.76	16.31
SW-5	6.89	6.09	6.12	5.94	6.03	23.60	23.29	22.42	21.78	17.13
SW-6	7.68	6.45	6.46	6.20	6.35	20.54	21.43	20.16	19.74	20.62
SW-7	7.14	6.49	6.48	6.64	6.88	20.02	20.33	19.64	18.94	18.01
SW-11	6.60	6.52	6.51	7.09	7.42	19.51	19.24	19.13	18.14	7.67
SW-12	7.14	6.49	6.48	6.64	6.88	16.94	22.56	21.52	20.63	22.44
SW-14	6.14	6.09	6.12	5.94	6.35	16.67	22.04	21.28	12.87	15.48
SW-16	7.29	6.27	6.29	6.07	6.19	19.01	20.77	20.27	19.95	18.46
SW-17	6.65	6.56	6.54	6.26	6.43	18.04	17.85	16.63	17.20	6.84
SW-18	6.87	6.50	6.50	6.86	7.15	15.48	15.48	15.48	15.48	15.48
SW-20	7.06	6.91	6.82	6.47	6.72	18.92	18.60	16.93	17.63	18.15
SW-25	9.53	7.22	7.08	6.65	8.56	18.41	16.00	12.03	7.87	19.29
SW-34	6.71	6.18	6.20	6.01	6.27	11.37	9.98	10.81	11.17	12.24
SW-37	6.97	6.42	6.41	6.16	6.31	13.79	7.33	7.37	7.87	10.03
SW-45	6.76	6.53	6.52	6.56	6.79	13.11	10.65	11.65	12.61	15.17
SW-50	6.96	6.70	6.66	6.67	6.94	16.75	16.00	14.33	16.00	16.60

In addition, the effect of future climate change has been also studied using post-BMP simulation as compare to the pre-BMP simulation. Results show horizon 2080 has high reduction in streamflow as compare to the other climate horizons (Figure 7.4). In case of sediment yield reduction, few sub-watersheds followed the same pattern of streamflow reduction at sub-watershed level, but in larger extent. In this analysis, the streamflow has nearly similar response in all critical sub-watersheds during future climate horizons, while the sediment yield has varying response to the conservation tillage treatment. Thus, the climate

change impact induces more variation in the sediment reduction under the same management practice. It may be due to varying soil erosion response to the future climatic changes.

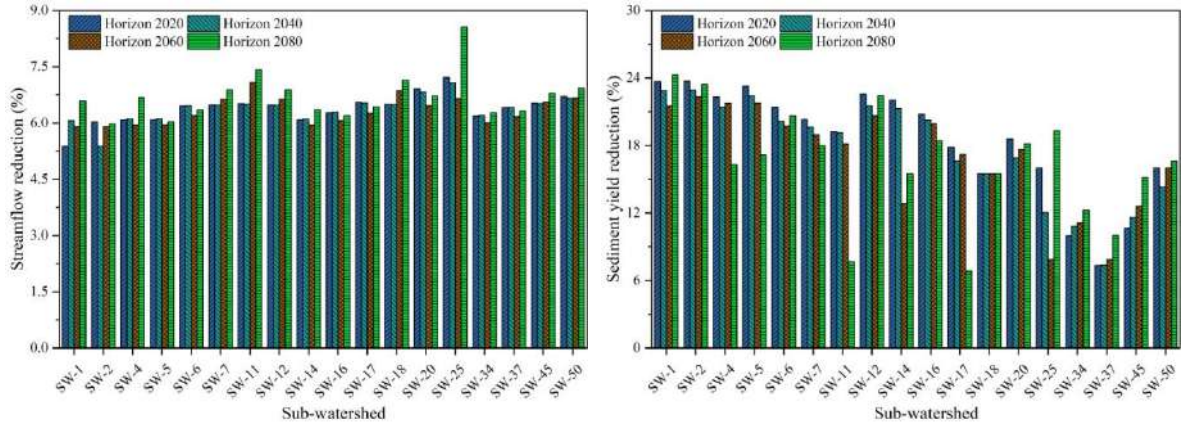

Figure 7.4: Effect of conservation tillage on future streamflow and sediment yield

7.7.2 Effective management of Contour farming

The effect of contour farming has been implemented by adjusting curve number (CN2) and USLE support practice factor (USLE_P), and then evaluated for critical sub-watersheds of the Betwa basin. In this practice, the USLE_P and CN2 have been decreased to reduce sheet erosion from the agriculture land. Results show that reduction in sediment yield (6.38% to 34.41%) is higher than the reduction in streamflow (9.78% to 13.25%) for baseline as well as future horizons (Table 7.5). It is observed that, percentage reduction in sediment yield has great variation due to varying response of the BMP parameters as compare to the response of streamflow reduction. Although the streamflow reduction in critical sub-watersheds (SW-25, SW-34, SW-37, SW-45 and SW-50) located at upper basin part is high, the contour farming can effectively reduce the sheet erosion by decreasing flow velocity and support practice factor. Thus, the BMP parameters, i.e. the CN2 and the USLE_P, have low sensitivity for streamflow and high sensitivity for sediment yield (Figure 7.3). The sub-watersheds located in lower basin part have high sensitivity of CN2 and USLE_P resulting high (more than 25%) sediment yield reduction (Figure 7.3 & Table 7.5). Sensitivity of these BMP parameters also reduces the flow (about 10%). Result shows that the USLE_P parameter increases the effect of contour farming on streamflow and sediment yield reduction. Thus, the contour farming is an effective management practice in the Betwa basin.

Table 7.5: % reduction in post-BMP simulation after implementation of contour farming

Sub-watershed	Streamflow (% reduction)					Sediment yield(% reduction)				
	Baseline 1986	Horizon 2020	Horizon 2040	Horizon 2060	Horizon 2080	Baseline 1986	Horizon 2020	Horizon 2040	Horizon 2060	Horizon 2080
SW-1	10.56	10.43	10.55	10.59	10.89	23.59	32.68	31.99	31.68	34.41
SW-2	10.56	9.78	10.55	10.59	10.89	22.16	33.78	32.05	31.75	33.61
SW-4	10.72	10.59	10.68	10.72	11.06	32.14	32.04	31.23	30.83	26.14
SW-5	10.75	9.90	9.96	10.74	11.09	32.18	33.05	31.26	30.16	26.98
SW-6	11.93	10.63	10.64	10.93	12.35	30.11	29.87	28.55	27.18	29.60
SW-7	11.02	10.36	10.64	10.86	11.62	32.14	23.19	31.23	22.63	22.90
SW-11	10.93	10.75	10.73	10.18	11.53	26.71	26.64	25.23	24.80	23.52
SW-12	10.77	10.89	10.54	11.09	10.74	26.14	23.20	30.30	22.64	31.60
SW-14	11.02	10.72	10.68	11.21	11.54	32.14	27.61	23.98	26.73	24.52
SW-16	10.93	10.60	10.50	11.20	11.58	29.44	29.84	28.25	27.48	25.25
SW-17	12.30	10.84	10.80	11.11	10.58	23.84	23.92	22.68	22.94	6.38
SW-18	11.26	10.80	10.85	11.25	10.66	32.14	25.40	27.61	24.68	23.71
SW-20	11.83	11.53	11.36	10.65	12.49	25.15	25.04	24.71	24.67	27.03
SW-25	12.63	12.15	11.87	11.02	13.25	24.82	20.37	16.41	10.75	23.65
SW-34	11.91	11.28	11.30	10.93	11.91	14.06	14.37	14.98	15.66	18.01
SW-37	11.57	11.15	10.94	11.56	11.29	12.37	7.01	8.11	9.12	11.60
SW-45	11.85	11.52	11.11	11.82	11.89	23.42	19.30	20.56	20.85	27.06
SW-50	11.92	11.66	11.30	11.59	12.57	23.10	20.37	18.70	20.37	20.37

Furthermore, the impact of future climate change on post-BMP simulation shows that horizon 2080 has high reduction in streamflow and sediment yield as compare to the other climate horizons (Figure 7.5). Similar to the previous analysis, the sediment yield reduction in few sub-watersheds followed the same pattern of streamflow reduction in lower part of the study area. In this analysis, the streamflow has nearly similar response in all critical sub-watersheds during future climate horizons, while the sediment yield has varying response to the contour farming practice. Thus, the climate change has impact on sediment reduction under the same management practice.

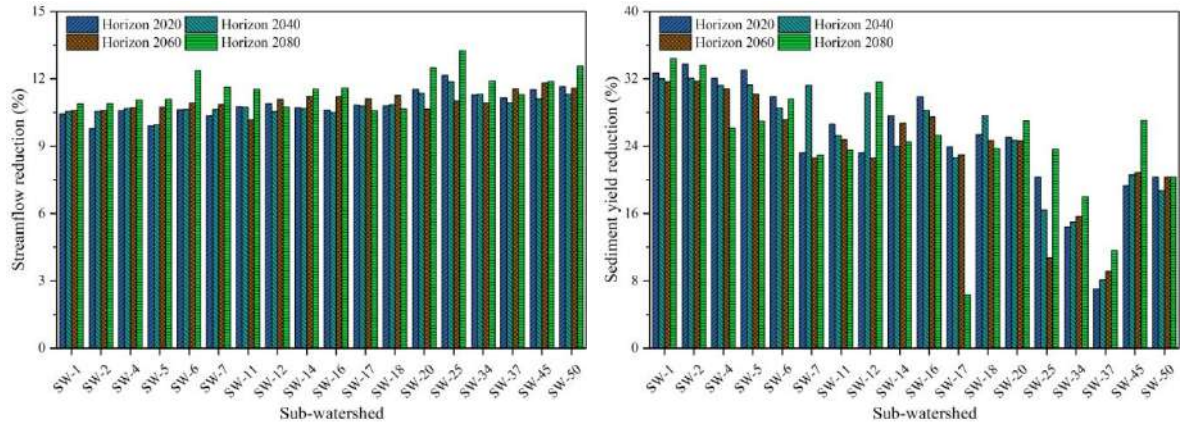

Figure 7.5: Effect of contour farming on future streamflow and sediment yield

7.7.3 Effective Residue management

Residue management has been implemented by considering changes in curve number (CN2), USLE cover factor (USLE_C), and Manning's roughness coefficient for overland flow (OV_N) in critical sub-watersheds of the Betwa basin. In this analysis, the CN2 and USLE_C decreased to reduce overland flow, sheet and rill erosion, while the OV_N increased to get more surface roughness. Results show that reduction in sediment yield (6.04% to 20.53%) is higher than the reduction in streamflow (6.44% to 9.08%) for baseline as well as future horizons (Table 7.6). Although the streamflow reduction in critical sub-watersheds (SW-25, SW-34, SW-37, SW-45 and SW-50) located at upper basin part is high, the residue management practice can effectively reduce the sheet and rill erosion by decreasing flow velocity and land cover factor with more surface roughness. The BMP parameters, i.e. the CN2, USLE_C and OV_N, have low sensitivity for streamflow and high sensitivity for sediment yield (Figure 7.3). Thus, in present analysis the sediment yield reduction is higher than the streamflow reduction. Mainly, the sub-watersheds located in lower basin area have high sensitivity of BMP parameters resulting high (about 18%) sediment yield reduction (Figure 7.3 & Table 7.6). Analysis shows that residue management practice has low effect on streamflow and sediment yield reduction, as compared to the contour farming.

Table 7.6: % reduction in post-BMP simulation after implementation of residue management

Sub-watershed	Streamflow (% reduction)					Sediment yield(% reduction)				
	Baseline 1986	Horizon 2020	Horizon 2040	Horizon 2060	Horizon 2080	Baseline 1986	Horizon 2020	Horizon 2040	Horizon 2060	Horizon 2080
SW-1	7.12	7.03	7.11	7.31	7.54	8.93	18.21	19.50	18.30	20.53
SW-2	7.12	7.03	7.11	7.31	7.54	8.92	20.32	18.50	18.35	19.71
SW-4	7.22	7.13	7.19	7.41	7.67	19.10	18.75	17.90	17.67	18.24
SW-5	7.24	6.44	6.47	7.42	7.69	19.13	18.78	17.92	16.99	19.09
SW-6	8.03	7.88	6.81	7.36	8.63	16.32	15.94	15.84	14.25	16.15
SW-7	7.49	7.37	6.83	7.40	8.20	16.12	12.82	18.58	12.26	12.53
SW-11	6.95	6.87	6.86	7.43	7.76	14.03	15.01	13.64	13.55	19.40
SW-12	7.12	8.14	7.21	7.42	7.60	18.07	12.83	16.91	12.27	17.20
SW-14	7.16	6.89	7.00	7.47	7.61	17.06	15.81	16.92	15.14	15.81
SW-16	7.23	7.16	7.14	7.49	8.15	14.39	16.51	13.91	13.44	17.78
SW-17	7.00	8.09	6.89	7.48	7.83	12.56	12.36	11.15	11.71	14.86
SW-18	7.45	7.19	7.02	7.66	8.20	14.64	15.91	14.28	15.29	17.60
SW-20	9.08	7.26	7.17	7.90	8.41	15.15	13.11	12.90	13.22	13.99
SW-25	7.80	7.56	7.42	8.27	8.91	12.41	7.85	6.04	14.88	10.00
SW-34	7.08	7.43	7.27	7.51	7.88	13.80	14.53	13.30	14.53	17.69
SW-37	7.11	7.37	7.12	7.70	7.72	14.54	13.25	13.11	14.18	14.43
SW-45	7.59	7.08	7.22	7.66	8.18	13.39	12.22	11.18	14.72	13.80
SW-50	7.76	7.45	7.24	7.86	8.12	10.00	10.00	8.33	10.00	10.00

The analysis of future climate change impact on post-BMP simulation shows that horizon 2080 has high reduction in streamflow and sediment yield (Figure 7.6). Sediment yield reduction in few critical sub-watersheds located at lower basin area is in similar pattern of streamflow reduction. In this analysis, the streamflow has increase in response in all critical sub-watersheds during future years, while the sediment yield has varying response to the residue management practice. Thus, the climate change also has an impact on streamflow and sediment reduction in the present study.

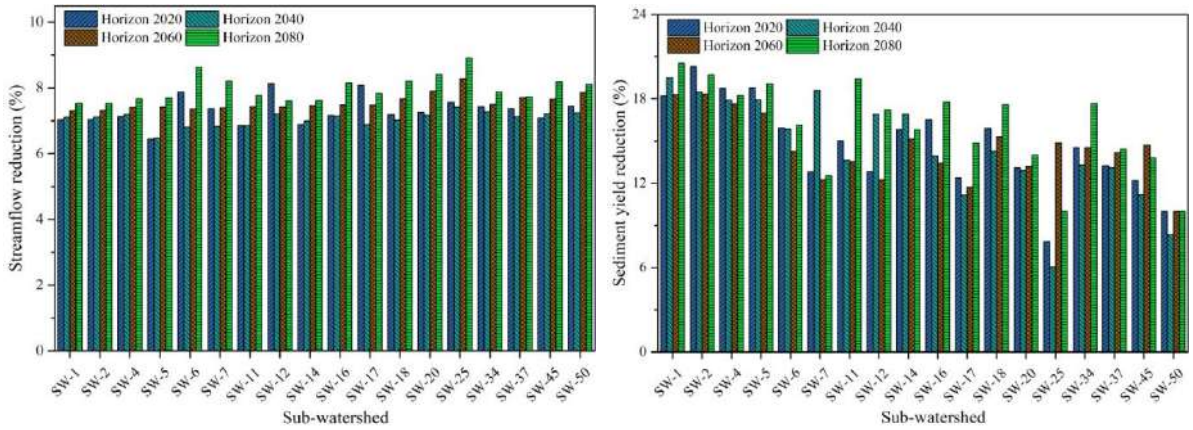

Figure 7.6: Effect of residue management on future streamflow and sediment yield

7.7.4 Effective management of Grassed waterways

In this study, the grassed waterway has been implemented on main river channel, and then evaluated for critical sub-watersheds of the Betwa basin. This practice increases channel cover (CH_COV) and channel roughness (CH_N2), as well as reduce the main channel erodibility (CH_EROD) to facilitate low flow velocity for sediment settling. Result shows that sediment yields of SW-45 reduce in large amount (from 50.54% to 56.42%) during baseline and future climate horizons (Table 7.7). Although the low amount of streamflow (about 1.77%) reduces in SW-45, this protection practice effectively reduces the main channel erosion due to high sensitivity of CH_COV, CH_EROD and CH_N2 as shown in Figure 7.3. Similarly, the SW-18 and SW-37 with high sensitivity of CH_COV, CH_EROD and CH_N2 resulting a large percent reduction in sediment yield (more than 45%). High sensitivity of CH_N2 at downstream river basin simulates more sediment yield reduction in SW-1, SW-2, SW-4 and SW-5 (Figure 7.3). The sensitivity of main channel roughness also reduces small percentages of streamflow (more than 3%) in lower basin sub-watersheds as compared to the upper basin sub-watersheds.

Furthermore, from SW-14 and SW-25 the sediment yield reduction is less as compare to other critical sub-watersheds. It may be due to low sensitivity of CH_COV (SI = 0.06) and

CH_EROD (SI = 0.18) in SW-14, and low negative sensitivity of CH_N2 (SI = -0.10) in SW-25. For all critical sub-watersheds, present study shows high percent sediment reduction ranges from 7.86% to 56.42%, and low streamflow reduction ranges from 1.62% to 3.62%. Thus, the grassed waterways in main channel of critical sub-watersheds can significantly reduce the sediment yield to protect the main river channel in critical sub-watersheds located in upper as well as lower basin area.

Table 7.7: % reduction in post-BMP simulation after implementation of grassed waterways

Sub-watershed	Streamflow (% reduction)					Sediment yield (% reduction)				
	Baseline 1986	Horizon 2020	Horizon 2040	Horizon 2060	Horizon 2080	Baseline 1986	Horizon 2020	Horizon 2040	Horizon 2060	Horizon 2080
SW-1	3.57	3.51	3.62	3.21	3.36	38.81	38.94	40.42	42.35	40.43
SW-2	3.58	3.53	3.62	3.21	3.36	39.16	39.31	40.76	42.75	40.79
SW-4	3.51	3.46	3.53	3.14	3.29	35.45	35.09	35.94	36.75	35.77
SW-5	3.41	3.37	3.45	3.06	3.21	35.60	35.24	36.08	36.89	35.91
SW-6	3.43	3.39	3.39	3.02	3.18	31.83	30.60	30.99	32.58	31.95
SW-7	2.20	2.20	2.22	2.16	2.16	21.67	19.85	20.02	24.36	22.96
SW-11	2.70	2.69	2.67	2.50	2.57	28.83	27.59	28.86	30.56	29.93
SW-12	1.98	1.98	1.98	1.99	1.98	21.76	19.90	20.04	24.44	23.02
SW-14	1.65	1.66	1.62	1.71	1.67	21.32	19.71	19.94	23.72	22.41
SW-16	1.74	1.76	1.73	1.79	1.77	21.76	20.15	20.36	24.10	22.82
SW-17	2.46	2.46	2.44	2.33	2.36	26.55	24.66	26.30	28.85	28.00
SW-18	1.86	1.85	1.84	1.88	1.86	46.08	46.15	46.68	47.00	46.59
SW-20	2.39	2.40	2.36	2.27	2.30	25.96	24.55	26.49	28.93	27.96
SW-25	2.21	2.21	2.19	2.13	2.17	29.96	24.77	18.70	13.36	7.86
SW-34	2.15	2.15	2.15	2.11	2.12	35.75	40.40	40.11	38.93	39.39
SW-37	1.99	2.00	2.00	2.00	1.99	48.41	52.24	51.77	50.95	51.41
SW-45	1.74	1.77	1.79	1.81	1.77	50.54	56.42	55.40	54.77	55.45
SW-50	1.77	1.79	1.83	1.84	1.79	44.61	44.58	44.04	43.19	43.52

In addition, the effect of future climate change on post-BMP simulation has also been analyzed in the study. Results show the SW-25 has sediment yield reduction variation from horizon 2020 (about 24.77%) to horizon 2080 (about 7.86%) as shown in Figure 7.7. It means SW-25 is most affected critical sub-watershed under climatic changes. Figure 7.7 illustrates that the critical sub-watersheds located at downstream of the Betwa basin have similar pattern between streamflow reduction and sediment yield reduction. However, four sub-watersheds (SW-34, SW-37, SW-45 and SW-50) located at upper part of the basin have high sensitivity to the sediment yield reduction. Result demonstrated that sensitivity of grassed waterways parameter is not very effective to reduce the streamflow in river channel.

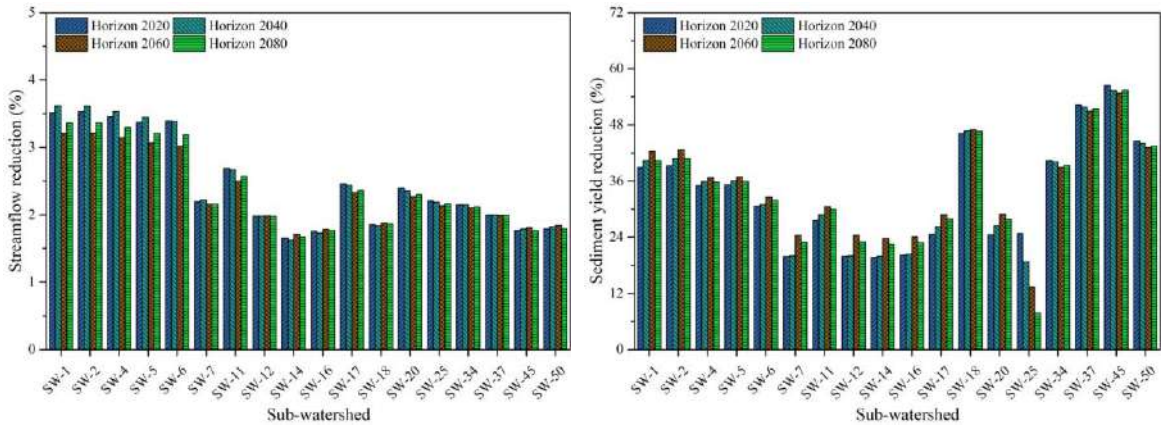

Figure 7.7: Effect of grassed waterways on future streamflow and sediment yield

7.7.5 Effective management of Streambank stabilization

Streambank stabilization, also called lined waterways, is used to reduce sediment loads while maintaining streamflow capacity in the main channel segment. This practice implemented by lowering channel erodibility (CH_EROD) and channel roughness (CH_N2) shows a high percent reduction of sediment yield in sub-watersheds SW-12 and SW-14 during all climate time-periods, i.e. from baseline to future horizons (Table 7.8). Streambank stabilization practice responds well to the sub-watersheds located upper and lower part of the study area. More sediment yield reductions with low streamflow changes are observed in upper basin sub-watersheds, mainly SW-37 and SW-45, where a negative sensitivity of CH_N2 is dominant over the sensitivity of CH_EROD (Figure 7.3). Thus, the streambank stabilization is an effective treatment to reduce large percent of sediment yields in the upper basin area. In case of lower basin, the SW-1, SW-2, SW-4 and SW-5 have high sediment yield reductions (more than 35%) and small streamflow reductions (about 3%) as compare to the upper basin streamflow reductions. In lower basin area also, the sensitivity of CH_N2 is dominant over the low sensitivity of CH_EROD. Thus, in streambank stabilization, the lined channel reduces a significant amount of sediment yield in the critical sub-watersheds. Nevertheless, the lower sediment yield reduction in SW-12 (about 20%) and SW-14 (about 22%) shows that the negative sensitivity of CH_N2 in SW-12 (SI = -0.17) and SW-14 (SI = -0.18) is less effective in these critical areas (Figure 7.3).

In this analysis, the percent reductions in sediment yield and streamflow by the streambank stabilization are nearly similar to the percent reductions obtained by grassed waterways. The grassed waterway parameter (mainly CH_COV) reduces more amount of streamflow as compare to the streamflow reductions obtained by streambank stabilization practice. Contrary, the sediment yield reductions are higher in case of streambank stabilization

treatment. It means the streambank stabilization is optimal in-stream BMP for river channel protection.

Table 7.8: % reduction in post-BMP simulation after implementation of streambank stabilization

Sub-watershed	Streamflow (% reduction)					Sediment yield (% reduction)				
	Baseline 1986	Horizon 2020	Horizon 2040	Horizon 2060	Horizon 2080	Baseline 1986	Horizon 2020	Horizon 2040	Horizon 2060	Horizon 2080
SW-1	3.37	3.31	3.42	3.01	3.16	41.08	41.51	42.55	44.12	42.49
SW-2	3.38	3.33	3.42	3.01	3.16	40.79	41.18	42.32	44.03	42.30
SW-4	3.31	3.26	3.33	2.94	3.09	36.36	36.14	36.82	37.46	36.62
SW-5	3.21	3.17	3.25	2.86	3.01	36.09	35.80	36.56	37.27	36.36
SW-6	3.23	3.19	3.19	2.82	2.98	31.83	30.60	30.99	32.58	31.95
SW-7	2.00	2.00	2.02	1.96	1.96	21.98	20.12	20.25	24.60	23.20
SW-11	2.50	2.49	2.47	2.30	2.37	28.92	27.69	28.93	30.62	30.00
SW-12	1.78	1.78	1.78	1.79	1.78	21.76	19.90	20.04	24.44	23.02
SW-14	1.45	1.46	1.42	1.51	1.47	21.60	19.96	20.18	23.98	22.69
SW-16	1.54	1.56	1.53	1.59	1.57	21.76	20.15	20.36	24.10	22.82
SW-17	2.26	2.26	2.24	2.13	2.16	26.55	24.66	26.30	28.85	28.00
SW-18	1.66	1.65	1.64	1.68	1.66	57.34	56.54	57.10	59.11	58.21
SW-20	2.19	2.20	2.16	2.07	2.10	25.96	24.55	26.49	28.93	27.96
SW-25	2.01	2.01	1.99	1.93	1.97	54.83	52.15	49.60	48.21	37.94
SW-34	1.95	1.95	1.95	1.91	1.92	54.30	56.06	56.71	57.08	56.91
SW-37	1.79	1.80	1.80	1.80	1.79	61.54	63.04	63.44	63.84	63.63
SW-45	1.54	1.57	1.59	1.61	1.57	60.06	63.36	63.41	63.74	63.70
SW-50	1.57	1.59	1.63	1.64	1.59	56.65	56.41	57.03	57.23	56.94

In future, the streambank stabilization can significantly decrease sediment yield from critical sub-watersheds with a lower amount of streamflow reductions (Figure 7.8). Based on the post-BMP simulation, this analysis reveals impact of climate change on the percent reductions in sediment yield and streamflow under varying response of BMP parameters in future. Mainly, in horizon 2060 the higher sediment yield reductions in all sub-watersheds are observed with low changes in streamflow (Figure 7.8). Except in SW-25, where a low sediment yield reduction is observed horizon 2020 (about 52.15%) to horizon 2080 (about 37.94%). This result reveals that in SW-25 the effect of streambank stabilization deceases in future under changing climate. Thus, the effect of streambank stabilization practice in main channel varies under changing climate in future.

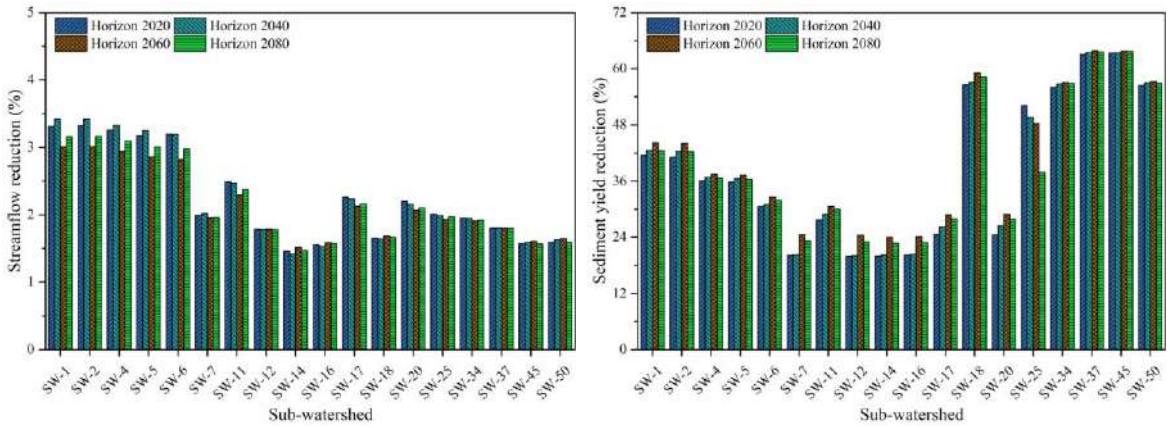

Figure 7.8: Effect of streambank stabilization on future streamflow and sediment yield

7.7.6 Effective management of Grade stabilization structures

In this study, grade stabilization structures have also been implemented and evaluated for main channel protection employing the SWAT model. This structural practice lowered the main channel erosion by decreasing the main channel erodibility (CH_EROD) and slope steepness (CH_S2). Analysis result shows a high percent sediment yield reduction (about 36%) from SW-12 compare to other critical sub-watersheds (Table 7.9). Due to structural intervention, the CH_S2 parameter in SW-12 has a large sensitivity to the high sediment yield reduction (35-37%) and low streamflow reductions (about 7-8%) as shown in Figure 7.3. In this analysis, low sediment reductions are observed for SW-37, located at downstream of Basoda gauging station, where main CH_S2 has a low sensitivity index value (SI = 0.19) affecting the model outputs (Figure 7.3). Further, the changes in streamflow increased from upper to lower basin (SW-50 to SW-1) due to varying CH_S2 sensitivity at sub-watershed level (Figure 7.3). Thus, the grade stabilization structure can be used as sustainable management practice to protect the main channel segment by reducing sediment yield as well as streamflow.

High sediment yield in SW-12 reduces during horizon 2060 (about 36.15%), and in SW-45 during horizon 2020 (about 8.25%) as illustrated in Figure 7.9. The SW-25 has increase in sediment yield reduction under changing climate, i.e. from horizon 2020 (about 14.42%) to horizon 2080 (about 23%), because of the low sensitivity of CH_S2 (SI = 0.13) and high sensitivity of CH_EROD (SI = 0.56) in main channel. Result shows that present sediment loads in the lower basin area can be minimized by implementation of grade stabilization structures, especially in SW-7, SW-12, SW-14, SW-16, SW-17 and SW-20 where a high sensitivities of CH_S2 (SI value more than 0.32) plays an important role (Table 7.9).

Table 7.9: % reduction in post-BMP simulation after implementation of grade stabilization structures

Sub-watershed	Streamflow (% reduction)					Sediment yield (% reduction)				
	Baseline 1986	Horizon 2020	Horizon 2040	Horizon 2060	Horizon 2080	Baseline 1986	Horizon 2020	Horizon 2040	Horizon 2060	Horizon 2080
SW-1	8.77	9.14	7.60	8.84	8.61	12.56	11.71	10.15	9.43	11.06
SW-2	8.06	6.97	7.27	9.07	9.29	12.83	11.91	10.31	9.51	11.23
SW-4	7.97	8.91	7.96	9.58	9.17	18.88	18.53	17.74	18.51	18.91
SW-5	7.56	7.88	7.81	10.43	8.91	19.17	18.74	17.97	18.72	19.17
SW-6	7.97	7.58	8.21	10.03	7.50	26.66	28.61	27.68	25.63	26.31
SW-7	7.66	7.35	8.65	8.74	8.11	36.09	35.47	36.76	35.96	35.73
SW-11	7.38	6.89	7.53	8.78	7.12	29.92	31.29	29.88	28.24	29.01
SW-12	7.90	7.23	7.72	7.19	7.12	36.33	35.72	37.04	36.15	35.96
SW-14	6.12	6.11	6.45	6.06	5.86	35.27	34.34	35.36	35.60	35.29
SW-16	5.83	5.83	5.83	6.59	5.83	34.93	33.95	34.98	35.35	35.00
SW-17	7.16	7.20	7.04	8.18	7.16	33.29	35.62	33.63	30.83	31.75
SW-18	5.83	5.83	5.83	5.83	6.12	15.57	15.42	15.52	14.58	14.92
SW-20	7.62	6.74	7.82	7.65	7.54	33.22	35.39	33.76	31.08	32.02
SW-25	6.82	6.13	6.63	7.81	6.58	13.53	14.42	16.72	18.23	23.00
SW-34	5.83	5.99	6.42	7.06	7.16	13.58	12.39	12.42	12.70	12.74
SW-37	6.23	6.01	6.50	6.37	6.16	9.12	8.25	8.29	8.53	8.62
SW-45	5.91	5.90	6.43	6.60	6.48	11.73	9.82	10.03	10.27	10.21
SW-50	6.10	6.01	6.35	6.01	6.16	13.04	13.22	13.14	13.78	13.88

Streamflow reductions are more in future horizon 2060, when a flooding may be possible owing to maximum rainfall events. Thus, this practice would be optimal solution to minimize flooding impact on river channel segment. From Figure 7.9, it is clearly observed that grade stabilization structures are more sensitive to the sediment yield reduction mainly in critical sub-watersheds located in the lower part of Betwa basin. In main channel, the CH_EROD parameter is less sensitive and the CH_S2 parameter is more sensitive for lower basin area (Table 7.9), which represents feasibility of structural practice to reduce the streamflow. Therefore, the present in-stream BMP intervention can be a value asset for reductions in sediment yield as well as streamflow during future years.

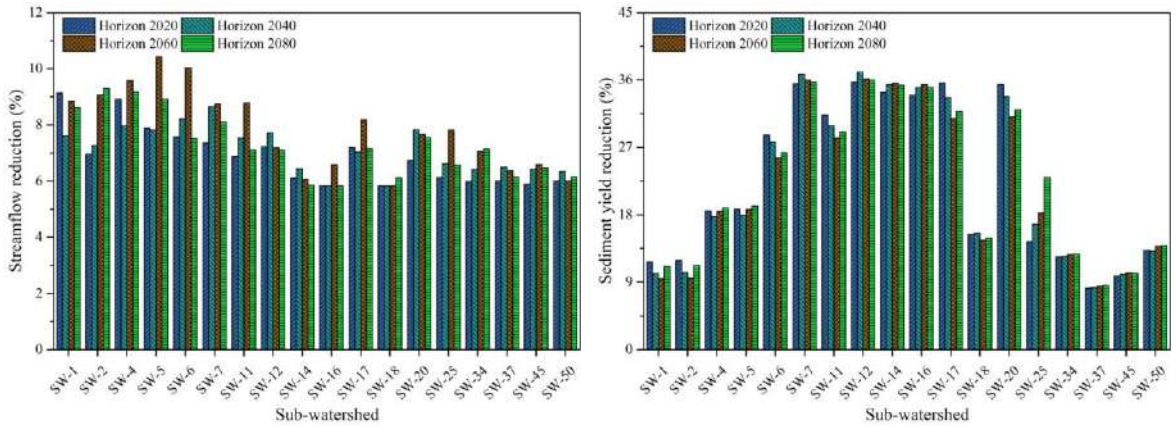

Figure 7.9: Effect of grade stabilization structures on future streamflow and sediment yield

Overall, this study significantly evaluated the overland as well as the river channel treatments to reduce streamflow and sediment yield in critical sub-watersheds of the Betwa basin. Streamflow is less sensitive than sediment yield in all BMP treatments.

7.8 SUMMARY

In the present study, the calibrated and validated SWAT model was employed for evaluation of overland as well as within channel BMPs, and recommendation of suitable soil and water conservation measures in the critical sub-watersheds of the Betwa basin. Initially, the soil erosion status based on the model simulation was accomplished to identify and prioritize critical sub-watersheds for BMP treatments. Then, the SWAT model was employed for evaluating the effectiveness of different management strategies to reduce streamflow and sediment yield considering conservation tillage, contour farming, residue management, grassed waterways, streambank stabilization and grade stabilization structures. Among these, first three BMPs were implemented for overland flow reduction, and last three were applied for protection of the river channel during future climate scenarios 2020, 2040, 2060 and 2080.

Following conclusions are drawn from the present study:

1. The SWAT model was effectively utilized for identification and prioritization of critical sub-watersheds for effective BMP treatments for agriculture land and river channels. About 2% of the total basin area were categorized as priority class-I; followed by 2.44% area under priority class-II, 3.18% area under priority class-III, 3.15% are under priority class-IV and 8.60% area under priority class-V, i.e. from very severe (more than 80 t $ha^{-1}year^{-1}$) to high (5-10 t ha^{-1} $year^{-1}$) soil erosion class.

2. Result of over-land BMPs showed that contour farming is the most effective treatment of agriculture land reducing streamflow about 9.78% to 13.25% and sediment yield about 6.38% to 34.41% for soil and water conservation in future. However, the conservation tillage could be the cost-effective treatment as none additional cost required to use this practice in the agriculture area.
3. The analysis of in-stream BMPs shows that both grassed waterways and streambank stabilization can be effective treatments for sediment yield reduction (about 20% to 60%) in critical areas of the upper basin (SW-34, SW-37, SW-45 and SW-50) and the lower basin (SW-1, SW-2, SW-4, SW-5, SW-6, SW-11, SW-18 and SW-25). The grade structural structure is the most effective treatment for streamflow reduction (about 6% to 10%) in the lower basin (SW-7, SW-12, SW-14, SW-16, SW-17 and SW-20).
4. The grade stabilization structure can effectively reduce the streamflow in main river channel during future horizon 2060, when flooding would be possible due to large precipitation events.
5. After BMP treatment, the percent reductions were varied in each horizon. It demonstrates that the sensitivity of each BMP parameter may alter in future under climatic changes.

Overall, an approach used in the study can be useful to prioritize the critical areas for intervention of effective BMPs for sustainable river basin management.

CHAPTER 8

CONCLUSIONS AND RECOMMENDATION OF THE STUDY

Various studies at a global to continental scale shows variability in the climate conditions. In this study, the effect of changing climatic conditions on hydrological processes for Betwa River basin, which is a tributary of Ganga river system, has been assessed. The basin is predominantly covered by agriculture areas playing important role in rural economy and food security. The study has been carried out with the following specific objectives:

1. To study the long-term changes in climatic variables in the Betwa basin.
2. To study the land use/land cover changes in the Betwa basin using satellite data.
3. To study the spatial correlation of land use/land cover with climate parameters in the Betwa basin.
4. Application of the Soil & Water Assessment (SWAT) model for estimation of runoff and sediment yield under changing climate.
5. Evaluation of optimal land use/land covers for the sustainable water resources development of the Betwa basin in changing climate.

To accomplish the above-mentioned objectives, analysis has been carried out using long term monthly data of climatic variables, discharge, sediment, satellite data for the basin. The SWAT model was used to estimate the runoff and sediment yield considering historical baseline (1986-2005) data as well as four future climate scenarios (downscaled GCM data) i.e. 2020-2039, 2040-2059, 2060-2079 and 2080-2099.

8.1 CONCLUSIONS

Based on the analysis, carried out in the report, the following conclusions are drawn:

1. The pre-monsoon rainfall is significantly increasing at 90% confidence level with time having the slope of 6.5 mm in 100 years over the Betwa river basin. The spatial trend analysis study has also been carried out utilizing the pre-monsoon rainfall data of all the rain gauge stations and the results are summarized in Chapter 3.
2. Minimum, maximum and average temperature during pre-monsoon, post-monsoon, and winter season as well as on annual basis are increasing at 99% confidence level. The rate of change varies from 0.7°C to 1.5°C per 100 years.

3. Minimum temperature is increasing at a faster rate than maximum temperature during winter season.
4. Potential Evapotranspiration is increasing at 99% confidence level during the winter season and the rate of increase is 3.8 mm per 100 years.
5. Aridity Index is increasing at 90% confidence level during the pre-monsoon season over.
6. Historical spatiotemporal LU/LC change analysis showed the accrued in agriculture area by 8.55% with increase in irrigation water availability from waterbody (0.89%) during the years 1972-2015. In 20^{th} century (from 2001-2015), about 3.10% agriculture area increased due to more water availability for irrigation (0.33%), especially from Rajghat reservoir located at central part of the Betwa basin.
7. Dense forest area reduced about 11.69% ceases to increase the degraded forest area about 3.33% during 1972-2015 in the Betwa basin.
8. Monthly rainfall exhibited a climatic greening response to vegetation (NDVI) change in dry, wet and all year analyses. However, T_{max} and T_{diff} exhibited a climatic degradation response to the NDVI. The positive response between monthly R_H and vegetation would not be altered under dry and wet spells.
9. The dominant crop land (CL) area showed significantly positive response with rainfall, T_{min}, Q, aridity index and sediment with values of r = 0.730, 0.801, 0.776, 0.654 and 0.801 respectively. The crop land was affected by the Tmax (-0.704) and Tdiff (-0.762) in the wet year analysis. However, in dry and all year analysis, none good correlation has been observed for CL area during the years 2001-2013.
10. About 10.77% area of the basin comes under the high to very severe soil erosion class (> 10 t $ha^{-1}year^{-1}$).
11. The temperature has shown significant increasing trend whereas the precipitation has shown significant decreasing trend under future climate scenario, except for the scenario 2060 (years 2060-2079) wherein an increasing trend is observed due to high precipitation, i.e. average annual precipitation is about 1152.55 mm.
12. Both runoff and sediment yield have shown almost similar variations under future climatic scenarios, i.e. increases in baseline 1986 and scenario 2060; however, it is expected to decrease for future scenarios of 2020, 2040 and 2080. It is observed that the flows at 50%,

75%, 90% and 99% dependability are likely to decrease in future resulting in a negative impact on river flows, particularly low flows, due to the expected climate change.

8.2 RECOMMENDATIONS

1. Increasing trend in pre-monsoon season rainfall may affect the harvesting of Rabi season crops. Thus, the early-growing crop variety should be introduced in agriculture.
2. Increase in the minimum and maximum temperature may lead to a significant change in the growing season, growth stages and crop water use that subsequently affects the yield. Therefore, the crop varieties, which can sustain in the high temperature, should be introduced in future.
3. Contour farming can be the most effective over-land BMP treatment for agriculture land reducing runoff (about 9.78% to 13.25%) and sediment yield (about 6.38% to 34.41%) for soil and water conservation under changing future climate.
4. The grade stabilization structure can effectively reduce the streamflow in main river channel during future horizon 2060, when flooding would be possible due to large precipitation events i.e. under future climatic changes.
5. Both grassed waterways and streambank stabilization practices can be the most effective in-stream BMP treatments reducing sediment yield (about 20% to 60%) by protecting river channel segment in future.

8.3 LIMITATIONS & FUTURE RESEARCH SCOPE

1. At the time of study, only monthly data of climatic variables were available, therefore extreme events and other important aspects of climate change on daily basis could not be analyzed.
2. In this study, monthly streamflow and sediment yield are simulated for sub-watershed level analysis. Thus, the SWAT model simulation study at daily time-scale and at HRU level need to be carried out to reduce the uncertainty in the results induced because of considering the larger temporal scale (i.e. monthly).
3. Cost-effectiveness of the BMP scenarios is required to be assessed based the evaluation of recommended interventions in the study area.
4. This study used only one GCM model with one RCP 8.5 GCM scenarios for future climate change analysis. Use of different RCP-scenarios (other than RCP 8.5) and different climate

models for future climate change impact assessment would be the scope of future research work. In addition to this, ensemble hydrological modelling may be carried out to reduce the uncertainty in the results.

5. Effect of Ken-Betwa River linking project on future change analysis was not considered during the study. Thus, this aspect may be considered as the scope of future research work in the Betwa river basin.

REFERENCES

Abbaspour, K. C. (2007). User manual for SWAT-CUP, SWAT calibration and uncertainty analysis programs. *Swiss Federal Institute of Aquatic Science and Technology, Eawag, Duebendorf, Switzerland*, *93*.

Abbaspour, K. C., Vejdani, M., Haghighat, S., & Yang, J. (2007). SWAT-CUP calibration and uncertainty programs for SWAT. In *MODSIM 2007 international congress on modelling and simulation, modelling and simulation society of Australia and New Zealand* (pp. 1596-1602).

Arnold, J. G., & Fohrer, N. (2005). SWAT2000: current capabilities and research opportunities in applied watershed modelling. *Hydrological processes*, *19*(3), 563-572.

Arnold, J. G., Allen, P. M., & Bernhardt, G. (1993). A comprehensive surface-groundwater flow model. *Journal of hydrology*, *142*(1-4), 47-69.

Arnold, J. G., Srinivasan, R., Muttiah, R. S., & Williams, J. R. (1998). Large area hydrologic modeling and assessment part I: model development. *JAWRA Journal of the American Water Resources Association*, *34*(1), 73-89.

ASCE Task Committee on Definition of Criteria for Evaluation of Watershed Models of the Watershed Management Committee, Irrigation and Drainage Division. (1993). Criteria for evaluation of watershed models. *Journal of Irrigation and Drainage Engineering*, *119*(3), 429-442.

Aziz, O. I. A., & Burn, D. H. (2006). Trends and variability in the hydrological regime of the Mackenzie River Basin. *Journal of hydrology*, *319*(1-4), 282-294.

Bannayan, M., Sanjani, S., Alizadeh, A., Lotfabadi, S. S., & Mohamadian, A. (2010). Association between climate indices, aridity index, and rainfed crop yield in northeast of Iran. *Field Crops Research*, *118*(2), 105-114.

Bari, M. A., Smith, N., Ruprecht, J. K., & Boyd, B. W. (1996). Changes in streamflow components following logging and regeneration in the southern forest of Western Australia. *Hydrological processes*, *10*(3), 447-461.

Barichivich, J., Briffa, K. R., Myneni, R. B., Osborn, T. J., Melvin, T. M., Ciais, P., ... & Tucker, C. (2013). Large-scale variations in the vegetation growing season and annual cycle of atmospheric CO2 at high northern latitudes from 1950 to 2011. *Global change biology*, *19*(10), 3167-3183.

Behera, S., & Panda, R. K. (2006). Evaluation of management alternatives for an agricultural watershed in a sub-humid subtropical region using a physical process based model. *Agriculture, ecosystems & environment*, *113*(1-4), 62-72.

Bian, L., Sun, H., Blodgett, C., Egbert, S., Li, W., Ran, L., & Koussis, A. (1996). An integrated interface system to couple the SWAT model and ARC/INFO. In *Proceedings of the 3rd International Conference on Integrating GIS and Environmental Modeling. US National Center for Geographic Information and Analysis, Santa Fe, New Mexico, CD-ROM.*

Blaney, H. F., & Criddle, W. D. (1962). *Determining consumptive use and irrigation water requirements* (No. 1275). US Department of Agriculture.

Bulygina, N., Ballard, C., McIntyre, N., O'Donnell, G., & Wheater, H. (2012). Integrating different types of information into hydrological model parameter estimation: application to ungauged catchments and land use scenario analysis. *Water Resources Research*, 48(6). doi: 10.1029/2011WR011207

Burn, D. H. (2008). Climatic influences on streamflow timing in the headwaters of the Mackenzie River Basin. *Journal of Hydrology*, *352*(1-2), 225-238.

Burn, D. H., & Elnur, M. A. H. (2002). Detection of hydrologic trends and variability. *Journal of hydrology*, *255*(1-4), 107-122.

Burn, D.H., Cunderlik, J.M., & Pietroniro, A. (2004). Hydrological trends and Variability in the Liard River basin, *Hydrological Sciences Journal*, 49(1), 53–68.

Chandramouli, C., & Sinha, S. (2014). Census of India 2011: District Census Handbook Bhopal. Directorate of Census Operations, Madhya Pradesh, Government of India, Series-24, Part XII-B.

Chaube, U.C. (1988). Model study of water use and water balance in Betwa Basin, *J. Institution of Engineers (India)*, 69:169–173.

Chauhan, M. S., & Quamar, M. F. (2010). Vegetation and climate change in southeastern Madhya Pradesh during Late Holocene, based on pollen evidence. *Journal of the Geological Society of India*, *76*(2), 143-150.

Chauhan, M. S., & Quamar, M. F. (2012). Pollen records of vegetation and inferred climate change in southwestern Madhya Pradesh during the last ca. 3800 years. *Journal of the Geological Society of India*, *80*(4), 470-480.

Chen, H., Guo, S., Xu, C. Y., & Singh, V. P. (2007). Historical temporal trends of hydro-climatic variables and runoff response to climate variability and their relevance in water resource management in the Hanjiang basin. *Journal of hydrology*, *344*(3-4), 171-184.

Chien, H., Yeh, P. J. F., & Knouft, J. H. (2013). Modeling the potential impacts of climate change on streamflow in agricultural watersheds of the Midwestern United States. *Journal of Hydrology*, *491*, 73-88.

Chiew, F. H. S., Teng, J., Vaze, J., Post, D. A., Perraud, J. M., Kirono, D. G. C., & Viney, N. R. (2009). Estimating climate change impact on runoff across southeast Australia: Method, results, and implications of the modeling method. *Water Resources Research*, *45*(10). doi:10.1029/2008WR007338

Chu, T. W., Shirmohammadi, A., Montas, H., & Sadeghi, A. (2004). Evaluation of the SWAT model's sediment and nutrient components in the Piedmont physiographic region of Maryland. *Transactions of the ASAE*, *47*(5), 1523-1538.

Dabral, P. P., & Pandey, A. (2007). Morphometric analysis and prioritization of eastern Himalayan River basin using Satellite data and GIS. *Asian J Geoinformatics*, *7*(3), 3-14.

Das, L., Dutta, M., Mezghani, A., & Benestad, R. E. (2018). Use of observed temperature statistics in ranking CMIP5 model performance over the Western Himalayan Region of India. International Journal of Climatology, 38(2), 554-570.

Dimyati, M. U. H., Mizuno, K., Kobayashi, S., & Kitamura, T. (1996). An analysis of land use/cover change in Indonesia. *International Journal of Remote Sensing*, *17*(5), 931-944.

Douglas, E. M., Vogel, R. M., & Kroll, C. N. (2000). Trends in floods and low flows in the United States: impact of spatial correlation. *Journal of hydrology*, *240*(1-2), 90-105.

Dubovyk, O., Landmann, T., Erasmus, B. F., Tewes, A., & Schellberg, J. (2015). Monitoring vegetation dynamics with medium resolution MODIS-EVI time series at sub-regional scale in southern Africa. *International Journal of Applied Earth Observation and Geoinformation*, *38*, 175-183.

Duhan, D., & Pandey, A. (2013). Statistical analysis of long term spatial and temporal trends of precipitation during 1901–2002 at Madhya Pradesh, India. *Atmospheric Research*, *122*, 136-149.

Ehsanzadeh, E., Ouarda, T. B., & Saley, H. M. (2011). A simultaneous analysis of gradual and abrupt changes in Canadian low streamflows. *Hydrological Processes*, *25*(5), 727-739.

Fontaine, T. A., Klassen, J. F., Cruickshank, T. S., & Hotchkiss, R. H. (2001). Hydrological response to climate change in the Black Hills of South Dakota, USA. *Hydrological Sciences Journal*, *46*(1), 27-40.

Foster, G. R., & Meyer, L. D. (1972). Closed-form soil erosion equation for upland areas. In *Sedimentation Symposium To Honor Professor HA Einstein, Berkeley, 1971. (Papers)*

Frederick, K. D., & Major, D. C. (1997). Climate change and water resources. *Climatic Change*, *37*(1), 7-23.

Geng, L., Ma, M., Wang, X., Yu, W., Jia, S., & Wang, H. (2014). Comparison of eight techniques for reconstructing multi-satellite sensor time-series NDVI data sets in the Heihe river basin, China. *Remote Sensing*, 6(3), 2024-2049. DOI: 10.3390/rs6032024

Goswami, B. N., Venugopal, V., Sengupta, D., Madhusoodanan, M. S., & Xavier, P. K. (2006). Increasing trend of extreme rain events over India in a warming environment. *Science*, *314*(5804), 1442-1445.

Gu, Y., Hunt, E., Wardlow, B., Basara, J. B., Brown, J. F., & Verdin, J. P. (2008). Evaluation of MODIS NDVI and NDWI for vegetation drought monitoring using Oklahoma Mesonet soil moisture data. *Geophysical Research Letters*, *35*(22). doi: 10.1029/2008GL035772

Guo, Y., Cao, J., Li, H., Wang, J., & Ding, Y. (2016). Simulation of the interface between the Indian summer monsoon and the East Asian summer monsoon: Intercomparison between MPI-ESM and ECHAM5/MPI-OM. Advances in Atmospheric Sciences, 33(3), 294-308.

Gupta, H. V., Sorooshian, S., & Yapo, P. O. (1999). Status of automatic calibration for hydrologic models: Comparison with multilevel expert calibration. *Journal of Hydrologic Engineering*, *4*(2), 135-143.

Haan, C.T., Johnson, H.P. and Brakensiek, D.L. (1982). Hydrological modeling of small watersheds, *American Society of Agricultural Engineers*, 2950 Niles Road, ASAE, St. Joseph, Michigan.

Hamed, K. H., & Rao, A. R. (1998). A modified Mann-Kendall trend test for autocorrelated data. *Journal of Hydrology*, *204*(1-4), 182-196.

Hargreaves, G. H., & Samani, Z. A. (1985). Reference crop evapotranspiration from temperature. *Applied engineering in agriculture*, *1*(2), 96-99.

Hirsch, R. M., & Slack, J. R. (1984). A nonparametric trend test for seasonal data with serial dependence. *Water Resources Research*, *20*(6), 727-732.

Hirsch, R. M., Slack, J. R., & Smith, R. A. (1982). Techniques of trend analysis for monthly water quality data. *Water resources research*, *18*(1), 107-121.

Huo, Z., Dai, X., Feng, S., Kang, S., & Huang, G. (2013). Effect of climate change on reference evapotranspiration and aridity index in arid region of China. *Journal of Hydrology*, *492*, 24-34.

Jang, S. S., Ahn, S. R., & Kim, S. J. (2017). Evaluation of executable best management practices in Haean highland agricultural catchment of South Korea using SWAT. *Agricultural Water Management*, *180*, 224-234.

Jönsson, P., & Eklundh, L. (2004). TIMESAT—a program for analyzing time-series of satellite sensor data. *Computers & Geosciences*, 30(8), 833-845. DOI: 10.1016/j.cageo.2004.05.006

Jothityangkoon, C., Sivapalan, M., & Farmer, D. L. (2001). Process controls of water balance variability in a large semi-arid catchment: downward approach to hydrological model development. Journal of Hydrology, 254(1-4), 174-198.

Kendall, M. G. (1975). Rank Correlation Measures [M]. *London: Charles Griffin*.

Kingston, D. G., & Taylor, R. G. (2010). Sources of uncertainty in climate change impacts on river discharge and groundwater in a headwater catchment of the Upper Nile Basin, Uganda. *Hydrology and Earth System Sciences*, *14*(7), 1297-1308.

Kulkarni, A. V., & Karyakarte, Y. (2014). Observed changes in Himalayan glaciers. *Current Science*, 237-244.

Kumar, K. K., Patwardhan, S. K., Kulkarni, A., Kamala, K., Rao, K. K., & Jones, R. (2011). Simulated projections for summer monsoon climate over India by a high-resolution regional climate model (PRECIS). *Current Science*, *101*(3), 312-326.

Kumar, K. R., & Hingane, L. S. (1988). Long-term variations of surface air temperature at major industrial cities of India. *Climatic Change*, *13*(3), 287-307.

Kuznetsov, M. S., Gendugov, V. M., Khalilov, M. S., & Ivanuta, A. A. (1998). An equation of soil detachment by flow. *Soil and tillage research*, *46*(1-2), 97-102.

Lal, M., Singh, K. K., Srinivasan, G., Rathore, L. S., Naidu, D., & Tripathi, C. N. (1999). Growth and yield responses of soybean in Madhya Pradesh, India to climate variability and change. *Agricultural and Forest Meteorology*, *93*(1), 53-70.

Lam, Q. D., Schmalz, B., & Fohrer, N. (2011). The impact of agricultural Best Management Practices on water quality in a North German lowland catchment. *Environmental monitoring and assessment*, *183*(1-4), 351-379.

Lanorte, A., Lasaponara, R., Lovallo, M., & Telesca, L. (2014). Fisher–Shannon information plane analysis of SPOT/VEGETATION Normalized Difference Vegetation Index (NDVI) time series to characterize vegetation recovery after fire disturbance. *International Journal of Applied Earth Observation and Geoinformation*, *26*, 441-446.

Leavesley, G. H. (1994). Modeling the effects of climate change on water resources—a review. In *Assessing the Impacts of Climate Change on Natural Resource Systems* (pp. 159-177). Springer, Dordrecht.

Legates, D. R., & McCabe, G. J. (1999). Evaluating the use of "goodness-of-fit" measures in hydrologic and hydroclimatic model validation. *Water resources research*, *35*(1), 233-241.

Lettenmaier, D. P., Wood, E. F., & Wallis, J. R. (1994). Hydro-climatological trends in the continental United States, 1948-88. *Journal of Climate*, *7*(4), 586-607.

Lewarne, M. (2009). *Setting up hydrological model for the Verlorenvlei catchment* (Doctoral dissertation, Thesis (PhD). Stellenbosch University, South Africa).

Lins, H. F., & Slack, J. R. (1999). Streamflow trends in the United States. *Geophysical research letters*, *26*(2), 227-230.

Mann, H. B. (1945). Nonparametric tests against trend. *Econometrica: Journal of the Econometric Society*, 245-259.

McIntyre, N., & Marshall, M. (2010). Identification of rural land management signals in runoff response. *Hydrological Processes*, *24*(24), 3521-3534.

Mehrotra, D., & Mehrotra, R. (1995). Climate change and hydrology with emphasis on the Indian subcontinent. *Hydrological Sciences Journal*, *40*(2), 231-242.

Millington, A. C. (1986). Reconnaissance scale soil erosion mapping using a simple geographic information system in the humid tropics. *Land evaluation for land-use planning and conservation in sloping areas*, 64-81.

Mirza, M. Q., Warrick, R. A., Ericksen, N. J., & Kenny, G. J. (1998). Trends and persistence in precipitation in the Ganges, Brahmaputra and Meghna river basins. *Hydrological Sciences Journal*, *43*(6), 845-858.

Mishra, A. K., Özger, M., & Singh, V. P. (2009). Trend and persistence of precipitation under climate change scenarios for Kansabati basin, India. *Hydrological processes*, *23*(16), 2345-2357.

Monteith, J.L. (1965). Evaporation and the environment. p. 205-234. In The state and movement of water in living organisms, *XIXth Symposium. Society for Experimental Biology, Swansea, Cambridge University Press*.

Moore, I. D., & Grayson, R. B. (1991). Terrain-based catchment partitioning and runoff prediction using vector elevation data. *Water Resources Research*, *27*(6), 1177-1191.

Moriasi, D. N., Arnold, J. G., Van Liew, M. W., Bingner, R. L., Harmel, R. D., & Veith, T. L. (2007). Model evaluation guidelines for systematic quantification of accuracy in watershed simulations. *Transactions of the ASABE*, *50*(3), 885-900.

Murty, P. S., Pandey, A., & Suryavanshi, S. (2014). Application of semi-distributed hydrological model for basin level water balance of the Ken basin of Central India. *Hydrological processes*, *28*(13), 4119-4129.

Narayana, D. (1993). *Soil and water conservation research in India*. Indian Council of Agricultural Research; New Delhi.

Nash, J. E., & Sutcliffe, J. V. (1970). River flow forecasting through conceptual models part I—A discussion of principles. *Journal of hydrology*, *10*(3), 282-290.

National Water Policy (2012). Draft as recommended by National Water Board, *Ministry of Water Resources*, http://mowr.gov.in/writereaddata/linkimages/DraftNWP2012_English9353289094.pdf, accessed on 20 September 2012.

Neitsch, S. L. (2004). ARNOLD, JG, KINIRY, JR. *SRINIVASAN, R., WILLIAMS JR "Soil and Water Assessment Tool. Input/Output File Documentation*.

Neitsch, S. L., Arnold, J. G., Kiniry, J. R., & Williams, J. R. (2011). *Soil and water assessment tool theoretical documentation version 2009*. Texas Water Resources Institute.

Neitsch, S. L., Arnold, J. G., Kiniry, J. R., Williams, J. R., & King, K. W. (2005). Soil and water assessment tool theoretical documentation. Grassland. *Soil and Water Research Laboratory, Temple, TX*.

Niraula, R., Kalin, L., Srivastava, P., & Anderson, C. J. (2013). Identifying critical source areas of nonpoint source pollution with SWAT and GWLF. *Ecological Modelling*, *268*, 123-133.

NWDA (1993). Technical study No. 70, Water Balance Study of lower Betwa Sub basin of Betwa Basin, *National Water Development Agency*, Government of India, pp 156.

Önöz, B., & Bayazit, M. (2003). The power of statistical tests for trend detection. *Turkish Journal of Engineering and Environmental Sciences*, *27*(4), 247-251.

Pal, I., & Al-Tabbaa, A. (2011). Assessing seasonal precipitation trends in India using parametric and non-parametric statistical techniques. *Theoretical and Applied Climatology*, *103*(1-2), 1-11.

Panday, P. K., & Ghimire, B. (2012). Time-series analysis of NDVI from AVHRR data over the Hindu Kush–Himalayan region for the period 1982–2006. *International journal of remote sensing*, *33*(21), 6710-6721.

Pandey, A., Chowdary, V. M., Mal, B. C., & Billib, M. (2008). Runoff and sediment yield modeling from a small agricultural watershed in India using the WEPP model. *Journal of Hydrology*, *348*(3-4), 305-319.

Pandey, A., Chowdary, V. M., Mal, B. C., & Billib, M. (2009d). Application of the WEPP model for prioritization and evaluation of best management practices in an Indian watershed. *Hydrological processes*, *23*(21), 2997-3005.

Pandey, V. K., Panda, S. N., & Sudhakar, S. (2005). Modelling of an agricultural watershed using remote sensing and a geographic information system. *Biosystems Engineering*, *90*(3), 331-347.

Pandey, V. K., Panda, S. N., Pandey, A., & Sudhakar, S. (2009c). Evaluation of effective management plan for an agricultural watershed using AVSWAT model, remote sensing and GIS. *Environmental Geology*, *56*(5), 993-1008.

Peel, M. C., & Blöschl, G. (2011). Hydrological modelling in a changing world. *Progress in Physical Geography*, *35*(2), 249-261.

Poveda, G., & Mesa, O. J. (1997). Feedbacks between hydrological processes in tropical South America and large-scale ocean–atmospheric phenomena. *Journal of climate*, *10*(10), 2690-2702.

Priestley, C. H. B., & Taylor, R. J. (1972). On the assessment of surface heat flux and evaporation using large-scale parameters. *Monthly weather review*, *100*(2), 81-92.

Quamar, M. F., & Chauhan, M. S. (2014). Signals of Medieval Warm Period and Little Ice Age from southwestern Madhya Pradesh (India): a pollen-inferred late-Holocene vegetation and climate change. *Quaternary International*, *325*, 74-82.

Ranade, A., Singh, N., Singh, H. N. and Sontakke, N. A. (2008). On variability of hydrological wet season, seasonal rainfall and rainwater potential of the river basins of India (1813–2006), *Journal of Hydrological Research and Development*, 23:79–108.

Rao, P. G. (1993). Climatic changes and trends over a major river basin in India. *Climate Research*, 215-223.

Rasmussen, M. S. (1997). Operational yield forecast using AVHRR NDVI data: reduction of environmental and inter-annual variability. *International Journal of Remote Sensing*, *18*(5), 1059-1077.

Refsgaard, J. C. (1987, August). A methodology for distinguishing between the effects of human influence and climate variability on the hydrologic cycle. In *Proceedings of the Vancouver Symposium 'The Influence of Climate Change Variability on the Hydrologic Regime and Water Resources* (pp. 557-570).

Riebsame, W. E., Meyer, W. B., & Turner, B. L. (1994). Modeling land use and cover as part of global environmental change. *Climatic change*, *28*(1-2), 45-64.

Roxy, M. K., Modi, A., Murtugudde, R., Valsala, V., Panickal, S., Prasanna Kumar, S., Ravichandran, M., Vichi, M., & Lévy, M. (2016). A reduction in marine primary productivity driven by rapid warming over the tropical Indian Ocean. Geophysical Research Letters, 43(2), 826-833.

Running, S. W. (1990). Estimating terrestrial primary productivity by combining remote sensing and ecosystem simulation. In *Remote sensing of biosphere functioning* (pp. 65-86). Springer, New York, NY.

Schulze, R. E. (2000). Modelling hydrological responses to land use and climate change: a southern African perspective. *AMBIO: A Journal of the Human Environment*, *29*(1), 12-22.

Shah, S. K., Bhattacharyya, A., & Chaudhary, V. (2007). Reconstruction of June–September precipitation based on tree-ring data of teak (Tectona grandis L.) from Hoshangabad, Madhya Pradesh, India. *Dendrochronologia*, *25*(1), 57-64.

Sharda, V. N., Dogra, P., & Dhyani, B. L. (2012). Indicators for assessing the impacts of watershed development programmes in different regions of India. *Indian Journal of Soil Conservation*, *40*(1), 1-12.

Sharmila, S., Joseph, S., Sahai, A. K., Abhilash, S., & Chattopadhyay, R. (2015). Future projection of Indian summer monsoon variability under climate change scenario: An assessment from CMIP5 climate models. Global and Planetary Change, 124, 62-78.

Singh, G., Babu, R., Narain, P., Bhushan, L. S., & Abrol, I. P. (1992). Soil erosion rates in India. *Journal of Soil and water Conservation*, *47*(1), 97-99.

Singh, J., Knapp, H. V., Arnold, J. G., & Demissie, M. (2005). Hydrological modeling of the Iroquois River watershed using HSPF and SWAT. *JAWRA Journal of the American Water Resources Association*, *41*(2), 343-360.

Singh, V. P. (1995). Computer models of watershed hydrology. Chapter 1: Watershed Modelling. *Water Resources Publications*, Colorado.

Sloan, P. G. (1983). Modeling surface and subsurface stormflow on steeply-sloping forested watersheds.

Small, E. E., & Kurc, S. A. (2003). Tight coupling between soil moisture and the surface radiation budget in semiarid environments: Implications for land-atmosphere interactions. *Water Resources Research*, *39*(10). doi: 10.1029/2002WR001297

Some'e, B. S., Ezani, A., & Tabari, H. (2012). Spatiotemporal trends and change point of precipitation in Iran. *Atmospheric research*, *113*, 1-12.

Subash, N., Sikka, A. K., & Mohan, H. R. (2011). An investigation into observational characteristics of rainfall and temperature in Central Northeast India—a historical perspective 1889–2008. *Theoretical and applied climatology*, *103*(3-4), 305-319.

Suryavanshi, S., Pandey, A., Chaube, U. C., & Joshi, N. (2014). Long-term historic changes in climatic variables of Betwa Basin, India. *Theoretical and applied climatology*, *117*(3-4), 403-418.

Tabari, H. and Aghajanloo, M.B. (2012). Temporal pattern of aridity index in Iran with considering precipitation and evapotranspiration trends, *International J. Climatology*. doi: 10.1002/joc.3432.

Tabari, H., Somee, B. S., & Zadeh, M. R. (2011). Testing for long-term trends in climatic variables in Iran. *Atmospheric Research*, *100*(1), 132-140.

Thrasher, B., Maurer, E. P., McKellar, C., & Duffy, P. B., 2012: Technical Note: Bias correcting climate model simulated daily temperature extremes with quantile mapping. Hydrology and Earth System Sciences, 16(9), 3309-3314.

Tripathi, M. P., Panda, R. K., & Raghuwanshi, N. S. (2005). Development of effective management plan for critical subwatersheds using SWAT model. *Hydrological Processes*, *19*(3), 809-826.

Tucker, C. J., & Nicholson, S. E. (1999). Variations in the size of the Sahara Desert from 1980 to 1997. *Ambio*, 587-591.

Turner, N. C. (2004). Agronomic options for improving rainfall-use efficiency of crops in dryland farming systems. *Journal of Experimental Botany*, *55*(407), 2413-2425.

Ullrich, A., & Volk, M. (2009). Application of the Soil and Water Assessment Tool (SWAT) to predict the impact of alternative management practices on water quality and quantity. *Agricultural Water Management*, *96*(8), 1207-1217.

UNEP (1992). United Nations Environment Programme (UNEP). World Atlas of Desertification.

USDA, S. (1972). Section 4: Hydrology. *National Engineering Handbook, Washington, DC, Soil Conservation Service*.

USDA-NRSC (2005). The PLANTS Database, Version 3.5. Data compiled from various sources by Mark W. Skinner. *National Plant Data Center, Baton Rouge, LA*, 70874-4490.

Vangelis, H., Tigkas, D., & Tsakiris, G. (2013). The effect of PET method on Reconnaissance Drought Index (RDI) calculation. *Journal of Arid Environments*, *88*, 130-140.

Vazquez-Amábile, G. G., & Engel, B. A. (2005). Use of SWAT to compute groundwater table depth and streamflow in the Muscatatuck River watershed. *Transactions of the ASAE*, *48*(3), 991-1003.

Wagener, T. (2007). Can we model the hydrological impacts of environmental change?. *Hydrological Processes*, *21*(23), 3233-3236.

Wardlow, B. D., & Egbert, S. L. (2008). Large-area crop mapping using time-series MODIS 250 m NDVI data: An assessment for the US Central Great Plains. *Remote sensing of environment*, *112*(3), 1096-1116.

WCDMP-45. (2000). World Climate Programme –Water, Detecting Trend and Other Changes in Hydrological Data, Zbigniew W. Kundzewicz and Alice Robson (Editors), Genva, May 2000, *United Nations Educational Scientific and Cultural Organization*, World Meteorological Organization.

Weiss, J. L., Gutzler, D. S., Coonrod, J. E. A., & Dahm, C. N. (2004). Seasonal and inter-annual relationships between vegetation and climate in central New Mexico, USA. *Journal of arid environments*, *57*(4), 507-534.

Wilcox, B. P., Rawls, W. J., Brakensiek, D. L., & Wight, J. R. (1990). Predicting runoff from rangeland catchments: a comparison of two models. *Water Resources Research*, *26*(10), 2401-2410.

Williams, J. R., Izaurralde, R. C., & Steglich, E. M. (2008). Agricultural policy/environmental extender model. *Theoretical Documentation, Version*, *604*, 2008-17.

Willmott, C. J. (1981). On the validation of models. *Physical geography*, *2*(2), 184-194.

Yue, S., & Pilon, P. (2004). A comparison of the power of the t test, Mann-Kendall and bootstrap tests for trend detection. *Hydrological Sciences Journal*, *49*(1), 21-37.

Yue, S., Pilon, P., & Cavadias, G. (2002). Power of the Mann–Kendall and Spearman's rho tests for detecting monotonic trends in hydrological series. *Journal of hydrology*, *259*(1-4), 254-271.

Zhang, Q., Jiang, T., Gemmer, M., & Becker, S. (2005). Precipitation, temperature and runoff analysis from 1950 to 2002 in the Yangtze basin, China/Analyse des précipitations, températures et débits de 1950 à 2002 dans le bassin du Yangtze, en Chine. *Hydrological Sciences Journal*, *50*(1).

Zhou, L., Tucker, C. J., Kaufmann, R. K., Slayback, D., Shabanov, N. V., & Myneni, R. B. (2001). Variations in northern vegetation activity inferred from satellite data of vegetation index during 1981 to 1999. *Journal of Geophysical Research: Atmospheres*, *106*(D17), 20069-20083.

Zribi, M., Paris Anguela, T., Duchemin, B., Lili, Z., Wagner, W., Hasenauer, S., & Chehbouni, A. (2010). Relationship between soil moisture and vegetation in the Kairouan plain region of Tunisia using low spatial resolution satellite data. *Water Resources Research*, *46*(6). doi:10.1029/2009WR008196

APPENDIX-A

Field Visit (August 2-3, 2013)

Place: Basoda-Ganj Village- near Rapta pul at right bank of Betwa River
Latitude: 23° 52' 41.0", **Longitude:** 77° 55' 05.6", **Elevation:** 400 m

Place: Basoda-Ganj Village- Farm near Rapta pul at right bank of the Betwa River
Latitude: 23° 52' 26.1", **Longitude:** 77° 55' 12.5", **Elevation:** 410 m

Place: Basoda-Ganj Village- river flow condition near Rapta pul, view from right bank of the Betwa River
Latitude: 23° 52' 41.0", **Longitude:** 77° 55' 05.6", **Elevation:** 400 m

Place: Basoda-Ganj Village- Sediment flow by Betwa River water near Rapta pul
Latitude: 23° 52' 41.0", **Longitude:** 77° 55' 05.6", **Elevation:** 400 m

Place: Basoda-Ganj Village- cutting of river bank by Betwa River water flow near Rapta pul
Latitude: 23° 52' 41.0", **Longitude:** 77° 55' 05.6", **Elevation:** 400 m

Place: Basoda- near Ambanagar pul water flow condition, view from right bank of the Betwa River
Latitude: 23° 53' 01.6", **Longitude:** 77° 55' 11.9", **Elevation:** 397 m

Place: Basoda- near Ambanagar pul, view from right bank of the Betwa River
Latitude: 23° 53' 01.6", **Longitude:** 77° 55' 11.9", **Elevation:** 397 m

Place: Basoda_Nandpura village- soyabeen farm at left bank of the Betwa River
Latitude: 23° 51' 08.6", **Longitude:** 77° 52' 45.6", **Elevation:** 414 m

Place: Basoda_Nandpura village- soyabeen farm observation by Prof. S.K. Sharma with farmer (after crossing Barighat pul) at left bank of the Betwa River- **Farmer:** Kushal Singh
Latitude: 23° 51' 08.6", **Longitude:** 77° 52' 45.6", **Elevation:** 414 m

Place: Vidisha - right bank view of the Betwa River before crossing the pul, near Mela ground
Latitude: 23° 32' 24.8", **Longitude:** 77° 48' 09.6", **Elevation:** 425 m

Place: Vidisha_ left bank view of the Betwa River after crossing the pul, near Mela ground
Latitude: 23° 32' 24.8", **Longitude:** 77° 48' 09.6", **Elevation:** 425 m

Place: Vidisha_ River divide in two way, view from right bank of the Betwa River, near Mela ground
Latitude: 23° 32' 24.8", **Longitude:** 77° 48' 09.6", **Elevation:** 425 m

Field Visit (May 7-8, 2014)

Place: Nandpura Village near Basoda
Latitude: 23° 51' 8.6" N, **Longitude:** 77° 56' 45.6" E, **Elevation:** 420 m

Place: Ambanagar pul
Latitude: 23° 52' 59.1", **Longitude:** 77° 55’12.4", **Elevation** 400 m

Place: Barrighat pul
Latitude: 23° 51' 0.08", **Longitude**: 77° 53' 09.8", **Elevation:** 400 m

Place: Field2 (Basoda)
Latitude: 23° 52' 50.0", **Longitude:** 77° 55’10.0"

Place: Field 3 (Behind Manorma colony, Sagar)
Latitude: 23° 49' 54.5", **Longitude**: 78° 45' 52.6"

Place: Forest (Sagar)
Latitude: 23° 49' 27.1", **Longitude**: 78° 45' 7.09"

Place: Forest2 (Sagar)
Latitude: 23° 49' 37.6", **Longitude**: 78° 45' 6.25"

Place: Water Body Sagar (Pond)
Latitude: 23° 49' 59.0", **Longitude:** 78° 44' 48.5"

Place: Field (Sihora)
Latitude 23° 47' 57.0", **Longitude**: 78° 35' 01.8"

Place: Field (Rahatgadh)
Latitude: 23° 47' 37.6", **Longitude:** 78° 24' 28.0"

Place: Field (Begamganj)
Latitude: 23° 36' 13.0", **Longitude**: 78° 20' 53"

Place: Barren Land (Geratganj)
Latitude: 23° 25' 11.2", **Longitude:** 78° 14' 42.0"

Place: Field (Garhi)
Latitude: 23° 23' 20.4", **Longitude:** 78° 08' 59.3"

Place: Field (Dehgaon)
Latitude: 23° 19' 32.0", **Longitude:** 78° 06' 05.4"

Place: Field (Narwar)
Latitude: 23° 18' 30.4", **Longitude:** 77° 57' 58.0"

Place: Field (Raisen)
Latitude: 23° 19' 08.8", **Longitude:** 77° 47' 39.8"

Place: Field (Bhopal)
Latitude: 23° 14' 52.6", **Longitude:** 77° 32' 56.3"

Place: Field (Bhopal)
Latitude: 23° 15' 27.4", **Longitude:** 77° 30' 29.8"

Place: Bhopal (Waterbody)
Latitude: 23° 15' 12.3", **Longitude:** 77° 23' 26.8"

Place: Begamganj (Barren Land)
Latitude 23° 36' 38.2", **longitude** 77° 20' 58.0"

Field Visit (November 19-22, 2014)

Place: Rajghat dam
Latitude: 24° 45.928' N, **Longitude**: 78° 14.264' E, **Elevation**: 345 m

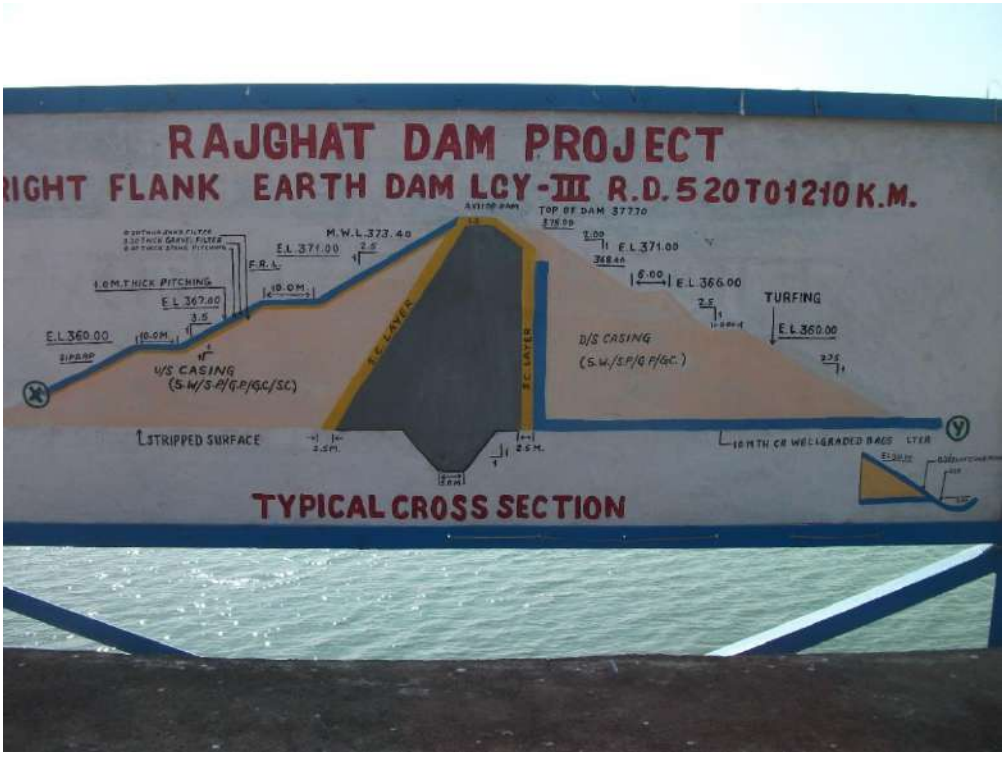

Place: Typical cross section board on Rajghat dam
Latitude: 24° 45.720' N, **Longitude**: 78° 14.198' E, **Elevation**: 380 m

Place: Side view from top-right side of the Rajghat dam
Latitude: 24° 45.720' N, **Longitude**: 78° 14.198' E, **Elevation**: 380 m

Place: Rajghat dam open gate
Latitude: 24° 45.720' N, **Longitude**: 78° 14.198' E, **Elevation**: 380 m

Place: Rajghat dam close gate
Latitude: 24° 45.720' N, **Longitude**: 78° 14.198' E, **Elevation**: 380 m

Place: Chanderi village view
Latitude: 24° 43.159' N, **Longitude**: 78° 08.372' E, **Elevation**: 437 m

Place: Fort near Chanderi village
Latitude: 24° 42.643' N, **Longitude**: 78° 08.417' E, **Elevation**: 501 m

Place: Near Roda village
Latitude: 24° 44.701' N, **Longitude**: 78° 25.807' E, **Elevation**: 349 m

Place: Near Maharra village
Latitude: 24° 47.440' N, **Longitude**: 78° 26.843' E, **Elevation**: 340 m

Place: Near Nadawara village
Latitude: 24° 47.711' N, **Longitude**: 78° 27.160' E, **Elevation**: 338 m

Place: Near Nadawara village
Latitude: 24° 48.322' N, **Longitude**: 78° 27.300' E, **Elevation**: 340 m

Place: Near Lakhanpura village
Latitude: 24° 50.360' N, **Longitude**: 78° 27.868' E, **Elevation**: 337 m

Place: Near Bansi village
Latitude: 24° 54.498' N, **Longitude**: 78° 28.069' E, **Elevation**: 337 m

Place: Shahjad reservoir
Latitude: 24° 56.761' N, **Longitude**: 78° 28.099' E, **Elevation**: 330 m

Place: Near Shahjad reservoir
Latitude: 24° 58.098' N, **Longitude**: 78° 27.987' E, **Elevation**: 329 m

Place: Near Matatila dam
Latitude: 25° 2.985' N, **Longitude**: 78° 23.040' E, **Elevation**: 306 m

Place: Matatila dam storage
Latitude: 25° 4.012' N, **Longitude**: 78° 22.778' E, **Elevation**: 305 m

Place: Downstream side of the Matatila dam
Latitude: 25° 5.887'N, **Longitude**: 78° 22.955' E, **Elevation**: 292 m

Place: Matatila dam
Latitude: 25° 5.887'N, **Longitude**: 78° 22.955' E, **Elevation**: 292 m

Place: Measure scale over gate
Latitude: 25° 5.705'N, **Longitude**: 78° 22.489' E, **Elevation**: 307 m

Place: Garden near Matatila dam
Latitude: 25° 5.887'N; **Longitude**: 78° 22.955' E; **Elevation**: 292m

Place: Near Khandi village
Latitude: 25° 4.128' N, **Longitude**: 78° 27.838' E, **Elevation**: 329 m

Place: Near Khandi village
Latitude: 25° 4.128' N, **Longitude:** 78° 27.838' E, **Elevation:** 329m

Place: Near Birdha village
Latitude: 25° 6.392' N, **Longitude**: 78° 31.395' E, **Elevation**: 302 m

Field Visit (16-17 Nov 2016)

Place: Ch. Charan Singh Lahchura Dam (Dhasan River)
Latitude: 25°13’41.8597”N **Longitude**: 79°13’50”E **Elevation**: 169 m

Place: Energy dissipators in Lahchura Dam near Mau-Ranipur
Latitude: 25°13’41.8597”N **Longitude**: 79°13’50”E **Elevation**: 169 m

Place: Downstream view from Lahchura Dam in Dhasan river
Latitude: 25°13’41.8597”N **Longitude**: 79°13’50”E **Elevation**: 169 m

Place: Canal diverted from Lahchura Dam in Dhasan river
Latitude: 25°13’41.8597”N **Longitude**: 79°13’50”E **Elevation**: 169 m

Place: Agricultural land near Ghat Lahchura
Latitude: 25°15’39.0356”N **Longitude**: 79°14.37’ E **Elevation**: 153 m

Place: Forest near Lahchura Village
Latitude: 25°18’6.8292”N **Longitude**: 79°13’10.1”E **Elevation**: 366 m

Place: Saprar Dam near Mau-Ranipur
Latitude: 25.14°56’69.71”N **Longitude**: 79.8° 14. **Elevation**: 826 m

Place: Reservoir of Saprar Dam
Latitude: 25.14°56’69.71”N **Longitude**: 79.8° 14. **Elevation**: 826 m

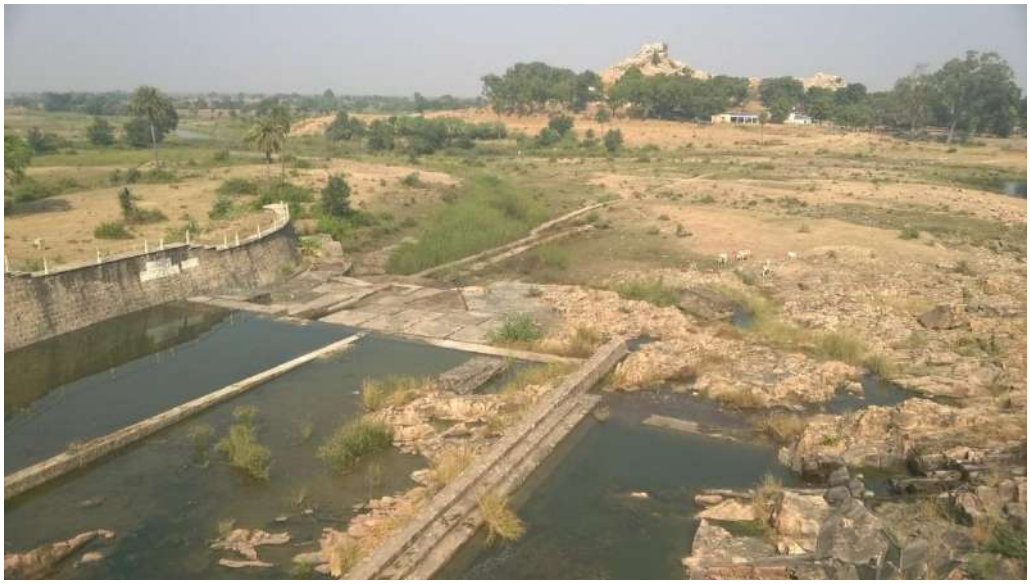

Place: Downstream view of Saprar Dam
Latitude: 25.14°56’69.71”N **Longitude**: 79.8° 14. **Elevation**: 826 m

Place: Downstream view of Saprar Dam
Latitude: 25.14°56’69.71”N **Longitude**: 79.8° 14. **Elevation**: 826 m

Place: Shrub Land near Rath
Latitude: 25.35°19.9836'N **Longitude**: 79°42'22"E. **Elevation**: 703m

Place: Bramhanand Dam Near Rath
Latitude: 25.35°20.1552'N **Longitude**: 79°42'25.1" E. **Elevation**: 202m

Place: Downstream view of Bramhanand Dam Near Rath
Latitude: 25.35°20.1552'N **Longitude**: 79°42'25.1" E. **Elevation**: 202m

Place: Downstream view of Bramhanand Dam Near Rath
Latitude: 25.35°20.1552'N **Longitude**: 79°42'25.1" E. **Elevation**: 202m

Place: Agricultural Land
Latitude: 25.55° 4.4058’N **Longitude**: 79°47’29.0” E. **Elevation**: 843m

Place: Scrub Land
Latitude: 25.55° 48.866’N **Longitude**: 79°47’57.2” E. **Elevation**: 369m

Place: Scrub Land
Latitude: 25.55° 48.866’N **Longitude**: 79°47’57.2” E. **Elevation**: 369m

Place: Agricultural Land
Latitude: 25.58° **7**.8570’N **Longitude**: 79°49’13.4” E. **Elevation**: 270m

Place: Agricultural Land
Latitude: 25°59’19.0920’N **Longitude**: 79°51’43.5” E. **Elevation**: 277m

Place: Agricultural Land
Latitude: 25°59’19.0920’N **Longitude**: 79°52’54.8” E. **Elevation**: 216m

Place: Scrub Land
Latitude: 25°57’20.2174’N **Longitude**: 80°5’52.7” E. **Elevation**: 984m

Place: Village Rameri Danda Near Hamirpur
Latitude: 25°92’39.09”’N **Longitude**: 80°18’94.9” E. **Elevation**: 490m

Place: Agricultural land near confluence of Betwa and Yamuna River at Hamirpur
Latitude: 25°91’99.40” N **Longitude**: 80°20’15” E. **Elevation**: 590m

APPENDIX B

Appendix B-1: Results of trend analysis for rainfall at various stations

Station	Pre-monsoon		Monsoon		Post-monsoon		Winter		Yearly	
	Z-MK	Trend*	Z-MK	Trend*	Z-MK	Trend*	Z-MK	Trend*	Z-MK	Trend*
Banda	1.91	10	-1.18	0	0.06	0	-0.35	0	-1.67	-10
Bhopal	1.40	0	-0.89	0	-0.39	0	1.71	10	-0.61	0
Damoh	-0.30	0	-0.49	0	-0.44	0	-0.37	0	-0.55	0
Datia	1.92	10	-0.76	0	0.61	0	-1.13	0	-0.42	0
Guna	1.45	0	0.76	0	-0.01	0	0.55	0	0.82	0
Hamirpur	2.48	5	-1.30	0	0.18	0	-0.83	0	-1.24	0
Hoshangabad	0.46	0	0.20	0	-1.01	0	0.23	0	0.26	0
Jhansi	1.88	10	-0.52	0	0.10	0	-0.25	0	-0.36	0
Kanpur	2.87	1	0.37	0	0.68	0	-0.21	0	0.41	0
Khajuraho	1.41	0	-0.58	0	0.47	0	0.27	0	-0.51	0
Lalitpur	1.47	0	-0.22	0	1.09	0	0.98	0	0.00	0
Mahoba	1.90	10	0.04	0	1.25	0	0.53	0	0.07	0
Narsinghpur	-0.94	0	-1.20	0	-1.28	0	-0.53	0	-1.23	0
Orai	2.76	1	-0.61	0	0.62	0	-1.01	0	-0.49	0
Panna	-0.20	0	-0.81	0	-0.03	0	-0.20	0	-0.79	0
Raisen	1.21	0	-0.90	0	-0.38	0	0.62	0	-0.75	0
Sagar	2.32	5	-0.52	0	-0.50	0	0.57	0	-0.19	0
Sehore	1.19	0	-1.04	0	-0.07	0	1.36	0	-0.75	0
Shivpuri	1.72	10	-0.72	0	-0.45	0	0.36	0	-0.47	0
Tikamgarh	1.71	10	-1.04	0	-0.06	0	-0.46	0	-1.09	0
Vidisha	1.91	10	-0.22	0	-0.38	0	0.55	0	0.15	0

* 0 = No Trend, 1 = Increasing trend at 1% significance level, 5 = Increasing trend at 5% significance level,
10 = Increasing trend at 10% significance level, -1 = Decreasing trend at 1% significance level,
-5 = Decreasing trend at 5% significance level, -10 = Decreasing trend at 10% significance level

Appendix B-2: Slope, Intercept and relative change values at various stations with significant trends for rainfall

Station	Pre-monsoon			Monsoon			Post-monsoon			Winter			Yearly		
	Sen's Slope	RC	Intercept	Sen's Slope	RC	Intercept	Sen's Slope	RC	Intercept	Sen's Slope	RC	Intercept	Sen's Slope	RC	Intercept
Banda	0.07	35.69	12.84	-	-	-	-	-	-	-	-	-	-1.25	-13.31	1125.50
Bhopal	-	-	-	-	-	-	-	-	-	0.05	25.72	15.55	-	-	-
Datia	0.06	42.83	10.69	-	-	-	-	-	-	-	-	-	-	-	-
Hamirpur	0.06	40.81	10.88	-	-	-	-	-	-	-	-	-	-	-	-
Jhansi	0.05	36.15	11.16	-	-	-	-	-	-	-	-	-	-	-	-
Kanpur	0.08	50.56	10.44	-	-	-	-	-	-	-	-	-	-	-	-
Mahoba	0.06	32.73	13.00	-	-	-	-	-	-	-	-	-	-	-	-
Orai	0.07	50.81	10.48	-	-	-	-	-	-	-	-	-	-	-	-
Sagar	0.09	50.74	11.66	-	-	-	-	-	-	-	-	-	-	-	-
Shivpuri	0.05	38.33	11.45	-	-	-	-	-	-	-	-	-	-	-	-
Tikamgarh	0.06	35.13	11.12	-	-	-	-	-	-	-	-	-	-	-	-
Vidisha	0.07	39.91	11.11	-	-	-	-	-	-	-	-	-	-	-	-

Appendix B-3: Results of trend analysis for minimum temperature at various stations

Station	Pre-monsoon		Monsoon		Post-monsoon		Winter		Yearly	
	Z-MK	Trend*	Z-MK	Trend*	Z-MK	Trend*	Z-MK	Trend*	Z-MK	Trend*
Banda	3.81	1	-0.45	0	4.86	1	5.23	1	3.44	1
Bhopal	3.03	1	0.97	0	5.31	1	8.61	1	3.91	1
Damoh	2.45	5	0.28	0	3.45	1	2.41	5	2.96	1
Datia	2.22	5	-2.05	-5	3.96	1	5.87	1	2.52	5
Guna	2.39	5	1.07	0	3.19	1	11.98	1	3.40	1
Hamirpur	2.93	1	-0.96	0	4.01	1	4.74	1	2.49	5
Hoshangabad	3.03	1	2.03	5	3.75	1	7.36	1	4.58	1
Jhansi	2.89	1	-0.46	0	3.59	1	4.18	1	2.44	5
Kanpur	1.78	10	-5.33	-1	4.42	1	6.58	1	2.79	1
Khajuraho	2.81	1	1.01	0	4.17	1	5.01	1	4.75	1
Lalitpur	1.78	10	-0.97	0	2.91	1	4.55	1	3.48	1
Mahoba	1.78	10	-1.56	0	3.35	1	6.87	1	4.37	1
Narsinghpur	3.05	1	1.59	0	3.80	1	13.89	1	4.21	1
Orai	3.27	1	-1.88	-10	4.81	1	7.33	1	3.55	1
Panna	1.41	0	-0.88	0	4.34	1	4.68	1	2.03	5
Raisen	1.95	10	0.94	0	3.46	1	4.00	1	3.32	1
Sagar	3.22	1	0.82	0	3.73	1	10.17	1	4.51	1
Sehore	2.56	5	0.39	0	3.67	1	6.51	1	3.47	1
Shivpuri	1.65	10	-1.70	-10	3.36	1	4.95	1	2.37	5
Tikamgarh	2.31	5	0.00	0	2.94	1	8.91	1	3.57	1
Vidisha	3.20	1	1.45	0	3.48	1	6.24	1	4.35	1

* 0 = No Trend, 1 = Increasing trend at 1% significance level, 5 = Increasing trend at 5% significance level,
10 = Increasing trend at 10% significance level, -1 = Decreasing trend at 1% significance level,
-5 = Decreasing trend at 5% significance level, -10 = Decreasing trend at 10% significance level

Appendix B-4: Slope, Intercept and relative change values at various stations with significant trends for minimum temperature

Station	Pre-monsoon			Monsoon			Post-monsoon			Winter			Yearly		
	Sen's Slope	RC	Intercept	Sen's Slope	RC	Intercept	Sen's Slope	RC	Intercept	Sen's Slope	RC	Intercept	Sen's Slope	RC	Intercept
Banda	0.011	6.12	20.26	-	-	-	0.017	12.57	14.37	0.015	19.40	8.00	0.008	4.78	18.00
Bhopal	0.007	3.79	21.73	-	-	-	0.016	10.92	15.30	0.011	11.26	10.55	0.008	4.67	18.47
Damoh	0.005	2.80	21.78	-	-	-	0.011	7.68	15.78	0.005	4.90	11.04	0.005	3.01	18.75
Datia	0.007	3.58	21.22	-0.005	-2.09	25.17	0.010	7.10	15.20	0.010	12.87	8.35	0.004	2.66	18.40
Guna	0.006	3.22	21.66	-	-	-	0.012	7.96	15.73	0.009	10.19	9.99	0.006	3.82	18.54
Hamirpur	0.012	6.72	20.23	-	-	-	0.019	13.63	14.32	0.017	22.14	7.66	0.008	5.14	17.98
Hoshangabad	0.006	2.97	22.23	0.006	2.72	22.95	0.017	11.86	15.27	0.010	9.61	11.41	0.009	5.15	18.63
Jhansi	0.011	5.74	21.00	-	-	-	0.015	10.31	15.00	0.012	14.45	8.51	0.006	3.51	18.29
Kanpur	0.005	2.67	20.77	-0.008	-3.43	26.64	0.009	6.68	15.12	0.012	15.79	7.92	0.003	2.00	18.57
Khajuraho	0.007	3.95	20.95	-	-	-	0.012	8.59	15.23	0.007	7.86	9.50	0.008	4.58	18.23
Lalitpur	0.006	2.80	21.63	-	-	-	0.013	7.97	15.72	0.011	10.25	10.06	0.006	3.15	18.57
Mahoba	0.005	2.32	20.56	-	-	-	0.013	8.65	14.63	0.010	12.08	8.28	0.005	2.86	17.99
Narsinghpur	0.007	3.56	21.42	-	-	-	0.018	13.01	14.57	0.009	9.33	10.63	0.008	5.12	17.89
Orai	0.009	4.79	20.74	-0.005	-2.23	25.93	0.014	10.31	14.78	0.014	18.89	7.74	0.006	3.80	18.26
Panna	-	-	-	-	-	-	0.015	10.60	15.02	0.008	9.49	9.58	0.005	2.98	18.33
Raisen	0.004	2.24	22.15	-	-	-	0.016	11.21	15.43	0.008	7.70	11.33	0.006	3.69	18.81
Sagar	0.009	4.59	21.82	-	-	-	0.018	12.02	15.57	0.013	12.98	10.73	0.009	5.20	18.56
Sehore	0.007	3.28	22.23	-	-	-	0.015	9.46	15.60	0.011	9.62	11.16	0.007	3.96	18.85
Shivpuri	0.005	2.45	21.58	-0.003	-1.53	24.57	0.010	7.05	15.68	0.009	10.17	9.28	0.004	2.49	18.55
Tikamgarh	0.007	3.59	21.42	-	-	-	0.010	7.20	15.62	0.008	9.15	9.59	0.006	3.80	18.50
Vidisha	0.009	4.68	21.44	-	-	-	0.017	11.95	15.25	0.012	12.86	10.23	0.009	5.44	18.25

Appendix B-5: Results of trend analysis for maximum temperature at various stations

Station	Pre-monsoon		Monsoon		Post-monsoon		Winter		Yearly	
	Z-MK	Trend*	Z-MK	Trend*	Z-MK	Trend*	Z-MK	Trend*	Z-MK	Trend*
Banda	3.20	1	0.29	0	5.72	1	6.27	1	4.11	1
Bhopal	2.52	5	-0.62	0	4.66	1	3.90	1	2.54	5
Damoh	3.94	1	1.53	0	4.53	1	5.89	1	3.97	1
Datia	3.47	1	-1.00	0	3.68	1	4.82	1	3.72	1
Guna	3.80	1	0.81	0	3.75	1	5.20	1	4.82	1
Hamirpur	3.17	1	-0.77	0	3.63	1	2.19	5	2.83	1
Hoshangabad	4.25	1	2.21	5	4.68	1	3.91	1	4.97	1
Jhansi	4.46	1	-0.81	0	4.02	1	4.38	1	3.89	1
Kanpur	1.22	0	-3.97	-1	1.93	10	2.44	5	0.41	0
Khajuraho	3.50	1	1.11	0	4.94	1	6.22	1	3.21	1
Lalitpur	2.14	5	-0.93	0	3.15	1	5.98	1	3.32	1
Mahoba	1.96	10	-1.67	-10	4.41	1	4.60	1	3.06	1
Narsinghpur	3.37	1	1.51	0	3.53	1	6.54	1	3.28	1
Orai	3.35	1	-2.24	-5	2.86	1	3.23	1	2.38	5
Panna	3.70	1	0.32	0	4.36	1	3.86	1	3.24	1
Raisen	2.06	5	0.48	0	4.10	1	4.12	1	3.77	1
Sagar	3.40	1	-0.23	0	4.03	1	7.64	1	4.61	1
Sehore	2.85	1	0.38	0	4.43	1	6.49	1	3.72	1
Shivpuri	2.38	5	-0.85	0	2.29	5	5.27	1	3.55	1
Tikamgarh	3.34	1	0.23	0	3.89	1	4.70	1	4.13	1
Vidisha	3.79	1	0.65	0	4.06	1	7.03	1	4.79	1

* 0 = No Trend, 1 = Increasing trend at 1% significance level, 5 = Increasing trend at 5% significance level,
10 = Increasing trend at 10% significance level, -1 = Decreasing trend at 1% significance level,
-5 = Decreasing trend at 5% significance level, -10 = Decreasing trend at 10% significance level

Appendix B-6: Slope, Intercept and relative change values at various stations with significant trends for maximum temperature

Station	Pre-monsoon			Monsoon			Post-monsoon			Winter			Yearly		
	Sen's Slope	RC	Intercept	Sen's Slope	RC	Intercept	Sen's Slope	RC	Intercept	Sen's Slope	RC	Intercept	Sen's Slope	RC	Intercept
Banda	0.010	3.06	37.03	-	-	-	0.018	6.78	29.42	0.011	4.85	24.18	0.008	2.90	31.62
Bhopal	0.005	1.51	37.86	-	-	-	0.012	4.50	30.19	0.007	2.81	26.77	0.005	1.67	31.95
Damoh	0.009	2.85	37.19	-	-	-	0.019	7.14	29.18	0.009	3.71	25.75	0.009	3.14	31.26
Datia	0.011	3.38	37.06	-	-	-	0.013	4.70	30.15	0.010	4.48	23.80	0.007	2.34	31.76
Guna	0.010	3.13	37.05	-	-	-	0.015	5.38	30.22	0.012	5.41	25.18	0.008	2.92	31.57
Hamirpur	0.008	2.25	37.43	-	-	-	0.011	4.02	30.17	0.006	2.83	24.32	0.004	1.55	32.12
Hoshangabad	0.009	2.65	37.77	0.004	1.49	31.39	0.018	6.63	29.63	0.006	2.46	27.35	0.009	3.05	31.71
Jhansi	0.011	3.24	37.16	-	-	-	0.014	5.18	29.99	0.009	3.91	24.20	0.006	2.21	31.75
Kanpur	-	-	-	-0.008	-2.52	35.82	0.006	2.24	30.81	0.005	2.48	24.18	-	-	-
Khajuraho	0.012	3.69	36.97	-	-	-	0.018	6.51	29.54	0.010	4.23	24.87	0.009	3.15	31.40
Lalitpur	0.006	1.65	37.15	-	-	-	0.013	4.36	29.87	0.010	4.05	25.02	0.006	1.78	31.55
Mahoba	0.005	1.27	37.16	-0.004	-1.22	33.93	0.014	4.52	29.79	0.009	3.79	24.30	0.005	1.56	31.70
Narsinghpur	0.012	3.57	36.18	-	-	-	0.017	6.48	28.11	0.010	4.34	25.36	0.008	3.06	30.20
Orai	0.007	2.12	37.43	-0.005	-1.46	35.22	0.010	3.57	30.46	0.007	3.17	23.96	0.003	1.21	32.20
Panna	0.007	2.15	37.15	-	-	-	0.015	5.61	29.27	0.008	3.49	25.17	0.007	2.35	31.44
Raisen	0.004	1.29	37.89	-	-	-	0.016	5.84	29.76	0.006	2.70	26.75	0.006	2.10	31.82
Sagar	0.007	2.18	37.18	-	-	-	0.016	6.07	29.48	0.010	4.52	25.61	0.007	2.45	31.31
Sehore	0.007	1.90	38.52	-	-	-	0.015	4.91	30.76	0.011	3.91	27.82	0.008	2.38	32.53
Shivpuri	0.007	2.11	36.99	-	-	-	0.008	2.93	30.44	0.009	4.02	24.43	0.005	1.73	31.68
Tikamgarh	0.008	2.44	37.17	-	-	-	0.013	4.87	29.93	0.010	4.61	24.75	0.007	2.33	31.62
Vidisha	0.009	2.85	37.06	-	-	-	0.016	6.05	29.69	0.012	5.10	25.57	0.008	2.79	31.34

Appendix B-7: Results of trend analysis for average temperature at various stations

Station	Pre-monsoon		Monsoon		Post-monsoon		Winter		Yearly	
	Z-MK	Trend*	Z-MK	Trend*	Z-MK	Trend*	Z-MK	Trend*	Z-MK	Trend*
Banda	3.37	1	-0.04	0	5.08	1	8.60	1	4.43	1
Bhopal	3.10	1	0.20	0	4.79	1	9.60	1	3.58	1
Damoh	3.67	1	1.41	0	4.64	1	4.50	1	4.75	1
Datia	4.00	1	-0.97	0	3.83	1	7.02	1	3.55	1
Guna	3.23	1	1.07	0	3.65	1	7.39	1	3.99	1
Hamirpur	3.58	1	-0.69	0	5.14	1	6.92	1	4.01	1
Hoshangabad	3.56	1	2.72	1	4.09	1	6.08	1	4.84	1
Jhansi	4.03	1	-0.36	0	3.91	1	6.14	1	3.64	1
Kanpur	1.67	10	-4.27	-1	3.37	1	4.21	1	1.45	0
Khajuraho	4.47	1	0.93	0	4.82	1	9.17	1	4.15	1
Lalitpur	2.05	5	-0.93	0	3.00	1	4.50	1	3.49	1
Mahoba	1.94	10	-1.57	0	3.44	1	7.04	1	4.15	1
Narsinghpur	3.89	1	1.72	10	3.68	1	7.68	1	3.97	1
Orai	3.81	1	-2.50	-5	4.15	1	6.92	1	3.68	1
Panna	1.89	10	-1.13	0	4.67	1	4.91	1	3.34	1
Raisen	2.04	5	0.92	0	3.73	1	4.85	1	3.93	1
Sagar	3.63	1	0.29	0	3.79	1	8.84	1	5.17	1
Sehore	2.86	1	0.38	0	4.41	1	6.45	1	3.61	1
Shivpuri	2.13	5	-1.13	0	2.75	1	8.99	1	3.90	1
Tikamgarh	2.78	1	-0.20	0	3.49	1	13.87	1	3.94	1
Vidisha	3.86	1	1.04	0	3.70	1	8.76	1	4.28	1

* 0 = No Trend, 1 = Increasing trend at 1% significance level, 5 = Increasing trend at 5% significance level,
10 = Increasing trend at 10% significance level, -1 = Decreasing trend at 1% significance level,
-5 = Decreasing trend at 5% significance level, -10 = Decreasing trend at 10% significance level

Appendix B-8: Slope, Intercept and relative change values at various stations with significant trends for average temperature

Station	Pre-monsoon			Monsoon			Post-monsoon			Winter			Yearly		
	Sen's Slope	RC	Intercept	Sen's Slope	RC	Intercept	Sen's Slope	RC	Intercept	Sen's Slope	RC	Intercept	Sen's Slope	RC	Intercept
Banda	0.011	4.25	28.73	-	-	-	0.018	8.89	21.88	0.013	8.83	16.07	0.008	3.63	24.77
Bhopal	0.006	2.23	29.77	-	-	-	0.014	6.82	22.82	0.009	5.09	18.65	0.006	2.75	25.20
Damoh	0.008	3.05	29.41	-	-	-	0.015	7.28	22.50	0.006	3.69	18.42	0.007	3.05	24.99
Datia	0.010	3.70	29.13	-	-	-	0.013	6.19	22.63	0.011	7.14	16.09	0.006	2.79	25.04
Guna	0.008	3.18	29.33	-	-	-	0.013	6.33	22.91	0.011	6.72	17.57	0.008	3.38	25.03
Hamirpur	0.011	4.08	28.82	-	-	-	0.016	7.76	22.21	0.010	6.95	16.03	0.007	3.33	24.96
Hoshangabad	0.008	2.87	29.99	0.005	2.12	27.17	0.018	8.65	22.42	0.008	4.76	19.36	0.009	3.95	25.15
Jhansi	0.012	4.49	29.04	-	-	-	0.016	7.67	22.46	0.011	7.10	16.31	0.007	3.11	24.95
Kanpur	0.004	1.64	29.23	-0.008	-2.85	31.19	0.008	3.81	22.92	0.008	5.60	16.06	-	-	-
Khajuraho	0.011	4.05	29.00	-	-	-	0.015	7.46	22.37	0.008	5.22	17.20	0.009	3.86	24.79
Lalitpur	0.006	1.94	29.39	-	-	-	0.013	5.61	22.77	0.010	5.93	17.52	0.006	2.35	25.03
Mahoba	0.005	1.63	28.88	-	-	-	0.013	5.74	22.19	0.010	6.01	16.32	0.005	1.99	24.85
Narsinghpur	0.009	3.56	28.76	0.005	2.22	26.26	0.018	8.85	21.27	0.010	6.34	17.93	0.009	3.99	24.02
Orai	0.008	3.22	29.06	-0.005	-1.88	30.56	0.012	5.95	22.59	0.011	7.38	15.81	0.005	2.33	25.22
Panna	0.004	1.70	29.18	-	-	-	0.015	7.27	22.16	0.008	4.94	17.36	0.006	2.54	24.89
Raisen	0.004	1.57	29.99	-	-	-	0.016	7.65	22.64	0.007	4.16	19.05	0.006	2.66	25.30
Sagar	0.008	3.15	29.48	-	-	-	0.017	8.35	22.50	0.012	7.39	18.13	0.008	3.55	24.94
Sehore	0.007	2.42	30.35	-	-	-	0.015	6.43	23.16	0.011	5.58	19.46	0.008	2.94	25.67
Shivpuri	0.005	2.10	29.28	-	-	-	0.009	4.53	23.02	0.008	5.51	16.84	0.005	2.17	25.08
Tikamgarh	0.006	2.47	29.30	-	-	-	0.011	5.49	22.76	0.009	5.80	17.14	0.006	2.67	25.05
Vidisha	0.010	3.65	29.24	-	-	-	0.017	8.22	22.45	0.013	7.73	17.84	0.009	3.87	24.78

Appendix B-9: Results of trend analysis for PET at various stations

Station	Pre-monsoon		Monsoon		Post-monsoon		Winter		Yearly	
	Z-MK	Trend*	Z-MK	Trend*	Z-MK	Trend*	Z-MK	Trend*	Z-MK	Trend*
Banda	-0.87	0	0.55	0	-1.08	0	-0.27	0	1.59	0
Bhopal	-0.53	0	0.69	0	-0.99	0	-0.25	0	0.40	0
Damoh	-1.02	0	0.60	0	-1.10	0	-0.37	0	1.52	0
Datia	-0.94	0	0.55	0	-1.41	0	-0.57	0	1.15	0
Guna	-0.59	0	0.77	0	-1.22	0	-0.36	0	2.06	5
Hamirpur	-0.87	0	0.62	0	-1.13	0	-0.47	0	1.27	0
Hoshangabad	-0.66	0	0.77	0	-0.94	0	-0.28	0	2.13	5
Jhansi	-0.77	0	0.60	0	-1.31	0	-0.50	0	1.13	0
Kanpur	-0.85	0	0.69	0	-1.24	0	-0.50	0	0.23	0
Khajuraho	-1.02	0	0.61	0	-1.11	0	-0.38	0	1.52	0
Lalitpur	1.63	0	-1.21	0	0.19	0	4.42	1	0.64	0
Mahoba	0.89	0	-1.42	0	0.29	0	2.98	1	0.38	0
Narsinghpur	-1.03	0	0.67	0	-0.71	0	-0.22	0	1.41	0
Orai	-0.90	0	0.62	0	-1.36	0	-0.51	0	0.90	0
Panna	-0.91	0	0.64	0	-0.91	0	-0.28	0	1.30	0
Raisen	-0.60	0	0.69	0	-0.91	0	-0.32	0	2.26	5
Sagar	-0.84	0	0.62	0	-1.14	0	-0.43	0	1.60	0
Sehore	1.94	10	-1.00	0	1.07	0	8.20	1	1.84	10
Shivpuri	-0.69	0	0.65	0	-1.27	0	-0.45	0	0.90	0
Tikamgarh	-0.78	0	0.63	0	-1.26	0	-0.50	0	1.14	0
Vidisha	-0.64	0	0.64	0	-1.05	0	-0.31	0	2.06	5

* 0 = No Trend, 1 = Increasing trend at 1% significance level, 5 = Increasing trend at 5% significance level,
10 = Increasing trend at 10% significance level, -1 = Decreasing trend at 1% significance level,
-5 = Decreasing trend at 5% significance level, -10 = Decreasing trend at 10% significance level

Appendix B-10: Slope, Intercept and relative change values at various stations with significant trends for PET

Station	Pre-monsoon			Monsoon			Post-monsoon			Winter			Yearly		
	Sen's Slope	RC	Intercept	Sen's Slope	RC	Intercept	Sen's Slope	RC	Intercept	Sen's Slope	RC	Intercept	Sen's Slope	RC	Intercept
Guna	-	-	-	-	-	-	-	-	-	-	-	-	0.219	1.03	2386.07
Hoshangabad	-	-	-	-	-	-	-	-	-	-	-	-	0.223	1.05	2386.65
Lalitpur	-	-	-	-	-	-	-	-	-	0.048	1.01	483.10	-	-	-
Mahoba	-	-	-	-	-	-	-	-	-	0.046	0.97	479.11	-	-	-
Raisen	-	-	-	-	-	-	-	-	-	-	-	-	0.165	0.78	2384.38
Sehore	0.040	0.53	768.84	-	-	-	-	-	-	0.062	1.19	532.44	0.105	0.43	2450.99
Vidisha	-	-	-	-	-	-	-	-	-	-	-	-	0.220	1.04	2376.42

Appendix B-11: Results of trend analysis for aridity index at various stations

Station	Pre-monsoon		Monsoon		Post-monsoon		Winter		Yearly	
	Z-MK	Trend*	Z-MK	Trend*	Z-MK	Trend*	Z-MK	Trend*	Z-MK	Trend*
Banda	2.11	5	-1.78	-10	0.09	0	-0.23	0	-1.82	-10
Bhopal	1.11	0	-1.44	0	-0.30	0	2.09	5	-0.50	0
Damoh	-0.15	0	-0.97	0	-0.44	0	-0.21	0	-0.72	0
Datia	1.97	5	-1.25	0	0.64	0	-1.00	0	-0.51	0
Guna	1.59	0	-0.31	0	-0.01	0	0.69	0	0.85	0
Hamirpur	2.17	5	-1.07	0	0.22	0	-0.66	0	-1.72	-10
Hoshangabad	0.54	0	-1.04	0	-0.93	0	0.44	0	0.07	0
Jhansi	1.98	5	-1.13	0	0.11	0	-0.15	0	-0.40	0
Kanpur	3.12	1	-0.42	0	0.72	0	0.08	0	0.52	0
Khajuraho	1.80	10	-1.19	0	0.50	0	0.45	0	-0.60	0
Lalitpur	1.43	0	-0.06	0	0.84	0	0.92	0	0.00	0
Mahoba	1.88	10	0.19	0	1.20	0	0.55	0	0.12	0
Narsinghpur	-0.90	0	-1.66	-10	-1.26	0	-0.26	0	-1.43	0
Orai	2.85	1	-1.13	0	0.65	0	-0.93	0	-0.66	0
Panna	0.01	0	-1.12	0	0.05	0	0.02	0	-0.69	0
Raisen	1.26	0	-1.51	0	-0.29	0	0.71	0	-0.83	0
Sagar	2.38	5	-1.14	0	-0.47	0	0.81	0	-0.43	0
Sehore	1.12	0	-0.84	0	-0.07	0	1.32	0	-0.77	0
Shivpuri	1.79	10	-1.24	0	-0.49	0	0.50	0	-0.52	0
Tikamgarh	1.79	10	-1.06	0	-0.05	0	-0.13	0	-1.21	0
Vidisha	2.02	5	-1.00	0	-0.26	0	0.74	0	-0.01	0

* 0 = No Trend, 1 = Increasing trend at 1% significance level, 5 = Increasing trend at 5% significance level,
10 = Increasing trend at 10% significance level, -1 = Decreasing trend at 1% significance level,
-5 = Decreasing trend at 5% significance level, -10 = Decreasing trend at 10% significance level

Appendix B-12: Slope, Intercept and relative change values at various stations with significant trends for aridity index

Station	Pre-monsoon			Monsoon			Post-monsoon			Winter			Yearly		
	Sen's Slope ($\times 10^{-5}$)	RC	Intercept	**Sen's Slope ($\times 10^{-5}$)**	RC	Intercept	**Sen's Slope ($\times 10^{-5}$)**	RC	Intercept	**Sen's Slope ($\times 10^{-5}$)**	RC	Intercept	**Sen's Slope ($\times 10^{-5}$)**	RC	Intercept
Banda	9.92	39.11	0.017	-244.9	-22.29	1.37	-	-	-	-	-	-	-55.93	-14.23	0.475
Bhopal	-	-	-	-	-	-	-	-	-	11.84	29.88	0.030	-	-	-
Datia	8.79	43.86	0.015	-	-	-	-	-	-	-	-	-	-	-	-
Hamirpur	8.58	44.84	0.014	-	-	-	-	-	-	-	-	-	-60.35	-17.27	0.440
Jhansi	7.91	38.77	0.014	-	-	-	-	-	-	-	-	-	-	-	-
Kanpur	11.25	55.10	0.014	-	-	-	-	-	-	-	-	-	-	-	-
Khajuraho	7.74	31.70	0.017	-	-	-	-	-	-	-	-	-	-	-	-
Mahoba	7.40	33.02	0.017	-	-	-	-	-	-	-	-	-	-	-	-
Narsinghpur	-	-	-	-273.6	-21.17	1.60	-	-	-	-	-	-	-	-	-
Orai	10.50	54.19	0.013	-	-	-	-	-	-	-	-	-	-	-	-
Sagar	12.52	52.36	0.015	-	-	-	-	-	-	-	-	-	-	-	-
Shivpuri	7.44	38.08	0.016	-	-	-	-	-	-	-	-	-	-	-	-
Tikamgarh	8.29	36.50	0.015	-	-	-	-	-	-	-	-	-	-	-	-
Vidisha	10.21	43.76	0.015	-	-	-	-	-	-	-	-	-	-	-	-